

MICROCOPY RESOLUTION TEST CHART
NATIONAL BUREAU OF STANDARDS-1963-A

AD-A145 441

6

AFWAL-TR-84-4007

CUMULATIVE DAMAGE MODEL FOR
ADVANCED COMPOSITE MATERIALS



GENERAL DYNAMICS
FORT WORTH DIVISION
P.O. BOX 748
FORT WORTH, TEXAS 76101

March 1984

Final Report for Period 23 May 1982 to 23 September 1983

Approved for public release; distribution unlimited

MATERIALS LABORATORY
AIR FORCE WRIGHT AERONAUTICAL LABORATORIES
AIR FORCE SYSTEMS COMMAND
WRIGHT-PATTERSON AIR FORCE BASE, OHIO 45433

DTIC
SEP 12 1984
S E D
A

DTIC FILE COPY

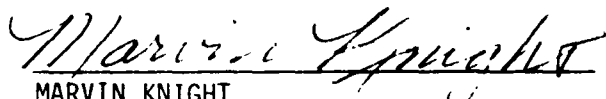
84 09 10 045

NOTICE

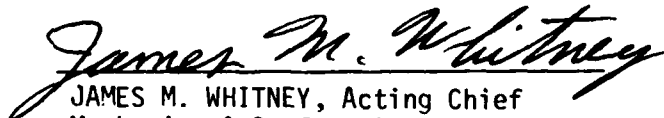
When Government drawings, specifications, or other data are used for any purpose other than in connection with a definitely related Government procurement operation, the United States Government thereby incurs no responsibility nor any obligation whatsoever; and the fact that the government may have formulated, furnished, or in any way supplied the said drawings, specifications, or other data, is not to be regarded by implication or otherwise as in any manner licensing the holder or any other person or corporation, or conveying any rights or permission to manufacture use, or sell any patented invention that may in any way be related thereto.

This report has been reviewed by the Office of Public Affairs (ASD/PA) and is releasable to the National Technical Information Service (NTIS). At NTIS, it will be available to the general public, including foreign nations.

This technical report has been reviewed and is approved for publication.



MARVIN KNIGHT
Materials Research Engineer
Mechanics & Surface Interactions Br



JAMES M. WHITNEY, Acting Chief
Mechanics & Surface Interactions Br
Nonmetallic Materials Division

FOR THE COMMANDER



F. D. CHERRY, Chief
Nonmetallic Materials Division

"If your address has changed, if you wish to be removed from our mailing list, or if the addressee is no longer employed by your organization please notify AFWAL/MLBM, W-PAFB, OH 45433 to help us maintain a current mailing list".

Copies of this report should not be returned unless return is required by security considerations, contractual obligations, or notice on a specific document.

| REPORT DOCUMENTATION PAGE | | READ INSTRUCTIONS BEFORE COMPLETING FORM |
|---|-------------------------------------|---|
| 1. REPORT NUMBER AFWAL-TR-84-4007 | 2. GOVT ACCESSION NO. AD-A145441 | 3. RECIPIENT'S CATALOG NUMBER |
| 4. TITLE (and Subtitle) CUMULATIVE DAMAGE MODEL FOR ADVANCED COMPOSITE MATERIALS | | 5. TYPE OF REPORT & PERIOD COVERED Technical - Final June 1982-October 1983 |
| | | 6. PERFORMING ORG. REPORT NUMBER FZM-7149 |
| 7. AUTHOR(s) H.R. Miller D.A. Ulman K.L. Reifsnider R.D. Bruner W.W. Stinchcomb K.M. Liechti | | 8. CONTRACT OR GRANT NUMBER(s) F33615-81-C-5049 |
| | | 10. PROGRAM ELEMENT, PROJECT, TASK AREA & WORK UNIT NUMBERS 24190327 |
| 9. PERFORMING ORGANIZATION NAME AND ADDRESS General Dynamics Corp. Fort Worth Division Fort Worth, TX | | 12. REPORT DATE March 1984 |
| 11. CONTROLLING OFFICE NAME AND ADDRESS Materials Laboratory Air Force Wright Aeronautical Laboratories AFSC, WPAFB, OH 45433 | | 13. NUMBER OF PAGES 270 |
| 14. MONITORING AGENCY NAME & ADDRESS (if different from Controlling Office) | | 15. SECURITY CLASS. (of this report) Unclassified |
| | | 15a. DECLASSIFICATION/DOWNGRADING SCHEDULE |
| 16. DISTRIBUTION STATEMENT (of this Report) Approved for Public Release; distribution unlimited | | |
| 17. DISTRIBUTION STATEMENT (of the abstract entered in Block 20, if different from Report) | | |
| 18. SUPPLEMENTARY NOTES | | |
| 19. KEY WORDS (Continue on reverse side if necessary and identify by block number) Cumulative damage, composite materials, stacking sequence, fa- tigue testing, multiple load histories, NDE, stiffness change, residual strength, models, property degradation. | | |
| 20. ABSTRACT (Continue on reverse side if necessary and identify by block number) The scope of the second phase of the investigation included in- terrelated analytical and experimental tasks. The major analyti- cal activities have been: (1) Determination of the values of parameters within the model and study of the sensitivity of the predictions of the model to those parameters. Associated with this task is a critical re-examination of the data generated (continued) | | |

20. (Continued)

Abstract (Continued)

in the previous phase along with the incorporation of Phase II data. (2) Refinement of the procedures for incorporating the effects of compressive load excursions within the framework of the cumulative damage model. (3). Incorporation of load history and R-value effects within the model. The experimental activities included: (1) Fabrication of AS1/3502 graphite-epoxy specimens using two differing lamination sequences. (2) Tensile and compressive testing to determine the moduli, Poisson's ratios, strength, quasistatic damage development, and ultimate strain of one of the laminates (the second laminate had been characterized in Phase I). (3) Fatigue testing of the two laminates in an extensive matrix including constant amplitude tension-tension, compression-compression, tension-compression, and simple two-stage block spectrum. Damage and stiffness change monitoring was employed in each test performed.

| | |
|----------------------|-------------------------------------|
| Accession For | |
| NTIS GRA&I | <input checked="" type="checkbox"/> |
| DTIC TAB | <input type="checkbox"/> |
| Unannounced | <input type="checkbox"/> |
| Justification | |
| By | |
| Distribution/ | |
| Availability Codes | |
| Dist | Avail and/or Special |
| A-1 | |



Unclassified

FOREWORD

The Cumulative Damage Model for Advanced Composite Materials program (F33615-81-C-5049) is sponsored by the Air Force Wright Aeronautical Laboratories, Materials Laboratory, Air Force Systems Command, Wright Patterson Air Force Base, Ohio 45433. Marvin Knight of AFWAL/MLBM is the Air Force Project Engineer.

The program is being performed jointly by the Structures and Design Department of General Dynamics, Fort Worth Division and by the Materials Response Group at Virginia Polytechnic Institute and State University. Harry R. Miller of the Materials Research Lab is the General Dynamics Program Manager. Mr. D. A. Ulman, Acting Program Manager during the period July 30, 1982 through October 11, 1982, is acknowledged for both his leadership during this period and his continuing participation in this program. His predecessors, Drs. K. M. Liechti and J. E. Masters, are acknowledged for their contributions to this program. Drs. K. L. Reifsnider, W. W. Stinchcomb and E. G. Henneke are the principal investigators at VPI & SU.

Also acknowledged for their contributions are R. D. Bruner of the Materials Research Lab of GD/FWD, J. H. Fruit of the Engineering Chemistry Lab of GD/FWD and VPI research assistant R. Simonds.

TABLE OF CONTENTS

| <u>SECTION</u> | | <u>PAGE</u> |
|----------------|--|-------------|
| I | INTRODUCTION | 1 |
| II | CUMULATIVE DAMAGE MODEL | 5 |
| | 1. Problem | 5 |
| | 2. Approach | 8 |
| | 3. Fundamental Formulations | 11 |
| | 4. Detailed Results | 31 |
| | A. Tension-Tension Loading | 31 |
| | B. Compression Loading | 96 |
| | C. Variable R-Value Testing and Modeling | 143 |
| | 5. Closure | 153 |
| III | CUMULATIVE DAMAGE EXPERIMENTAL INVESTIGATION | 159 |
| | 1. Background | 159 |
| | A. Specimen Description | 161 |
| | B. Nondestructive Test Techniques | 167 |
| | C. Test Procedures | 169 |

TABLE OF CONTENTS, CONTINUED

| <u>SECTION</u> | | <u>PAGE</u> |
|----------------|--|-------------|
| III | CUMULATIVE DAMAGE EXPERIMENTAL INVESTIGATION, CONTINUED | |
| | 2. Summary of Test Results | 171 |
| | A. Laminate Type C | 171 |
| | B. Laminate Type F | 186 |
| IV | SUMMARY | 197 |
| | APPENDIX: TABULAR DAMAGE DATA | 201 |
| | REFERENCES | 255 |

LIST OF ILLUSTRATIONS

| <u>FIGURE</u> | | <u>PAGE</u> |
|---------------|---|-------------|
| 1 | Damage Modes During Fatigue Loading of Composite Laminates | 13 |
| 2 | Longitudinal Young's Modulus Reduction for a $[\theta/45/-45/\theta]_s$ Graphite Epoxy Laminate Cycled at 85% of the Static Ultimate Strength, and a $[\theta/90_2]_s$ Glass Epoxy Specimen Cycled at 60% of the Static Ultimate Strength | 14 |
| 3 | Schematic Diagram of Regions of Damage Development for Composite Laminates | 15 |
| 4 | Schematic Diagram of Laminate Strength Reduction-Life Relationship | 19 |
| 5 | Schematic Diagram of Critical Element Strength-Life Relationship | 20 |
| 6 | Schematic Diagram of Critical Element Strength-Life Relationship for Three Dimensional Formulation | 21 |
| 7 | An Example of the Interpretation of Terms in the Summation Equation for Tension-Tension Constant Amplitude Loading | 24 |
| 8 | Conceptual Flow Chart of the Damage Accumulation Model | 28 |
| 9 | Crack Spacing in the -45 Ply of $[\theta/90/45/-45]_s$ Graphite Epoxy Laminates Under Cyclic and Quasi-Static Loading | 37 |
| 10 | Moire Fringe Pattern of a $[\theta/90_2]_s$ Laminate between Cracked Sections of the 90 Plies | 41 |
| 11 | Predicted and Observed Strain Distributions in the θ Plies of a $[\theta/90_2]_s$ Laminate between Cracked Sections of the 90 Plies | 42 |
| 12 | General Schematic Representation of Local Net-Section Stress Situation near a Matrix Crack | 43 |
| 13 | Linear Fit of Normalized Stress in the θ Plies During Cyclic Loading | 49 |

LIST OF ILLUSTRATIONS, CONTINUED

| <u>FIGURE</u> | | <u>PAGE</u> |
|---------------|--|-------------|
| 14 | Residual Strength Prediction and Observation for Specimen B2-6 | 51 |
| 15 | Change of b Parameter from -0.07 to -0.073 for Specimen B2-6 | 52 |
| 16 | Predicted and Observed Residual Strength for Applied T-T Stress Range of 44.1 ksi for $b=-0.07$ | 53 |
| 17 | Same Results Shown in Fig.16 with b Changed to -0.075 | 54 |
| 18 | Predictions and Observations for Specimens B2-6, B2-8, and a Hypothetical High Stress Case Plotted on Semi-Log Paper | 56 |
| 19 | Illustration of the Influence of Various Model Parameters on Predicted Results | 57 |
| 20 | Normalized Fiber Direction Stress in 0 Degree Plies Estimated from Laminate Analysis and Stiffness Changes | 61 |
| 21 | Predicted Residual Strength for Data Shown in Fig. 20 | 62 |
| 22 | Normalized Local Stress in 0 Plies Calculated from Laminate Analysis and Stiffness Changes | 63 |
| 23 | Residual Strength Calculation and Observed Data Point for Data in Fig. 22 | 64 |
| 24 | Same Prediction Shown in Fig. 23 Except b Has Been Changed from -0.073 to -0.077 | 65 |
| 25 | Curve Fit of Typical Stiffness Change Data for T-T Loading of Type D Specimens | 71 |
| 26 | Estimate of Local 0 Ply Stress for Data in Fig. 25 | 72 |
| 27 | Predicted Variation of Residual Strength for a Type D Laminate | 73 |
| 28 | Change in Stiffness for T-T Loading with a Maximum Strain Level of $5000 \mu e$ | 74 |

LIST OF ILLUSTRATIONS, CONTINUED

| <u>FIGURE</u> | | <u>PAGE</u> |
|---------------|--|-------------|
| 29 | Schematic of Geometry Used for Shear-Lag Analysis in Type D Laminates | 76 |
| 30 | Cases of Crack Growth Analyzed for Type D Damage Analysis | 77 |
| 31 | Crack Face Opening Geometry Predicted from Shear-Lag Analysis for a Long Coupled Crack in the Type D Laminate | 79 |
| 32 | Comparison of Calculated Stiffness Change and Change in Local Axial Stress in the θ Plies for Crack Coupling | 80 |
| 33 | Residual Strength Prediction and Typical Observation for Shear-Lag Refinement of the Damage Accumulation Model | 82 |
| 34 | Residual Strength and Life Predictions for Uncorrected Model, Showing Effect of Stress Redistribution | 84 |
| 35 | Predictions and Observations for Model in which F_1 , the Local Failure Function, was Set Equal to the Ratio of Applied Stress to Undamaged Strength | 86 |
| 36 | Semi-Log Plot of Data in Fig. 35 Showing Life Prediction for Specimen F4-6 | 88 |
| 37 | Predicted and Observed Data for Type F Laminate in T-T Loading for Model with Biaxial Correction | 93 |
| 38 | Summary of Refinements to the Tension-Tension Cumulative Damage Model | 95 |
| 39 | Stiffness Retention Fraction for Several C-C Tests of Type B Specimens | 100 |
| 40 | Fractional Stiffness Change for a Typical Type B Specimen Loaded in C-C at $4500\mu\epsilon$ | 102 |
| 41 | Fractional Stiffness Change in a Type B Specimen for C-C Loading at $5000\mu\epsilon$ | 103 |
| 42 | Fractional Stiffness Change in a Type B Specimen for C-C Loading at $5500\mu\epsilon$ | 104 |

LIST OF ILLUSTRATIONS, CONTINUED

| <u>FIGURE</u> | | <u>PAGE</u> |
|---------------|--|-------------|
| 43 | Residual Strength Prediction for C-C Loading | 105 |
| 44 | Residual Strength Prediction for C-C Loading | 106 |
| 45 | Residual Strength Prediction for C-C Loading | 107 |
| 46 | Summary of Predictions and Observations for C-C Loading of Type B Laminates | 108 |
| 47 | Observed Fractional Stiffness Change for T-C Loading with Strain Amplitude of $4000\mu\epsilon$ | 110 |
| 48 | Predicted Residual Strength Change for $4500\mu\epsilon$ | 112 |
| 49 | Predicted Residual Strength Change for Data in Fig. 47 with $\epsilon_c=4364\mu\epsilon$ | 113 |
| 50 | Summary of Observations and Predictions for T-C Loading Using Stiffness Based Model (Simple Form) for Type C Laminates | 114 |
| 51 | Fractional Stiffness Change Measured During T-C Loading of Type D Laminates | 116 |
| 52 | Observed Fractional Stiffness Change for Specimen D1-10 | 117 |
| 53 | Observed Fractional Stiffness Change for Specimen D2-8 | 118 |
| 54 | Observed Fractional Stiffness Change for Specimen D2-5 | 119 |
| 55 | Predicted Residual Strength Data for Specimen D1-10 | 120 |
| 56 | Predicted Residual Strength Data for Specimen D2-8 | 121 |
| 57 | Predicted Residual Strength Data for Specimen D2-5 | 122 |
| 58 | Summary of Observed and Predicted Data for T-C Loading of Type D Laminates Using Critical Stiffness Model | 123 |

LIST OF ILLUSTRATIONS, CONTINUED

| <u>FIGURE</u> | | <u>PAGE</u> |
|---------------|--|-------------|
| 59 | Parameter Study of the Power of Delamination Growth Law | 131 |
| 60 | Predicted and Observed Life Data for T-C Model which Uses Observed Stiffness Changes | 138 |
| 61 | Stiffness Change During Block Loading of Three Specimens | 139 |
| 62 | Fatigue Life Observations for Five Different R Values | 146 |
| 63 | Residual Strength Prediction for R=-1, Type C | 147 |
| 64 | Life Predictions and Observations for R=-0.5 Tests | 149 |
| 65 | Predicted and Observed Life for R=-2 Tests | 150 |
| 66 | Specimen Geometry | 163 |
| 67 | Interlaminar Normal Stress Distribution: Type C Laminate | 165 |
| 68 | Interlaminar Normal Stress Distribution: Type F Laminate | 166 |
| 69 | S-N Comparison: Phase I to Phase II Test Results | 173 |
| 70 | Longitudinal Stiffness Retention, Type C | 175 |
| 71 | Edge Replicas of Specimen C5-5 | 177 |
| 72 | Edge Replicas of Specimen C8-3 | 184 |
| 73 | Edge Replicas of Specimen C8-5 | 185 |
| 74 | Edge Replicas of Specimen C5-6 | 187 |
| 75 | Stress-Strain Results for Type F Tension Loading | 190 |
| 76 | Stress-Strain Results for Type F Compression Loading | 191 |
| 77 | Type F Stiffness Change, Monotonic Tension | 193 |
| 78 | Type F Longitudinal Stiffness Retention | 194 |

LIST OF TABLES

| <u>TABLE</u> | | <u>PAGE</u> |
|--------------|--|-------------|
| 1 | EXAMPLE: [0/90/45/-45]s T300-5208 | 39 |
| 2 | EXAMPLE: [0/90/45/-45]s3s | 46 |
| 3 | VARIATION OF RESIDUAL STRENGTH FOR FOUR "IDENTICAL" SPECIMENS | 66 |
| 4 | TYPE C 7500pe DATA | 69 |
| 5 | STRESSES IN 0 PLYS OF TYPE F LAMINATES DURING DAMAGE DEVELOPMENT | 89 |
| 6 | RESULTS OF BLOCK LOADING TESTS AND PREDICTIONS | 132 |
| 7 | RESULTS OF BLOCK LOADING TESTS AND PREDICTIONS | 141 |
| 8 | SUMMARY OF RESULTS FOR VARIABLE R SERIES | 152 |
| 9 | PHASE II TEST MATRIX | 160 |
| 10 | LAMINATE STACKING SEQUENCES | 162 |
| 11 | DAMAGE PROGRESSION IN SPECIMEN C5-5 | 176 |
| 12 | TEST MATRIX FOR LOAD HISTORY EFFECTS: TYPE C | 179 |
| 13 | FATIGUE LIFE DATA FROM LOAD HISTORY TESTS | 181 |
| 14 | CHANGE IN STATIC SECANT MODULUS: TYPE C | 183 |
| 15 | LAMINATE TENSILE AND COMPRESSIVE PROPERTIES | 192 |
| 16 | TYPE F BLOCK LOADING TESTS | 195 |
| 17 | DAMAGE PROGRESSION IN SPECIMEN C5-5 | 202 |
| 18 | DAMAGE PROGRESSION IN SPECIMEN C7-3 | 203 |
| 19 | DAMAGE PROGRESSION IN SPECIMEN C5-7 | 204 |
| 20 | DAMAGE PROGRESSION IN SPECIMEN C5-1 | 205 |
| 21 | DAMAGE PROGRESSION IN SPECIMEN C6-10 | 206 |
| 22 | DAMAGE PROGRESSION IN SPECIMEN C6-4 | 207 |
| 23 | DAMAGE PROGRESSION IN SPECIMEN C4-4 | 208 |
| 24 | DAMAGE PROGRESSION IN SPECIMEN C6-2 | 209 |

LIST OF TABLES, CONTINUED

| <u>TABLE</u> | | <u>PAGE</u> |
|--------------|--------------------------------------|-------------|
| 25 | DAMAGE PROGRESSION IN SPECIMEN C7-1 | 210 |
| 26 | DAMAGE PROGRESSION IN SPECIMEN C8-8 | 211 |
| 27 | DAMAGE PROGRESSION IN SPECIMEN C5-11 | 212 |
| 28 | DAMAGE PROGRESSION IN SPECIMEN C6-6 | 213 |
| 29 | DAMAGE PROGRESSION IN SPECIMEN C7-11 | 214 |
| 30 | DAMAGE PROGRESSION IN SPECIMEN C8-4 | 215 |
| 31 | DAMAGE PROGRESSION IN SPECIMEN C8-12 | 216 |
| 32 | DAMAGE PROGRESSION IN SPECIMEN C6-8 | 217 |
| 33 | DAMAGE PROGRESSION IN SPECIMEN C8-6 | 218 |
| 34 | DAMAGE PROGRESSION IN SPECIMEN C7-9 | 219 |
| 35 | DAMAGE PROGRESSION IN SPECIMEN C8-10 | 220 |
| 36 | DAMAGE PROGRESSION IN SPECIMEN C5-3 | 221 |
| 37 | DAMAGE PROGRESSION IN SPECIMEN F2-7 | 222 |
| 38 | DAMAGE PROGRESSION IN SPECIMEN F5-6 | 223 |
| 39 | DAMAGE PROGRESSION IN SPECIMEN F4-2 | 224 |
| 40 | DAMAGE PROGRESSION IN SPECIMEN F3-4 | 225 |
| 41 | DAMAGE PROGRESSION IN SPECIMEN F4-6 | 226 |
| 42 | DAMAGE PROGRESSION IN SPECIMEN F1-9 | 227 |
| 43 | DAMAGE PROGRESSION IN SPECIMEN F3-1 | 228 |
| 44 | DAMAGE PROGRESSION IN SPECIMEN F5-5 | 229 |
| 45 | DAMAGE PROGRESSION IN SPECIMEN F2-2 | 230 |
| 46 | DAMAGE PROGRESSION IN SPECIMEN F4-1 | 231 |
| 47 | DAMAGE PROGRESSION IN SPECIMEN F5-8 | 232 |
| 48 | DAMAGE PROGRESSION IN SPECIMEN F4-7 | 233 |

LIST OF TABLES, CONTINUED

| <u>TABLE</u> | | <u>PAGE</u> |
|--------------|--------------------------------------|-------------|
| 49 | DAMAGE PROGRESSION IN SPECIMEN F1-7 | 234 |
| 50 | DAMAGE PROGRESSION IN SPECIMEN F1-10 | 235 |
| 51 | DAMAGE PROGRESSION IN SPECIMEN F2-5 | 236 |
| 52 | DAMAGE PROGRESSION IN SPECIMEN F2-9 | 237 |
| 53 | DAMAGE PROGRESSION IN SPECIMEN F4-4 | 238 |
| 54 | DAMAGE PROGRESSION IN SPECIMEN F3-9 | 239 |
| 55 | DAMAGE PROGRESSION IN SPECIMEN F5-7 | 240 |
| 56 | DAMAGE PROGRESSION IN SPECIMEN F2-6 | 241 |
| 57 | DAMAGE PROGRESSION IN SPECIMEN F3-11 | 242 |
| 58 | DAMAGE PROGRESSION IN SPECIMEN F1-5 | 243 |
| 59 | DAMAGE PROGRESSION IN SPECIMEN F1-11 | 244 |
| 60 | DAMAGE PROGRESSION IN SPECIMEN F1-1 | 245 |
| 61 | DAMAGE PROGRESSION IN SPECIMEN F1-4 | 246 |
| 62 | DAMAGE PROGRESSION IN SPECIMEN F3-12 | 247 |
| 63 | DAMAGE PROGRESSION IN SPECIMEN F5-1 | 248 |
| 64 | DAMAGE PROGRESSION IN SPECIMEN F2-1 | 249 |
| 65 | DAMAGE PROGRESSION IN SPECIMEN F4-12 | 250 |
| 66 | DAMAGE PROGRESSION IN SPECIMEN F3-5 | 251 |
| 67 | DAMAGE PROGRESSION IN SPECIMEN F2-8 | 252 |
| 68 | DAMAGE PROGRESSION IN SPECIMEN F3-10 | 253 |
| 69 | DAMAGE PROGRESSION IN SPECIMEN F5-2 | 254 |

SECTION I
INTRODUCTION

The use of advanced composite materials for aerospace structural applications has evolved as a result of the advantages they offer in such areas as strength-to-weight ratio and ease of manufacture. As the use of advanced composites as primary load carrying structural elements becomes more attractive and realistic, so the need to analytically predict their performance and, particularly, life increases. A life prediction methodology can also be used in the optimization of designs and materials.

➤ The overall objective of this program is to develop a cumulative damage model for advanced composite materials. This involves the development of analytical models and experimental procedures for accurately predicting and characterizing the mechanical responses of advanced composites which have been subjected to conditions representative of those seen in service.

➤ This report reviews the achievements of the second of the three phases into which this program has been divided. The objective of this second phase was to refine the model developed in the first phase of the program. With the model developed and refined, a third and final phase will be conducted for the purpose of model verification.

The scope of the second phase of the investigation included interrelated analytical and experimental tasks. The major analytical activities have been:

- Determination of the values of parameters within the model and study of the sensitivity of the predictions of the model to those parameters. Associated with this task is a critical re-examination of the data generated in the previous phase along with the incorporation of Phase II data.
- Refinement of the procedures for incorporating the effects of compressive load excursions within the framework of the cumulative damage model.
- Incorporation of load history and R-value effects within the model.

The experimental activities included:

- Fabrication of AS1/3502 graphite-epoxy specimens using two differing lamination sequences.
- Tensile and compressive testing to determine the moduli, Poisson's ratio, strength, quasi-static damage development, and ultimate strain of one of the laminates (the second

laminate had been characterized in Phase I).

- Fatigue testing of the two laminates in an extensive test matrix including constant amplitude tension-tension, compression-compression, tension-compression, and simple two stage block spectrum. Damage and stiffness change monitoring was employed in each test performed.

The results of these activities will be completely described in the following sections. Section 2 details the analytical model refinement and contains many examples of the use of the model through the incorporation of the experimental data. Section 3 then follows with a summary of the test matrix, testing procedures, and results.

SECTION II

CUMULATIVE DAMAGE MODEL

1. Problem

In order to understand the approach that was taken to the modeling of cumulative damage in composite laminates, it is desirable to define precisely the problem that was addressed. The basic objective of the effort was to develop a mechanistic cumulative damage model that would have the capability of describing and predicting the strength and life of composite laminates during cyclic loading. The major point of departure of this research effort from prior modeling activities is the mechanistic approach. In fact, for the most part, the major thrust of the entire research program can be characterized as an attempt to make a major step in philosophy from phenomenological descriptions of composite laminate fatigue behavior to mechanistic modeling based on the physics and mechanics of the details of laminate response during cyclic loading.

While the basic objective of this research effort is certainly ambitious, the scope of the program actually presents the greatest challenge. The investigation is to address the residual strength and life of several types of composite laminates in unnotched coupon (plate) specimen form subjected to tension-tension, compression-compression, tension-compression, and spectral cyclic loading. While this scope may seem, at first reading, to be almost unreasonable, it is actually the consequence of a rational a priori decision regarding the approach to be used in this investigation that was made when the program was originally conceived. While it may appear to be more logical and academically reasonable to pick one aspect of composite laminate fatigue behavior

under one type of loading to investigate and model in a rigorous way, and then continue to another aspect of the problem, it is highly unlikely that such an approach will produce a major new unified, consistent, and efficacious theory of cumulative damage in composite laminates for engineering purposes. In the present case, then, it was decided to attempt to construct a framework, a lattice of rational rigor and sound physical philosophy into which the intricacies of more precise representations, physical insights, and mathematical sophistication can be subsequently interwoven as better understandings of the physical phenomena involved are developed. The modeling effort which is described in the following pages is entirely a result of this commitment to a general approach. Since the scientific and engineering community is at a very early stage of development of an understanding of the behavior of composite laminates under cyclic loading, and a great number of questions regarding the strength, stiffness and life of laminates under those conditions are presently unanswered, the penalty of initial imprecision of such an approach will certainly be evident in our results. However, if we are (as we believe) successful in establishing a valid, general approach to the mechanistic description of cumulative damage under the arbitrary cyclic loading modes and loading histories mentioned above, then it is reasonable to expect that a strong foundation has been laid for the construction of a rigorous general philosophy for the anticipation of residual response of such laminates under a variety of practical situations with an acceptable amount of precision.

From our conceptual definition of the problem at hand, the following specific requirements of the modeling effort can be stated:

- It is required that the models be mechanistic, i.e., that they be based on mechanisms which are defined by generic damage modes and failure modes.
- It is required that models be developed at the engineering level in such a way that a minimum amount of phenomenological characterization of material systems can be used to anticipate the behavior of various laminate configurations under arbitrary loading conditions.
- It is required that models be based on measurable parameters which can be used to characterize the development and current state of damage in a composite laminate so that an assessment of the current condition and anticipated behavior of a given specimen can be made based on measurements of immediate physical characteristics (in contrast to statistical predictions of group behavior based on statistical sample characterization).
- It is required that a definition of "equivalent damage states" be established so that cumulative damage under arbitrary load spectra can be correctly assessed.
- It is required that the models form a basic framework based on a single philosophy which has at least two primitive characteristics: a. the framework must be constructed in such a way that representations of individual events (damage modes, etc.) can be removed and inserted as understandings of those

events allow, b. the framework must be constructed in such a way that it can be easily translated into operational codes which allow engineers to use the philosophy in a direct and straightforward way for initial design and subsequent inspection interpretations.

With the basic problem and specific requirements stated above in mind, we are now prepared to describe in more detail the approach that was taken to the present modeling effort.

2. Approach

There are three basic elements of the approach we have used to solve the problem defined above. These will be outlined below. Each of them will be discussed in some detail in subsequent sections. The basic foundation of the present approach, and the fundamental contribution of the present modeling effort, is the concept that damage caused by the cyclic loading of composite laminates develops into characteristic (generic) patterns which can be used as the basis for a mechanics analysis (of the damage state) that is sensitive to local stress redistributions, and which can, in turn, be used in a philosophy that predicts the remaining strength, stiffness and life of the laminates.

There are three basic elements of this approach:

- (a) Fatigue is, by definition, a cycle-dependent process of micro-damage events which collectively influence the strength, stiffness, and life of materials and engineering components. In composite laminates subjected to cyclic tensile and compressive load excursions, that process generally consists of discreet

events which are peculiar to the properties of the individual plies of the laminate, their geometry and stacking sequence. Examples of such events are matrix cracking, debonding, delamination, and localized fiber fracture. One of the major peculiarities of fatigue damage development in composite laminates is the fact that many of these events occur in specific plies or groups of plies of the laminate while other plies remain virtually unaffected and uninvolved throughout most of the fatigue life. Hence, the first basic element of our approach to the cumulative damage modeling process is to identify those plies which are actively involved in fatigue damage development as "subcritical elements," so defined because of the fact that while the degradation of those elements may contribute to a reduction in stiffness and residual strength, those degradation processes are not life limiting in the sense that they cause fracture of the specimen or engineering component on the occasion of their occurrence. The degradation of these subcritical elements will be handled in a special way. The physical events that are associated with that degradation will be modeled mechanistically using the discipline of mechanics. The consequence of those events will be judged on the basis of the results of that modeling process.

- (b) The second basic element of our approach is a direct consequence of the reasoning behind the first. As mentioned above, during fatigue damage development in composite laminates it is common for certain elements of the laminate to be relatively unaffected

and uninvolved in the progressive fatigue damage process. However, when these elements do sustain significant damage and subsequently fail, that event causes the fracture of the specimen or engineering component and defines the life. In that sense, those elements are "critical." As we will describe in detail, it happens that the number of types of damage and combinations of damage (damage modes) that are involved in the damage development process in subcritical elements is large, while the number of critical elements and the processes of degradation in the failure of those elements is quite small by comparison. Since any strength or life model must involve some phenomenological input, we choose, as the second basic element of our approach, to describe the degradation of critical elements in a laminate by phenomenological relationships established experimentally as basic input.

- (c) The third basic element of our approach to the cumulative damage modeling effort is the choice of a basic operating scheme which can be used to perform a summation of the effects of various fatigue loading spectra and micromechanical processes on the residual properties of the laminates.

For this scheme we have chosen a generalized equation expressed in normalized form which represents the incremental reduction in normalized residual strength as a function of increments of cyclic load application. The equation includes terminology which accounts for the internal stress states that are created by damage events in the subcritical elements as

modeled by the mechanistic concepts appropriate for each of the damage modes. The equation is arranged in such a way that it provides a generalized receptor for the input of the various models of individual microdamage events in such a way that variable spectra of loading can be easily accommodated. In that context, it should be mentioned that the equation is arranged in such a way that equivalent damage is defined by equivalent reduction in strength. The summation of damage is actually carried out by a numerical integration process but the operation itself is extremely simple and lends itself nicely to convenient coding for engineering use.

3. Fundamental Formulations

The approach taken to modeling cumulative damage in composites is to model the internal stress redistributions that are associated with the damage mechanisms observed, and to anticipate residual strength when these internal stress states are associated with failure criteria identified by observed failure modes. The life of the specimens (or components) is predicted by associating the rate of strength reduction with the remaining difference between the loading level and the current strength level, using observed damage rates to establish interim strength reduction rates. Life is determined simply as the coincidence of the residual strength curve with the applied load level--actually life is the locus of those coincidences. Hence the general scenario is to observe the damage and damage rates associated with generic loading types, model the appropriate micromechanisms associated with that

damage, and predict the remaining residual strength and life for a given situation.

Some of the damage modes which can be observed during the fatigue loading of a laminate with off-axis plies are illustrated in Fig. 1. The slope of the representative damage curve is the damage rate. There are numerous damage modes which develop in a multitude of combinations depending upon loading level and mode, orientation of plies in the laminate, and specimen or component geometry. Since the engineer will not, in general, wish to make laboratory investigations of microdamage in each component in order to establish residual properties, it is necessary to establish some means of nondestructively measuring the degree of damage development in an arbitrary laminate for which the applied load history is unknown. Change in stiffness is used for that purpose in the model. The association between damage, stiffness change, and residual strength is illustrated in Figs. 2 and 3 for laminates under tension-tension fatigue. As discussed in the previous section, experimental observations show that matrix cracks develop in off-axis plies early in the loading history (stage I) accompanied by an initial but small change in laminate stiffness and strength. Fiber fractures also develop near the matrix cracks in stage I but they are thought to be inconsequential to our modeling process. As the cracks couple along ply interfaces to form delaminations (stage II), stiffness and strength change only slightly. As advanced damage states develop, (stage III) and large delaminations and interfacial cracks form throughout the laminate, the rate of stiffness change and strength degradation increase markedly. Thus, stiffness changes are nondestructive measurements which are directly related to the microdamage and attendant reduction in

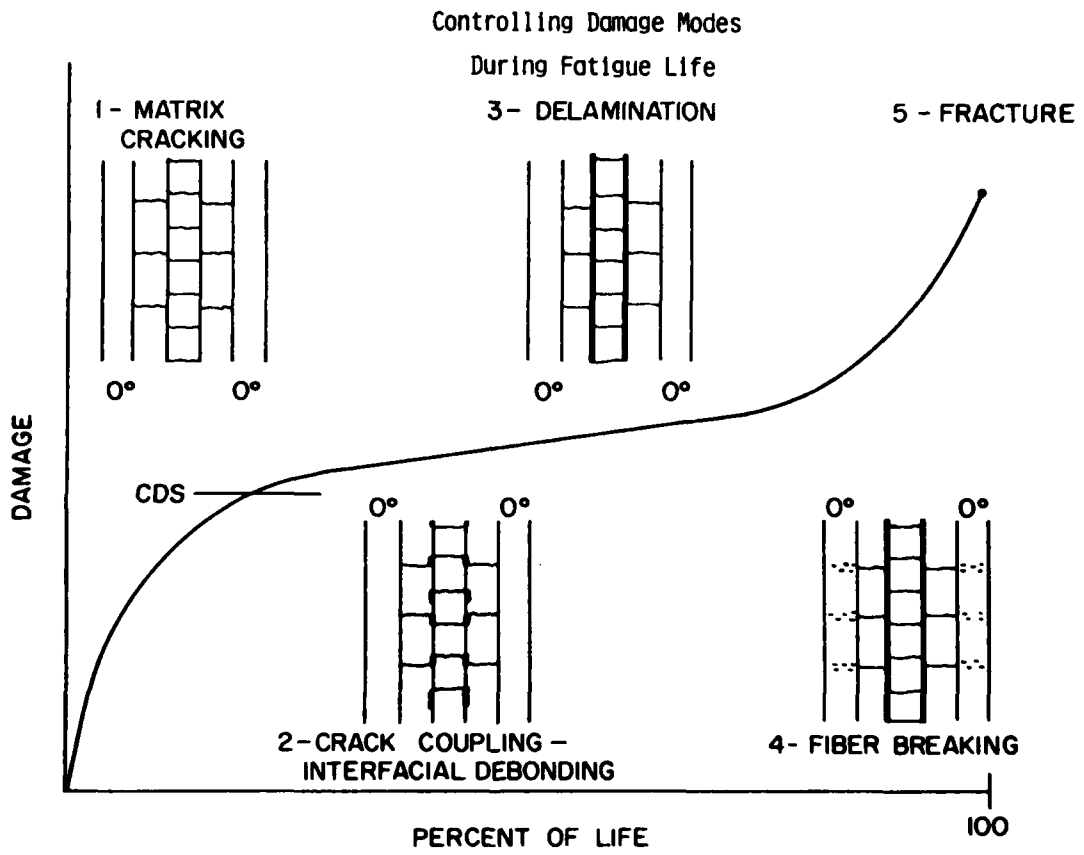


Figure 1: Damage Modes During Fatigue Loading of Composite Laminates

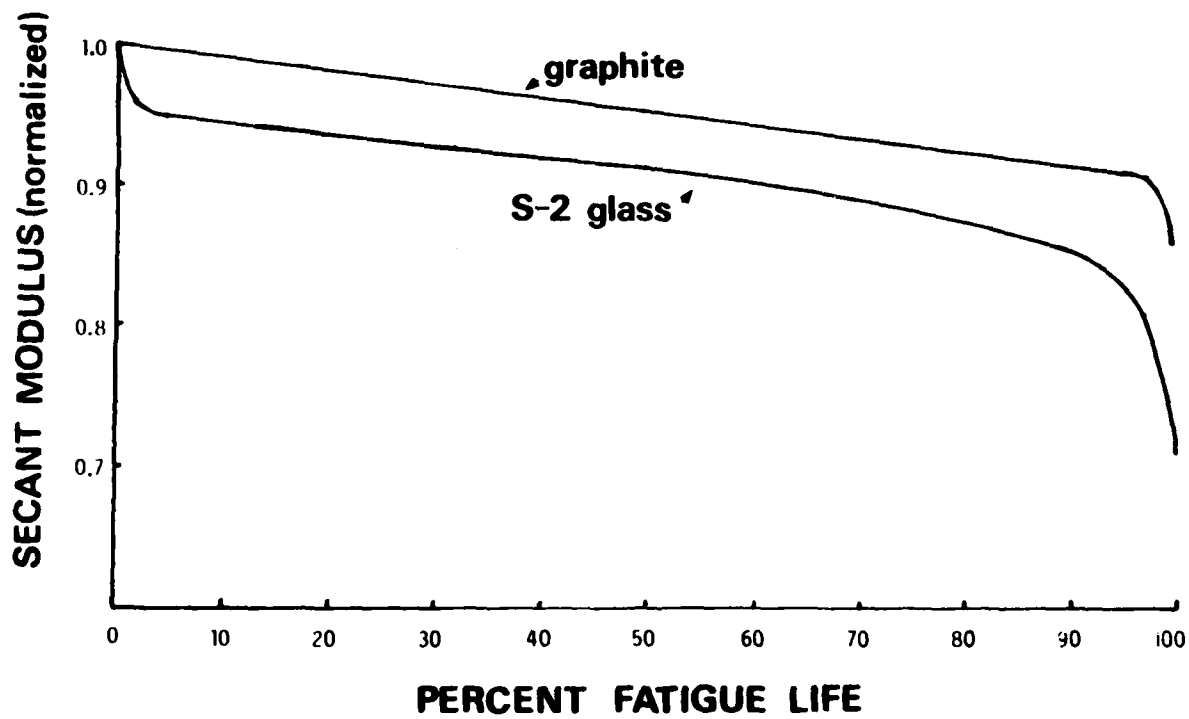


Figure 2: Longitudinal Young's Modulus Reduction for a $[0/45/-45/0]_s$ Graphite Epoxy Laminate Cycled at 85% of the Static Ultimate Strength, and a $[0/90_2]_s$ Glass Epoxy Specimen Cycled at 60% of the Static Ultimate Strength

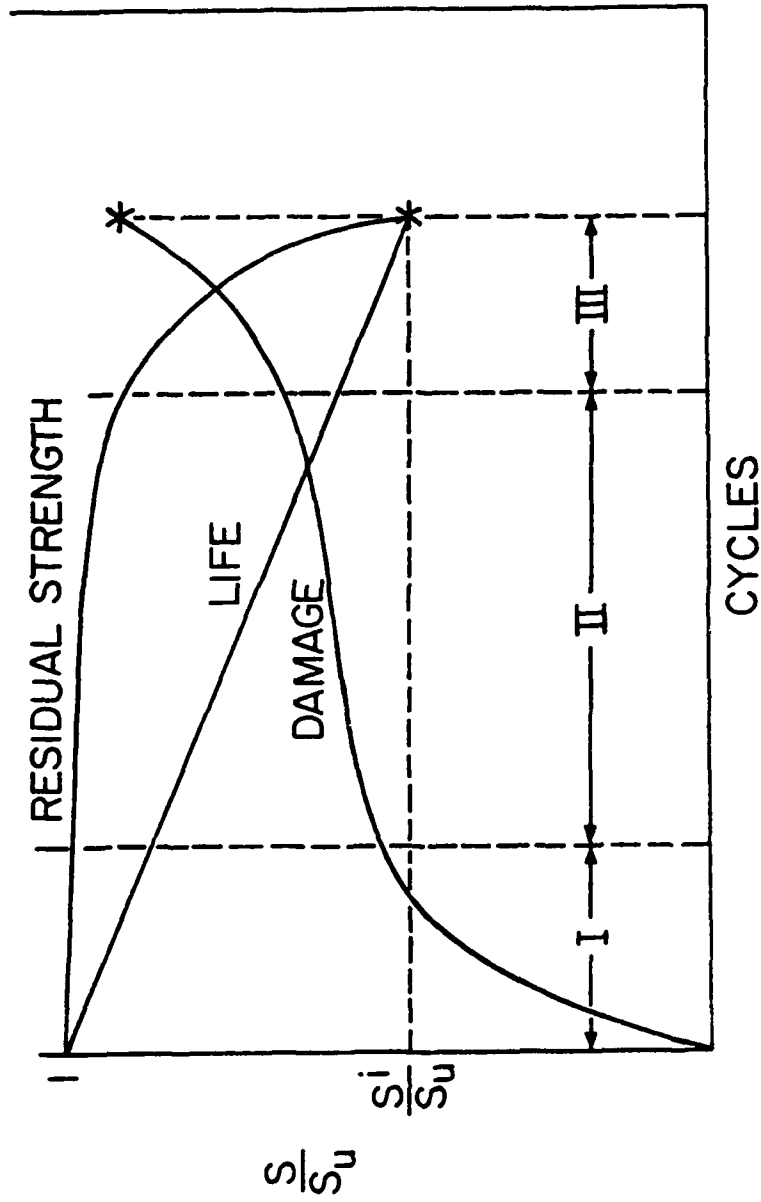


Figure 3: Schematic Diagram of Regions of Damage Development for Composite Laminates

residual strength. Furthermore, stiffness changes are directly related to internal stress redistributions since the same damage events produce both effects in proportion. Details and examples of stiffness change and stress redistribution due to the various damage modes are included in Ref. [1].

In contrast to the complexity of the damage modes, there are relatively few failure modes. For example, under tensile loading, the zero degree plies (or nearest-on-axis plies) are responsible for the residual strength and life of composite laminates regardless of the complexity of damage that develops in the off-axis plies during fatigue loading. Although one may change the stacking sequence and, therefore, the general nature of matrix cracking, delamination, and debonding throughout a fatigue test, the final fracture event is still controlled by the zero degree plies. In this case, the failure can be modeled using an appropriate failure theory, such as Tsai-Hill, applied to the zero degree plies. For laminates subjected to compression-compression or tension-compression loading, the 'failure' may be due to buckling instability enhanced by delamination. The delamination that occurs is used to anticipate the remaining buckling resistance of the laminate by altering elements of the bending stiffness matrix and using the new stiffness values in an appropriate buckling criterion.

Based on the observations, the cumulative damage model is constructed on the basis of critical and subcritical elements. Critical elements are, quite simply, the parts of a composite laminate which control the strength and life of that laminate. Subcritical elements are the remaining parts of the laminate which, although they may be severely damaged during a fatigue loading situation, do not cause

failure of the laminate, per se, but rather introduce stress redistribution in the laminate which influences the strength or life indirectly. This philosophy affects the model in two ways. First of all, it incorporates into the cumulative damage modeling process the concept of internal stress redistribution at the micro level due to the formation of damage in off-axis plies (subcritical elements). And second, it influences a major decision regarding the phenomenological input into the model. All strength and life models must include some phenomenological information, but it is desirable to maintain an absolute minimum of complexity and uncertainty associated with that input. The fatigue behavior of the critical elements in each laminate is represented phenomenologically, and the fatigue damage that is observed in the other plies or elements of the laminate is accounted for by stress redistribution as determined from models of the mechanics of those damage processes and of the resultant micro stress fields.

Before continuing on to the detailed results, we will discuss the third major element of our model. As we have mentioned earlier, we have chosen to introduce a generalized equation expressed in normalized form which computes the incremental reduction in normalized residual strength as a function of the increments of cyclic load application. We shall call this equation the generalized summation equation. The motivations for constructing and using such an equation include the need for a conceptual generalization of the complex processes involved, and a need for a unified computational approach which was compatible with and amenable to computer coding.

The rationale behind the generation of that equation can be understood by examining some simple fatigue concepts. We begin with

Fig. 4, which is a schematic representation of some of the basic relationships for laminate fatigue behavior. We imagine that this representation is essentially one-dimensional, i. e., that the residual strength, S_r , and the life locus represent laminate values determined from unidirectional loading. The residual strength curve can be written in terms of the applied stress, S_a , as shown in Eqn. (1) where i is a parameter introduced to accommodate the nonlinearity in the residual strength reduction curve.

$$S_r(n) = 1 - \left(1 - \frac{S_a}{S_u}\right) \left(\frac{n}{N}\right)^i \quad (1)$$

where $\frac{n}{N}$ = life fraction

It is further assumed that the applied stress amplitude, S_a , is constant throughout the test. The residual strength, S_r , is a function of the number of applied cycles.

We have indicated that the modeling approach that we have taken is based on a phenomenological characterization of the critical elements in the laminate, and not on the laminate itself. Hence, the next step in the construction of our generalized summation equation is to consider the fatigue behavior of the critical elements, as schematically indicated in Fig. 5. Since these critical elements are imbedded within a laminate, and since, as we have emphasized, the internal stress state is constantly changing as damage develops in the subcritical elements causing internal stress redistribution, the applied stress, S_a , is no longer constant as a function of the number of cycles. Since it is a variable, we cannot simply multiply all of our terms in a degradation equation by the ratio of applied cycles to life, the so-called life fraction. Instead, an equation such as (2) is more appropriate.

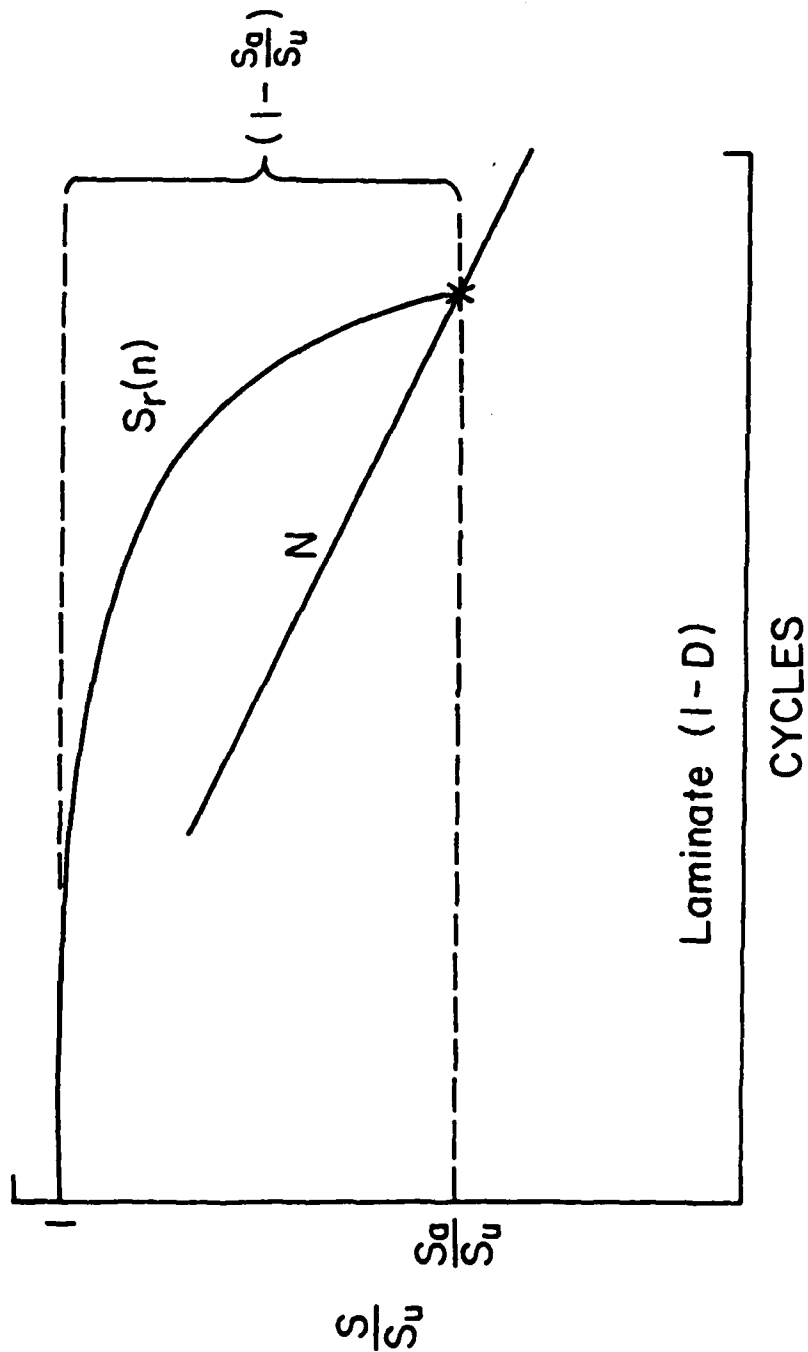


Figure 4: Schematic Diagram of Laminate Strength Reduction-Life Relationship

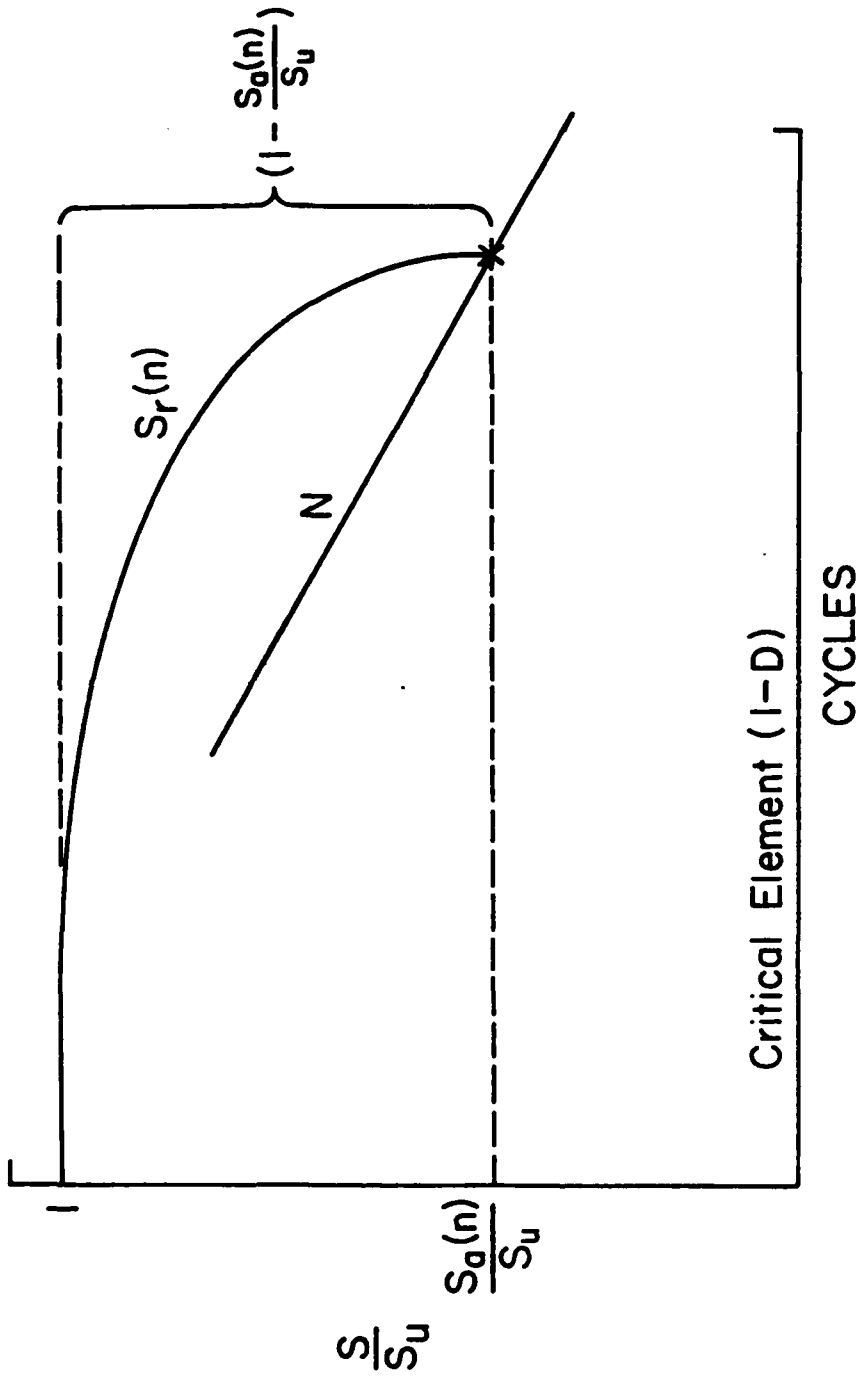


Figure 5: Schematic Diagram of Critical Element Strength-Life Relationship

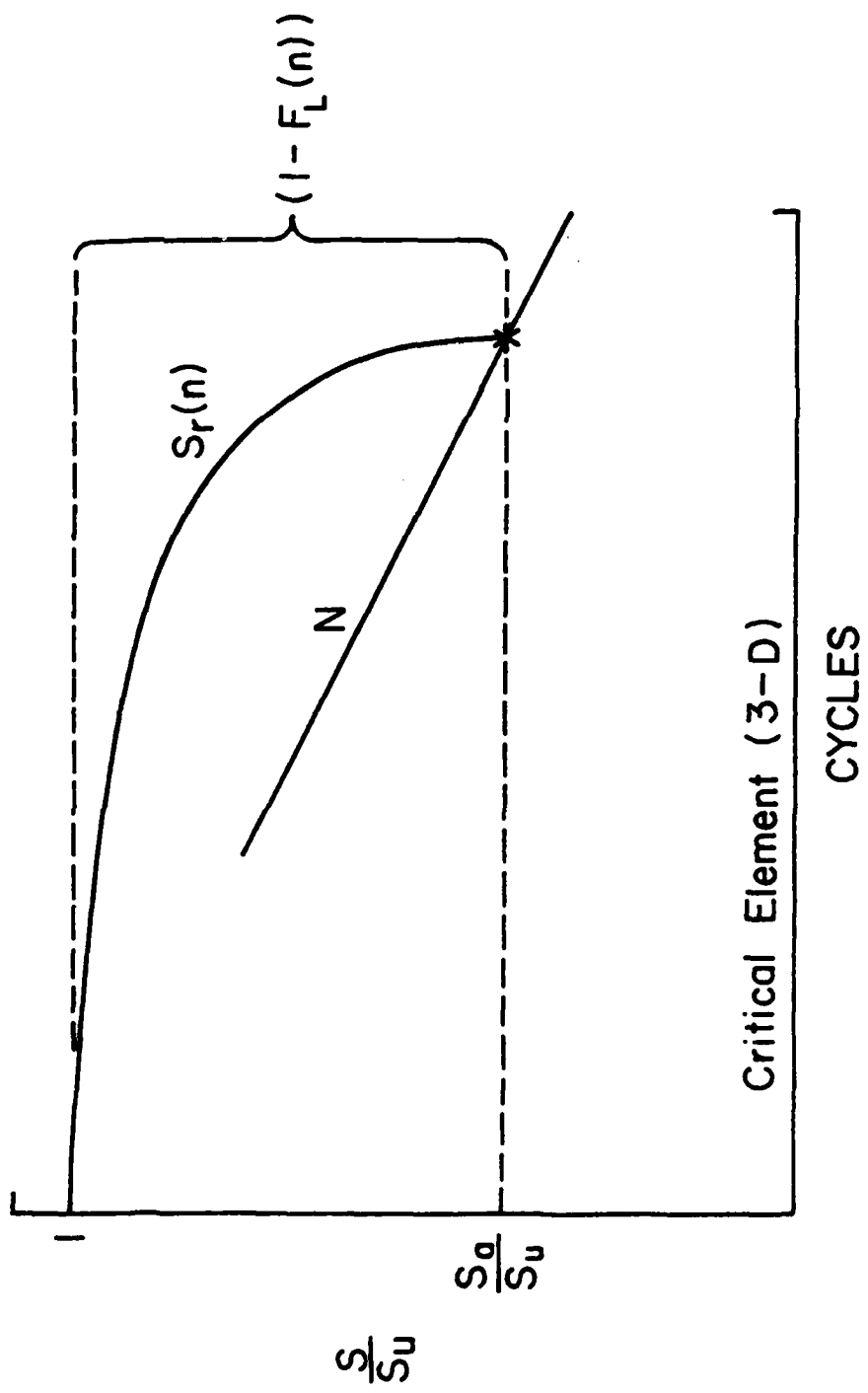


Figure 6: Schematic Diagram of Critical Element Strength-Life Relationship for Three Dimensional Formulation

$$S_r(n) = 1 - \int_0^{\gamma} \left(1 - \frac{S_a(n)}{S_u}\right) i \left(\frac{n}{N(n)}\right)^{i-1} d\left(\frac{n}{N(n)}\right) \quad (2)$$

where γ = specific value of $\frac{n}{N}$

Here it should be noted that the integrand is a function of the number of applied cycles, not only because of the variation of the applied stress on the critical element, S_a , but also because of the fact that the life that is calculated from a given applied stress (from the equation which fits the phenomenological data for the critical element) is also a function of the number of applied cycles, i. e., N is a function of n .

The last major item to be added to our derivation incorporates the reality that the stress state of the critical element is almost never one-dimensional. Since it is imbedded in a laminate, the internal stresses are generally predominantly two-dimensional, and occasionally three-dimensional. In order to correct our model for that fact, we introduce a local failure function, F_L , to replace the local applied stress ratio, S/S_u . This local failure function is unspecified at this point, except to the extent that it must represent the tendency for the internal stress state in the critical elements to cause failure of those elements. There is an obvious relationship between the concept behind the local failure function and the familiar "failure theories" introduced by a variety of investigators such as Tsai-Hill, Tsai-Wu, and others. For this refinement, Eqn. (2) becomes Eqn. (3), the final form of our generalized summation equation.

$$\Delta S(n) = \int_0^{\gamma} (1 - F_L(n)) i \left(\frac{n}{N(n)}\right)^{i-1} d\left(\frac{n}{N(n)}\right) \quad (3)$$

This equation functions by producing a normalized residual strength estimate (a fraction of the static ultimate strength) as a continuous function of loading history indicated by the number of cycles of load application, n . The equation produces that estimate by integrating and convoluting the influence of two fundamental types of microdamage development consequences. This formulation reflects the opinion of the investigators that fatigue damage in composite laminates can generally be discussed in terms of microevents which occur in "non-critical" elements of the laminate (events that influence the degradation of the laminate primarily by internal stress redistribution and adjustment of geometry), and microevents which act directly on "critical elements" (elements which control the final fracture of the laminate). Rather than attempt to provide an elaborate and complex discussion of the various nuances of this equation in this document, two scenarios will be briefly described in order to demonstrate its use.

The first scenario is based on tension-tension fatigue loading of an angle ply laminate which is constructed in such a way that no significant edge delamination occurs. The various terms in Eqn. (3) are identified in Fig. 7. We will discuss the figure from right to left. The life locus described by the function N is a phenomenological representation of the life of the critical element, taken to be the 0 degree plies in this case. The equation is written as a function of the applied unidirectional stress, $S(n)$, normalized by the ultimate strength of the element, S_u . The material constants, A , B , and C , are determined by fitting the data obtained from fatigue testing of unidirectional material of the type from which the laminate was constructed. Since, in this case, we are concerned only with the unidirectional performance of

Tension-Tension

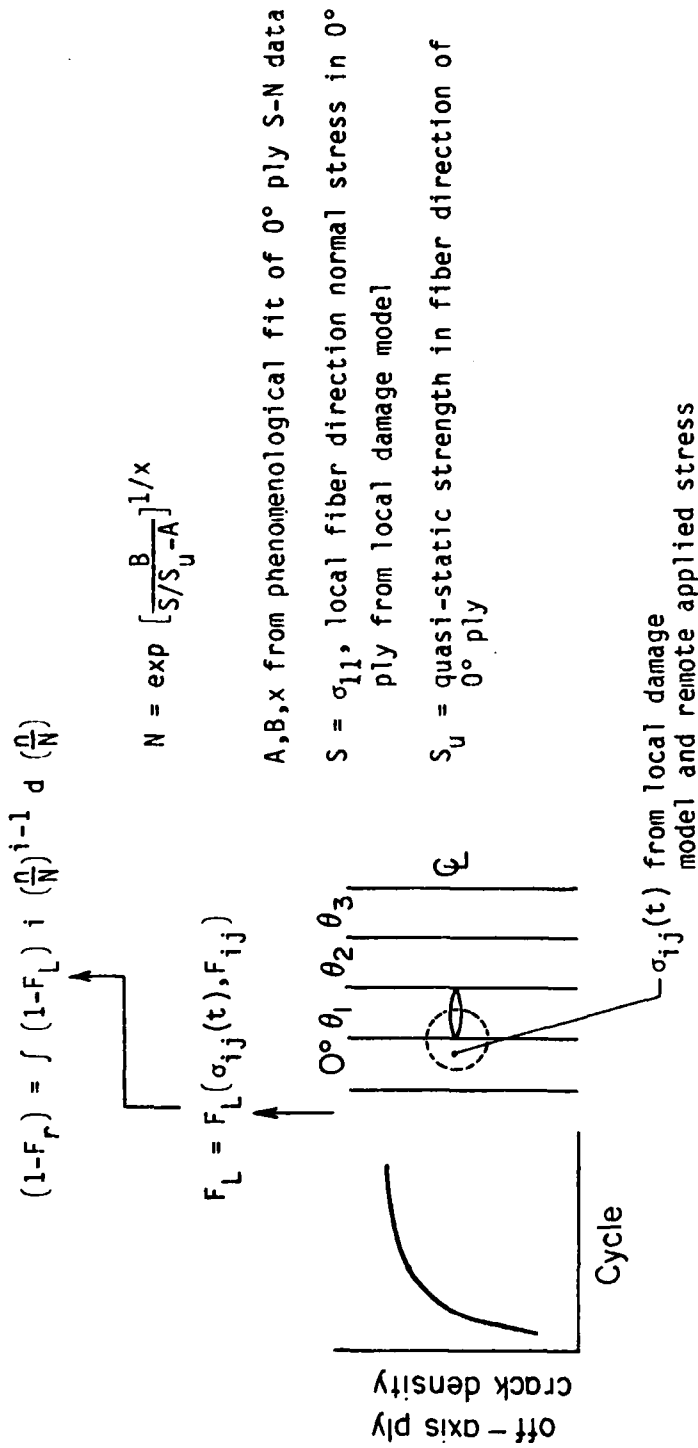


Figure 7: An Example of the Interpretation of Terms in the Summation Equation for Tension-Tension Constant Amplitude Loading

the 0 degree plies, (the critical elements) one such relationship will suffice for all laminates regardless of their construction (stacking sequence, etc.). Since it is recognized that the 0 degree plies in the laminate may carry different amounts of the total load as the damage development in noncritical elements redistributes stress and alters internal geometry, the applied stress on the critical element, $S(n)$, is stated as a continuous function of the number of applied cycles, n . It should also be mentioned that the local internal applied stress, $S(n)$, can be determined from measurements of changes in laminate stiffness which the authors have found, by experience and through a number of mechanics models (1,2,3), to be related to internal stress redistributions.

The choice of variable of integration, $\frac{n}{N}$, is important since that variable is a continuous function, even in circumstances when the applied loading spectrum is continuously varying in time. Hence, the damage accumulation Eqn. (3) can be used to determine the effect of cumulative damage under spectrum loading. The parameter i in Eqn. (3) is a material parameter which is associated with the nonlinearity of degradation (sometimes referred to as a tendency for sudden death) in composite laminates, and is also obtained from curve fitting of data. However, that constant generally has a value close to unity and does not appear, at this writing, to be a function of the construction of the laminate.

Continuing to move to the left in Fig. 7, the term in parentheses determines the total amplitude of allowable strength reduction, the sense that the laminate is expected to fail when the laminate strength (determined from the computation achieved by the equation) is reduced to

the level of the normalized failure function, $F^L(n)$. The failure function for the critical element, the 0 degree plies in this case, can be taken to be any of the typical phenomenological characterizations of strength computed at the load level. However, it is especially important that the stresses that enter into such an equation may be functions of n since internal stress redistribution will generally change the local stresses that cause failure of the critical element. Hence, the first term in parentheses in Eqn. (3) is also altered by the microdamage that occurs in subcritical elements causing internal stress redistributions and changes in internal geometry. Those changes are, as mentioned earlier, detected and interpreted based on stiffness changes in the scenario described. The choice of the failure function (and indeed a choice of the critical element) is dependent upon an anticipated failure mode of the laminate itself. This anticipation must be based on prior experience or guiding experiments. When the integral is performed, a normalized change in residual strength is produced as a function of the applied cycles, n , as indicated on the left of the equation shown in Fig. 7.

For load spectra which include compression excursions, other micromechanical models are used to provide input to the damage accumulation equation. The choice of approach in each case is controlled by the failure mode that is appropriate for the dominant damage development mode or modes. When failure involves buckling (as a consequence of delamination for example) the failure function may take the form of stiffness ratios. Since stiffness is the only material property which appears in stability equations, it is not surprising that such a parameter seems to provide a good representation of the

compression-controlled behavior. Some of these results were discussed in earlier reports.

Regardless of the micromechanical model that is used to represent the prefracture damage patterns, the scheme for application of the damage accumulation equation is unchanged, a fact that makes application of the model in computer coded form very convenient. A conceptual flow chart of the application scheme appears in Fig. 8.

It may also be instructive to examine the proper equations, configuration, and application scheme for the present model in the case of self-similar crack propagation in the sense normally identified with single crack dominated fatigue damage in homogeneous materials such as metals. In the present case, this particular type of formulation is needed to treat the case when delamination propagates in a self-similar fashion as is sometimes the case for edge-initiated delamination, especially for tension-compression loading. In order to demonstrate the form of the model in that case, we consider the instance when the crack-opening mode dominates the delamination propagation. We also assume that adequate stress analysis is available so that the crack-opening normal stress can be identified; that normal stress is used in the equations below. If the mode I toughness of the material interface involved is K_{Ic} , then it is possible to define an initial flaw size, a_0 , which corresponds to the initial strength (the tensile ultimate strength for the corresponding stress state) according to the equation

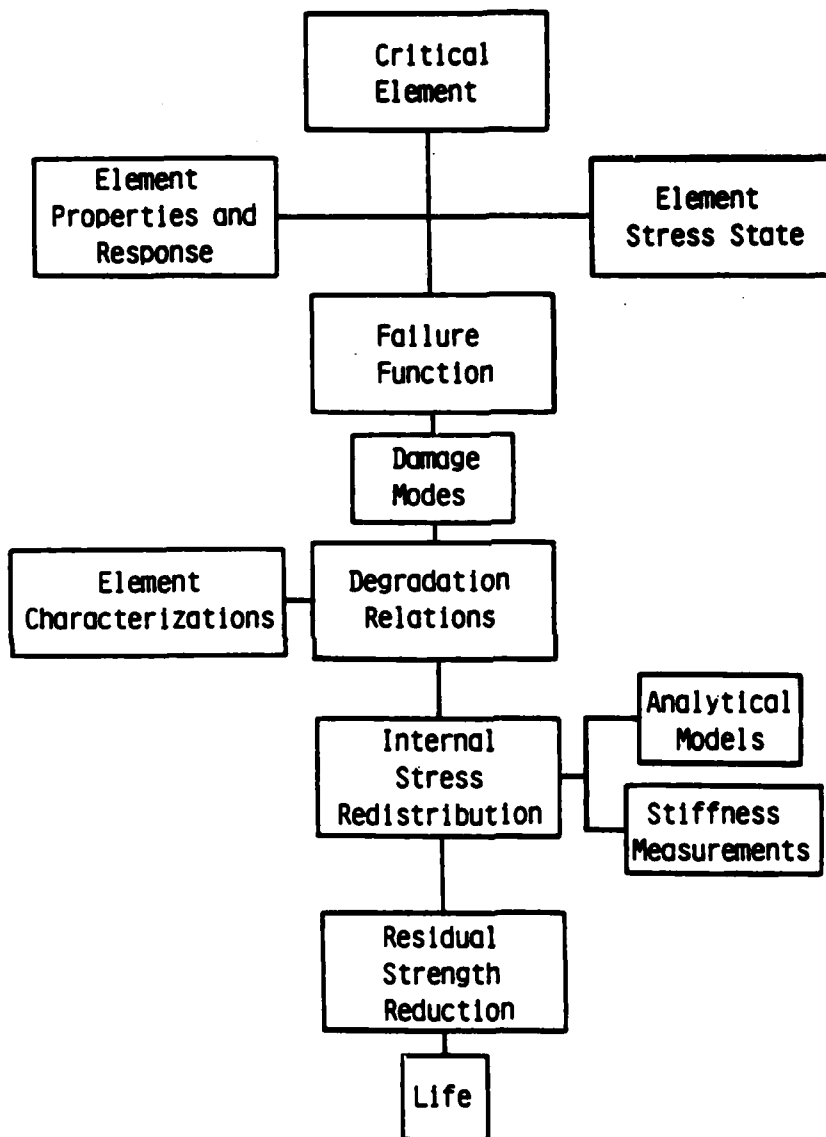


Figure 8: Conceptual Flow Chart of the Damage Accumulation Model

$$K_{IC} = \sigma_i \beta \pi a_0 = \sigma_i = \frac{K_{IC}}{\beta \pi a_0} \quad (4)$$

σ_i = initial strength, β = geometry factor

a_0 = initial flaw size

If the applied stress level is maintained at a constant amplitude, it is also possible to calculate a critical crack length for the current level of applied stress, σ^a , using the same relationship as stated in Eqn. (4).

$$K_{IC} = \sigma^a \beta \pi \frac{a}{c} \quad \sigma^a = \frac{K_{IC}}{\beta \frac{a}{c} \pi} \quad (5)$$

σ^a = current applied stress level

a_c = critical crack length for the current applied stress level, σ^a

Hence, the damage summation equation stated earlier takes on the form shown in Eqn. (6).

$$(1 - F_r(n)) = \int_0^1 \left(1 - \frac{a_0}{a_c}\right) i \left(\frac{n}{N}\right)^{i-1} d\left(\frac{n}{N}\right) \quad (6)$$

It should be noted in this equation that the critical crack length for the current applied stress level is constant only if the applied stress σ^a is constant. In instances when the global stress state is nonuniform or in other situations where the crack-opening normal stress varies as a function of the number of applied cycles, the current

critical crack length is not constant and must enter Eqn. (6) as a variable.

The life locus represented by N in Eqn. (6) is obtained by integrating equations which represent crack propagation rate data as a function of the applied field stress intensity. An example of such an equation is given below.

$$n_1 - n_0 = \frac{2}{\beta^2 \pi C (1-R)^2 \sigma_{\max}^2} \left[\frac{K_C}{K_0} - \frac{K_C}{K_I} - \ln \frac{K_I}{K_0} \right] \quad (7)$$

$$R = \sigma_{\min} / \sigma_{\max}$$

K_0, K_I, K_C = initial, final and critical field stress intensity

C = a material constant

In the instance when cycling continues until final failure the current number of cycles, n_1 becomes the total life, N , and the current field stress intensity K_I becomes the critical field stress intensity, K_C . If the initial number of cycles, n_0 , is zero, Eqn. (7) reduces to Eqn. (8).

$$N = \frac{2}{\beta^2 \pi C (1-R)^2 \sigma_{\max}^2} \left[\frac{K_C}{K_0} - 1 - \ln \frac{K_C}{K_0} \right] \quad (8)$$

In that equation, the initial field stress intensity K_0 is assumed to correspond to the initial flaw size, a_0 introduced in Eqn. (4). Since the life specified by Eqn. (8) depends on the maximum stress amplitude, σ_{\max} , if spectrum loading is applied to the specimen so that

the applied stress is a function of time or number of cycles, the life locus becomes a function of the variable of integration in Eqn. (6). This complication is easily handled by numerical integration schemes. Hence, for self-similar crack propagation we see that Eqn. (6) can be used to predict the residual strength in a very straightforward and familiar way. It should also be noted that the crack lengths a_0 , a_c , etc. can be associated with other damage zone dimensions in the instance when single, planar, self-similar cracks do not form but a localized damage zone grows in length instead. Such an interpretation may indeed be appropriate for several situations encountered in notched materials.

Having examined various forms of the model and the basic premises involved, we will now describe some of the detailed results obtained from application of the model to tension-tension, tension-compression, and compression-compression loading, as well as to block loading and variable R loading situations.

4. Detailed Results

A. Tension-Tension Loading

The mechanistic cumulative damage model that has been developed will be demonstrated in the following section by examples. Because of the basic nature of the model and of the data to be represented, the section will be divided into three major discussions. The first of these discussions will address the application of the model to tension-tension (T-T) loading situations. The second major discussion will focus on the application of the model to tension-compression (T-C) loading situations for which the cyclic load is completely reversed

($R=-1$). The third major discussion will be concerned with more general situations for which the tensile and compressive load amplitudes are unequal, and for which changes in amplitude during a given test (block loading) are considered. The logic of this presentation is to move from the simplest most basic application and demonstration of the model to more complex, more realistic, and more general applications. This same presentation concept will also be used in each of the major discussions in the sense that situations which require only rudimentary aspects of the model for successful description will be discussed before those requiring various refinements of the model which are introduced in order to describe more complex and sophisticated aspects of the fatigue behavior under discussion.

We begin, then, with a simple discussion of the tension-tension loading case for which Eqn. (3) is interpreted as indicated in Fig. 7. It should be recalled that the residual strength, F_r , and the local failure function, F_L , are both normalized quantities so that an undamaged residual strength would correspond to a F_r value of unity and incipient failure would correspond to a value of F_L of unity. As mentioned earlier, the power of the degradation ratio, i , is a parameter which is determined by the laminate tendency to demonstrate "sudden death", a behavior whereby the residual strength remains unchanged through a large fraction of the total life of the specimen and drops precipitously just prior to fracture. While some variations in that parameter will be introduced for demonstration purposes, it should be mentioned that ultimately a constant value of i equal to 1.2 was used throughout this entire research program for all computations.

It is assumed in Fig. 1 that the critical elements which define the residual life and strength of the laminates to be considered are the zero deg plies since that was in fact the case for all six laminates considered in this program. Hence, the phenomenological characterization of S-N behavior used in Eqn. (3) is taken to be a somewhat idealized form of the fatigue behavior of the zero degree plies. Actually, this characterization of fatigue behavior should be obtained under the two- or three-dimensional stress state that is appropriate for each of the laminates in which the zero degree plies are tested. However, since recovering such data would essentially require testing all laminates, and such a practice would preclude any predictive information obtained from the model, a single one-dimensional phenomenological characterization was assumed to be adequate for all cases. Hence, it is only necessary to establish that single relationship for the zero degree plies in order to predict the residual strength and life for all laminates made from that material for which the critical elements are zero degree plies. Moreover, since the object of this research project was to establish a philosophy rather than become engrossed in the nuances of data representation, a further simplification of the phenomenological representation was introduced; it was assumed that the parameter A was equal to unity, an assumption that is equivalent to requiring that the half cycle residual strength be equal to the ultimate strength of the zero degree plies. It was further assumed that the power, x , was equal to -1 , so that the only variable to be considered was the constant, B. Hence, one test of the applicability and validity of the present model is the extent to which the value of the constant, B, is the same for all laminates tested and modeled when

reasonable agreement between the observations and predictions are obtained. Variations of B will be introduced for demonstration purposes and illustration of its influence, but ultimately a value of 0.07 was used for all data predictions. To that extent, the model appears to have been self-consistent.

The value of the local stress, S , in the zero degree plies is obtained from models of local damage that is known to occur and from a measurable damage parameter which indicates the extent of damage development; the change in longitudinal stiffness was used as a damage parameter in the present case. We will provide more discussion of the local stress concepts below. At this point, it should be noted that the local stress which is used as an input to the phenomenological equation to calculate the expected life, N , becomes a function of the number of applied cycles, since the progressive development of damage has the effect of changing the local stress values which control the rate of degradation of the critical elements (the zero degree plies in this case) as cyclic damage develops. This local stress redistribution is due to the release of load in the plies (or regions of plies) which crack or break, and possibly also due to local stress concentrations caused by the internal geometry of cracks that form in the off-axis plies, between plies, and between matrix and fiber phases. These local redistributed stresses also enter into the computation of the local failure function, F_L , which appears in the integrand of the damage summation equation.

This stress redistribution concept is perhaps the most important central feature of the mechanics of the present modeling philosophy. The modeling of these local stress redistributions controls the accuracy

with which we are able to make predictions of strength and life. The generality of the model is greatly enhanced by the fact that all damage events beyond (the phenomenological representation of) the degradation of the critical plies for all of the complex damage modes that occur in all possible laminates are handled by stress redistribution modeling. Of course, this continues to be an area of fertile and vigorous research activity. As our understandings of the nature and consequence of local damage events improve with time these representations will improve correspondingly. In the next few paragraphs we introduce a discussion of how these local stresses are computed based on laminate analysis as a starting point for more sophisticated treatments mentioned later.

As suggested earlier, there is an early "stage of adjustment" to tensile cyclic loading which is characterized by a rapid (and rapidly decreasing) rate of damage development. For laminates which have off-axis plies, such as the common quasi-isotropic stacking sequences, this early stage involves matrix cracking, usually by the formation of matrix cracks through the thickness of the off-axis (90,+45,-45 degree) plies parallel to the fibers and perpendicular (at least in transverse projection) to the dominant load axis (the 0 degree direction). This type of transverse crack formation has received a great deal of attention and is, by comparison to other micro-events, fairly well described and understood. Formation of the cracks can be anticipated reasonably well by laminate analysis coupled with a common "failure theory" such as the maximum strain, Tsai-Wu or Tsai-Hill concepts. The prediction of the occurrence (or absence) of such cracks is, however, of relatively little consequence in the engineering sense. It is possible,

however, to anticipate the number and arrangement of such cracks, information which can be used for subsequent analysis of behavior.

Figure 9 shows the spacing between cracks in a -45 degree ply in a Type B laminate as a function of quasi-static load level and cycles of loading at about two-thirds of the ultimate strength ($R=0.1$). As one can see, cracks develop quite early in the life and quickly stabilize to a very nearly constant pattern with a fixed spacing. The same behavior occurs for quasi-static loading, in the sense that crack development occurs over a small range of load and quickly stabilizes into a pattern which has the same spacing as the fatigue crack pattern. In fact, the two patterns are essentially identical regular crack arrays in that ply regardless of load history. Similar behavior is observed for the other off-axis plies and in other laminates. We have named these crack patterns "characteristic damage states" (CDS for short) for matrix cracking in laminates having off-axis plies. The CDS is a laminate property, i.e. it is completely defined by the properties of the individual plies, their thickness, and the stacking sequence of the variously oriented plies. The CDS is independent of extensive variables such as load history and environment (except as the ply properties are altered) and internal affairs such as residual or moisture related stresses. A more thorough discussion of the CDS can be found in Refs. [1-9].

The stability of the off-axis crack pattern, the CDS, is the reason for the sudden decrease in damage rate between regions I and II in Fig. 3 and also accounts for the relatively flat nature of the damage development curve in region II. The regular crack patterns can be predicted with engineering accuracy as we show in the references just

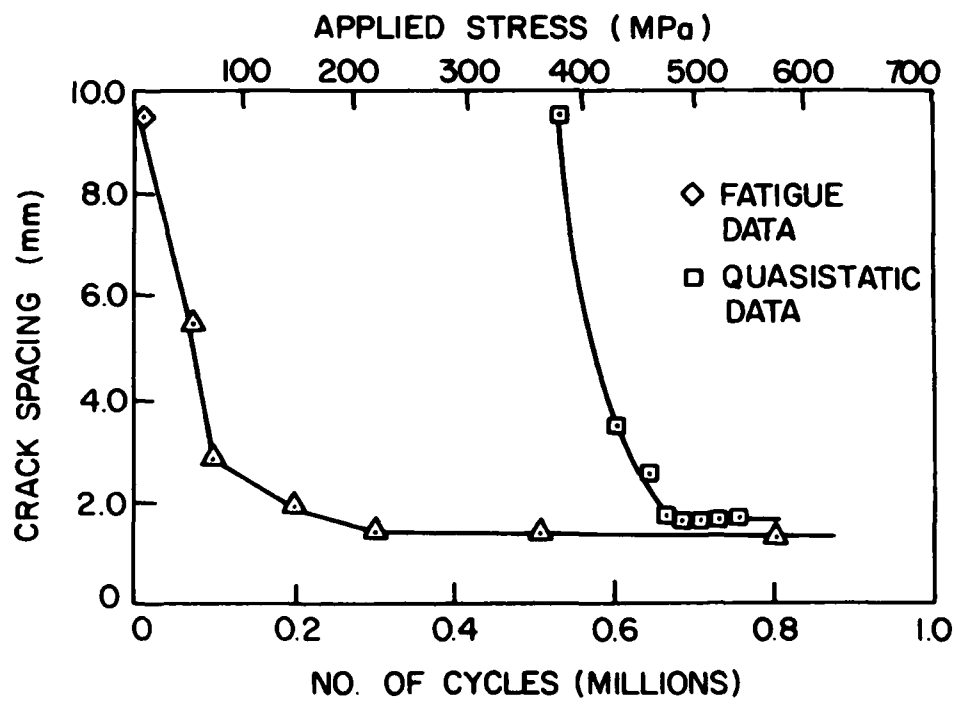


Figure 9: Crack Spacing in the -45 Ply of $[\theta/90/45/-45]_s$ Graphite Epoxy Laminates Under Cyclic and Quasi-Static Loading

noted, and the stress state in the neighborhood of such cracks can be accurately anticipated [1]. Using these predicted crack densities, the corresponding stiffness changes can be calculated. Such calculations have been made by the authors, and reasonable agreement with measured changes has been obtained [1].

The model for residual strength (and life) for cyclic tensile loading is based on the local stress state near the matrix cracks discussed above. A net section strength concept is also used based on the following argument.

When calculating the quasi-static strength of an unnotched laminate, the common scheme is to calculate the ply stresses using laminate analysis, invoke some failure criterion to predict first ply failure (usually matrix cracking), reduce the moduli in the broken ply (usually E_2 perpendicular to the fibers and the in-plane shear stiffness G), recalculate ply stresses, test for second ply failure, etc. until "last ply failure" is predicted. This scheme, commonly referred to as the ply discount method, has been widely used over a period of at least fifteen years and is known to provide good engineering estimates of laminate strength when edge effects do not dominate the failure process. Table 1 shows the stresses in the individual plies of an example laminate before and after matrix cracks form in the 90 degree and ± 45 degree plies (for which E_2 and G are then set equal to zero). The stress in the fiber direction of the 0 degree plies (which control final fracture) is increased from 2631 to 2993 MPa, a jump of 14% which is then used in a failure analysis of some type to predict the "correct" strength (if both off-axis plies fail before laminate failure). In general, failure of the off-axis plies will cause stress redistribution

Table 1.

Example: $[0,90,+45]_5$ T300-5208

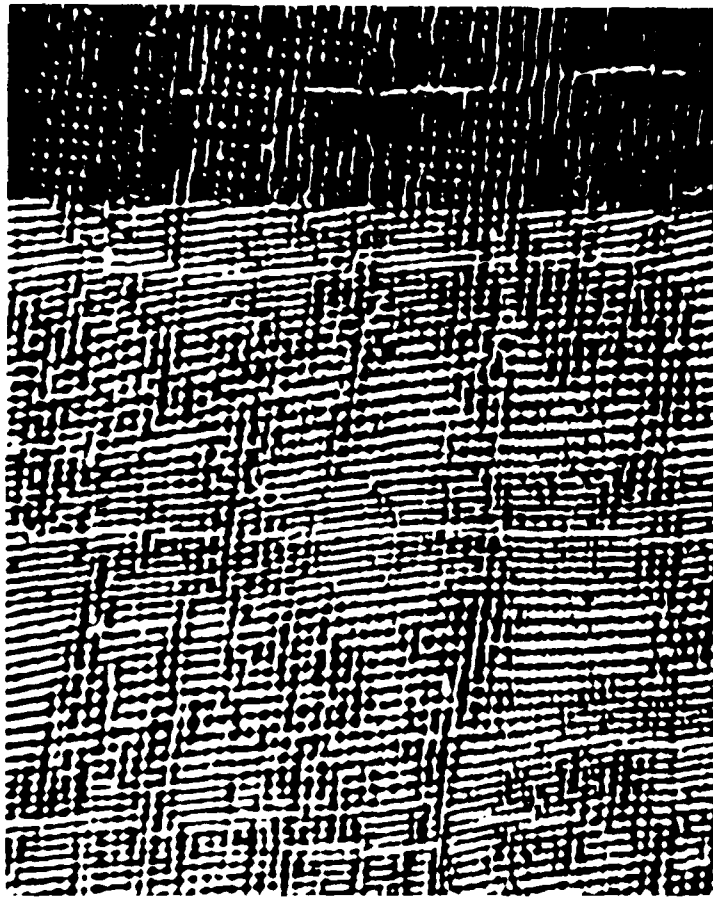
Applied stress $\sigma = 1000$

| Ply | σ_x | | σ_y | | σ_{xy} | |
|-----|------------|-------|------------|-------|---------------|-------|
| | Before | After | Before | After | Before | After |
| 0 | 2631 | 2993 | - 2.3 | - 4.7 | 0 | 0 |
| 90 | 167 | 0 | -796 | -1000 | 0 | 0 |
| +45 | 600 | 503 | 400 | 503 | 417 | 503 |
| -45 | 600 | 503 | 400 | 503 | -417 | -503 |

of this type which, based on some 15 years of literature, must be properly accounted for to predict "good" values of laminate strength.

It is easy to forget, however, that these stress redistributions (and the stiffness reductions that caused them) are not, in reality, uniform. They exist only near the matrix cracks in the off-axis plies. The first direct proof of that (to our knowledge) was provided by Highsmith and Jamison [38,39] who (with the able help of Prof. Post at Virginia Tech) constructed a very high resolution moiré diffraction device which was used to resolve strain distributions in the 0 degree ply of several different laminates in regions near cracks in adjacent off-axis plies during quasi-static loading. An example of their results is shown in Fig. 10. That figure was produced by the interference between a reference beam and a beam which was incident on a diffraction grating having about 800 lines per mm which was bonded to the specimen surface. The cracks in the off-axis 90 degree plies of the $[0,90_3]_S$ glass epoxy specimen can be seen as white horizontal bars having a spacing of about 4 mm in the original photograph. The constant displacement diffraction lines are more dense in the region of the off-axis cracks, indicating a strain concentration in the 0 degree plies which are being observed. The strain distribution between two of the cracks is shown in Fig. 11 along with strain plots from a simple one-dimensional model for three choices of the (only) parameter in that model.

Figure 12 is a general schematic representation of the situation shown in Figs. 10 and 11. The most important point to be made has to do with the local nature of the stress redistribution discussed above. The increased stresses (as discussed in Table 1) and increased strains (as



— 4.0mm.

↑
— 0.0mm.

Figure 10: Moire Fringe Pattern of a $[0/90_3]_s$ Laminate between Cracked Sections of the 90 Plies

STRAIN DISTRIBUTION BETWEEN CRACKED SECTIONS

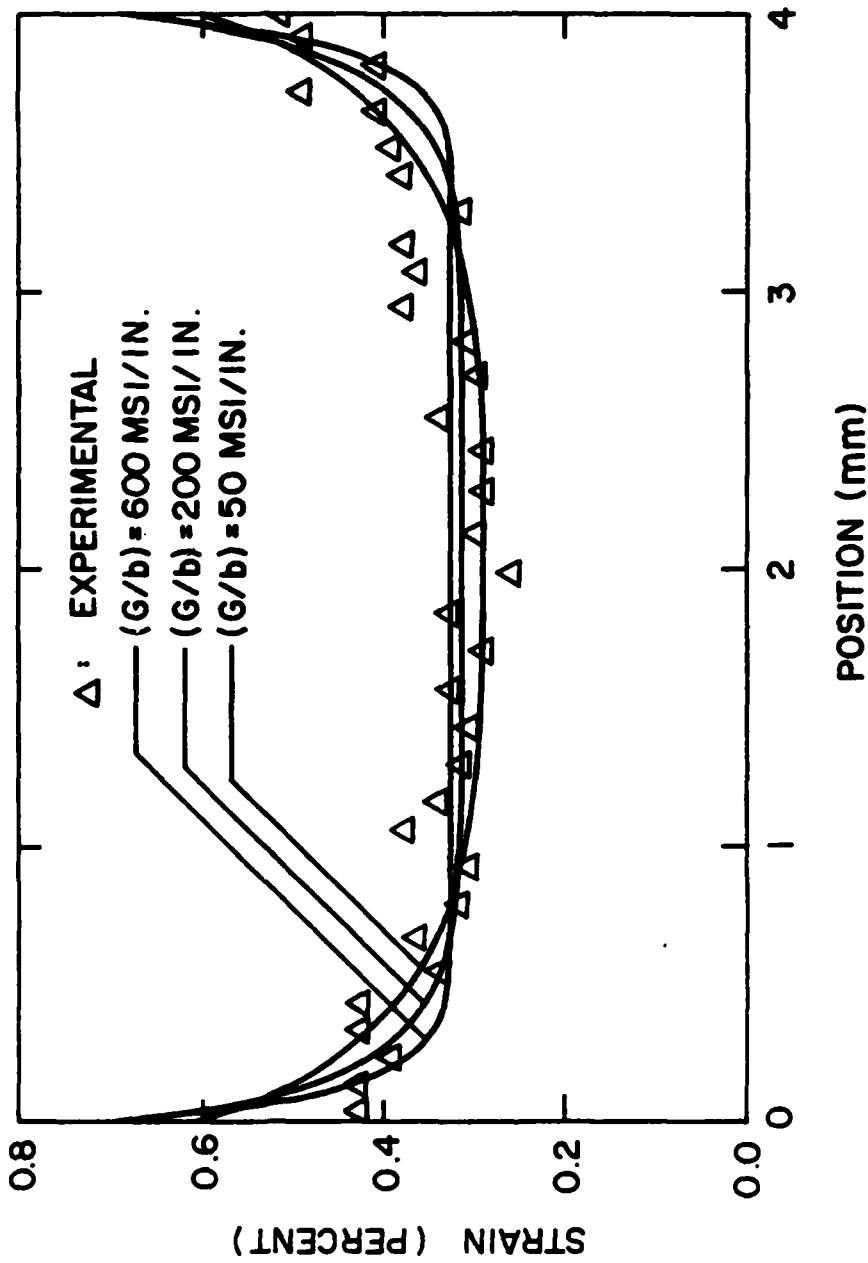


Figure 11: Predicted and Observed Strain Distributions in the \emptyset Plies of a $[\emptyset/90_3]_s$ Laminate between Cracked Sections of the $9\emptyset$ Plies

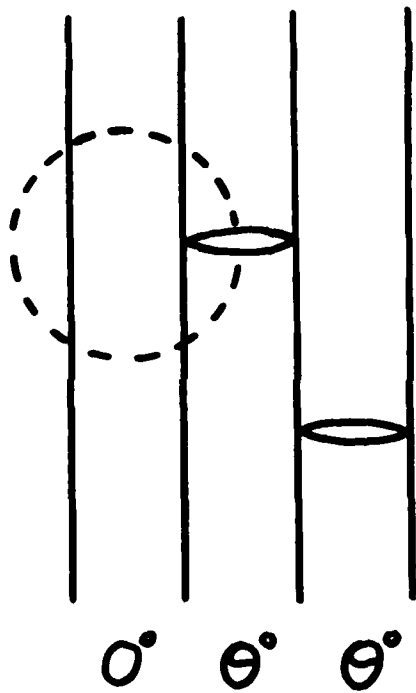


Figure 12: General Schematic Representation of Local Net-Section Stress Situation near a Matrix Crack

discussed in Figs. 10 and 11) exist only in the region of the off-axis cracks as indicated by the dotted circle in Fig. 12, and are in fact the average or net section values at the crack position. To that extent, then, some fifteen years of data appear to show that the net section strength of the 0 degree plies in the neighborhood of off-axis ply cracks controls the quasi-static laminate strength, at least to an engineering approximation level. Since this type of stress redistribution occurs if a specimen is quasi-statically loaded to failure or if the cracks form during fatigue loading, no reduction of residual strength (during fatigue) is expected or observed due to CDS formation, as suggested by Fig. 3. However, we shall see that the stress redistribution that occurs during that period can be critically important, and the present model incorporates those changes in an essential way.

The average net section stress in the fiber direction of the zero degree plies can be recovered from laminate analysis. The simplest possible interpretation of the fatigue behavior of those plies would be to claim that the fatigue behavior of any laminate can be predicted by calculating the fiber-direction stress for that laminate and estimating the resulting fatigue life from the curve that fits the data for one-dimensional fatigue behavior of that zero degree ply. In subsequent sections we shall see that this process is, at the same time, an excellent starting point and an inadequate simplification in some cases. We shall use it here as a starting point. When matrix cracking is the damage mode which is causing the local stress redistributions, we can calculate approximate values for the increased local stresses by the discount scheme described above.

However, when a specimen is actually tested, it must be determined to what extent the cracking in various plies develops so that the proper amount of local stress redistribution can be assigned. As we have suggested earlier, we have chosen (measured or predicted) stiffness changes as the damage parameter which allows us to monitor damage development and interpret that development in terms of internal stress redistributions. (In a sense, these stiffness changes replace the measurable crack length in a comparable fracture mechanics treatment in homogeneous materials.) Another positive consequence of this choice is the fact that axial stiffness changes are almost identical to local axial stress changes in the zero degree plies in a laminate. Such a relationship is demonstrated for quasi-isotropic stacking sequences by the information shown in Table 2. It is shown there for a Type B laminate that the axial fiber direction stress (calculated from laminate analysis) is 2.54 times as great as the applied stress when no other plies are broken in that laminate. When the 90° plies are cracked, however, the local axial stress in the zero degree plies increases to 2.64 times the applied value, an increase of 4.2%. The corresponding decrease in the stiffness of the total laminate is 4.1%, a nearly identical figure. When all of the 90° plies and all of the 45° plies are cracked, the discount scheme suggests that the local applied stress in the zero degree plies is 2.99 times the laminate applied stress, an increase of about 18% over the original value in that ply. The corresponding decrease in stiffness for that case is 15.3%, a very similar number. These computations have been made for literally dozens of laminates, with similar results. Hence, for our starting point, we make the assumption that the local axial stress in the fiber direction

Table 2.

Example: $[0,90,\pm 45,\mp 45,90,0]_{3s}$

Applied Stress $\sigma = 1000$

| Cracked Plies | σ_x in 0° plies | $\Delta\sigma_x$ due to ply cracking (%) | ΔE due to ply cracking (%) |
|----------------------|----------------------------------|---|---------------------------------------|
| none | 2540 | ---- | ---- |
| all 90's | 2646 | 4.2 | 4.1 |
| all 90's and 45's | 2992 | 18 | 15.3 |

in the zero degree plies can be estimated from an initial calculation of that stress using laminate analysis and knowledge of the stiffness change measured in a given specimen which can, in turn, be interpreted directly as percentage increases in the local stress that controls the rate of degradation of those zero degree plies.

In the instance that stiffness change observations are not available, it is possible to anticipate and estimate those changes for a given laminate and a given amplitude of applied load in tension. That estimation can be made by using any common failure theory (such as the Tsai-Hill or Tsai-Wu concepts) to estimate which off-axis plies will crack for a given maximum applied cyclic stress. The corresponding laminate stiffness change can be calculated from laminate analysis using the discount method and a corresponding local stress change can then be estimated. Of course, more sophisticated concepts and analyses can be used for these purposes, and we will demonstrate the use of several of those including shear lag schemes and finite difference as well as finite element analyses in a later section.

We begin by considering a simple application of the model to the test conditions used for specimen B2-6. That specimen was subjected to a nominal stress level of 45.6 ksi which corresponds to a strain level of about 5,000 $\mu\epsilon$. The axial stress in the fiber direction of the zero degree plies for that applied stress level was 2.54 times the applied stress or about 115.8 ksi (c.f. Table 2). During the actual test of specimen B2-6 a change of 4.5% in the axial stiffness of that specimen was observed. Hence, over the term of testing, the nominal stress in the zero degree plies will increase to a value of about 120.5 ksi. It should be noted that if the experimental observations were not

available, it would have been possible to anticipate this stiffness change of about 4% since the threshold of cracking of the 90° plies is thought to be about 41 ksi, calculated from laminate analysis, and the predicted stiffness change from the cracking of those plies is about 4%. The average quasi-static fracture strength of the Type B laminates was about 77.9 ksi according to our baseline data. From laminate analysis, the ratio of applied stress to local axial stress in the zero degree plies at fracture is about 2.99. Hence, the strength of the zero degree plies in that laminate should be about 77.9×2.993 or about 233 ksi. This value is used to normalize the calculated stresses in the zero degree plies as a function of cyclic loading. A linear fit of that data is shown in Fig. 13. It should be noted that the baseline experimental data for the quasi-static fracture strength of each laminate type has the effect of adjusting the influence of the applied cyclic stresses according to the strength demonstrated by the zero degree plies under the internal stresses peculiar to each laminate type, since that number is used to normalize all inputs. We shall see that this rather subtle piece of philosophy has a great deal to do with the ultimate success of the model.

Recalling Eqn. (3), we have established a relationship for the uniaxial fatigue behavior of the zero degree plies, thereby specifying $N(n)$, and we have established the local stresses in the zero degree plies that must be used to determine that function. We need only provide one additional function in Eqn. (3) so that the integration as a function of the number of applied cycles can be computed. That function is the local failure function, $F_L(n)$, which reflects the severity of the local stress state in proportion to the strength of the zero degree

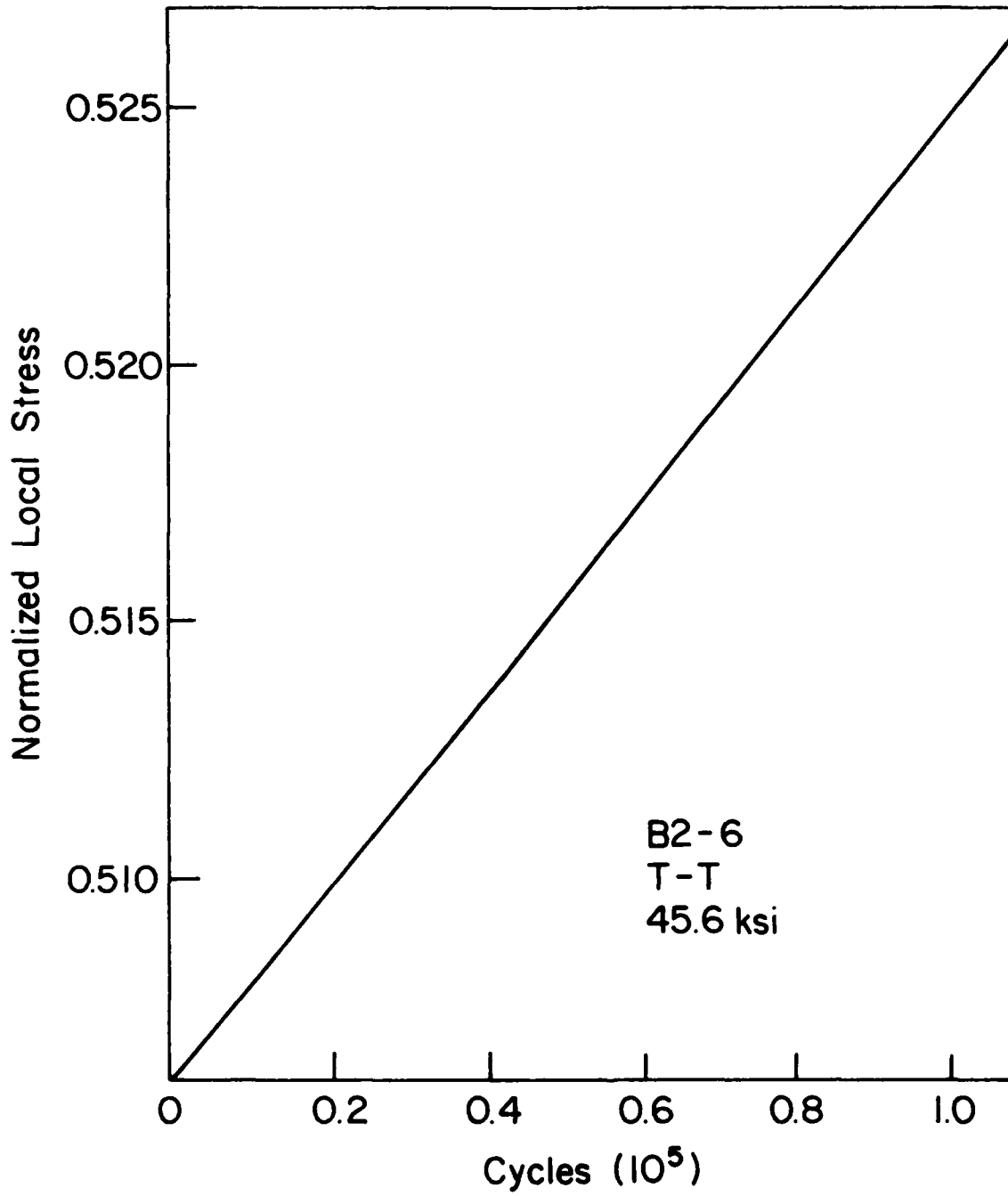


Figure 13: Linear Fit of Normalized Stress in the \emptyset Plies During Cyclic Loading

plies. For purposes of the present computation we will assume that this function is identical to the normalized axial stress ratio just determined and plotted in Fig. 13. This is equivalent to assuming that a maximum stress criterion controls the failure of the zero degree plies. More will be said of this choice later.

For those choices made, a computer program that increments the local stress function and performs the numerical integration of the integrand shown in Eqn. (3) is executed, the predicted data output and plotted. For the present inputs, the results are shown in Fig. 14. After one million cycles of loading, specimen B2-6 was loaded to failure to determine its residual strength; the data from that test is plotted as a triangle in Fig. 14, and indicates that the predictions are reasonable. For general information at this point, the information in Fig. 15 indicates that if the damage rate in the S-N equation is changed to $B = -0.073$ the agreement is virtually coincident with the data.

A result similar to the experience described for specimen B2-6 is shown in Figs. 16 and 17 which represent data for specimen B2-8. In those figures the local unidirectional stress in the zero degree plies was calculated using laminate theory, and changes in that stress were computed directly from measured stiffness changes as before. Also, the local failure function was set equal to the normalized local unidirectional stress calculated as just described. The two figures provide a comparison of the results obtained when the slope, B , of the logarithmic degradation equation used to describe the S-N behavior of the zero degree plies has two different values, a value of -0.07 and -0.075 . It can be seen that the observed data, represented by triangles

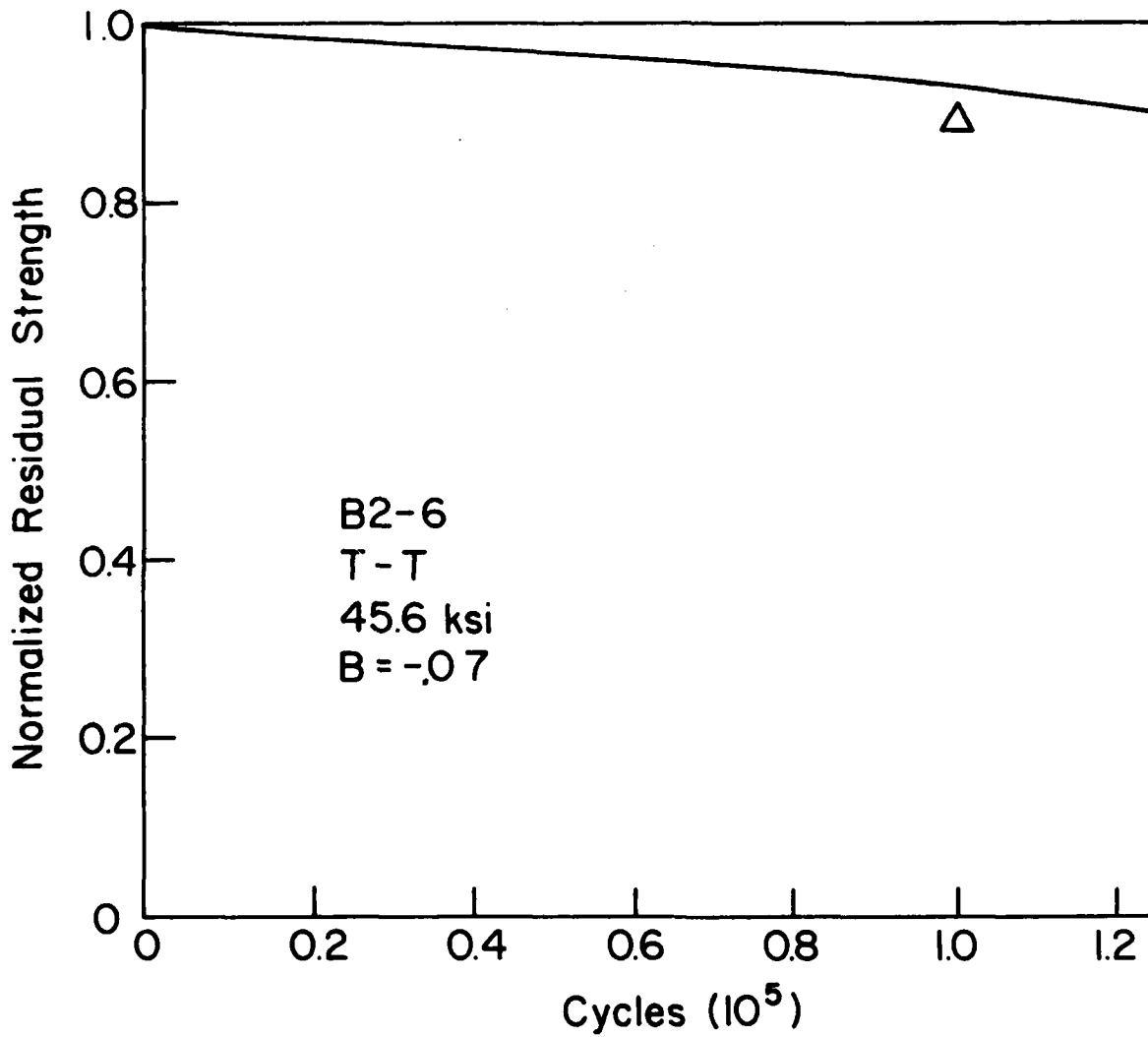


Figure 14: Residual Strength Prediction and Observation for Specimen B2-6

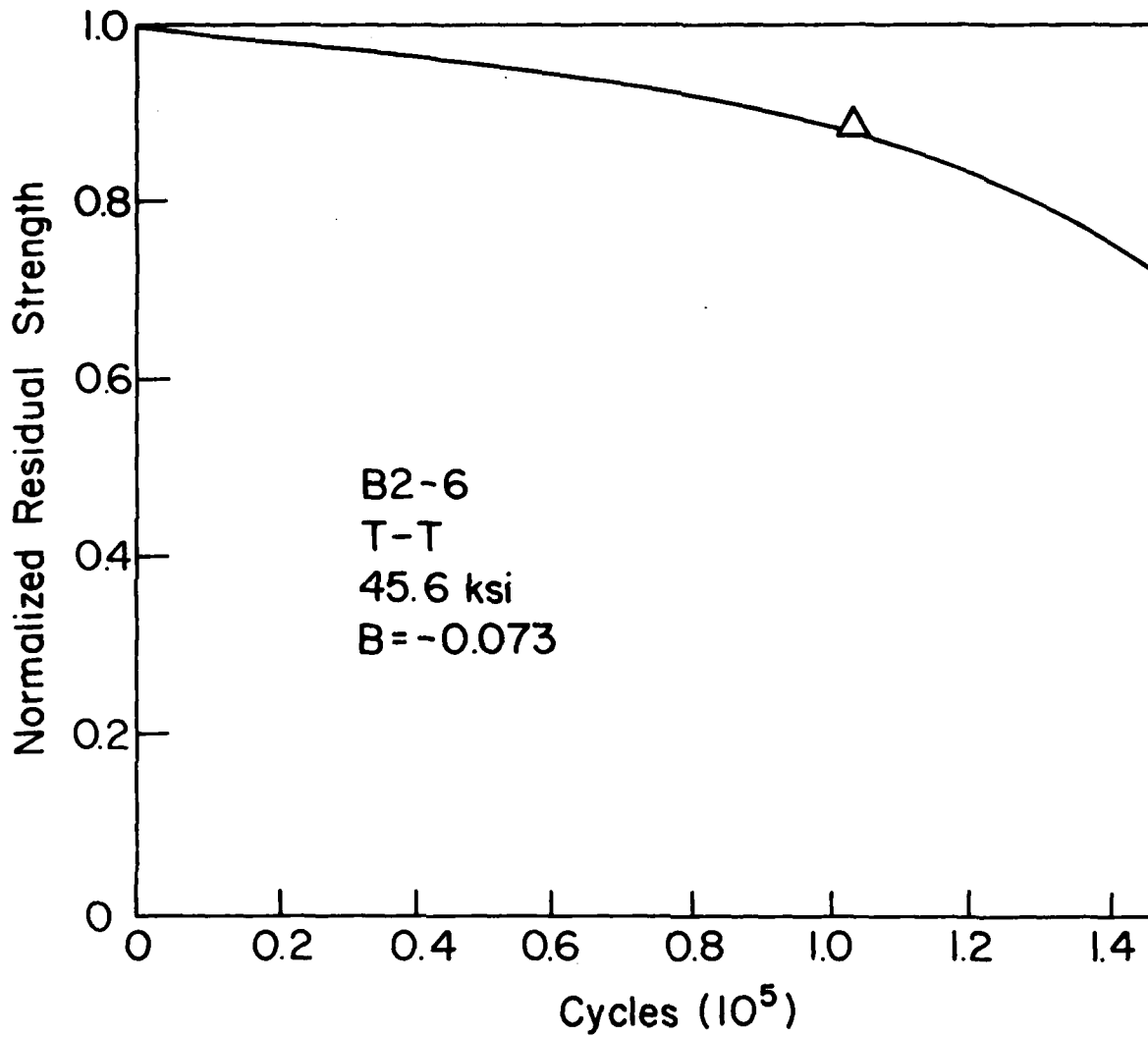


Figure 15: Change of b Parameter from -0.07 to -0.073 for Specimen B2-6

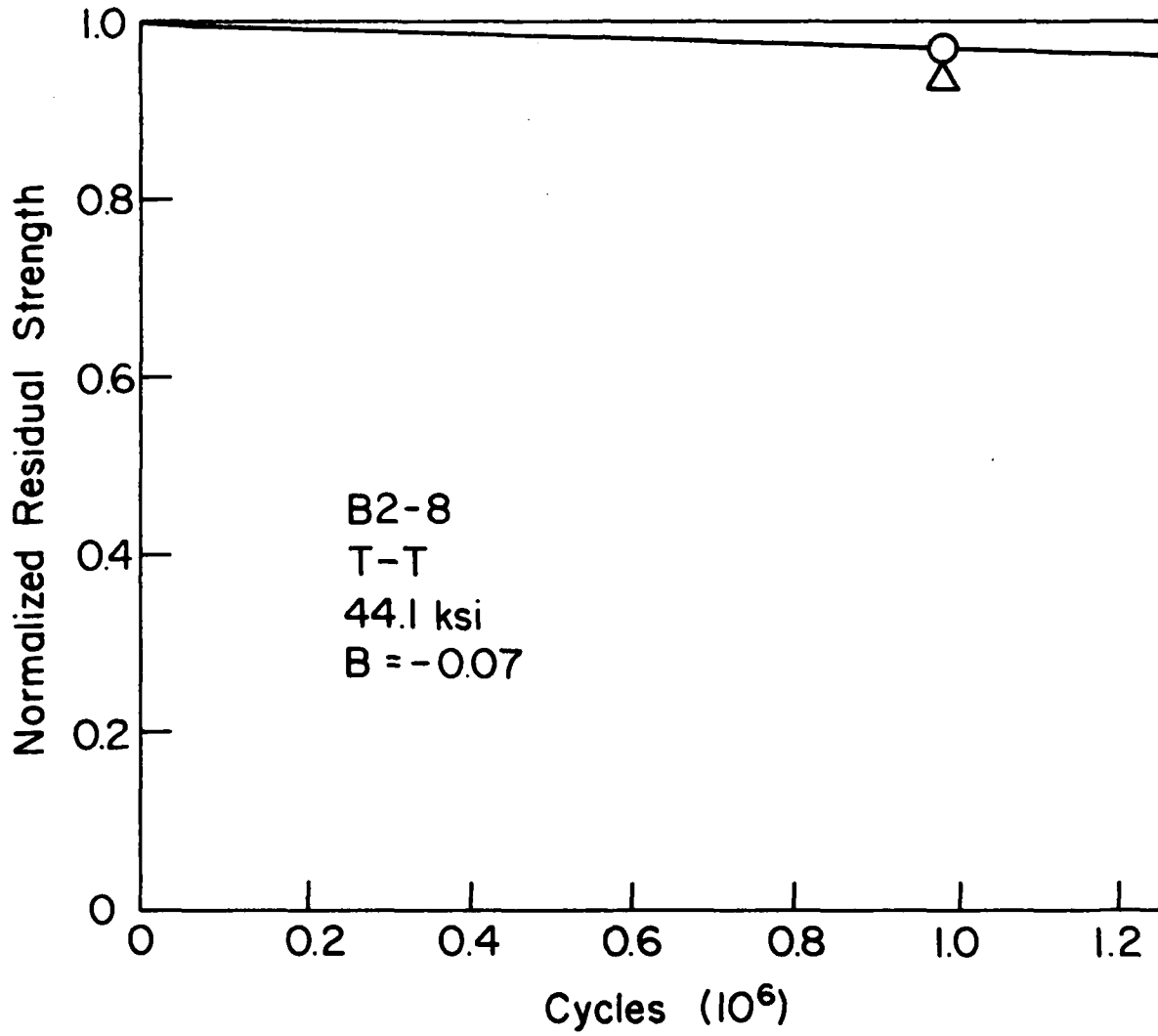


Figure 16: Predicted (0) and Observed (Δ) Residual Strength for
 Applied T-T Stress Range of 44.1 ksi for
 $b = -0.07$

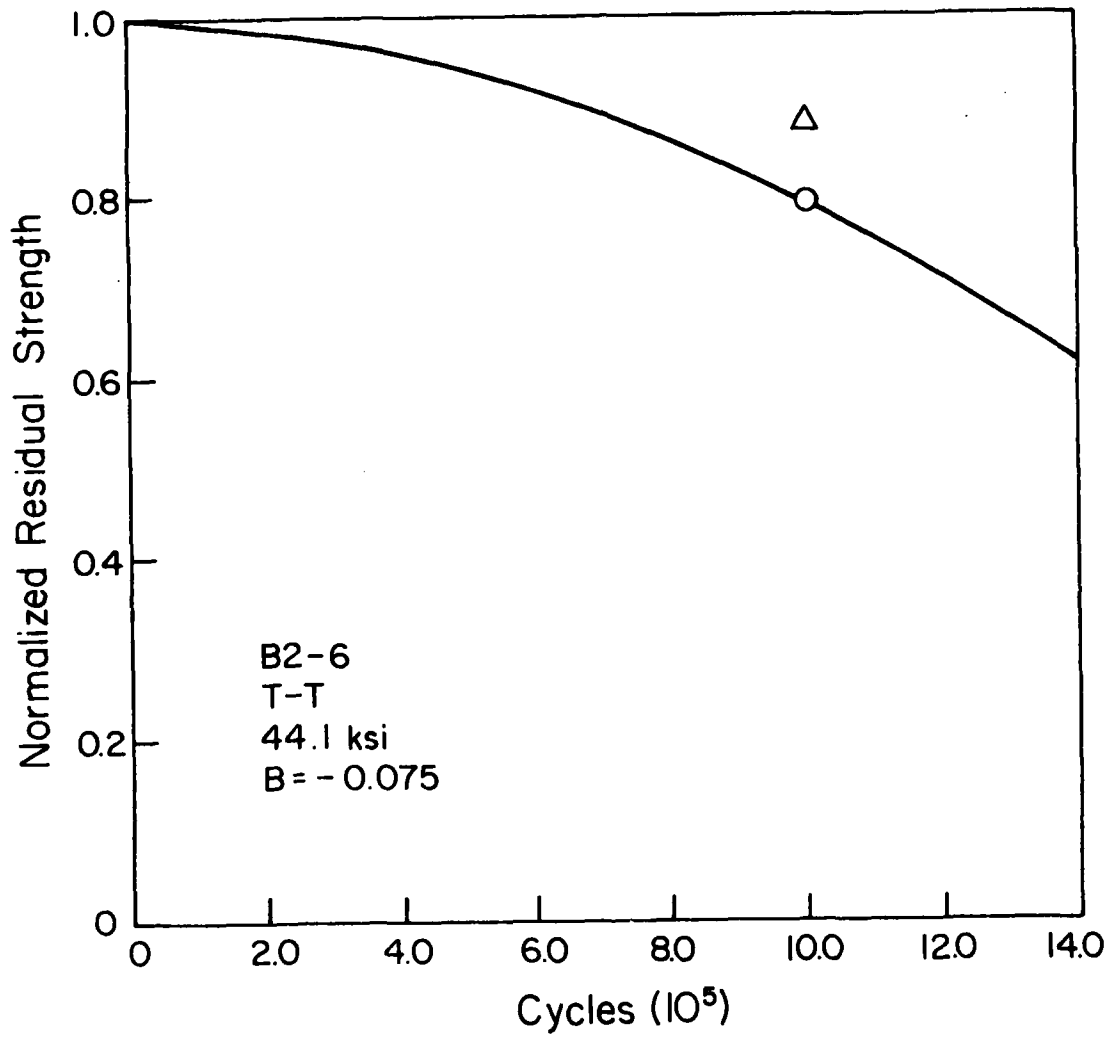


Figure 17: Same Results Shown in Fig.16 with b Changed to -0.075

in those figures, lies in between the two predicted curves for those slopes.

Figure 18 illustrates a general feature of these results which is sometimes misleading. In that figure, the results just demonstrated in Figs. 15 through 17 for specimens B2-6 and B2-8 are plotted on semi-log paper. Of course, plotting the results that way emphasizes the curvature of the residual strength curves predicted by the model. Indeed, when the results are displayed in this format, there is an apparent "sudden death" of the specimens. (A hypothetical high-stress case for which we have only predicted results is also shown in that figure.) While it is true that the rate of damage development appears to increase near the end of the life of the specimen, a significant part of the rapid drop off observed in Fig. 18 is contributed by the plotting technique alone. The physical data regarding damage development, stiffness change, etc. do not support the conclusion that the residual strength of these specimens has the precipitous drop suggested by Fig. 18 or by other figures plotted in that manner.

Figure 19 shows a variety of predictions (in a range of observed data for tension-tension fatigue testing of Type B laminates at about $6,000 \mu\epsilon$) which illustrate the influence of two of the parameters which enter into the damage accumulation model, the slope of the phenomenological fatigue characterization of the zero degree plies, B , and the power of the degradation ratio in Eqn. (3), i . It also illustrates the influence of internal stress redistribution for this case where changes in stiffness (and internal stress) are small, of the order of about 5 to 6%. Curves A and B show that internal stress redistribution contributes significantly to the nonlinearity of the

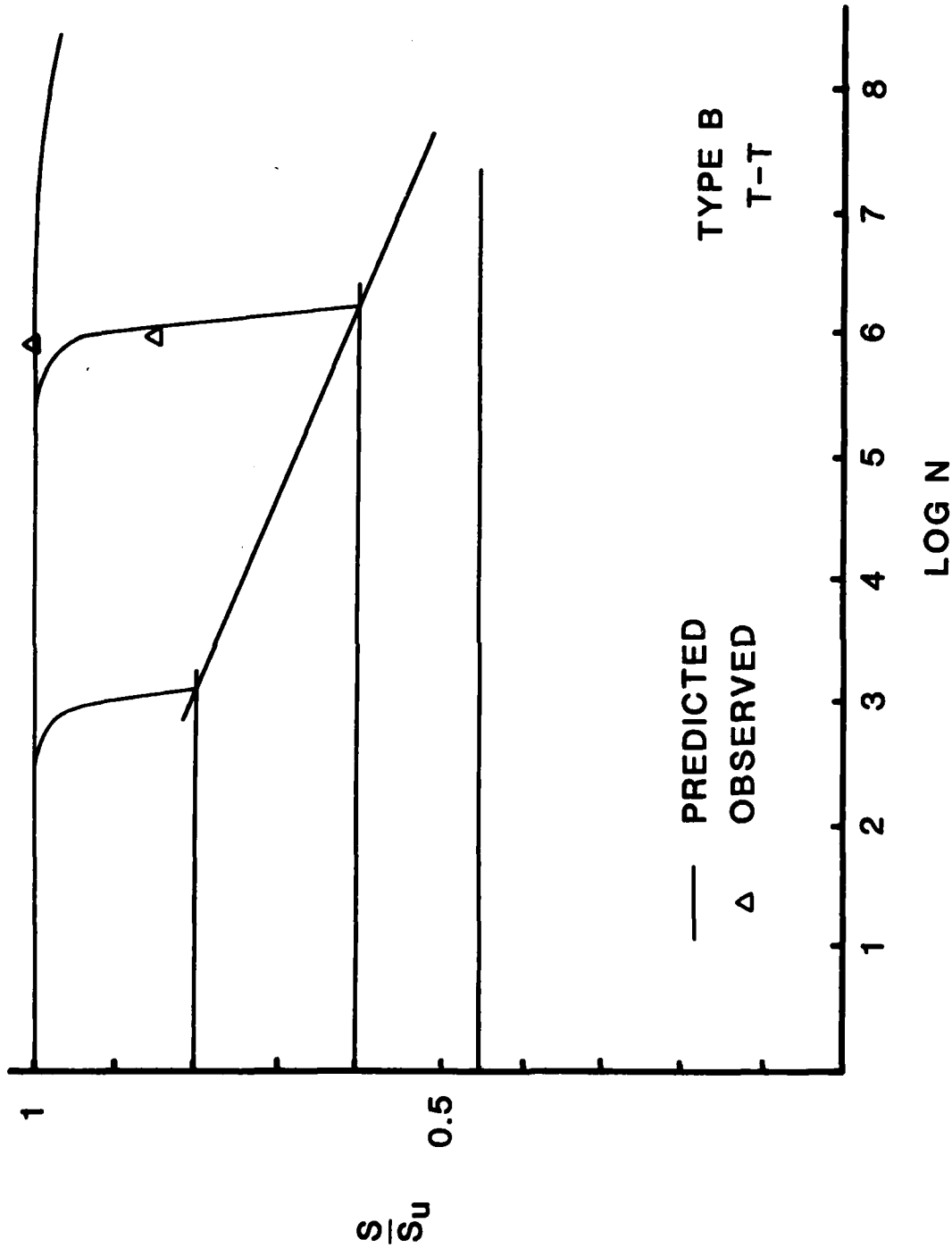


Figure 18: Predictions and Observations for Specimens B2-6, B2-8, and a Hypothetical High Stress Case Plotted on Semi-Log Paper

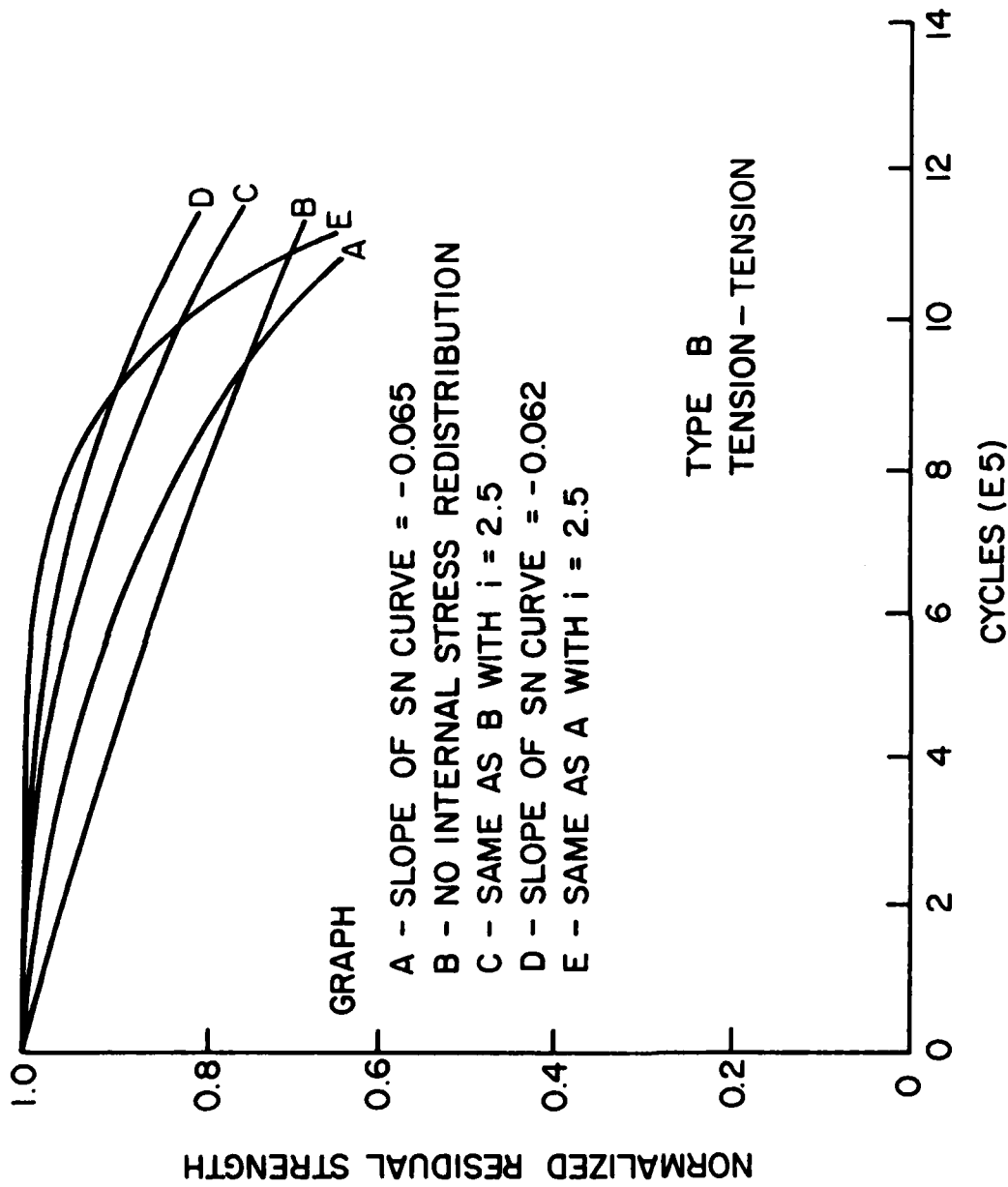
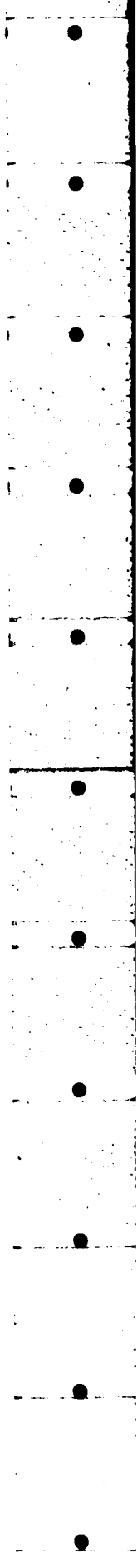


Figure 19: Illustration of the Influence of Various Model Parameters on Predicted Results



residual strength degradation curve, especially near the end of the specimen life. While the predictions through the early part of the fatigue life for those two cases are relatively similar, the residual strength and especially the life predictions of those two approaches to modeling can be radically different, even for relatively small amounts of damage development and rather long life situations. The power of the degradation ratio, i , is equal to 1.2 for curves A and B. If that power is changed to 2.5, one obtains the curve shown in C instead of the curve shown in B (both of which include no stress redistribution). One can see that the otherwise-straight curve B does become more curved with an increase in that power as would be expected. It should also be noted, however, that curve C is considerably higher (less residual strength reduction) in the early part of the fatigue life of the specimen than is curve B. Mathematically, this is a result of the fact that the small damage ratios in Eqn. (3) experienced in the early part of the fatigue life are raised to a higher power, making them smaller fractions during that period.

Curve D in Fig. 19 represents the predictions of residual strength when the degradation slope is equal to -0.062 and the power of the degradation ratio is equal to 1.2. Hence, that curve can be compared with curve A which differs from it only the the value of the degradation slope. Curve E is also similar to curve A except for a change in the power of the degradation ratio. The nonlinearity is very obvious in that curve and shows that relatively small changes in that power can make large differences in the strength predictions for a given specimen. Although it isn't obvious from the figure, several hundred calculations with the model suggest that the influence of the power on

life is minor by comparison to the influence of the degradation slope, B.

We will use our discussion of the model applied to laminate B as a baseline for the remainder of our discussion of tension-tension results. To reiterate, we have used laminate theory to estimate the local fiber direction normal stress in the zero degree plies and estimate the change in that stress when cracks develop in other off-axis plies using the discount method. We have used that calculated stress (as a function of the number of cycles) in the phenomenological fatigue life relationship to estimate the number of cycles to failure, N , in the local stress state that is continually changing because of stress redistribution. We have fixed the power of the degradation ratio in Eqn. (3), i , to be 1.2 and have assumed that the local failure function in the zero degree plies is equal to the normalized local normal stress in the zero degree plies in the fiber direction, the same input that we used in the phenomenological life equation of the zero degree plies. Those quantities have been used in the Eqn. (3) in a computer code which requires the basic properties of the laminate, the value of the parameters i , A , B , x , and functional relationships for the variation of the local normal stress in the fiber direction of the zero degree plies as a function of the number of applied cycles and a similar functional relationship for the local failure function, F_L . A numerical integration then produces a predicted residual strength as a function of the number of applied cycles as shown in the figures described above.

We now continue our discussion of T-T fatigue loading by changing the stacking sequence of the quasi-isotropic laminates from the Type B sequence to the Type C sequence which differs only in the respect that

the 45° plies are separated by 90° plies as indicated earlier. Figures 20 and 21 indicate typical results for the normalized local stress and predicted normalized residual strength variations, respectively, cyclically loaded with a maximum strain of about 6,000 $\mu\epsilon$ which corresponds to a maximum stress level of about 43.6 ksi. At those levels of loading, very little change in residual strength is predicted or observed (the slope of the S-N curve was taken to be -0.065 for those calculations).

The results of a similar calculation are shown in Figs. 22, 23, and 24 for specimen C6-10 which was oscillated at an essentially identical maximum stress of about 43.6 ksi. Figure 22 shows the normalized local stress for specimen C6-10 as determined from laminate analysis and the observed stiffness changes. Figures 23 and 24 indicate the predicted residual strength changes for two choices of the slope of the phenomenological S-N curve, both of which are slightly higher than the value of -0.07 that was eventually used as a "standard" value. The observed change in residual strength for that specimen is shown as a triangle in Fig. 24. It is apparent from Figs. 20 through 24 that the degradation of the zero degree plies in a Type C laminate and the consequent degradation of the laminate itself appears to be somewhat less for comparable maximum strain levels than was observed for the Type B laminates. One could speculate that the net section stress increase in the zero degree plies due to matrix cracking in the 90 and -45 (double) plies is not as great as one might expect due to the "protection" offered by the +45° plies which are observed to develop matrix cracks very late in the life of the specimens and which have considerable strength and stiffness. Table 3 shows the results of

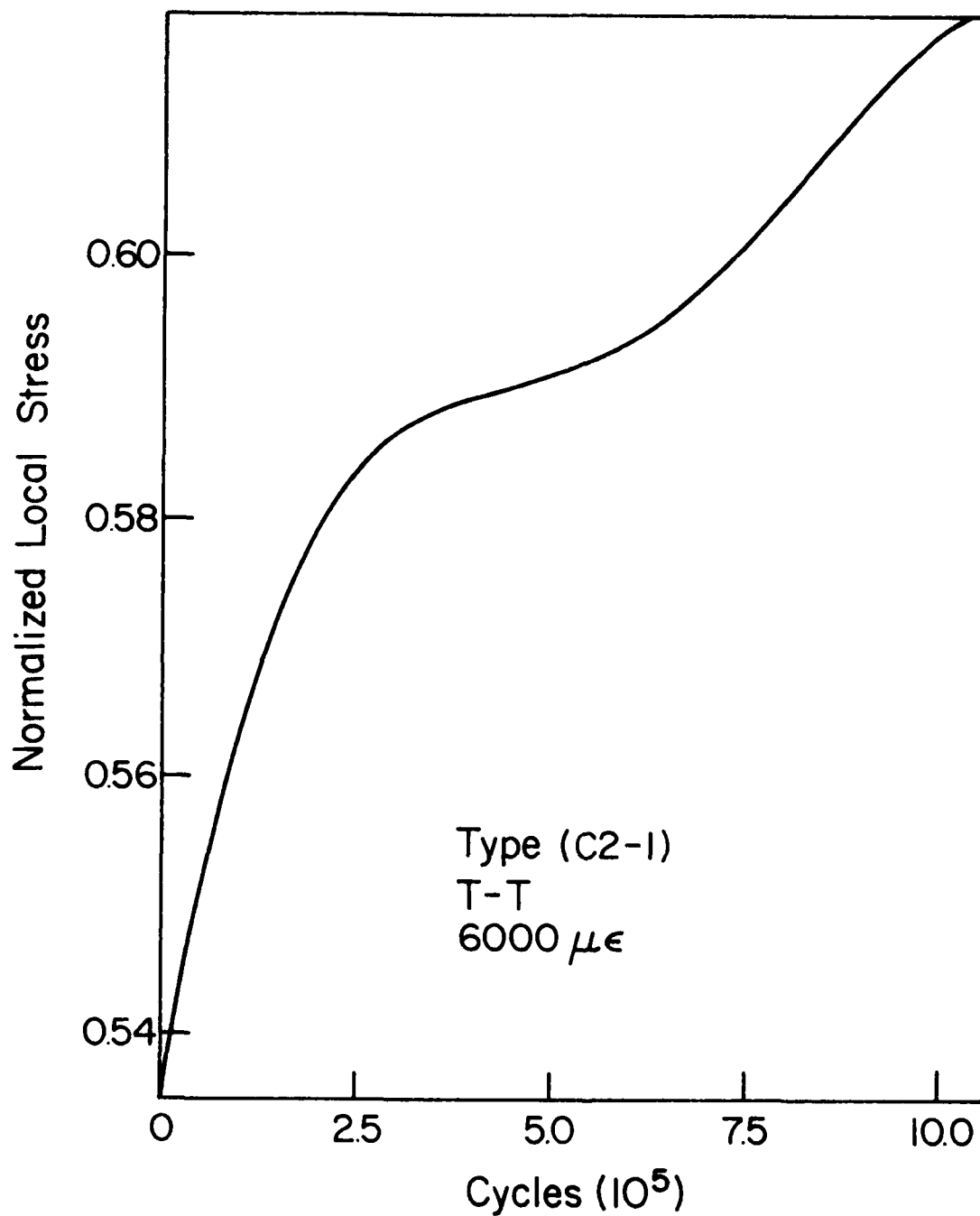


Figure 20: Normalized Fiber Direction Stress in 0 Degree Plies Estimated from Laminate Analysis and Stiffness Changes

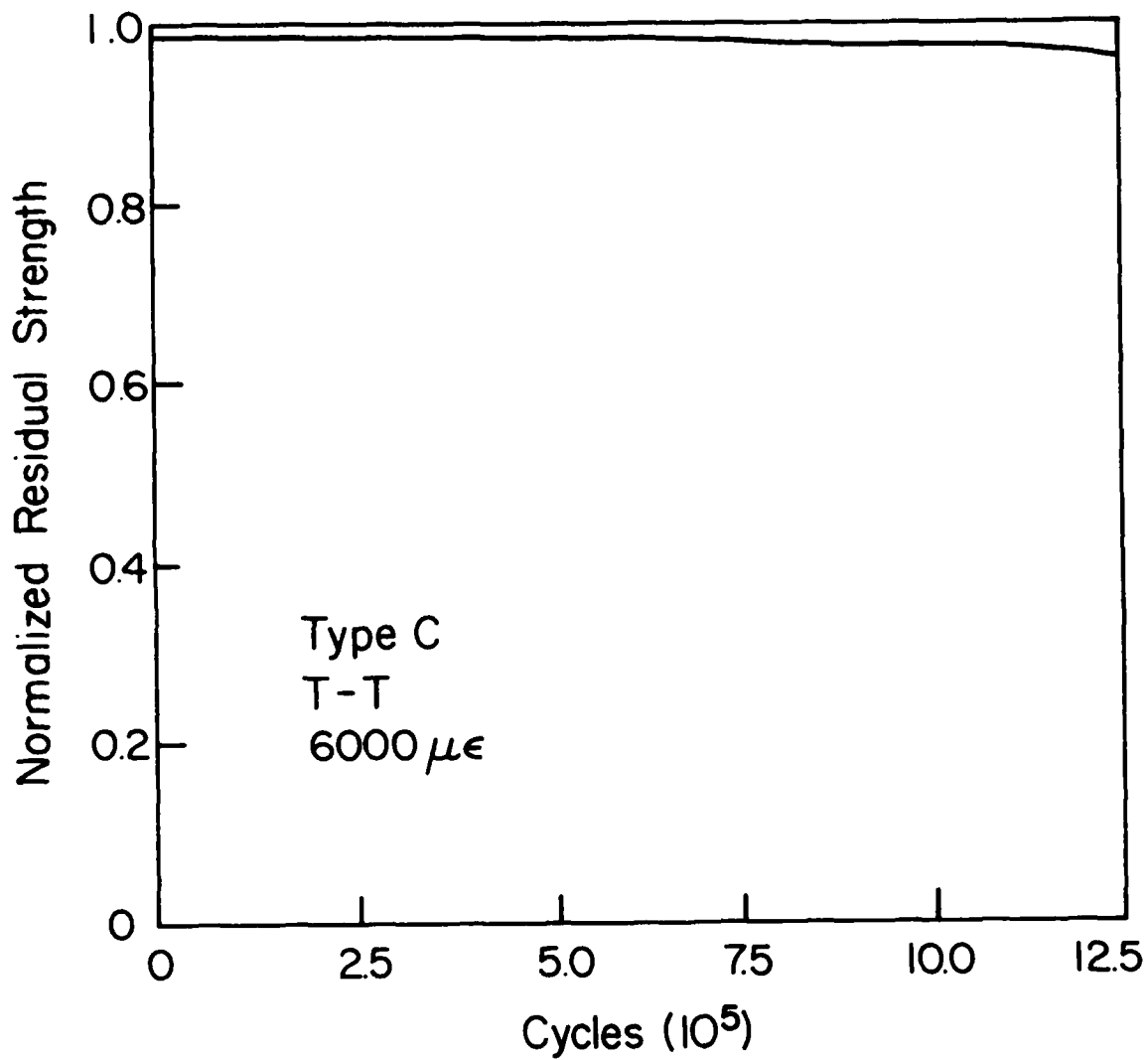


Figure 21: Predicted Residual Strength for Data Shown in Fig. 20

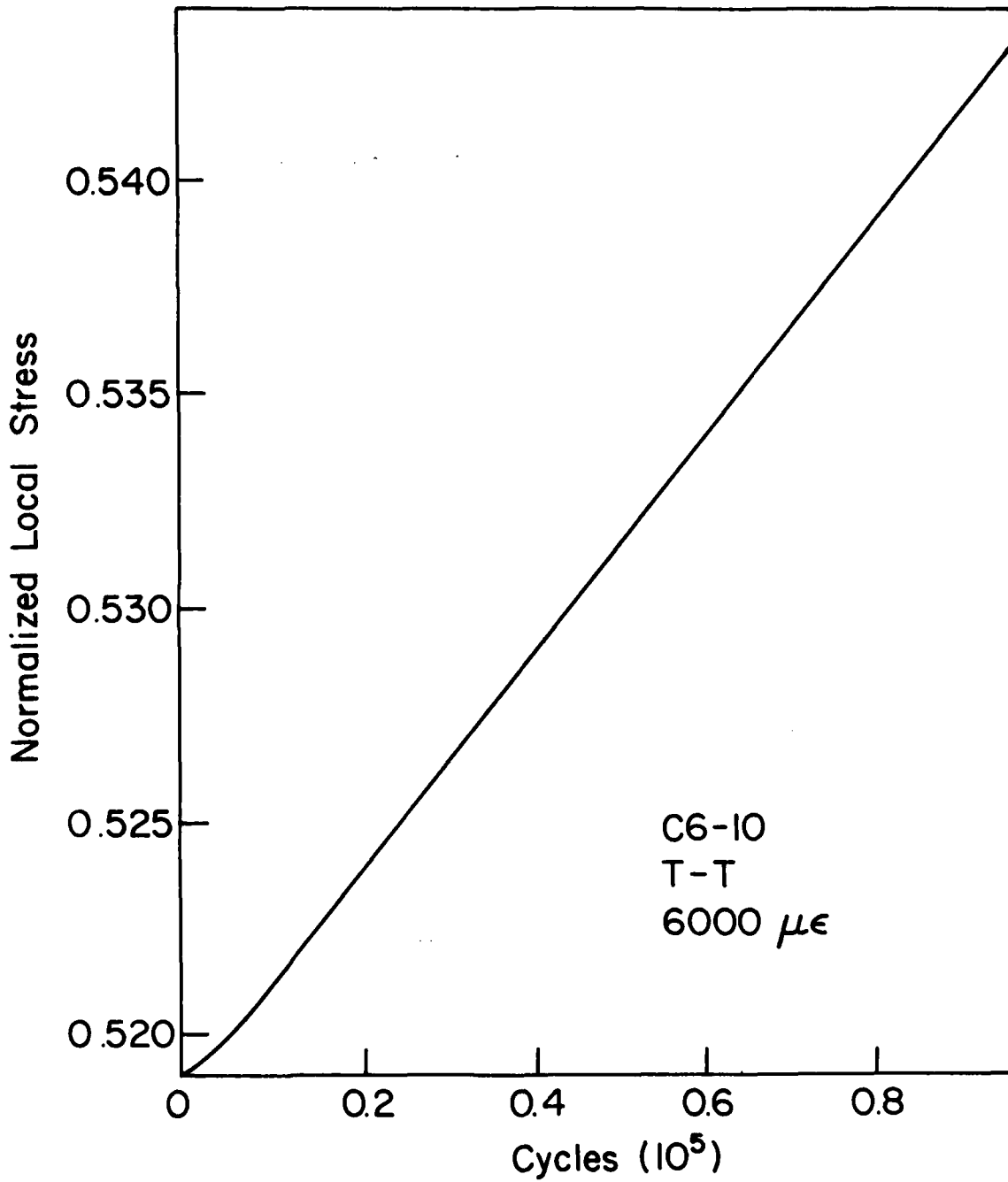


Figure 22: Normalized Local Stress in θ Plies Calculated from Laminate Analysis and Stiffness Changes

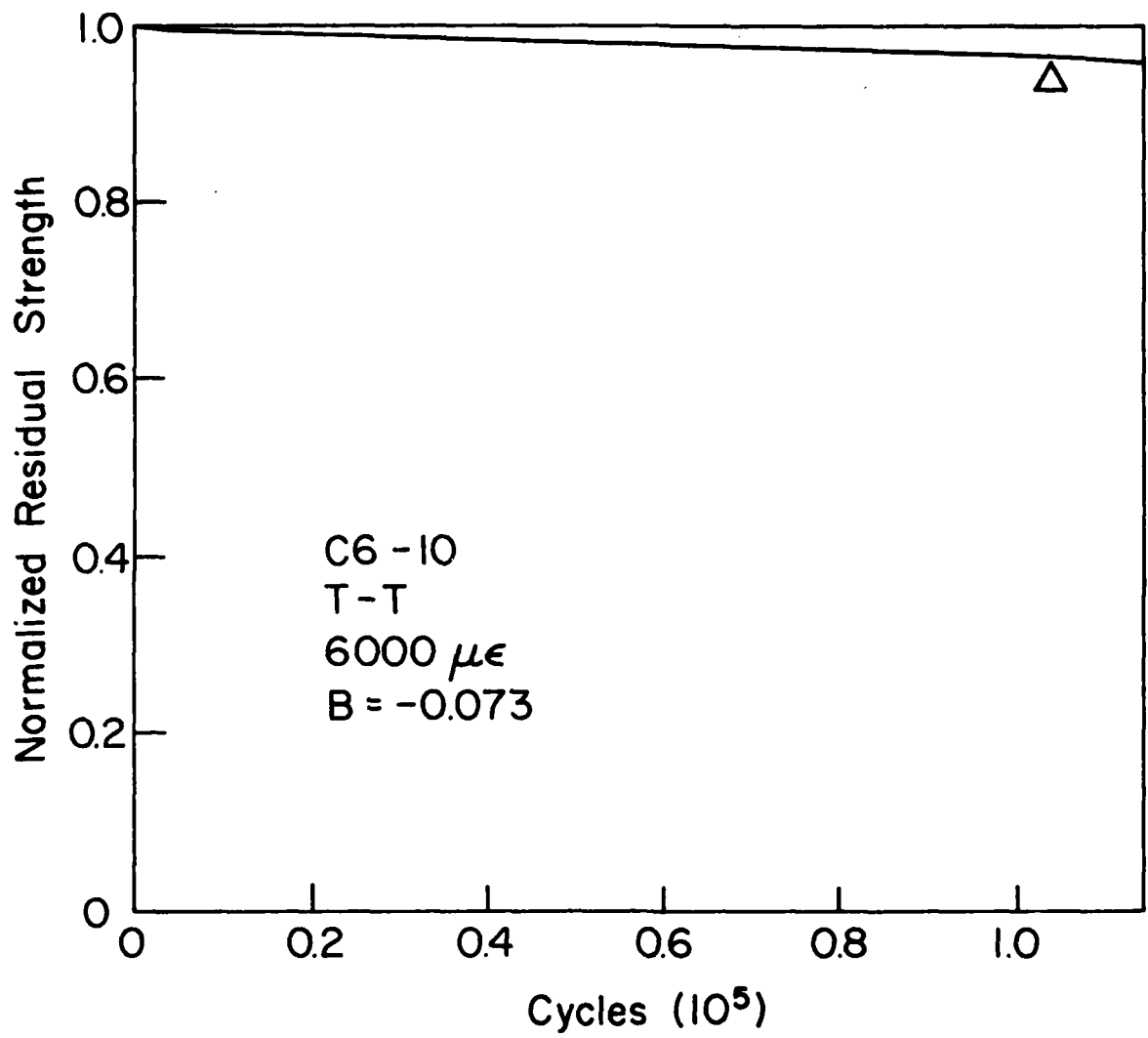


Figure 23: Residual Strength Calculation and Observed Data Point for Data in Fig. 22

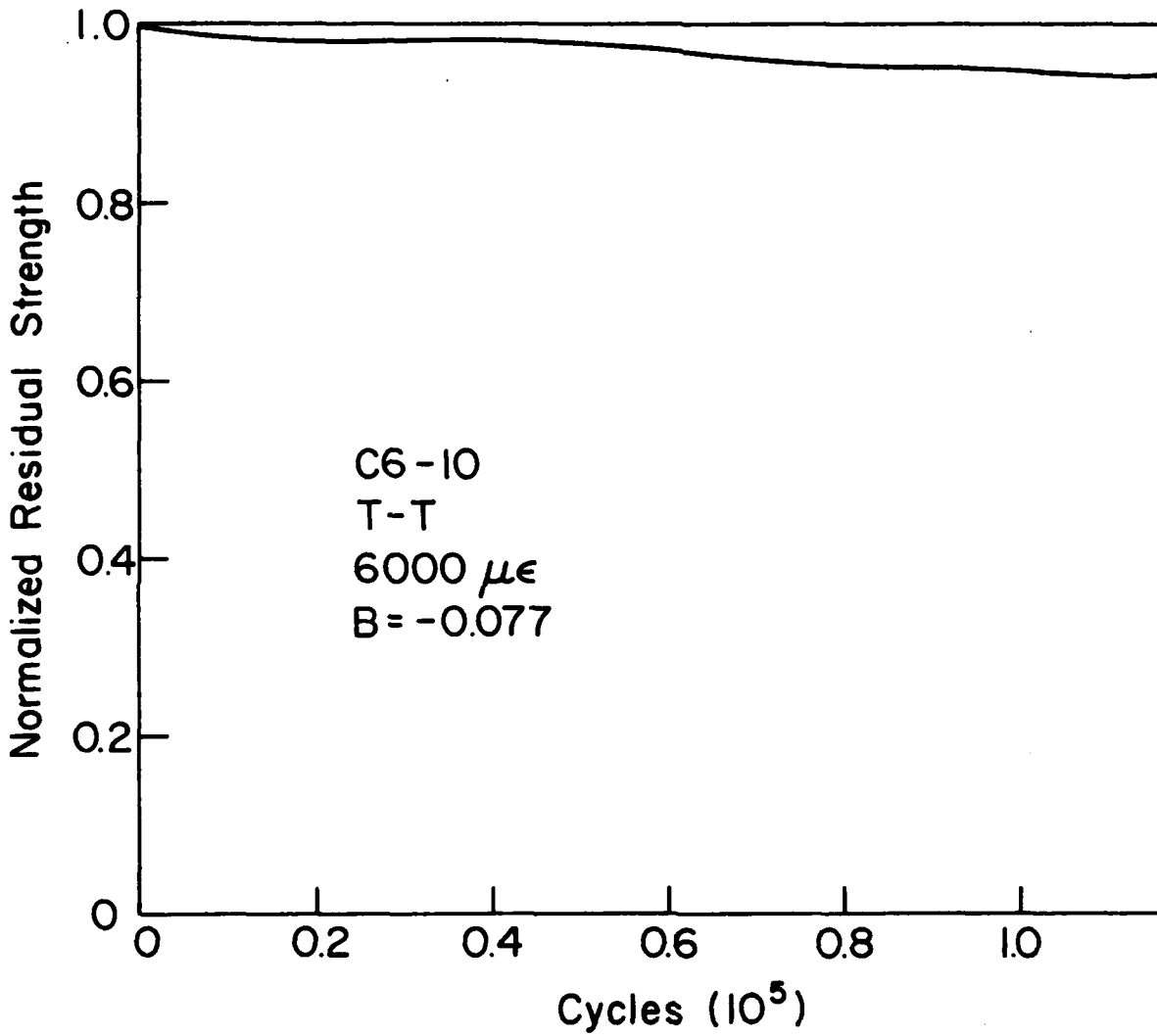


Figure 24: Same Prediction Shown in Fig. 23 Except b Has Been Changed from -0.073 to -0.077

Table 3.

| Specimen | Max. Stress (ksi) | Residual Strength Reduction | | |
|----------|----------------------|-----------------------------|----------|------------------------|
| | | Predicted | Observed | (after n cycles) |
| C6-4 | 54.0 | 6.3 | 2.2 | (10 ⁴) |
| C6-10 | 43.3 | 1 | 5.7 | (10 ⁵) |
| C2-1 | 43.6 | 5.4 | 0 | (10 ⁶) |
| C4-2 | 43.5 | 1 | 0 | (186x10 ³) |

several calculations and corresponding observations for the model with parameters having the values mentioned above, the same values used for the Type B laminates. While the agreement appears to be quite reasonable, especially considering the variability between individual specimen results, the predicted results are generally more severe than the observed ones.

Perhaps the matter of data spread for fatigue tests should be mentioned here. Table 4 presents a sample of experimental data for Type C specimens subjected to essentially identical test conditions at a maximum strain amplitude of about 7,500 $\mu\epsilon$. The maximum stress for each specimen is listed along with the life that was observed or the residual strength if the test was terminated before failure. It can be seen that one specimen failed after about 32,000 cycles of loading while two specimens went beyond one million cycles without failure. In fact, one of the specimens which went more than a million cycles without failure was subsequently tested and found to have a residual strength which was 9% greater than the average value determined from the quasi-static tests for that laminate. It can also be observed that the largest stiffness change did not correspond to the shortest specimen life although on the average it is true that the largest stiffness changes occurred in the specimens which failed after the smallest number of cycles of loading. The reader who is experienced in the field of fatigue will recognize that this variation in behavior is not unusual, nor is it peculiar to composite materials. From the standpoint of modeling, however, it does present a particular challenge, especially if one chooses to construct a model which is sensitive to the peculiarities of damage development in a given specimen and which is also capable of producing useful and

representative behavior of laminates in general. The authors regard one of the particularly important strengths of the present model to be its capability to account for specimen differences because of its sensitivity to stiffness changes if they are available as inputs to the model. For example, in Table 4 three predicted lives for widely different test data are shown for illustration. For specimen C5-5, the observed stiffness change in about 30,000 cycles was only 6%. The predicted life for that specimen was about 30,000 cycles compared to the observed life of about 32,200 cycles. For specimen C5-7 the stiffness change in 80,000 cycles was about 17% with a somewhat slower rate of stiffness change in the early part of the test than was observed for specimen C5-5. The corresponding life prediction was 35,000 cycles compared to about 81,000 for the observed test. If we then consider specimen C8-4 which had a stiffness change in one million cycles of only 5.4% we see that the model predicts a life of about 440,000 cycles which is an order of magnitude greater than the predictions for specimens C5-5 and C5-7 which were subjected to nominally identical test conditions. This sensitivity to degradation rates in individual specimens could not have been obtained from any other modeling approach which does not consider internal stress redistribution. From the standpoint of the practicing engineer, it means that the residual strength and life of individual specimens or engineering structural components can be anticipated by a model which is sensitive to the actual degradation that has occurred in that structure or specimen. This is believed to be a critically important point since the load history of many structures is not generally known or cannot be anticipated precisely. The present model, however, could be used to predict the residual strength and life

TABLE 4.

TYPE C 7500 $\mu\epsilon$ DATA

| Specimen | Max. Stress (ksi) | Observed Life(10^3) | Predicted Life(10^3) | Change in Stiffness(%) | Change in Strength(%) |
|----------|----------------------|----------------------------|-----------------------------|---------------------------|--------------------------|
| C7-3 | 53.8 | 58.9 | --- | 22.6 | --- |
| C5-7 | 53.6 | 81.5 | 35 | 17.6 | |
| C5-5 | 54.2 | 32.2 | 30 | 6 | |
| C6-4 | 54.0 | 10+ | --- | 5.1 | -2.2 |
| C7-11 | 54.2 | 1000+ | --- | 6 | -6.7 |
| C8-4 | 53.4 | 1000+ | 440 | 5.4 | +9 |

of such structures or components based on the results of periodic inspection.

We can continue our discussion by considering the tension-tension behavior of the Type D laminates. These laminates are peculiar and special in the sense that only 10% of the laminates are zero degree plies, 45% are 45° plies and 45% are 90° plies. The stacking sequence was indicated earlier; the zero degree plies are on the exterior surfaces and on either side of the center line of the laminates. This particular stacking sequence was picked purely for its potential to create an extreme which would give us an opportunity to examine the limitations of our modeling procedure. The testing of specimens from that laminate produced exactly that kind of challenge. Figure 25, 26, and 27 illustrate typical results for an application of the model in the form described in the previous stages. A degradation slope of $B = -0.07$ was used for those computations. The total amount of stiffness change observed for the data modeled in those figures was only about 8%. Figure 27 indicates that the strength reduction at one million cycles is predicted to be virtually zero. Figure 28, however, indicates that the residual strength reduction for one million cycles is typically about 6 or 7%. These results are typical of our attempts to apply the unrefined model to the Type D laminate. It is clear that the situation is characterized by strength reductions which exceed by considerable amounts the predicted strength reductions based on the observed stiffness changes and the local stress redistribution calculated from laminate analysis.

Experimental observations during the testing of these laminates indicated that the cracks that formed in the off-axis plies (which are

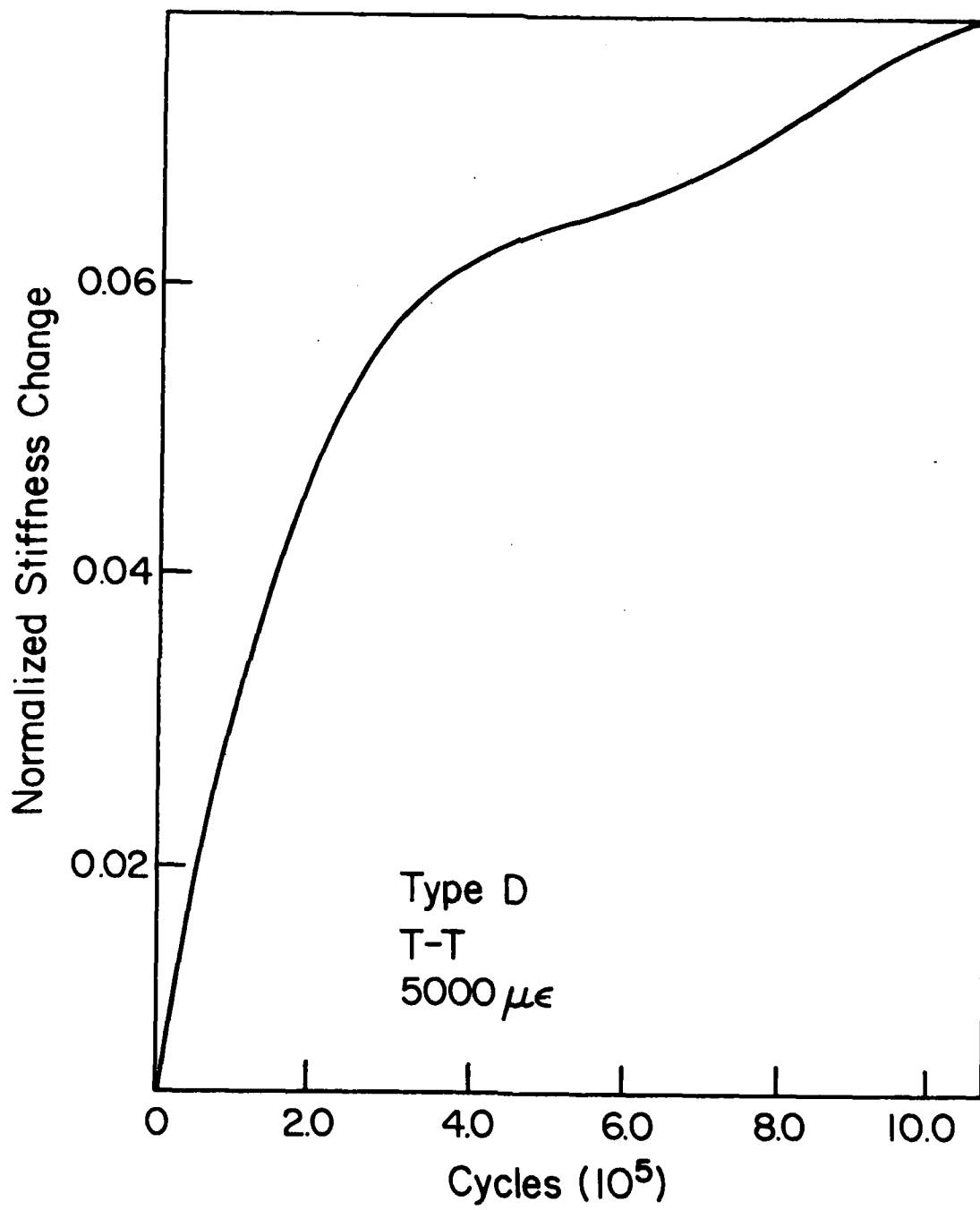


Figure 25: Curve Fit of Typical Stiffness Change Data for T-T Loading of Type D Specimens

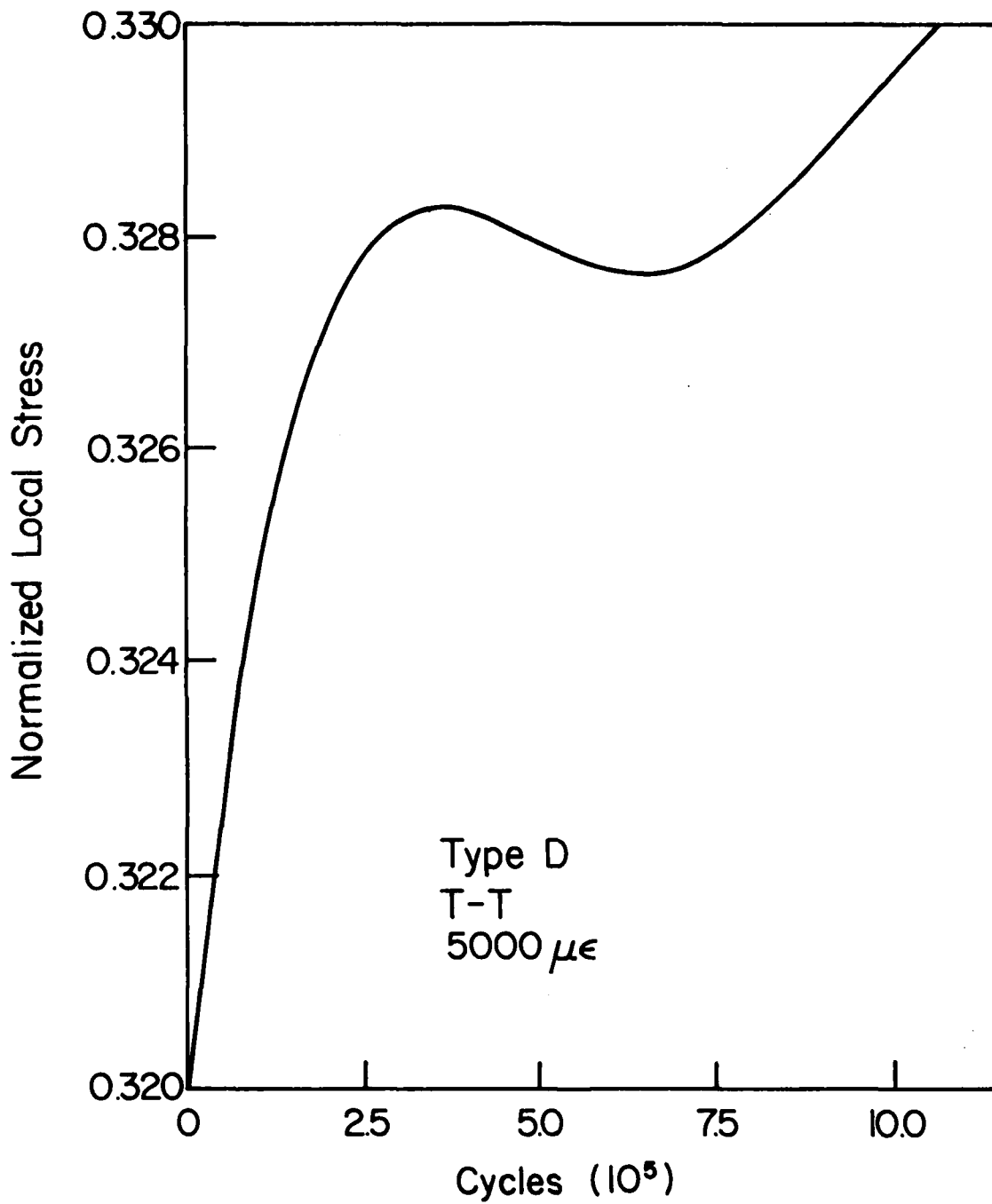


Figure 26: Estimate of Local \emptyset Ply Stress for Data in Fig. 25

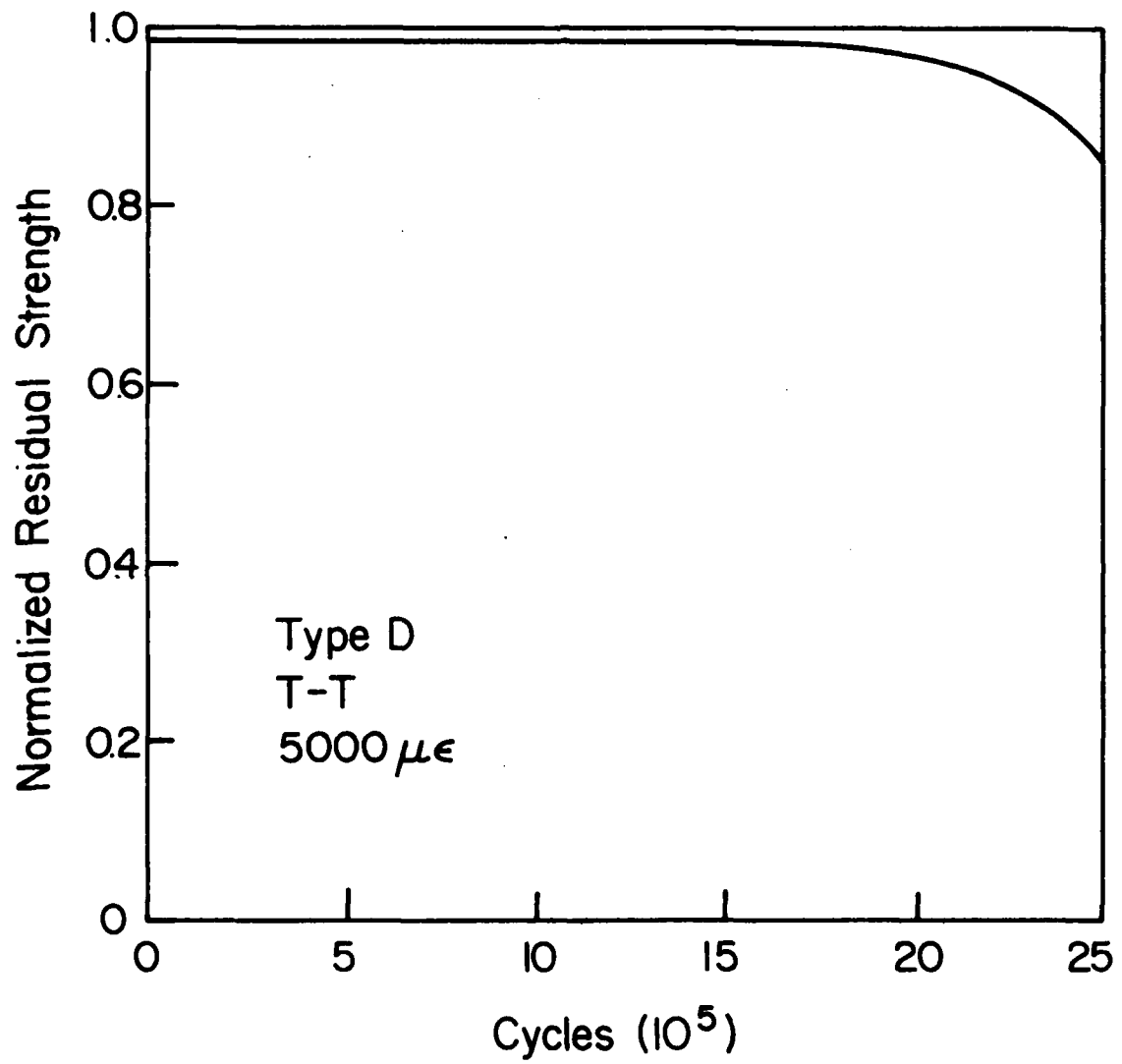


Figure 27: Predicted Variation of Residual Strength for a Type D Laminate

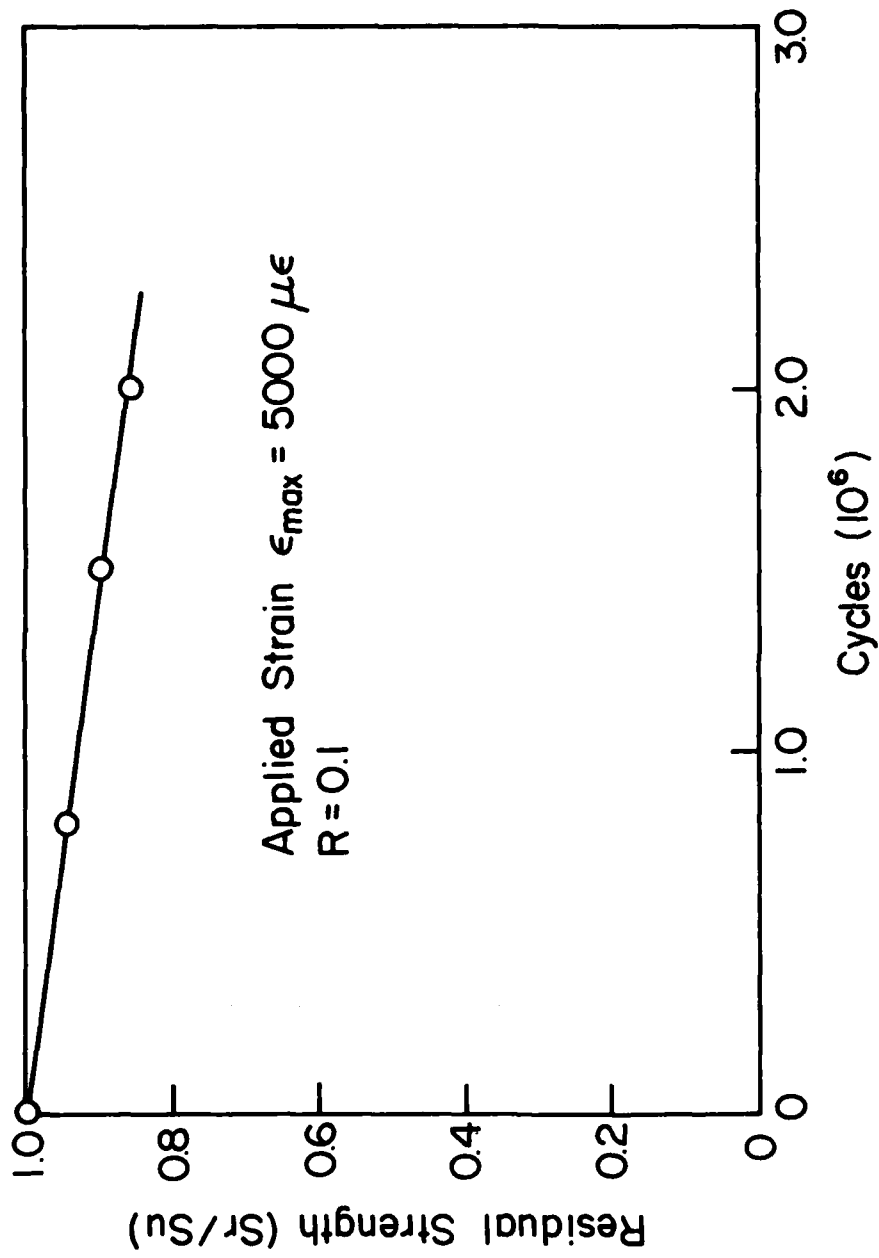


Figure 28: Change in Stiffness for T-T Loading with a Maximum Strain Level of $5000 \mu\epsilon$

grouped in the sections between the 0° plies) had a strong tendency to couple together at a given cross-sectional position during the course of fatigue loading. It was hypothesized that this coupling process created a local geometry which resembled a crack having a total length equal to the combined length of the matrix cracks that coupled together, at least to the extent that they exerted a stress concentration on the remaining zero degree plies on the exterior and near the centerline. In order to estimate the resultant zero degree ply stresses which were caused by this process of coupling, it was decided to apply a shear-lag model to the local stress computation problem. However, it was important to recall that the geometry that is used for analysis must include the effect of the characteristic spacing of matrix cracks described earlier. That is, it is necessary to analyze the stresses in the zero degree plies when cracks forming in all of the off-axis plies couple together, but it is also essential to include in the problem the presence of a similar crack (or extended crack) at a distance which corresponds to the characteristic spacing of cracks in those off-axis plies that form a stable pattern with regular spacing, the so-called characteristic damage state. A shear-lag analysis (described in Ref.[9]) which was generated by Highsmith, et al., was chosen for this problem. Figure 29 shows a schematic of the geometry used for the analysis. The problem was formulated by considering an element of material between two cracks having a spacing corresponding to the equilibrium spacing measured (and predicted) for this laminate. Free surfaces at the crack faces and at the exterior surface of the zero degree ply in the laminate were required. Figure 30 shows the cases that were actually analyzed. Progressive crack growth from the first

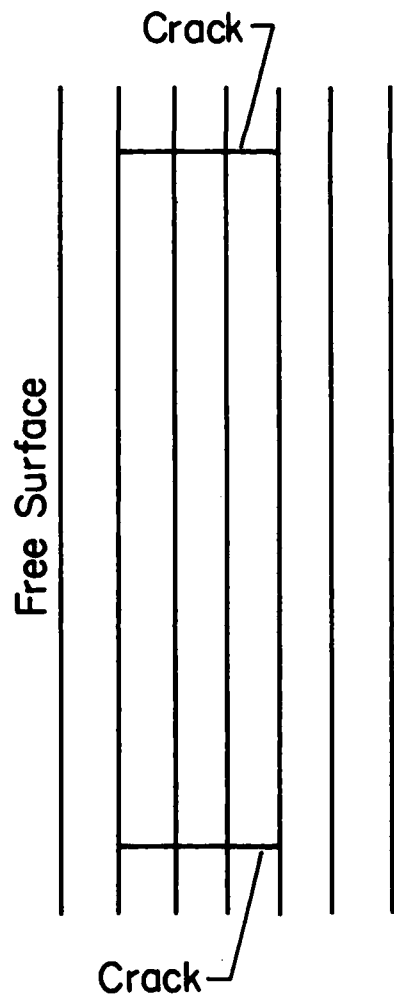


Figure 29: Schematic of Geometry Used for Shear-Lag Analysis in Type D Laminates

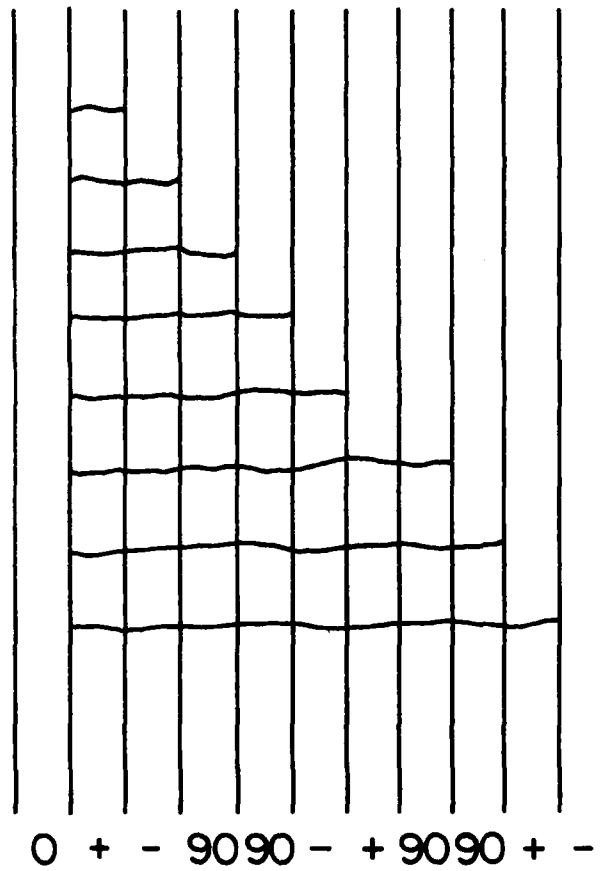


Figure 30: Cases of Crack Growth Analyzed for Type D Damage Analysis

+45° plies through the subsequent -45°,90°,90°,-45°,+45°,90°,90°, and remaining +45° plies were considered successively. Figure 31 indicates the crack opening displacement of the crack face for the longest crack considered as predicted from the analysis for a crack spacing of 0.035 inches. (The absolute amount of displacement is arbitrary.) It should be remembered that the shear-lag analysis is a net-section analysis in the sense that only one displacement function is used for each ply, so that the points in Fig. 31 are really computed average values of the displacement in each of the plies indicated.

Figure 32 shows the results of the predictions of local stress using that analysis compared to the changes in stiffness which are also calculated from that analysis. If we were determining these quantities from a laminate analysis using the discount scheme, as indicated earlier, there would be a direct proportionality between the percent change in stress and the percent change in laminate modulus as indicated by the diagonal trend line in Fig. 32. The calculations, indicated by the curved line in that figure, show clearly that the local stress increases at a more rapid rate than the change in laminate modulus. For example, a change of 3% in the modulus yields a 12% local change in the axial normal stress in the zero degree plies, corresponding to the crack formation in the 45° plies next to them. When both 45° plies and one 90° ply have cracked, the change in axial modulus is 13%, but the local stress changes by 32%. If the crack coupling extends throughout all of the off-axis plies indicated in Fig. 30, a 34% modulus change should be observed and a 77% increase in the local stress is predicted.

In order to apply this to our cumulative damage model, we consider the test results for specimens D1-5, D2-10, and D2-12 which are observed

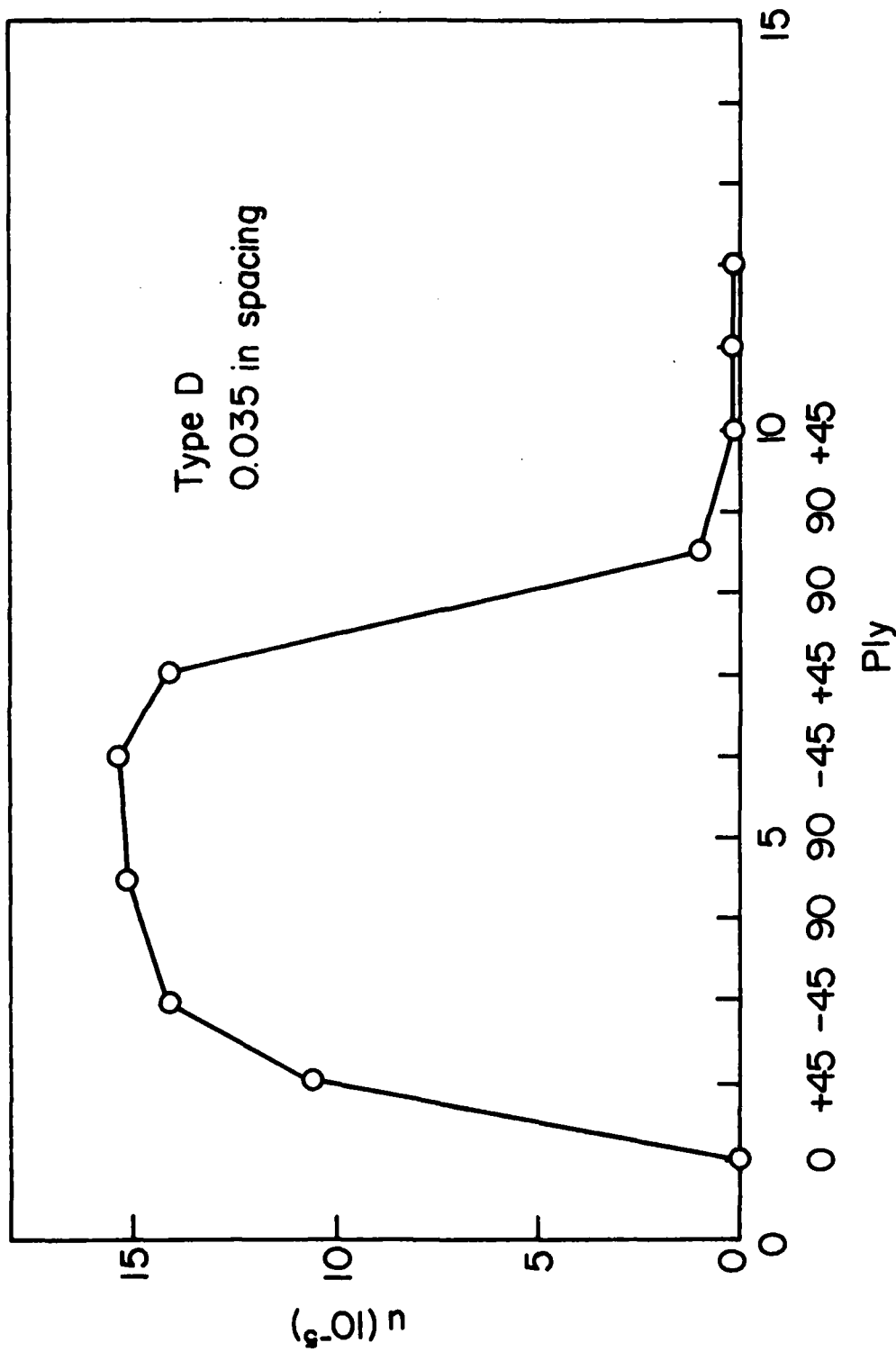


Figure 31: Crack Face Opening Geometry Predicted from Shear-Lag Analysis for a Long Coupled Crack in the Type D Laminate

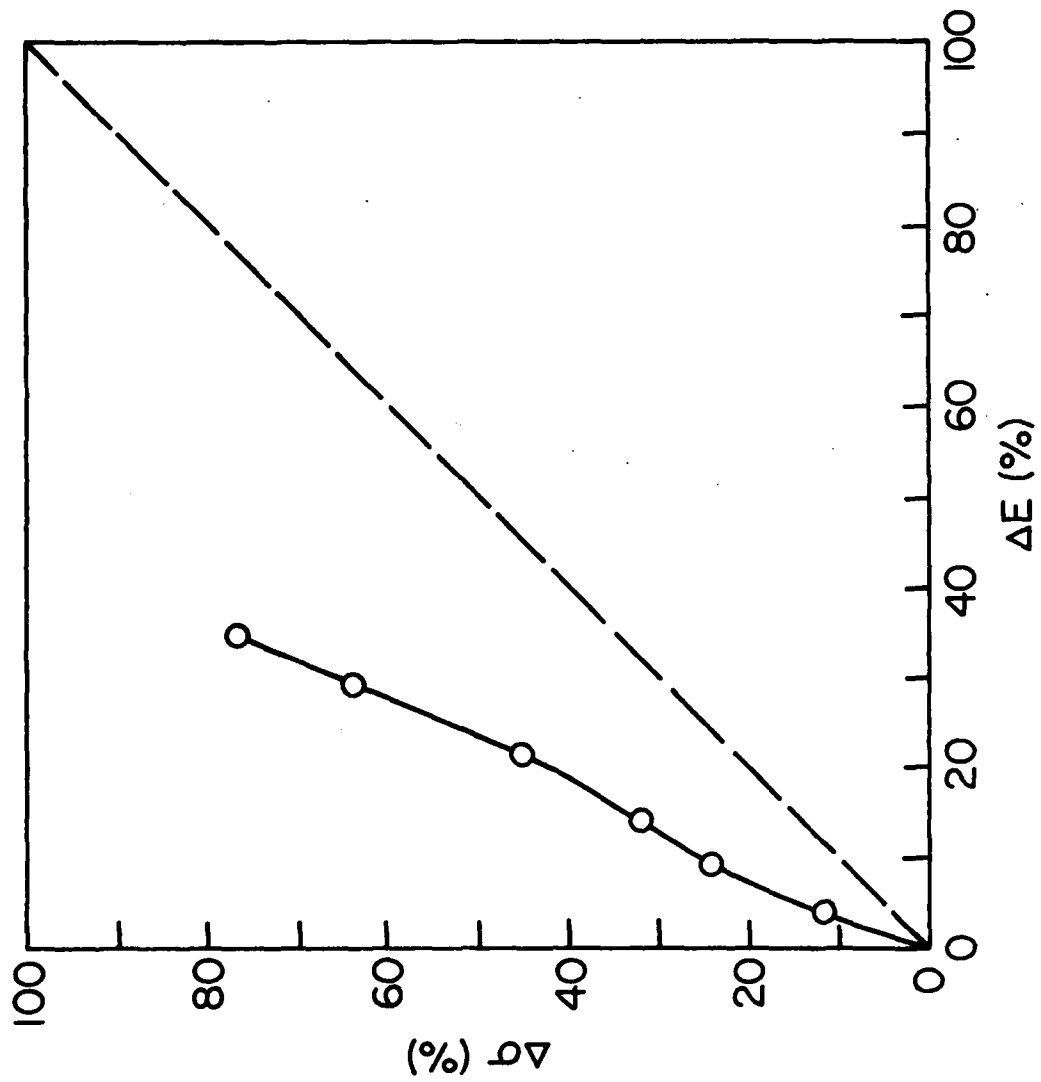


Figure 32: Comparison of Calculated Stiffness Change and Change in Local Axial Stress in the \emptyset Plies for Crack Coupling

to have a stiffness change of about 10% during tension-tension loading. According to our calculation, that stiffness change corresponds to a 26% change in local stress. Initially, the laminate applied stress is 21.4 ksi for those tests, which produces an axial normal stress in the 0° plies of 90.61 ksi calculated from laminate analysis. At one million cycles, after a 10% stiffness change and 26% local stress change, the stress in the zero degree plies is 113.3 ksi. If the strength of those zero degree plies is 230 ksi the local stress ratio begins at a value of 0.394 and rises to a value of 0.492 (which equals $113.3 \div 230$) during the test. If a linear interpretation of that change is used in the cumulative damage model as described earlier, the predicted residual strength change shown in Fig. 33 is obtained. A typical data point for the residual strength of 1.4 million cycles is also shown in that figure. It can be seen that the predictions are much more closely aligned with the observation. Comparison with the predictions in Fig. 33 with the observations in Fig. 28 confirm that in general the predictions are brought into much better agreement with the data for this extreme case of stress redistribution. It is also possible to infer that better estimates of the local stresses in the zero degree plies obtained from more precise analyses, as they become available, can be used to obtain further improvements in the predictions of the model. It is important to note that local stress redistribution is an absolutely essential element of the correct modeling of cumulative damage in this laminate under fatigue loading. Finally, it is well to mention that the basic structure of the model was not altered to account for this extreme case; it was only necessary to improve the micromechanics (or mini-mechanics) models that are used to obtain

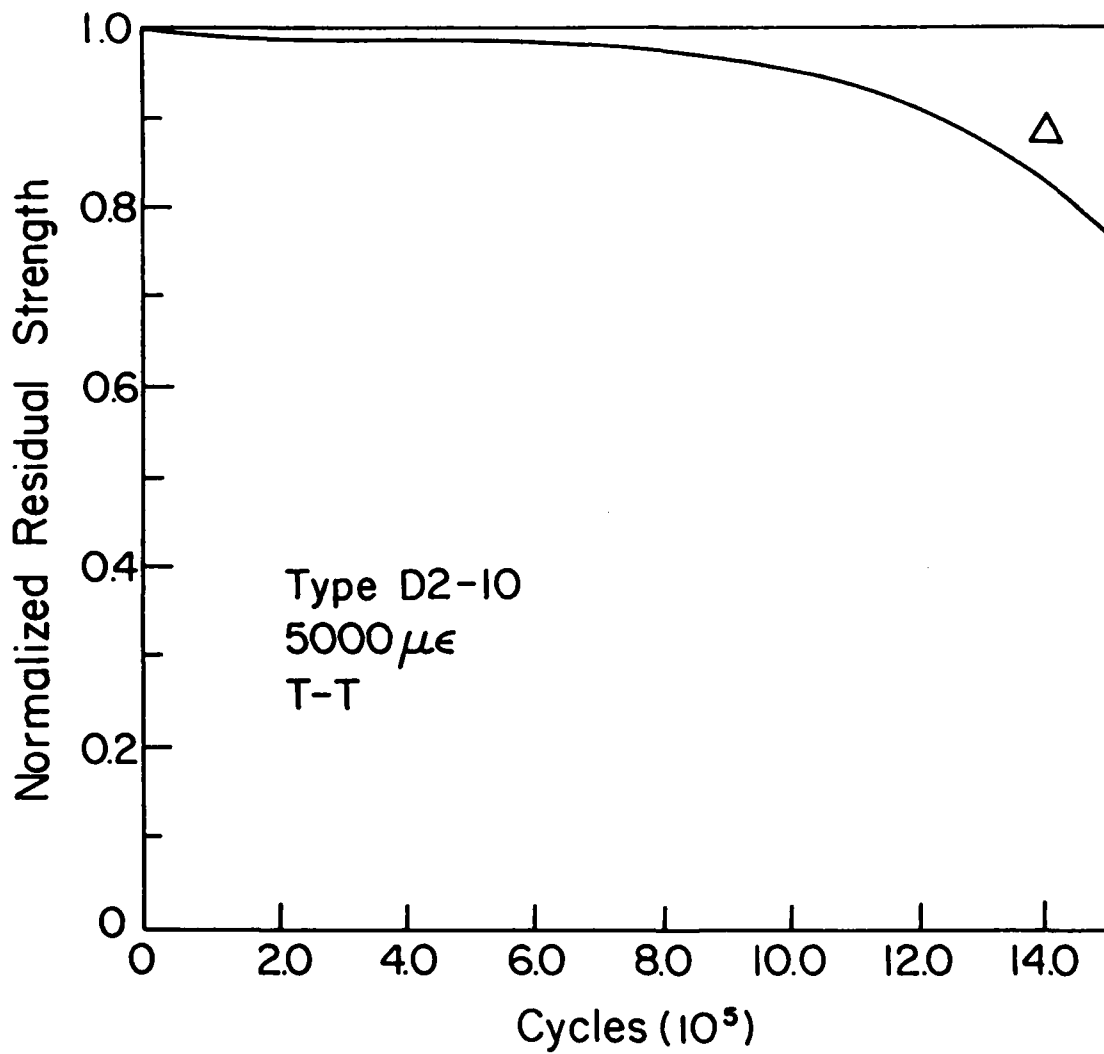
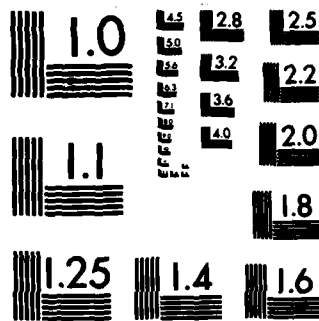


Figure 33: Residual Strength Prediction and Typical Observation for Shear-Lag Refinement of the Damage Accumulation Model



MICROCOPY RESOLUTION TEST CHART
NATIONAL BUREAU OF STANDARDS-1963-A

information about the internal stress field near the damage development events.

We continue our discussion by considering the Type F laminate which has a stacking sequence of $[(0,\pm 45)_s]_{4s}$. This laminate has a very high loading of zero degree plies and is very strong under axial and shear loading. The quasi-static properties are given in Section III. Initially the ratio of axial normal stress in the fiber direction of the zero degree plies to the applied stress on the laminate in that direction is 2.3. If the discount method is used, when the -45° plies crack the ratio changes to a value of 2.5, a 10.5% change. When the $+45^\circ$ plies also crack the ratio changes to 2.87, a total change of about 25%. Generally, during the fatigue testing of these laminates, the stiffness changes were rarely more than 10 to 15%. We note in passing that the calculated strength of the Type F laminate using the discount method was 81 ksi compared to an average value for the quasi-static tests of this laminate of about 80 ksi. (A Tsai-Hill theory of failure was used.) For the purpose of demonstration, a second interpretation of the local failure function, F_L , was introduced. Up to this point, that function had been taken to be equal to the local stress ratio in the zero degree plies. When that interpretation is used to predict the residual strength reduction for specimen F2-2, which was cycled with a maximum stress of 71 ksi, a life of about 14,000 cycles is predicted as shown in Fig. 34, compared to an observed life of about 21,000 cycles. At 10,000 cycles the residual strength is predicted to have been reduced to a normalized value of 0.88. Specimen F5-5 run at essentially identical stress levels had a strength retention of 0.97 which compares reasonably with the predicted number. Also shown in Fig. 34 is a curve

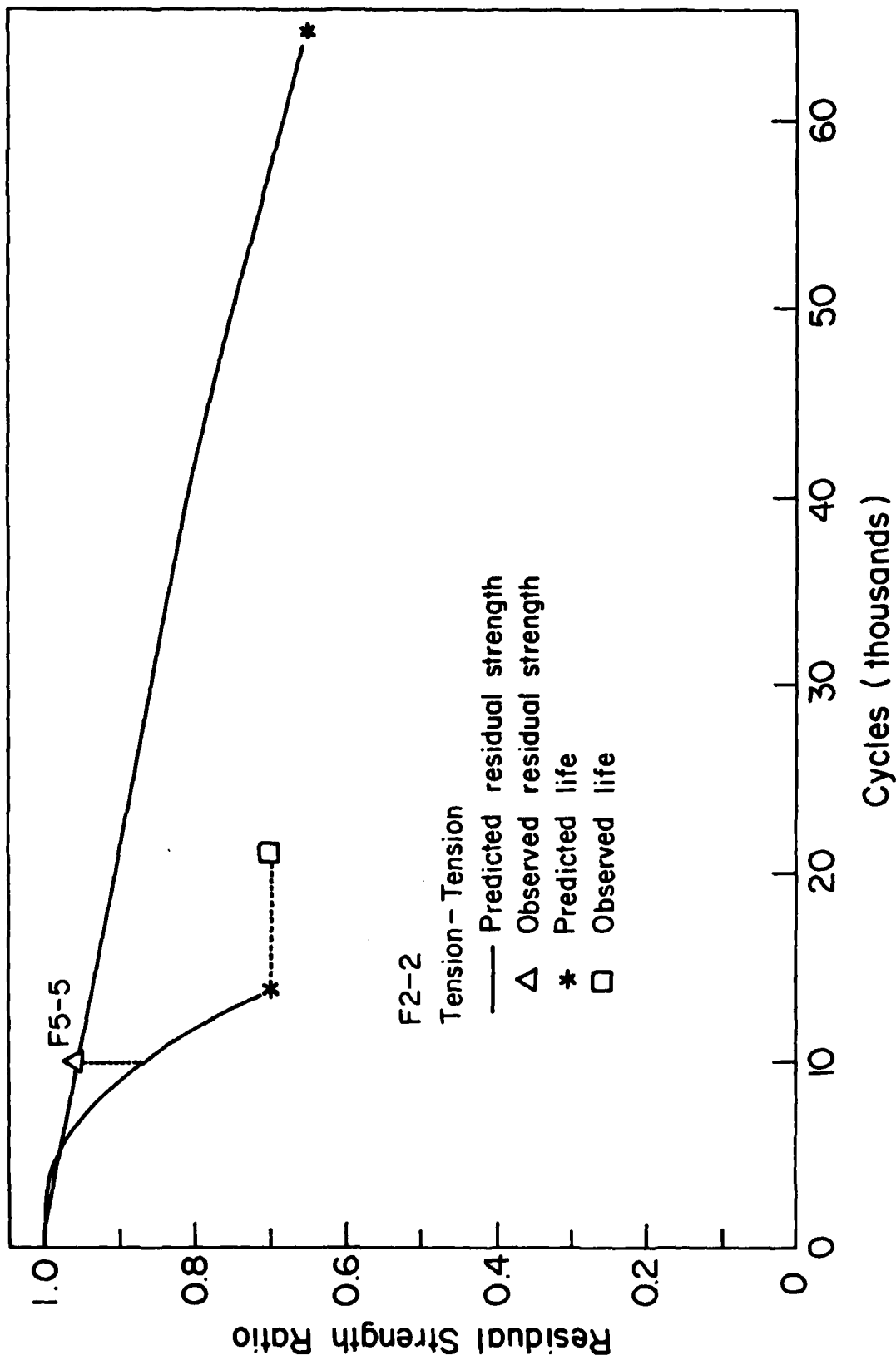


Figure 34: Residual Strength and Life Predictions for Uncorrected Model, Showing Effect of Stress Redistribution

of predicted residual strength which ends in a life prediction of over 60,000 cycles. That curve corresponds to the same cumulative damage model when stress redistribution is ignored. It is clear that the influence of stress redistribution is extremely great in this highly fiber-dominated laminate. The predictions of this model would make no sense at all if the internal stress redistribution due to damage development were ignored.

As we mentioned above, the local failure function, F_L , was reinterpreted in this series of tests. Figure 35 illustrates some of the results of that variation. It was decided to consider the case when the local failure function was set equal to the ratio of the applied laminate stress to the predicted laminate undamaged strength from the Tsai-Hill criterion used in the laminate analysis mentioned earlier. The predicted undamaged strength is used since the applied stress is thought to cause damage in the laminate in proportion to the strength of the laminate before damage occurs, rather than to the measured strength of the laminate after damage has occurred due to the increase in stress beyond the level of maximum stress during cyclic loading, i.e., the final quasi-static strength. Hence, for specimen F2-2 the initial value of the local failure function was taken to be $71.2 + 104.42$ or a ratio of 0.683. The 10% modulus change and corresponding increase in laminate strain was assumed to cause an increase in that ratio of about 10% as well over the period of the test. The results of that computation are shown on the left-hand side of Fig. 35, again for a calculation for which the stress redistribution was considered and for which it was ignored. The corrected calculation of life for specimen F2-2 is shown as a prediction "with stress redistribution and Tsai-Hill failure

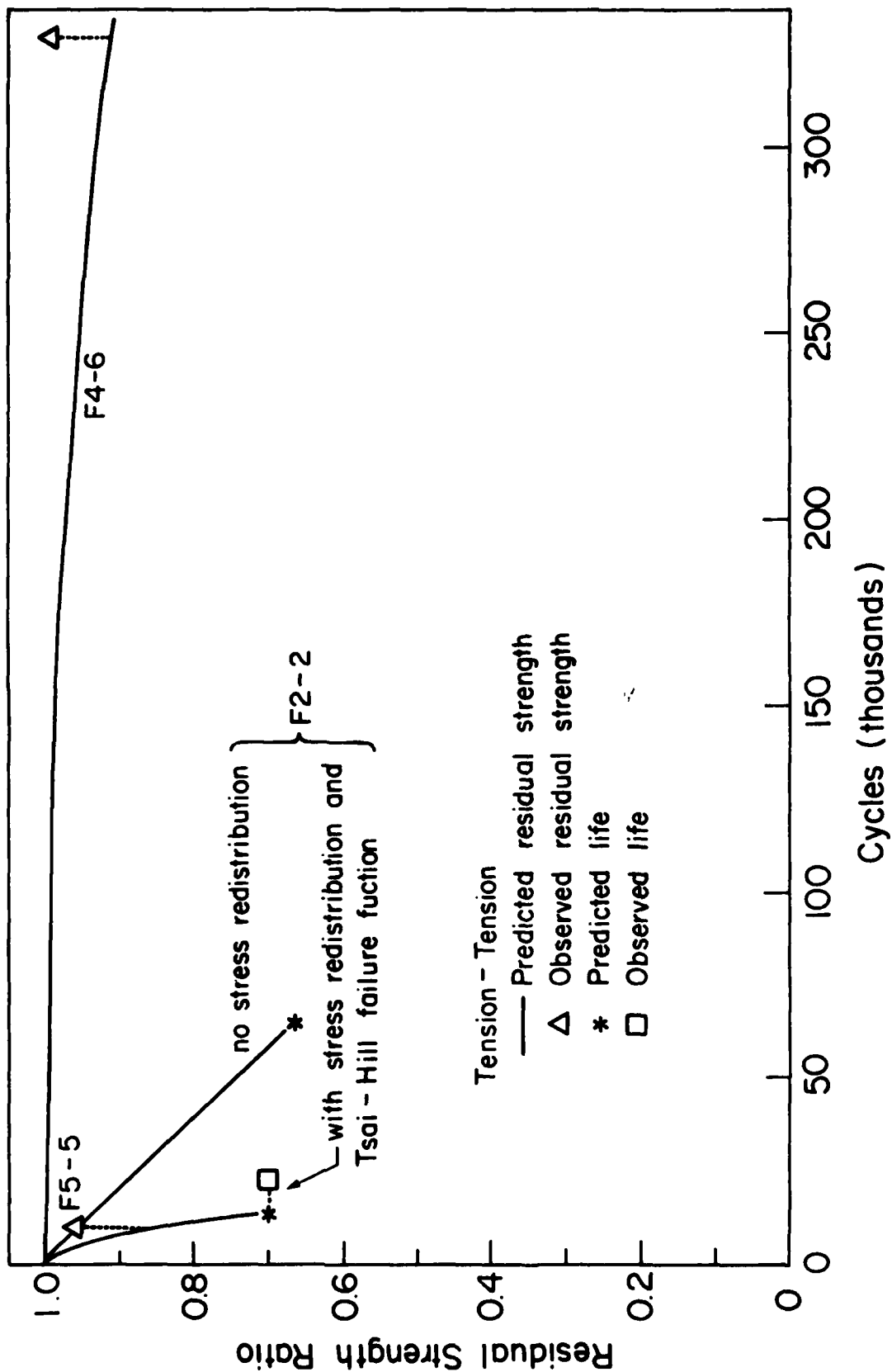


Figure 35: Predictions and Observations for Model in which F1, the Local Failure Function, was Set Equal to the Ratio of Applied Stress to Undamaged Strength

function" and compares quite well with the observed life of that specimen. Again, the predictions which ignore stress redistribution are widely different from the observed data. A similar computation is shown for specimen F4-6. The maximum stress for that specimen was 57.1 ksi. Hence, the initial value of the failure function was 0.55 increasing by about 8% (corresponding to an 8% change in stiffness) to about 0.6. The local stress in the zero degree plies for that case begins at a stress ratio of about 0.53 and increases to about 0.575. The estimated life for that case is about 550,000 cycles. The predicted residual strength retention at 330,000 cycles was 0.93. The measured strength retention at that number of cycles for specimen F4-6 was essentially 1.0.

Specimen F1-9 was also modeled, and represents an intermediate loading level. The maximum stress in that test was about 63.8 ksi. The specimen demonstrated approximately a 10% stiffness change at about 250,000 cycles and failed at 290,000 cycles. However, the predicted life for that specimen was 150,000 cycles and the predicted residual strength reduction was too great. Figure 36 shows the data indicated in Fig. 35 on a semi-logarithmic scale which allows the life prediction to be indicated. The figure also serves to illustrate the "exaggeration" of the nonlinearity in the residual strength reductions caused by the plotting procedure as noted earlier.

At this point, another refinement will be discussed based on the biaxiality of the stress in the zero degree plies in this particular laminate. The data in Table 5 illustrates this biaxiality. That table presents the stresses in the zero degree plies of a Type F laminate during damage development as determined from laminate analysis using the discount method described earlier. The stress in the zero degree plies for both a Type F and a Type C laminate are shown for comparison

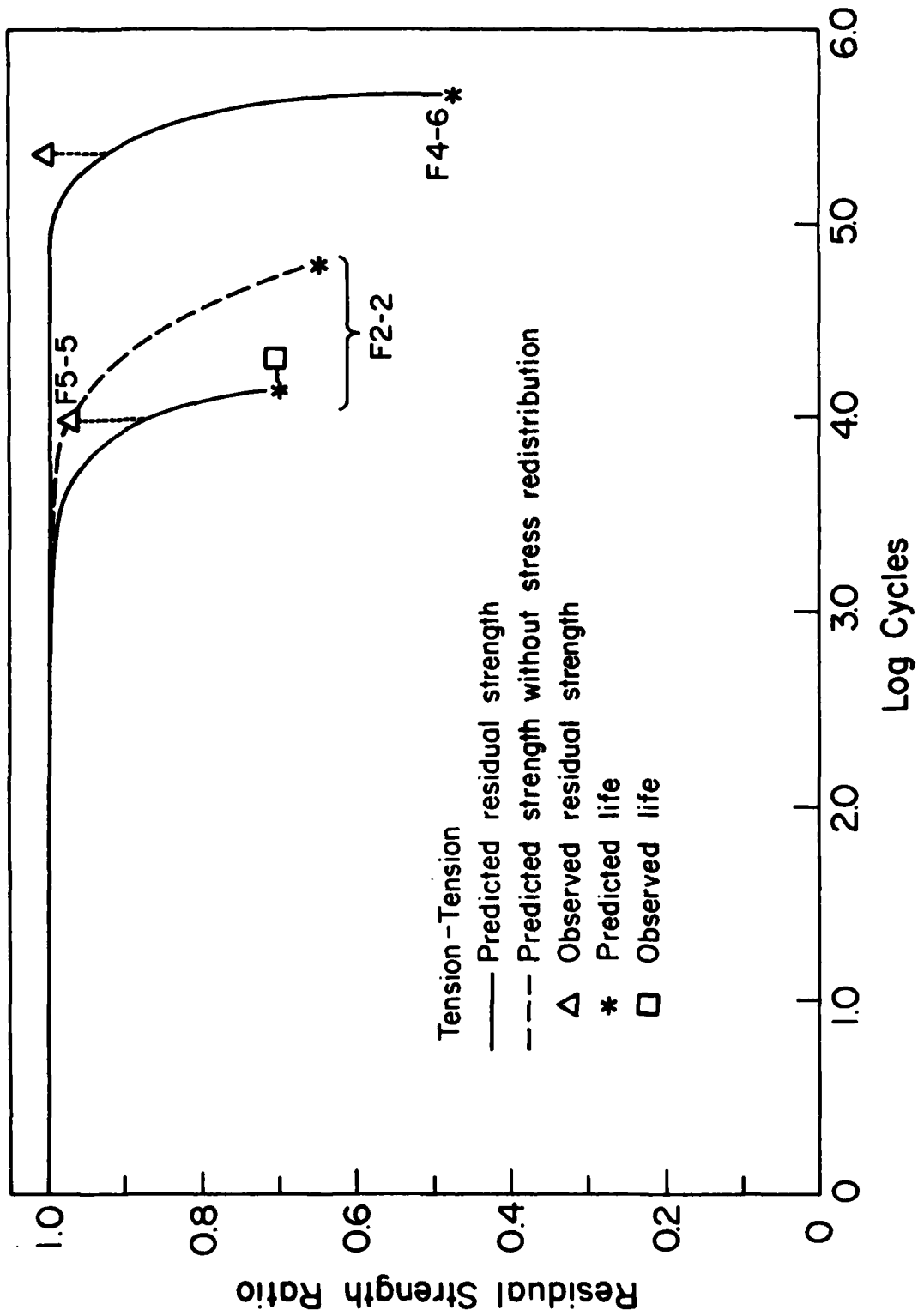


Figure 36: Semi-Log Plot of Data in Fig. 35 Showing Life Prediction for Specimen F4-6

TABLE 5.

STRESSES IN 0° PLYS OF TYPE F LAMINATES DURING DAMAGE DEVELOPMENT
(APPLIED STRESS = 1000 UNITS)

| | σ_x | σ_y | τ_{xy} | f.f.(1) |
|-------------------------------|------------|------------|-------------|---------|
| Type F Laminate: | | | | |
| Undamaged | 2295 | - 65.9 | 0 | 0.94 |
| One 45° ply cracked | 2536 | - 90.2 | 0 | 0.92 |
| Two 45° plies cracked | 2873 | -126.9 | 0 | 0.89 |
| Type C Laminate: | | | | |
| Undamaged | 2541 | 1.2 | 0 | 1.00 |
| 90° plies cracked | 2646 | 3.9 | 0 | 0.998 |
| All off-axis plies cracked | 2993 | - 5 | 0 | 0.994 |

purposes. The last column of that table shows the computed value of the first term of the Tsai-Hill failure function (which corresponds to the normalized axial stress in the zero degree plies in the fiber direction) for the situations described. In the Type F laminate (for an applied stress of 1,000 units) the axial normal stress in the two laminates begins at a similar value. However, the transverse normal stress is compressive in the Type F laminate and tensile in the Type C laminate. Moreover, that transverse normal stress in the zero degree plies is more than 60 times as large in magnitude in the Type F laminate as it is for Type C specimens. The initial failure function is 0.94 for Type F and 1.0 for Type C. As damage develops, an even greater contrast develops between the types of laminates. The fiber-direction normal stress in both laminates increases, to 2,536 units in the case of Type F and to 2,646 units in the case of Type C. However, the transverse normal stress increases in the case of the Type F laminate and decreases in the case of the Type C laminate. When all of the off-axis plies are cracked, the axial normal stress in the zero degree plies is 2,873 units for Type F and 2,993 units for the Type C laminate. However, the transverse normal stress in the Type C laminate has passed through zero and has become slightly compressive, but still small in magnitude. The transverse normal stress in the Type F laminate has gained another order of magnitude to reach a compressive value of 126.9 units. This increase in biaxiality for the Type F laminate is also illustrated by the progression of the failure function values from 0.94 to 0.92 to 0.89. In the case of the Type C laminate the values of the failure function remain very close to unity beginning at a value of 1.0, changing to 0.998, and ending up at 0.994. Hence, we have a situation where the

internal stress redistribution is increasing the biaxiality of the internal state of stress and is influencing the rate of degradation in the zero degree plies. The reader may recall that one of the justifications for choosing a one-dimensional characterization of the internal stress in the zero degree plies and of the change in that stress with internal redistribution is the fact that, for most common laminates, the state of stress in the zero degree plies becomes more uniaxial as damage develops in the other off-axis plies. The Type F laminate is a distinct (and intentional) exception to that generality.

An experienced experimentalist might be quick to point out that the large values of transverse compressive stress (only one order of magnitude smaller than the axial normal stress) in the zero degree plies might produce a reduction in the rate of degradation of the zero degree plies by helping to prevent longitudinal cracking and related types of damage in those plies. Such an observation is certainly consistent with the fact that the model overestimates the degradation of these materials when only one-dimensional stresses are considered. With those observations as a starting premise, we pose the critical question. How is it possible to incorporate the "positive" aspect of the "negative" transverse normal stress in the zero degree plies into our phenomenological representation of the S-N behavior of those plies? A relationship such as Eqn. (9) could be solved for the number of cycles to failure for an arbitrary biaxial stress state as in Eqn. (10) if all of the parameters in that equation were known.

$$\left(\frac{n}{N_1(\sigma_1)}\right)^2 + \left(\frac{n}{N_2(\sigma_2)}\right)^2 - \frac{n^2}{N_1(\sigma_1)N_2(\sigma_2)} + \left(\frac{n}{N_5(\sigma_{12})}\right)^2 = 1 \quad (9)$$

$$n = \frac{1}{\frac{1}{N_1(\sigma_1)^2} + \frac{1}{N_2(\sigma_2)^2} - \frac{1}{N_1(\sigma_1)N_2(\sigma_2)} + \frac{1}{(N_s(\sigma_{12}))^2}}^{1/2} \quad (10)$$

That would require characterization of the zero degree plies under fiber direction normal stress (to produce N_1), under transverse normal stress (to determine N_2), and under shear stress (to determine N_s) with a sufficient data base to establish Eqn. (9). That information was not (and generally is not) available.

As an interim measure, we postulate that the local fiber direction stress is diminished in its influence on the degradation of that ply by an amount which is proportional to the absolute value of the first term in the Tsai-Hill failure function according to the data presented in Table 5. Hence, if half of the 45° plies crack in that laminate, the local fiber stress ratio would be multiplied by 0.92 to account for the fact that the compressive normal stress in the transverse direction is diminishing the effect of the increased axial normal stress in the fiber direction. While this refinement is somewhat artificial, it is at least rational. Using that refinement, and the refinement of the local failure function mentioned earlier, all of the data predictions were recalculated and plotted in Fig. 37. The predictions are seen to agree surprisingly well with the experimental data for both residual strength and life. For specimen F2-2, for example, the predicted life is about 27,000 cycles compared to the observed life of about 20,000. The predicted residual strength retention at 10,000 cycles is about 0.98 which compares nicely with the experimental data for specimen F5-5 which

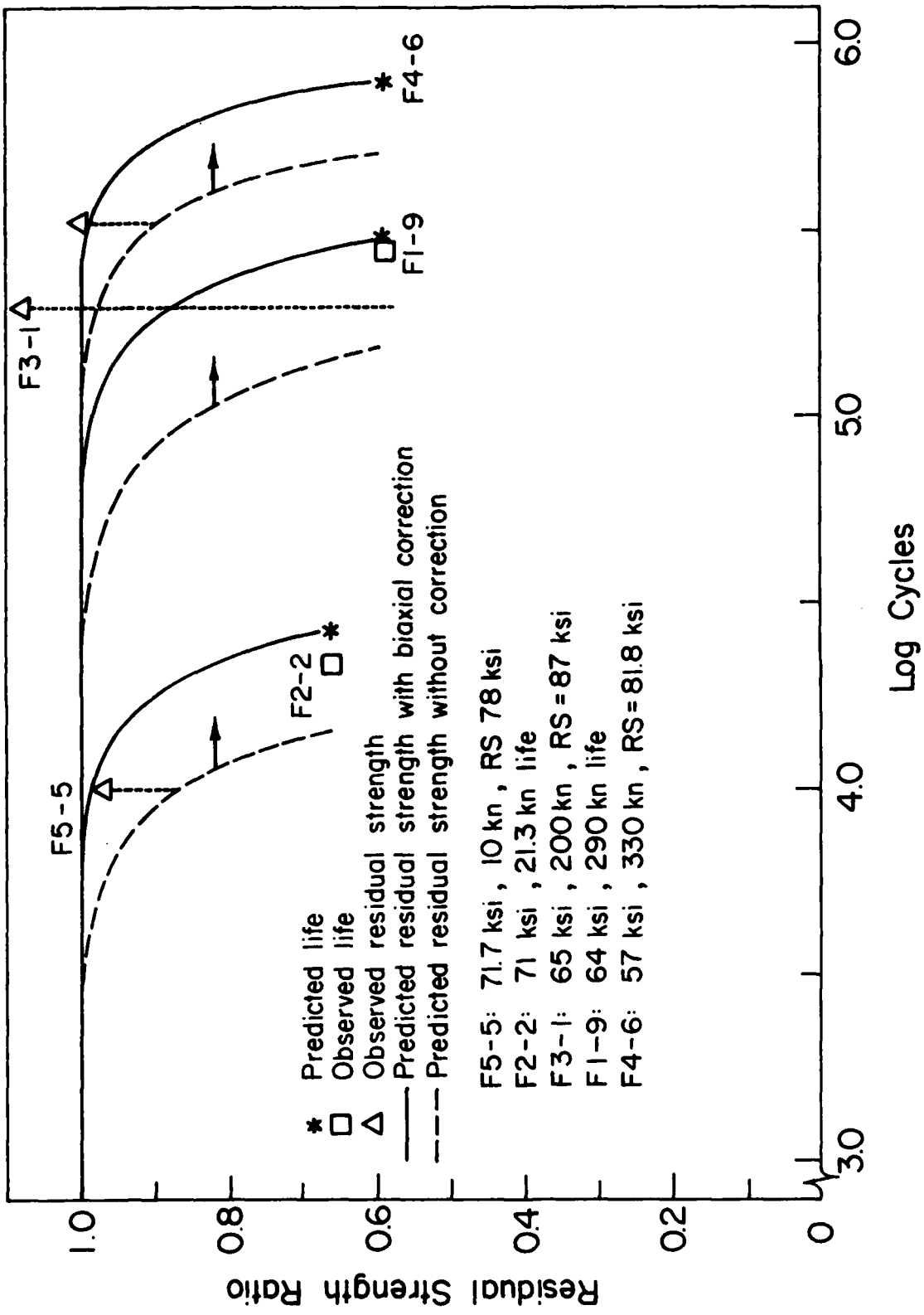


Figure 37: Predicted and Observed Data for Type F Laminate in T-T Loading for Model with Biaxial Correction

was 0.97. For specimen F4-6, the predicted life becomes 800,000 cycles and the residual strength retention at 330,000 cycles is predicted to be 0.98 which compares well with the measured value of about 1.0. The life prediction for specimen F1-9 is virtually coincident with the observed data. The residual strength retention for that load level is considerably less than the experimental observation for specimen 3-1, but that value is certainly suspect since it is nearly 115% of the average quasi-static measured value. In general, the biaxial correction appears to be reasonable.

It should be mentioned that this biaxial correction scheme cannot be extrapolated. In the limit, it predicts the ridiculous result that an infinitely large compressive normal stress in the transverse direction in the zero degree plies would completely suppress the degradation of those plies! In reality, of course, no such "huge" values are observed. And, the correction scheme should be interpreted more in the sense of having the degradation of the zero degree plies suppressed in deference to another damage mode or simply suppressed altogether. It is also possible, that one could discuss this behavior in terms of stress interaction concepts. These points cannot be resolved without substantive further physical information and a considerable amount of basic research effort. Until such information and data is available, the present scheme is judged to be a reasonable alternative interim practice.

This completes our discussion of the tension-tension cumulative damage model. Figure 38 provides a summary of the refinements generated for that model. It is clear from our discussion that a number of further refinements can be made. However, the authors suggest that there is considerable evidence that the basic tenets of the model (such

Refinements:

1. Static strength of 0 degree plies (used to normalize all inputs) calculated from each laminate type quasi-static data.
2. Local stress redistribution corrected for crack coupling.
3. Local failure function corrected for individual laminate type behavior.
4. Local stress in 0 degree plies adjusted to compensate for effects of strong biaxiality of the stress state.

Figure 38. Summary of Refinements to Tension-tension Cumulative Damage Model.

as stress redistribution, critical elements, subcritical elements, and the cumulative damage integral concept) are valid and generally useful.

B. Compression Loading

We now consider fatigue loading spectra which have compression components. The modeling of fatigue degradation, especially for the purpose of determining residual strength and life, is greatly complicated by a number of factors. Perhaps the most important of these is the fact that failure in compression loading is usually a stability problem, at least when the specimen is not side-supported as was the case in the present experiments. Parenthetically, it should be noted that for most applications in practical situations for which composite materials are commonly used compressive failure usually involves macro- or micro-buckling of some type. The presence of buckling seriously constrains and complicates the interpretation of test data and the generality of any model of that behavior. Factors such as the precision with which the specimens are made, the degree to which the alignment of the specimen in the test machine is perfect, the accuracy with which the specimens are cut from the original plates, the absolute repeatability of all testing conditions, the degree of identity between the internal microstructure of each of the laminate specimens tested, and a variety of other realities contribute to an apparent variability in behavior which can be a serious obstacle to rational modeling.

In the paragraphs that follow, we will include a considerable amount of our experience, a limited amount of which actually contributed to the final form of the model that was used to describe the behavior

under this type of loading. However, it is believed that the other experiences were constructive and might provide guidance and useful stimulation to the reader.

One of the ideas which seemed to produce interesting modeling results was the use of a critical stiffness concept. The basis of this idea really lies within the association between stiffness and buckling. One possible scenario for the present objectives based on that association can be demonstrated by considering Eqn. (11)

$$\sigma_c = \frac{\pi^2 EI}{l^2 A} + \epsilon_c = \frac{\sigma_c}{E} = \frac{\pi^2 I}{l^2 A} \quad (11)$$

which is the familiar Euler Buckling Formula for a simple column. When that formula is rearranged in such a way that it describes a critical strain value, the remaining terms on the right-hand side of the equation are geometric (or otherwise) constant. It is possible, then, to make the premise that buckling failure in compression loading occurs when the stiffness of the laminate (specimen) is reduced to the point where the critical strain is realized in the specimen for a given applied load, as suggested by Eqn. (12).

$$\epsilon_c = \frac{\sigma \text{ (applied, constant)}}{E(n) \text{ (measured, cycle dependent)}} \quad (12)$$

It is also possible to associate these concepts with the terms that one finds in Eqn. (3). One way of doing that is to associate the compressive aspects of damage development with edge delamination, an idea that is strongly supported by physical observations. Let us say, for example, that the stiffness reduction of the specimen during cyclic

compressive loading corresponds to the stiffness reduction predicted by a linear relationship first stated by O'Brien as given in Eqn. (13).

$$E(n) = E_L + (E^* - E_L) \frac{a}{b} \quad (13)$$

In that equation, E_L is the initial modulus of the laminate, E^* is the completely delaminated modulus of the laminate, a is the length of the delamination growth, and b is the half-width of the specimen which is delaminating. Hence, The equation states that as the delamination grows across a fraction of the width of the specimen given by a/b , the modulus of the laminate will be reduced to the value given by Eqn. (13) as a function of the number of cycles of loading. If one now combines Eqns. (13) and (12), and solves for the critical crack length, a_c , which corresponds to a critical reduction in stiffness, one obtains the expression given in relationship (14).

$$a_c = \frac{b(\sigma^0 / \epsilon_c - E_L)}{E^* - E_L} \quad (14)$$

The stress entered in Eqn. (14) is the maximum absolute value of the applied stress in compression, a constant. Then in Eqn. (3), we take the ratio of the number of applied cycles to the total life of the specimen to be equal to the ratio of the current crack length to the critical crack length for buckling of the specimen as shown in Eqn. (15).

$$\frac{n}{N} + \frac{a}{a_c} = \frac{\sigma^0 / \epsilon(n) - E_L}{\sigma^0 / \epsilon_c - E_L} = \frac{E(n) - E_L}{\sigma^0 / \epsilon_c - E_L} \quad (15)$$

As the equation shows, it is apparent that such a ratio is equal to the current change in stiffness divided by the critical change in stiffness. In order to maintain our normalized form of all the quantities to be entered into Eqn. (3), and to make our data interpretation scheme simpler, the final ratio to be used is expressed in normalized form as shown in Eqn. (16).

$$\frac{n}{N} \rightarrow \frac{\Delta E(n)/E_L}{\Delta E_c/E_L} \quad (16)$$

Hence, Eqn. (3) takes the form shown in Eqn. (17).

$$\Delta S(n) = \int (1-F_L(n)) \left(\frac{\Delta E(n)/E_L}{\Delta E_c/E_L} \right)^{i-1} d \left(\frac{\Delta E(n)/E_L}{\Delta E_c/E_L} \right) \quad (17)$$

We will examine the results obtained for two choices of the local failure function, F_L . In one case, that function was set equal to the critical value of the change in stiffness divided by the initial laminate stiffness. In the second case, that function was set equal to the simple ratio of the laminate applied stress to the buckling stress of the laminate measured in quasi-static compression. Similar results were obtained for the two situations. We will examine some of those results below, and follow that discussion with another development which differs considerably from the present details.

Stiffness changes observed during cyclic compression-compression (C-C) loading were large. An example of those changes is shown in Fig. 39 for four levels of cyclic loading corresponding to the microstrain ranges indicated in that figure on each of the curves.

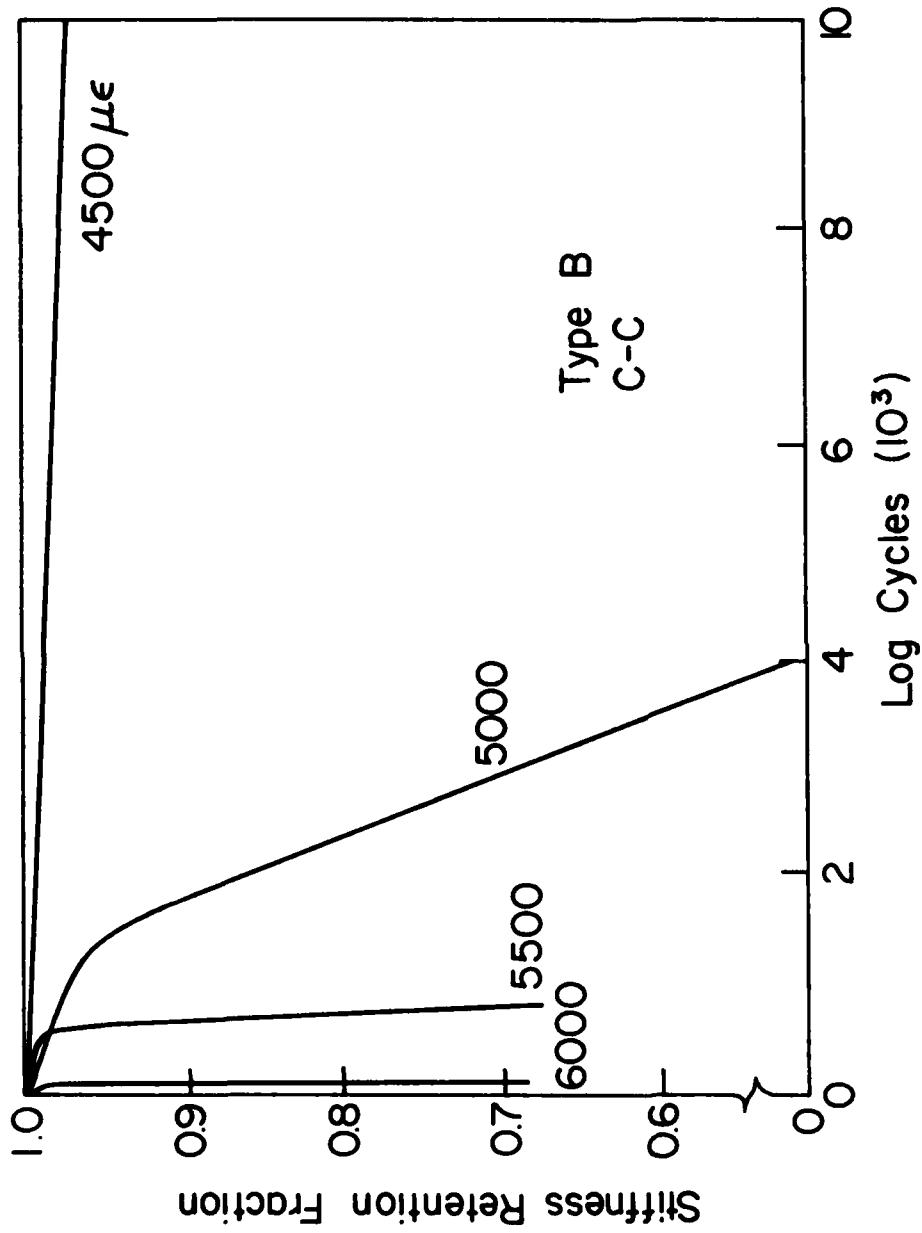


Figure 39: Stiffness Retention Fraction for Several C-C Tests of Type B Specimens

Fifty percent reductions in (compressive) stiffness were common. In order to enter those changes into Eqn. (17), the fractional stiffness change as a function of cycles is needed. Curves were fitted to the data for those fractional stiffness changes. Figures 40 through 41 show the normalized stiffness changes for the three lower stress amplitudes shown in Fig. 39. These fractional stiffness changes were entered into Eqn. (12) as described earlier, and the local failure function, F_L , was set equal to the ratio of the applied strain level to the critical strain level for buckling, a ratio which is equivalent to the ratio of applied to ultimate stress. However, it was found that the buckling strain under quasi-static loading was not appropriate as a critical (normalizing) strain for the ratio to be used for F_L . It should be remembered that failure under C-C loading was controlled not only by the buckling of the specimen, but by the dynamic response of the test system including the test machine and the specimen itself. Failure was actually defined under cyclic loading as that point at which the specimen became so compliant that the test machine was unable to cycle over the compressive stress range that had been set as a required constant. Such a situation can hardly be ascribed the significance of a material constant! It was found that the critical dynamic strain for buckling under cyclic loading was about 12,400 $\mu\epsilon$. That quantity was used in the denominator of the ratio F_L . The applied strain range was the numerator.

The resulting calculations of residual strength and life are shown in Figs. 43 through 45 for the data indicated in Figs. 40 through 42. The results of these modeling efforts are shown in summary form in Fig. 46. The corresponding maximum compressive stress ranges are also

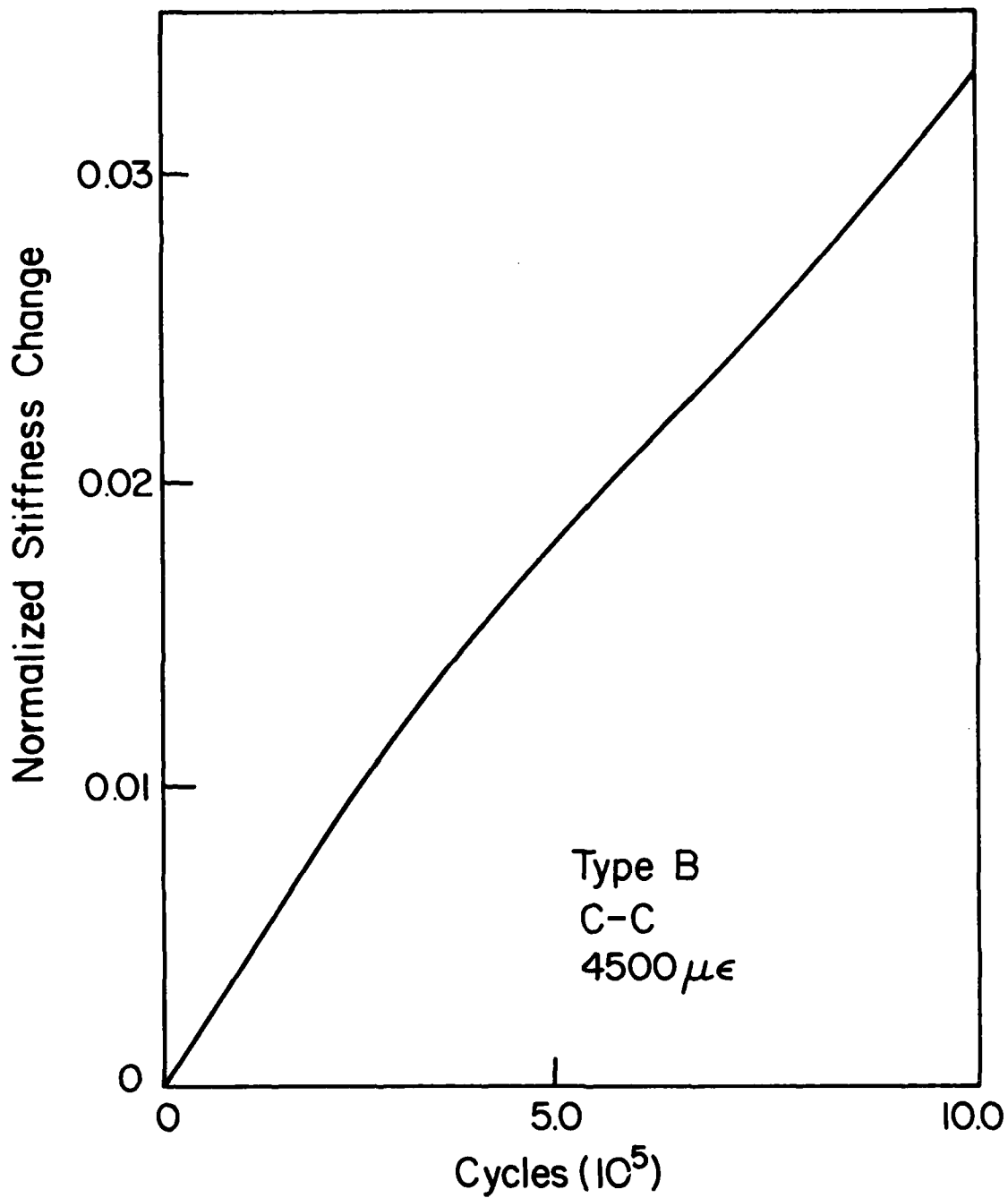


Figure 40: Fractional Stiffness Change for a Typical Type B Specimen Loaded in C-C at 4500 $\mu\epsilon$

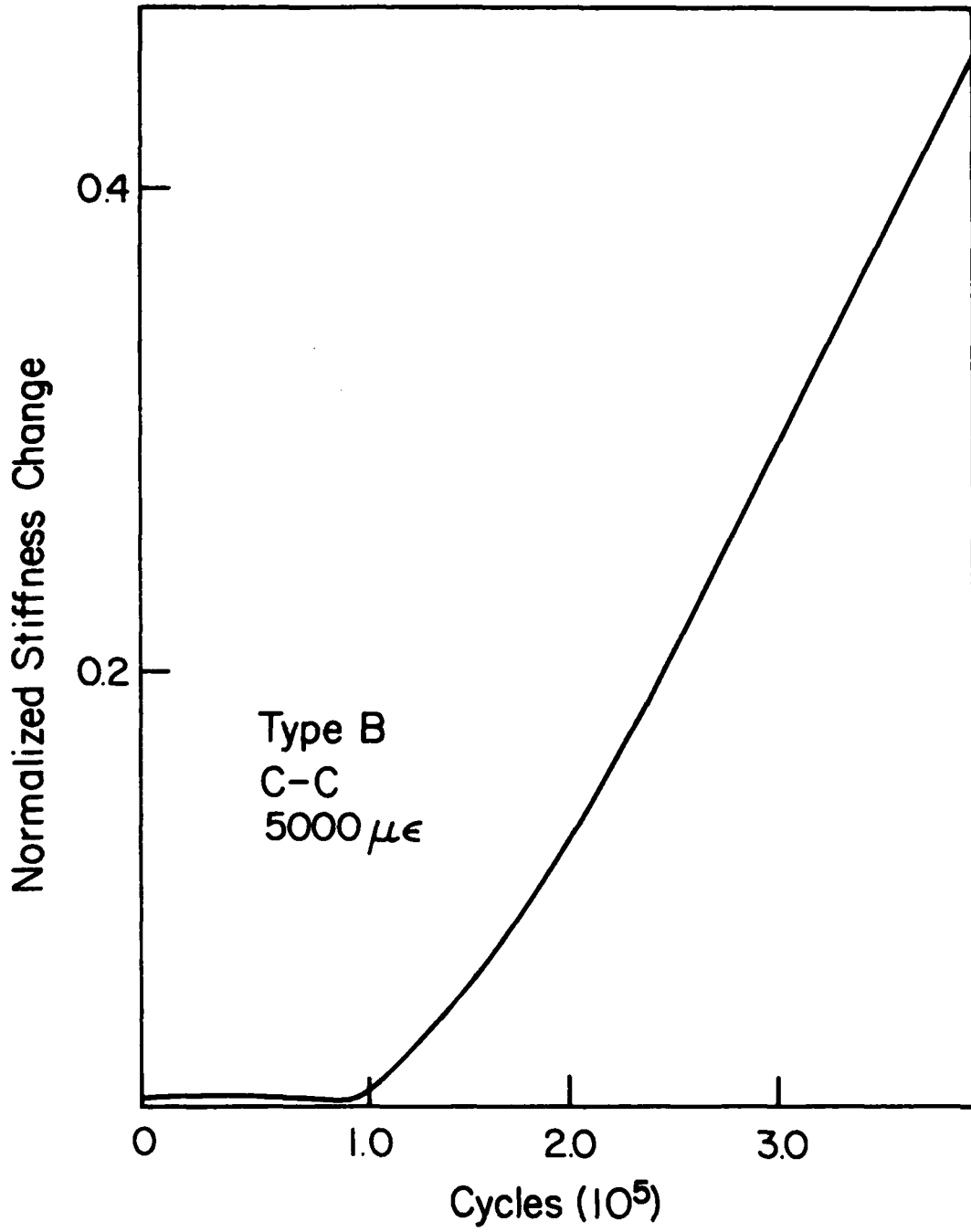


Figure 41: Fractional Stiffness Change in a Type B Specimen for C-C Loading at $5000\mu\epsilon$

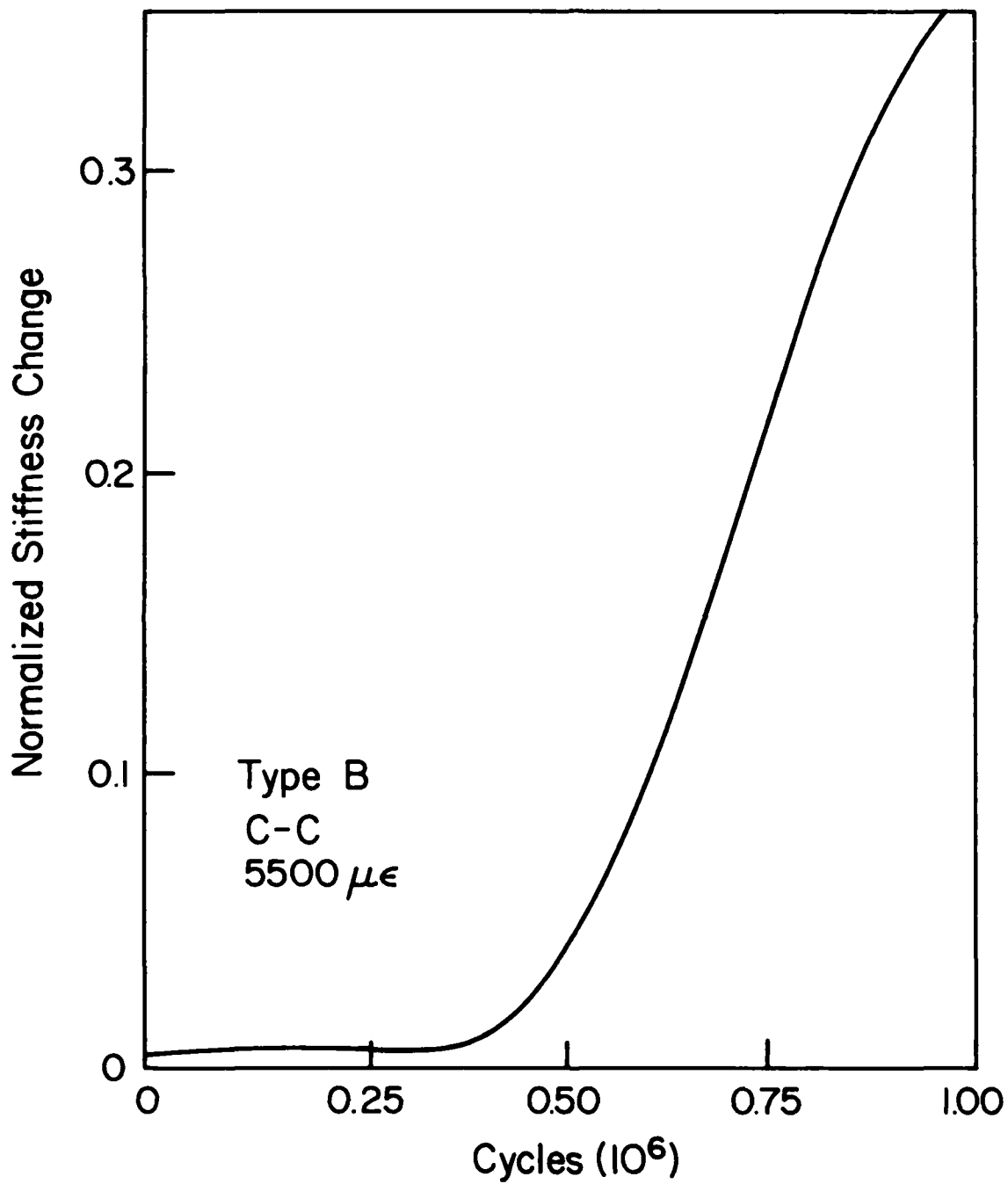


Figure 42: Fractional Stiffness Change in a Type B Specimen for C-C Loading at 5500 $\mu\epsilon$

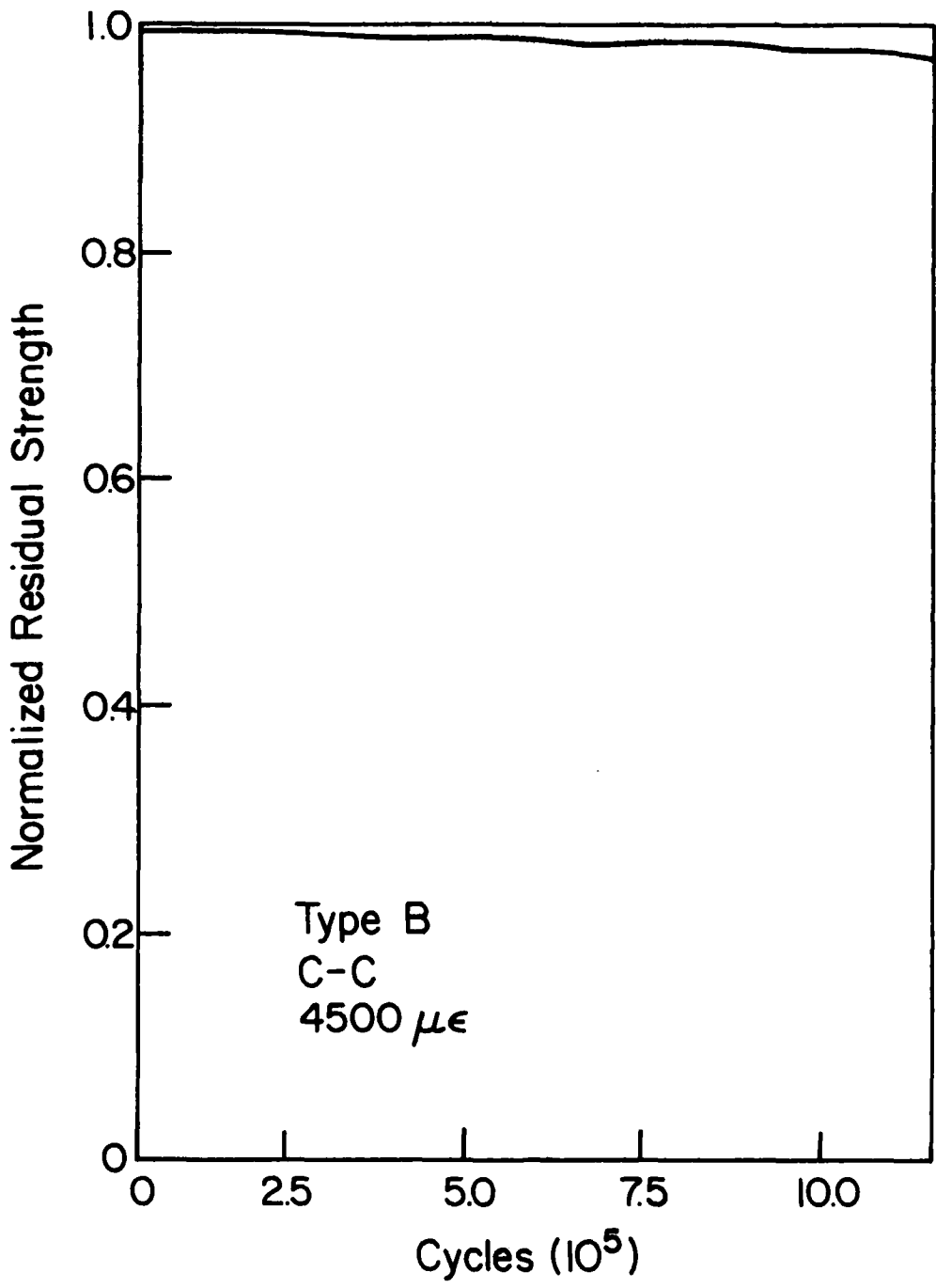


Figure 43: Residual Strength Prediction for C-C Loading

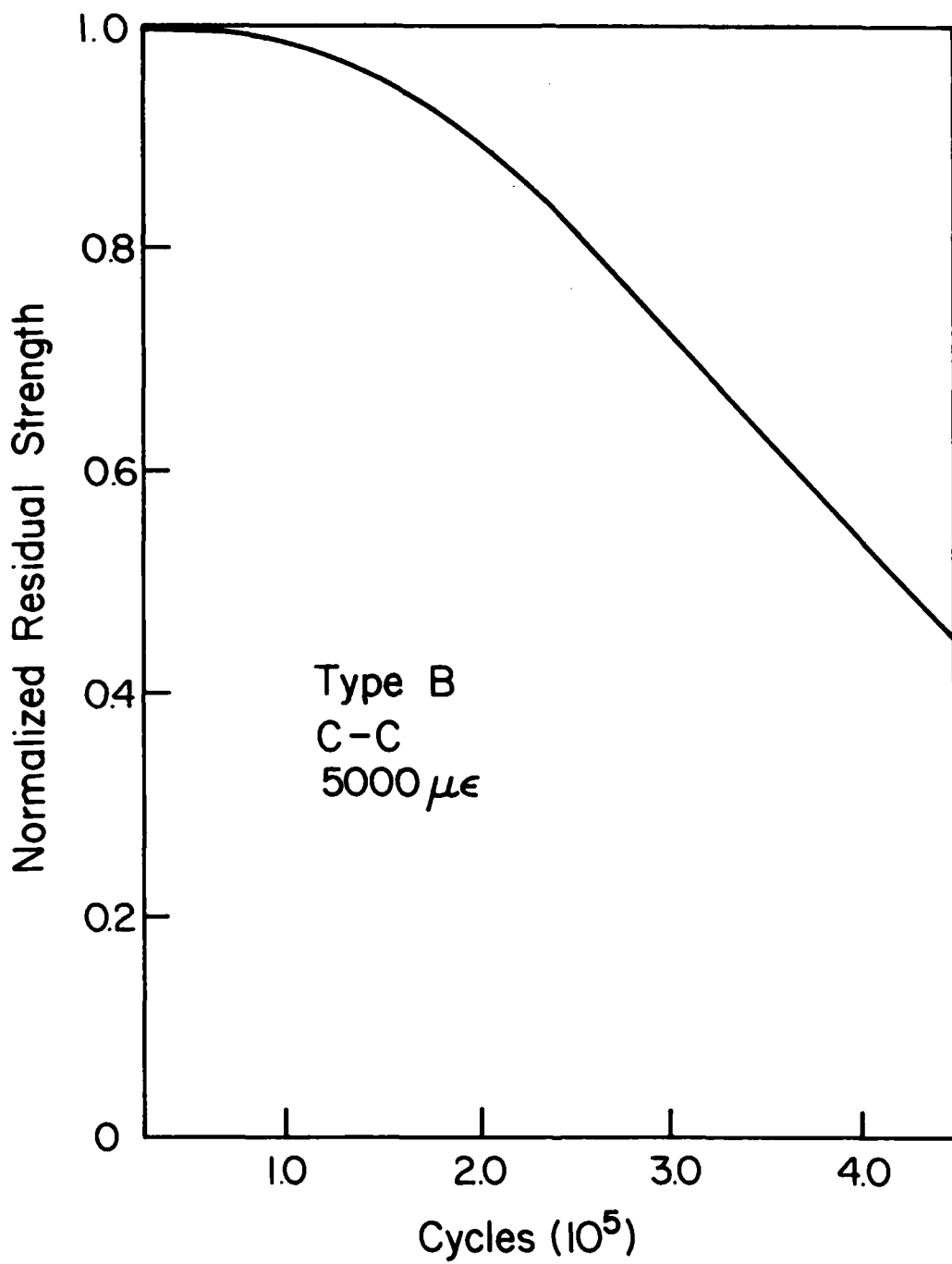


Figure 44: Residual Strength Prediction for C-C Loading

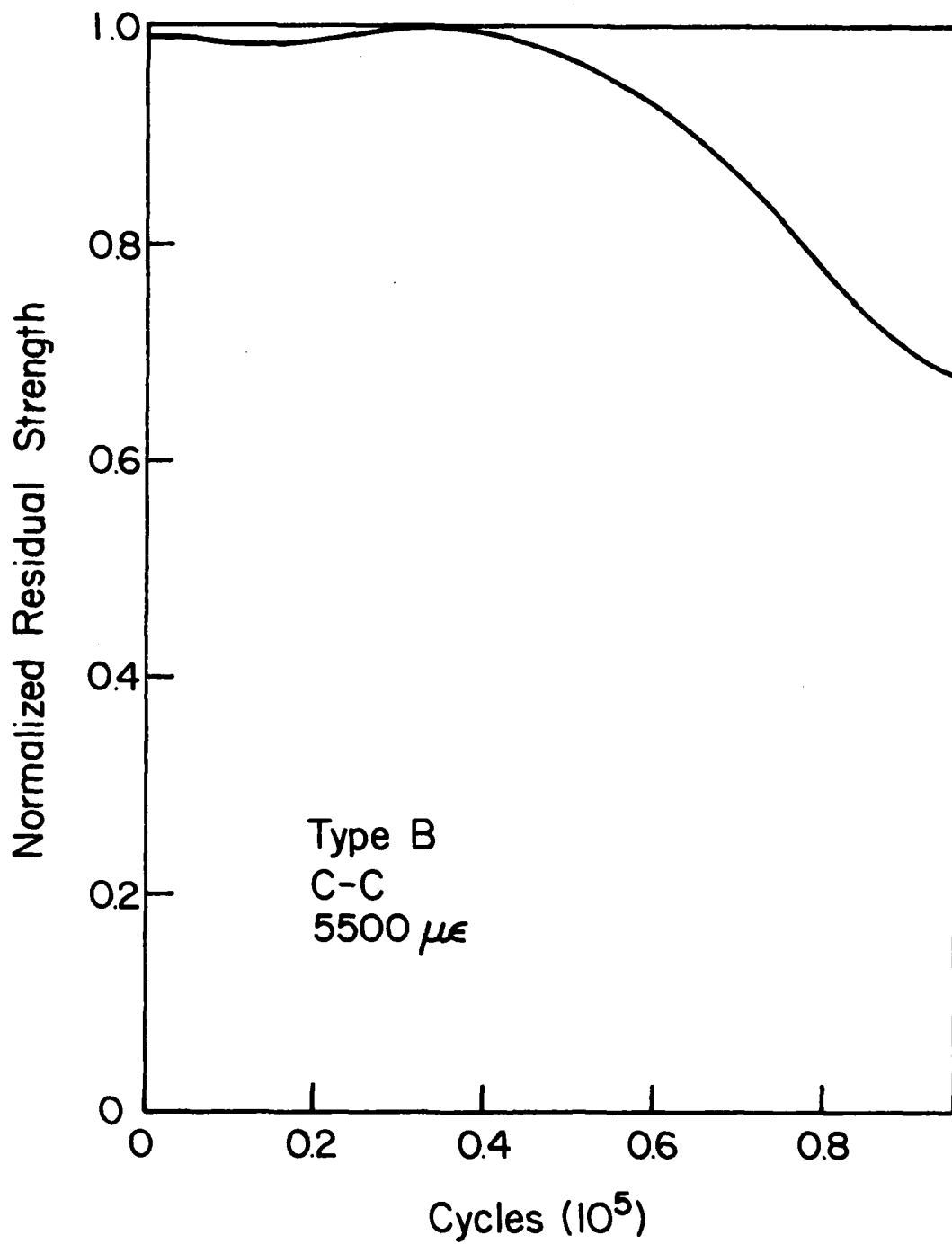


Figure 45: Residual Strength Prediction for C-C Loading

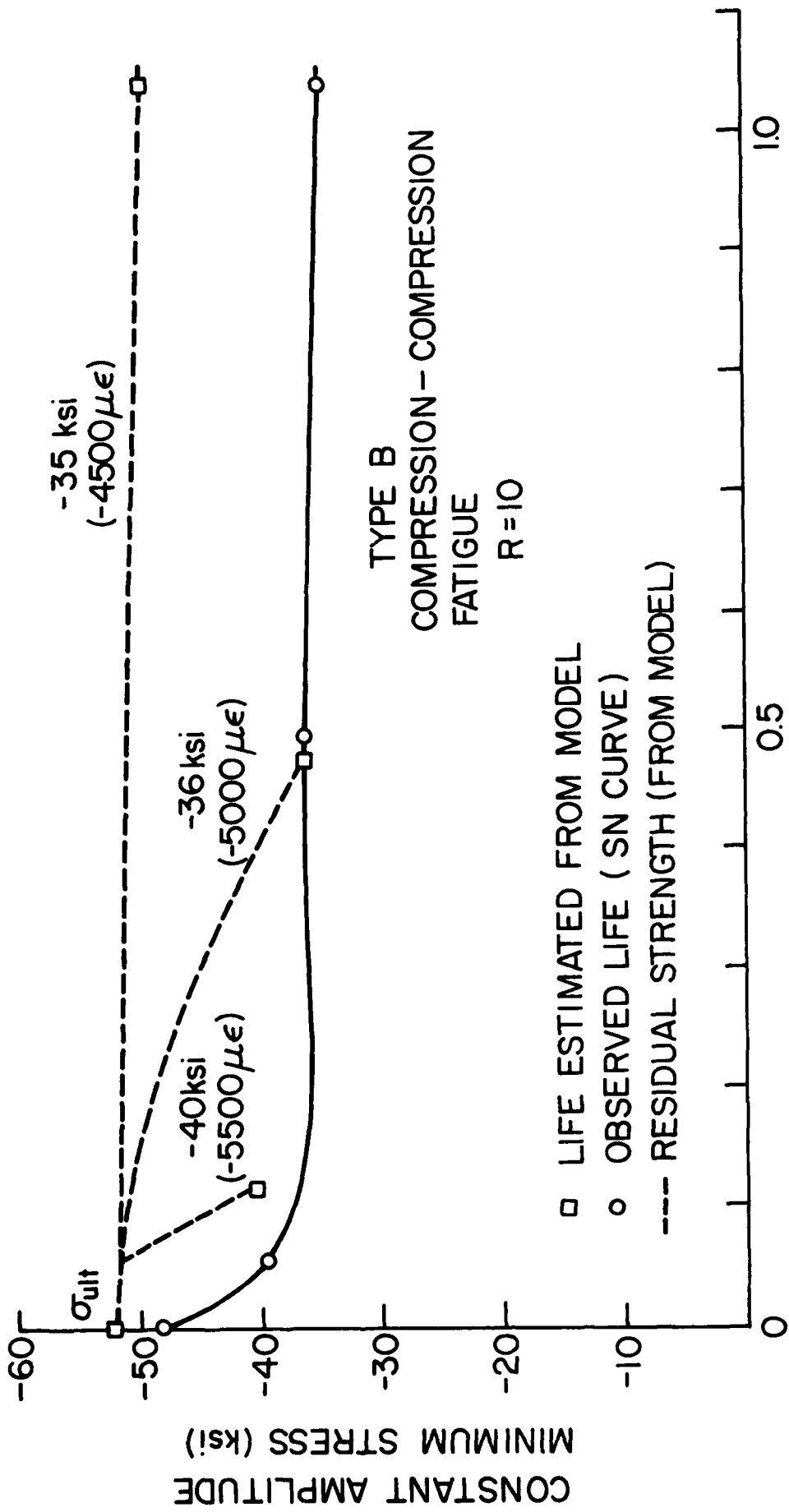


Figure 46: Summary of Predictions and Observations for C-C Loading of Type B Laminates

indicated on that figure. The data in that figure indicates that the agreement between the cumulative damage model and the experimental information is reasonably good. It is important to recall, however, that the model in this form includes relatively little information about the specific degradation mechanisms that are responsible for the fatigue performance in compression loading. Only the concepts of stiffness reduction and critical strain to failure have been used. Although edge delamination was mentioned and used to establish a model for the stiffness reduction, strictly speaking no specific information from the delamination concept is used in this form of the model.

As a further illustration of the applicability of this simple stiffness change based model to compression loading, we will now consider the tension-compression (T-C) loading of the Type C and Type B laminates. As noted in the section on Experimental Data, T-C loading is special in every sense. The development of damage for that type of loading is more rapid and more severe than for tensile or compressive loading alone, regardless of the manner of comparison, and failure of the laminates occurs very rapidly after initiation of severe damage. Because of this behavior, the change in stiffness of these specimens was hard to determine, especially near the end of the tests. Hence the measured stiffness changes before failure was observed were generally unrealistically small, partly because of our inability to measure the stiffness changes quite close to the failure events. More will be said of this problem later.

Figure 47 shows the fractional stiffness change for a Type C specimen oscillated in T-C with an amplitude of about 4,000 $\mu\epsilon$. Observations of that test and other tests in the series suggested that a

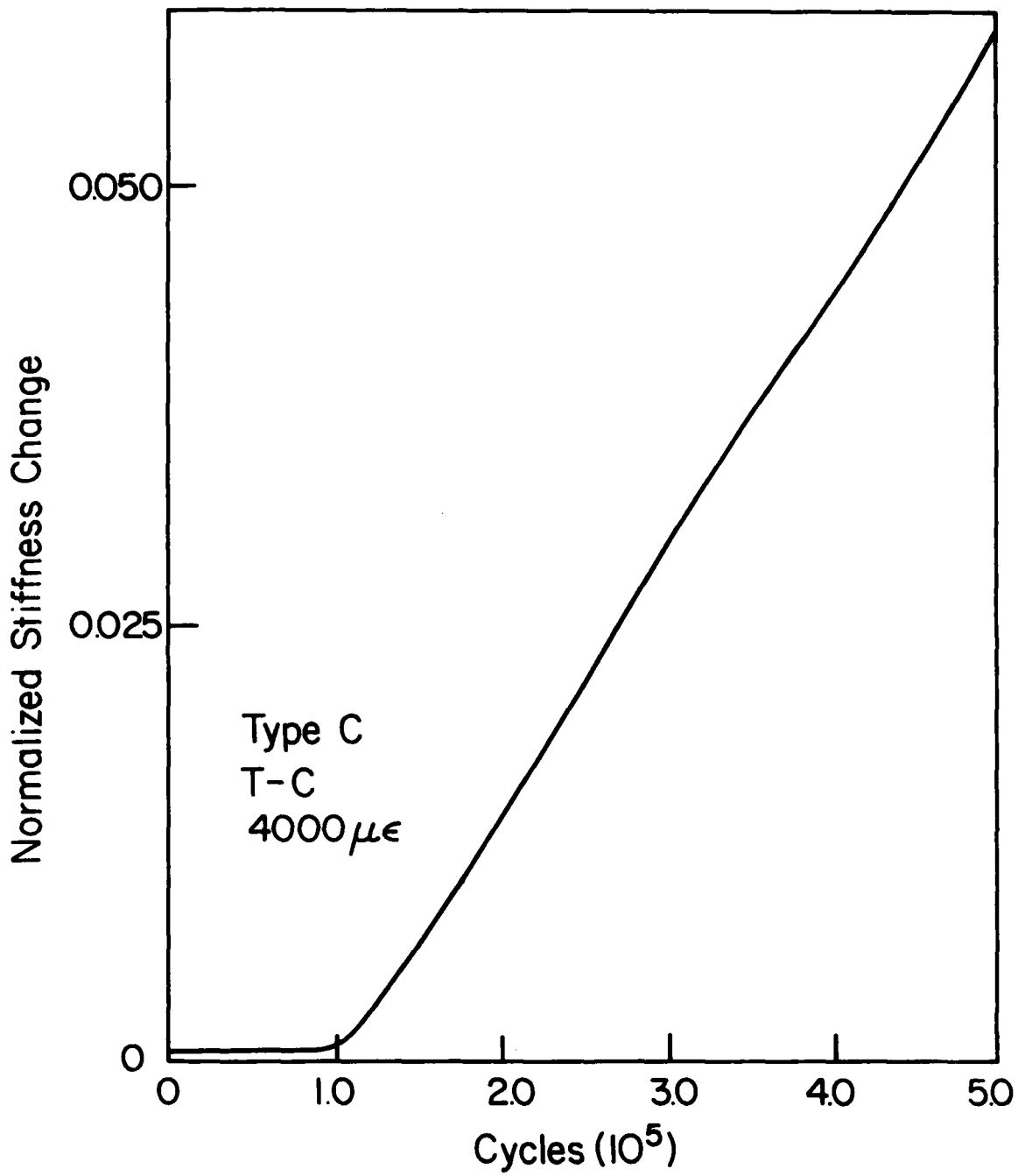


Figure 47: Observed Fractional Stiffness Change for T-C Loading with Strain Amplitude of 4000 $\mu\epsilon$

critical strain to failure was very low, probably a value between 4,000 and 4,600 $\mu\epsilon$. Figure 48 indicates the predicted residual strength reductions when the model was applied for a critical strain value of 4,600 $\mu\epsilon$. Figure 49 shows a similar prediction when that critical strain value was changed to 4,354 $\mu\epsilon$. The life predicted by the model demonstrated in Fig. 49 was 595,000 cycles, while the life predicted by the model shown in Fig. 48 was about 700,000 cycles. The latter value is closer to the measured experimental data. Calculations were also conducted for a strain amplitude of about 4,500 $\mu\epsilon$ with a critical strain to failure of about 4,600 $\mu\epsilon$. The predicted life for that computation was about 25,000 cycles. A summary of those predictions and a variety of observations is shown in Fig. 50. The predictions appear to agree reasonably well with the observations. It should be noted that this type of testing produces results which are extremely sensitive to the amplitude of loading. Strain amplitudes of about 4,000 $\mu\epsilon$ produce nearly a million cycles of life while strain amplitudes of only 4,500 $\mu\epsilon$ or so produce lives that are of the order of 10^4 cycles or less. The fact that the model is able to follow these rather radical changes is a result of the fact that it is entirely controlled by the stiffness changes observed during those tests. If the stiffness change data were not available, those changes would have to be estimated or this form of the model could not be applied.

Before continuing our discussion we recall that the local failure function in Eqn. (17), F_L , has been estimated in the calculations discussed so far by dividing the applied strain amplitude by a critical dynamic buckling strain (or instability strain) determined from observations of the degradation behavior. The critical change in

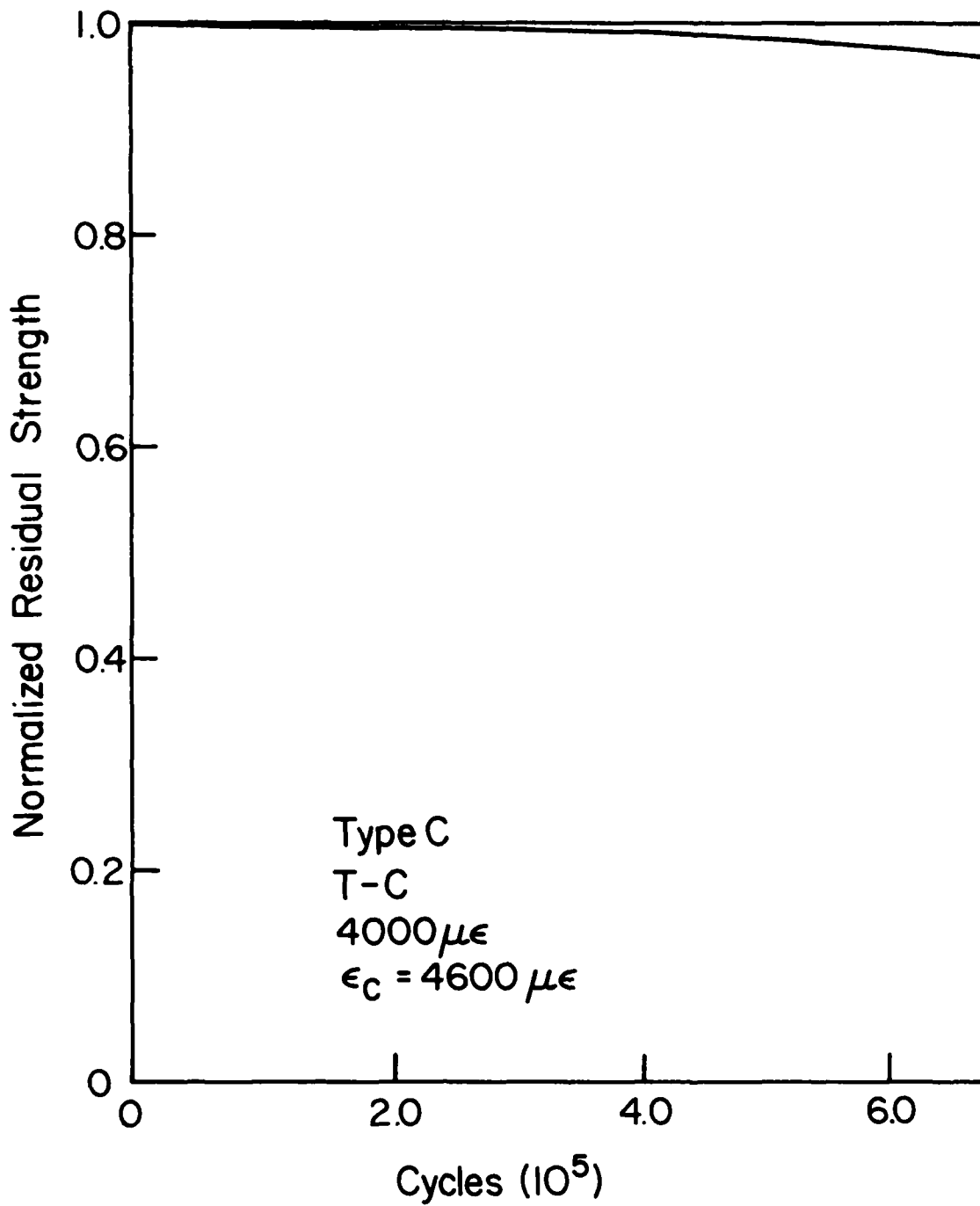


Figure 48: Predicted Residual Strength Change for 4500 $\mu\epsilon$

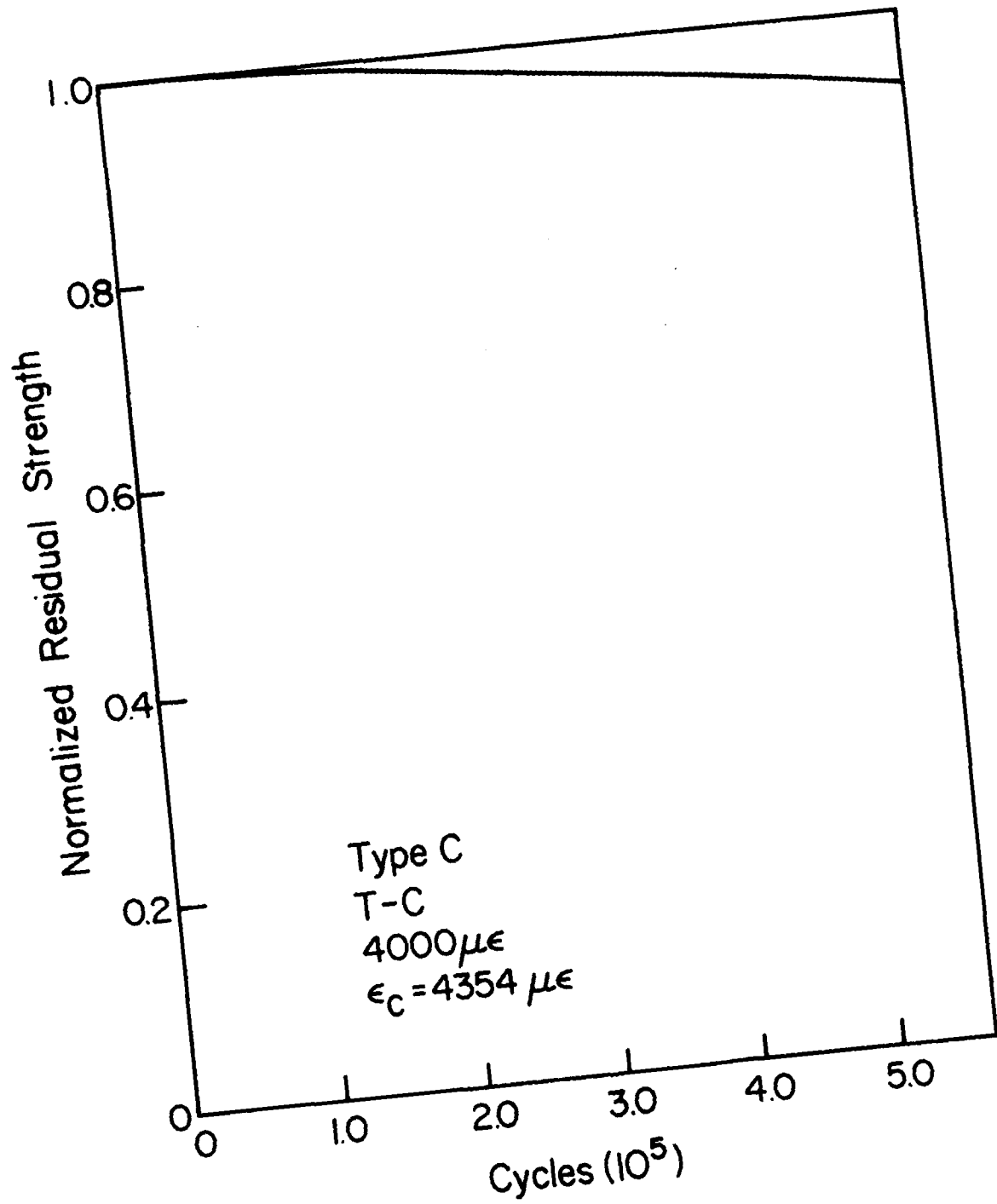


Figure 49: Predicted Residual Strength Change for Data in Fig. 47 with $\epsilon_c = 4364 \mu\epsilon$

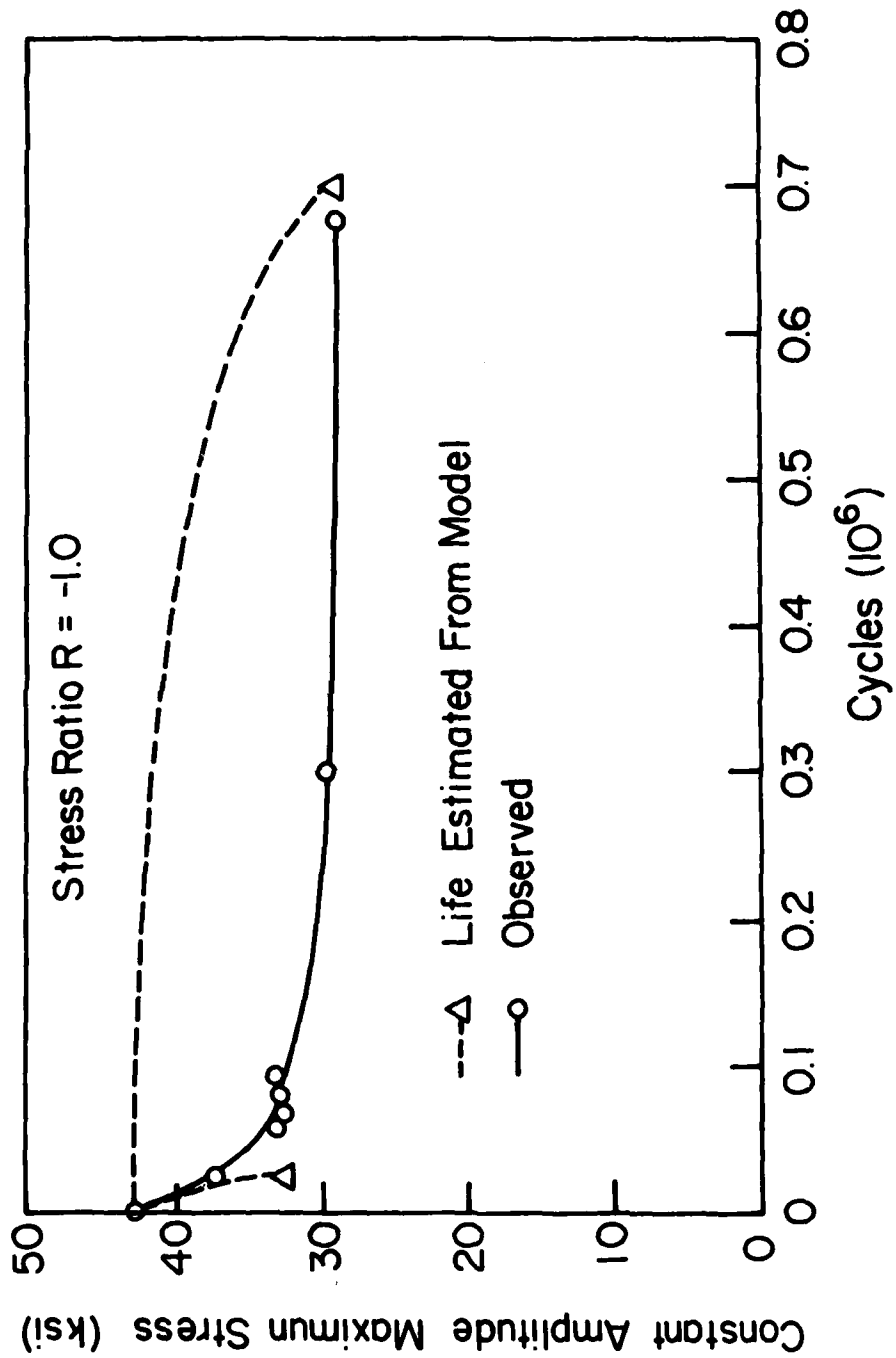


Figure 50: Summary of Observations and Predictions for T-C Loading Using Stiffness Based Model (Simple Form) for Type C Laminates

stiffness, δE_c , was determined in each case from the quasi-static buckling strain. The calculation is made automatically in the computer program used for the computation. The program requests the value of the buckling strain obtained from quasi-static testing and computes the amount of stiffness reduction necessary to reach that buckling strain at the applied stress amplitude. For the Type C laminate data which we have just described, those calculated values of critical stiffness change were generally between about 2 to 10%.

A typical set of stiffness retention curves measured from specimens tested at several stress amplitudes (the corresponding strain amplitudes are indicated in the figure) are shown in Fig. 51. However, the specimens did not fail at the point which corresponds to the last measurement of stiffness change that could be made before the specimen failed. Specimen D2-5 failed at 440,000 cycles, and specimen D2-8 failed at about 110,000 cycles, for example. From a variety of these kinds of observations, it was decided to attempt to extrapolate the stiffness retention curves to the number of cycles at failure to estimate the critical stiffness change for these laminates. The value obtained from that procedure for several widely different test conditions was surprisingly similar and was averaged to obtain a critical stiffness change fraction of about 0.27. That critical fraction was used as the normalizing denominator in Eqn. (17) for the calculations for the Type D laminates. The local failure function, F_L , was taken to be simply the strain amplitude divided by the critical strain amplitude for buckling determined from the quasi-static tests for each case. The fractional stiffness change for the tests shown in Fig. 51 are shown in Figs. 52, 53, and 54. A summary of some of the

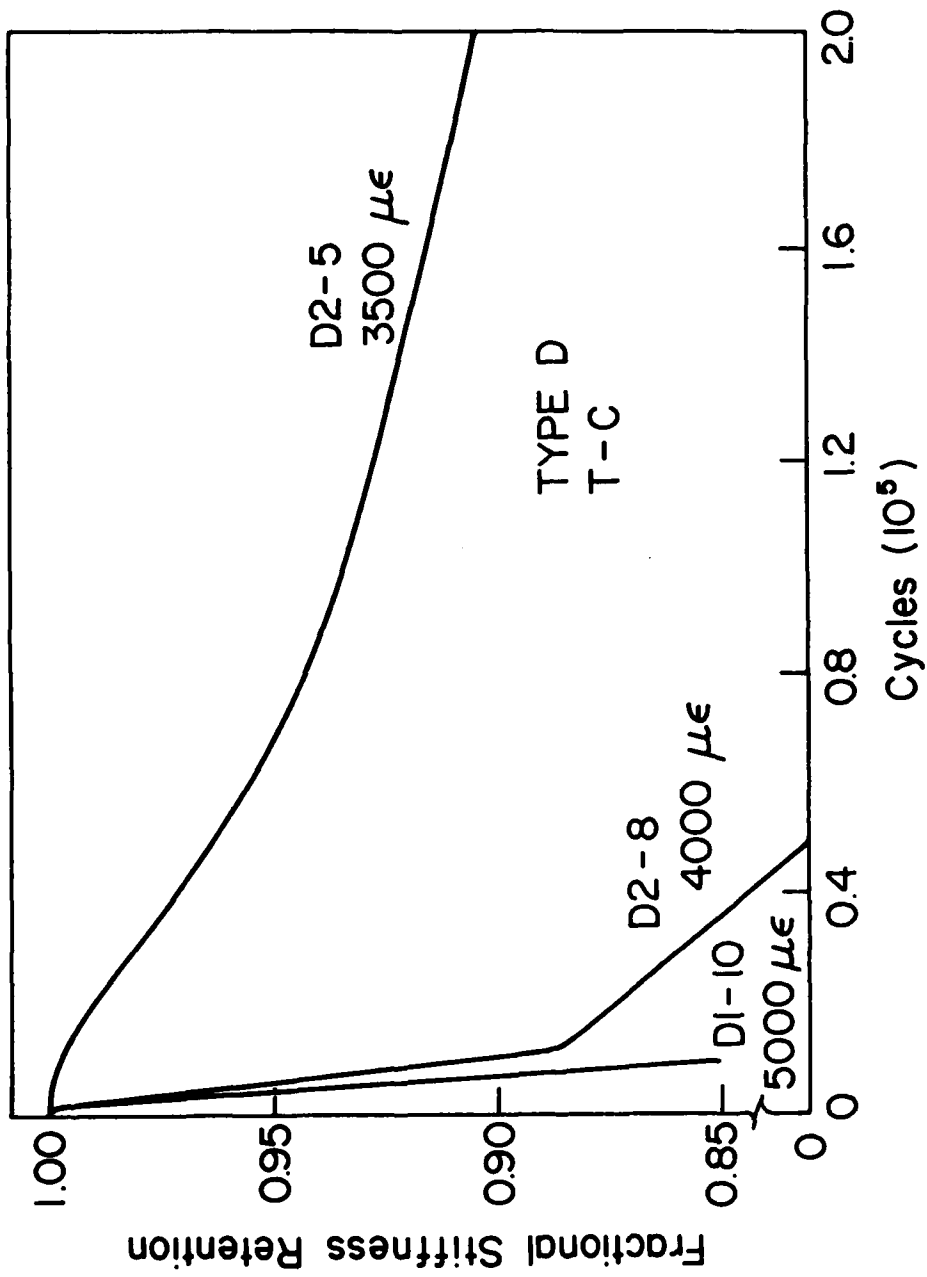


Figure 51: Fractional Stiffness Change Measured During T-C Loading of Type D Laminates

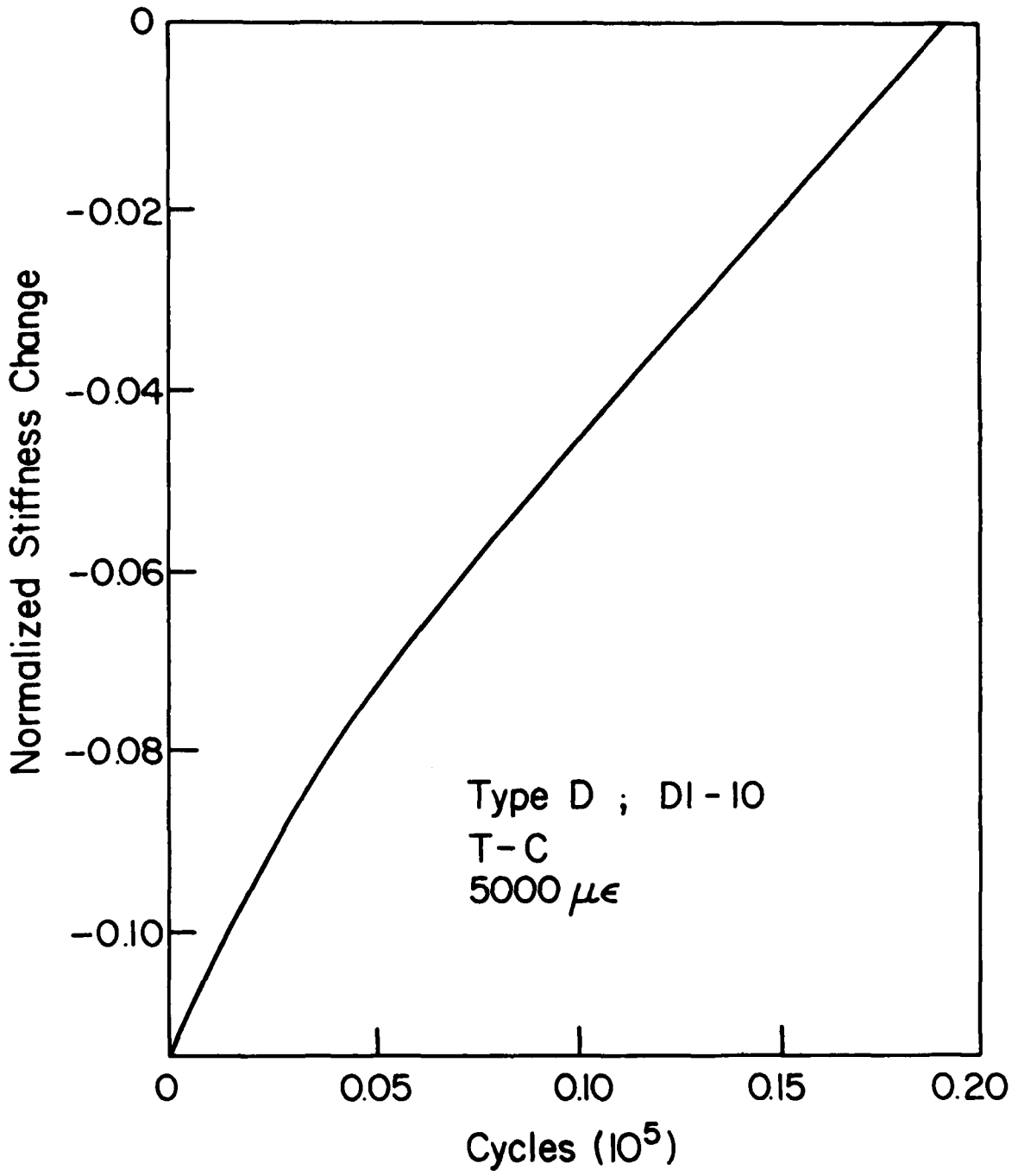


Figure 52: Observed Fractional Stiffness Change for Specimen DI-10

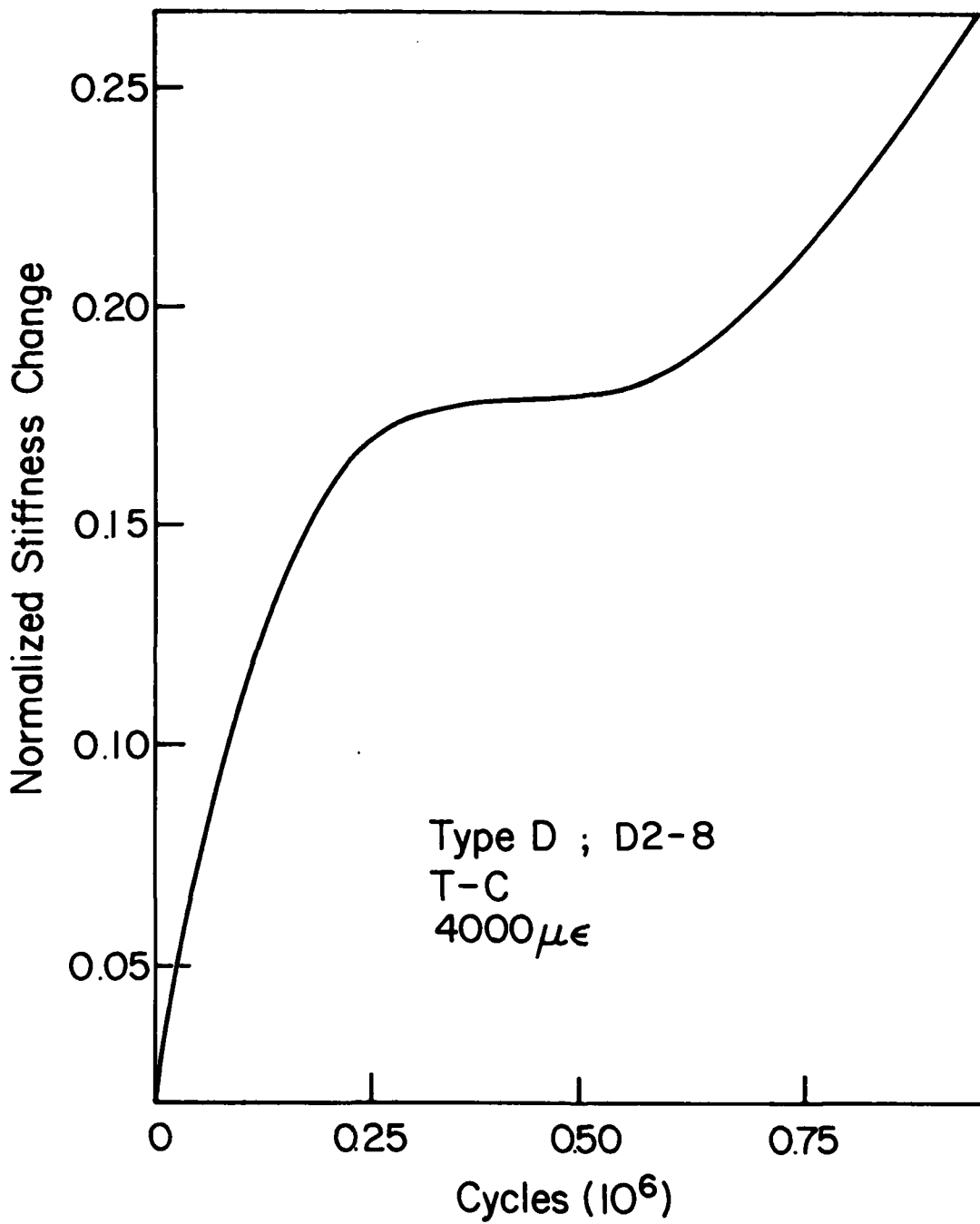


Figure 53: Observed Fractional Stiffness Change for Specimen D2-8

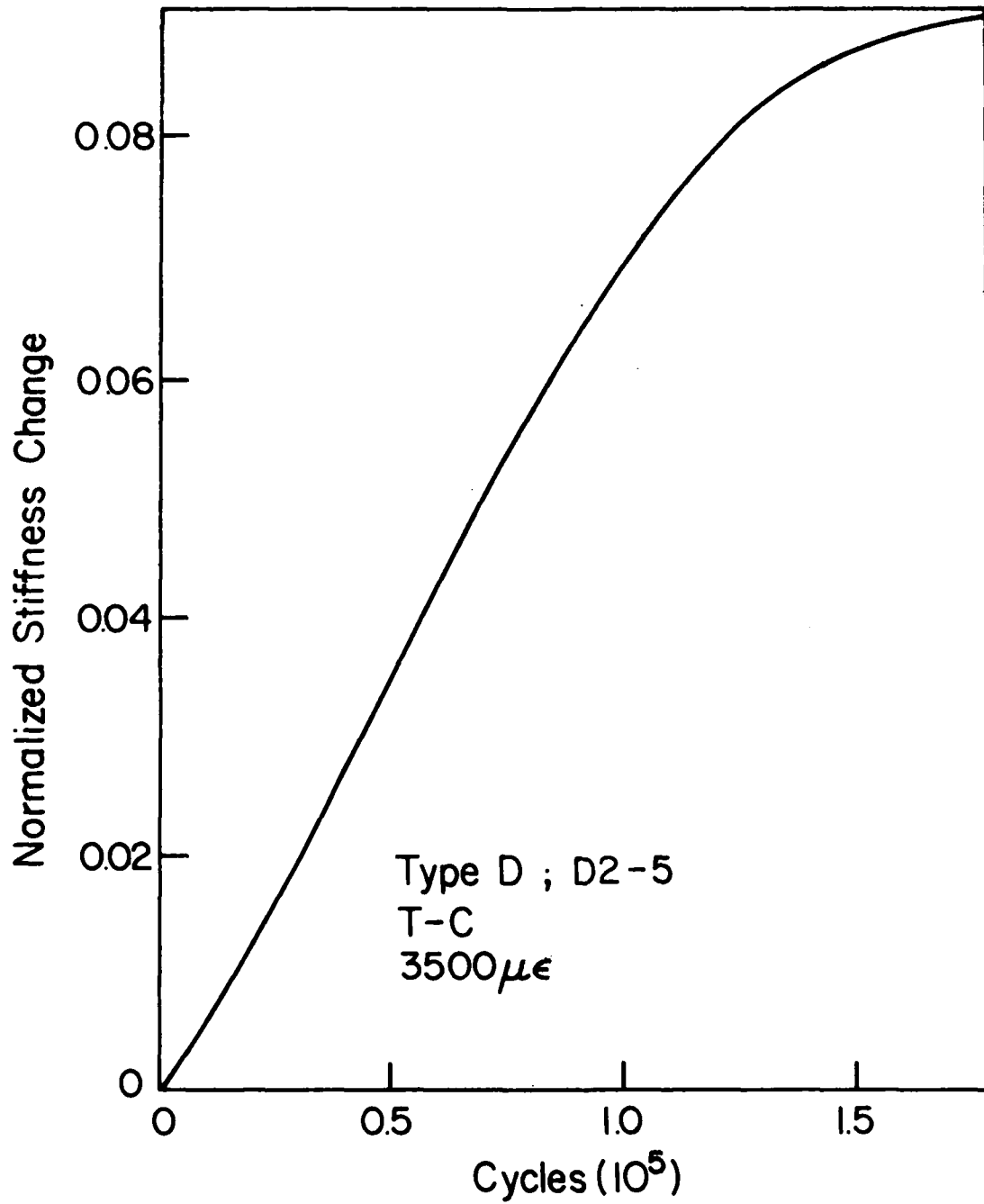


Figure 54: Observed Fractional Stiffness Change for Specimen D2-5

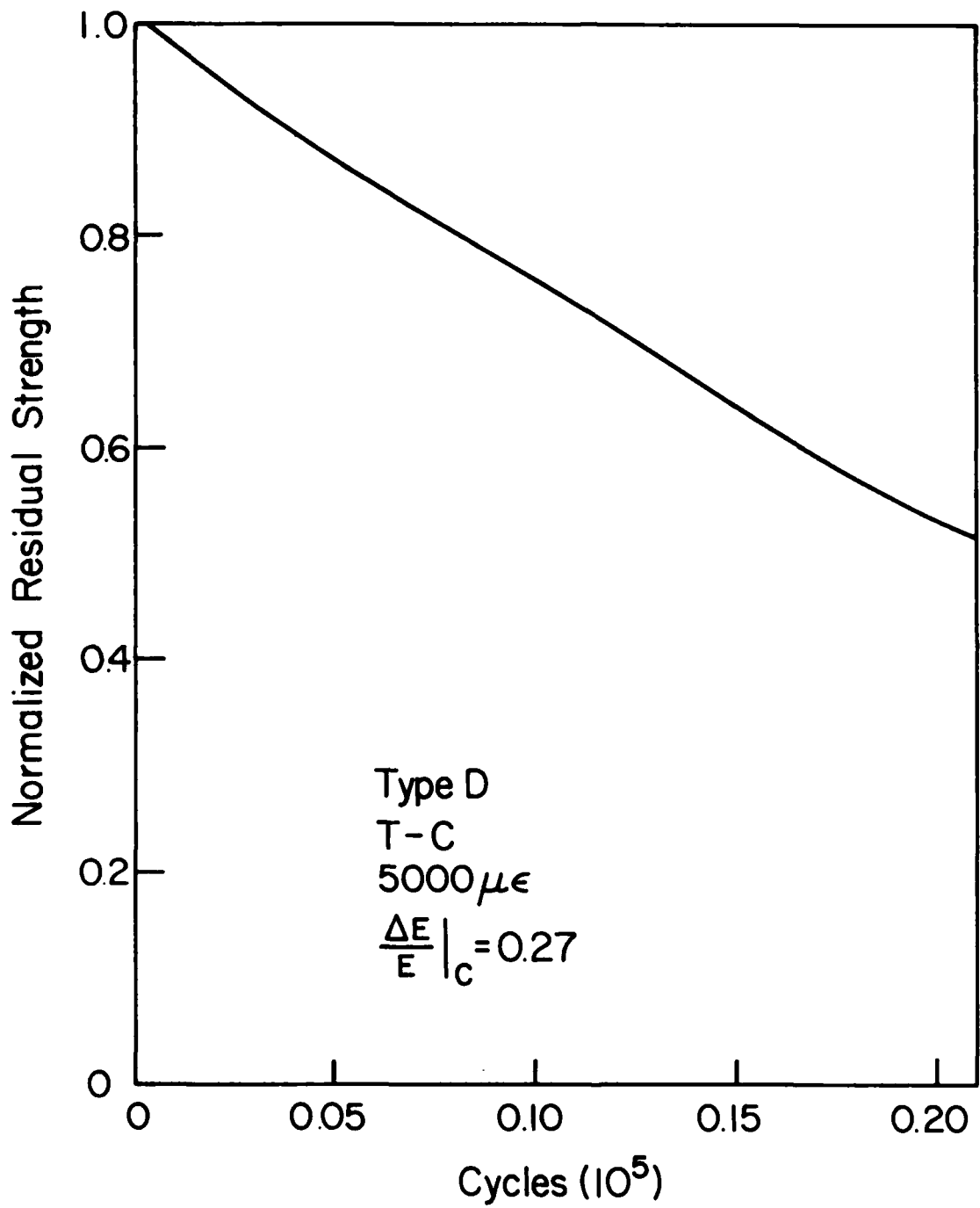


Figure 55: Predicted Residual Strength Data for Specimen D1-10

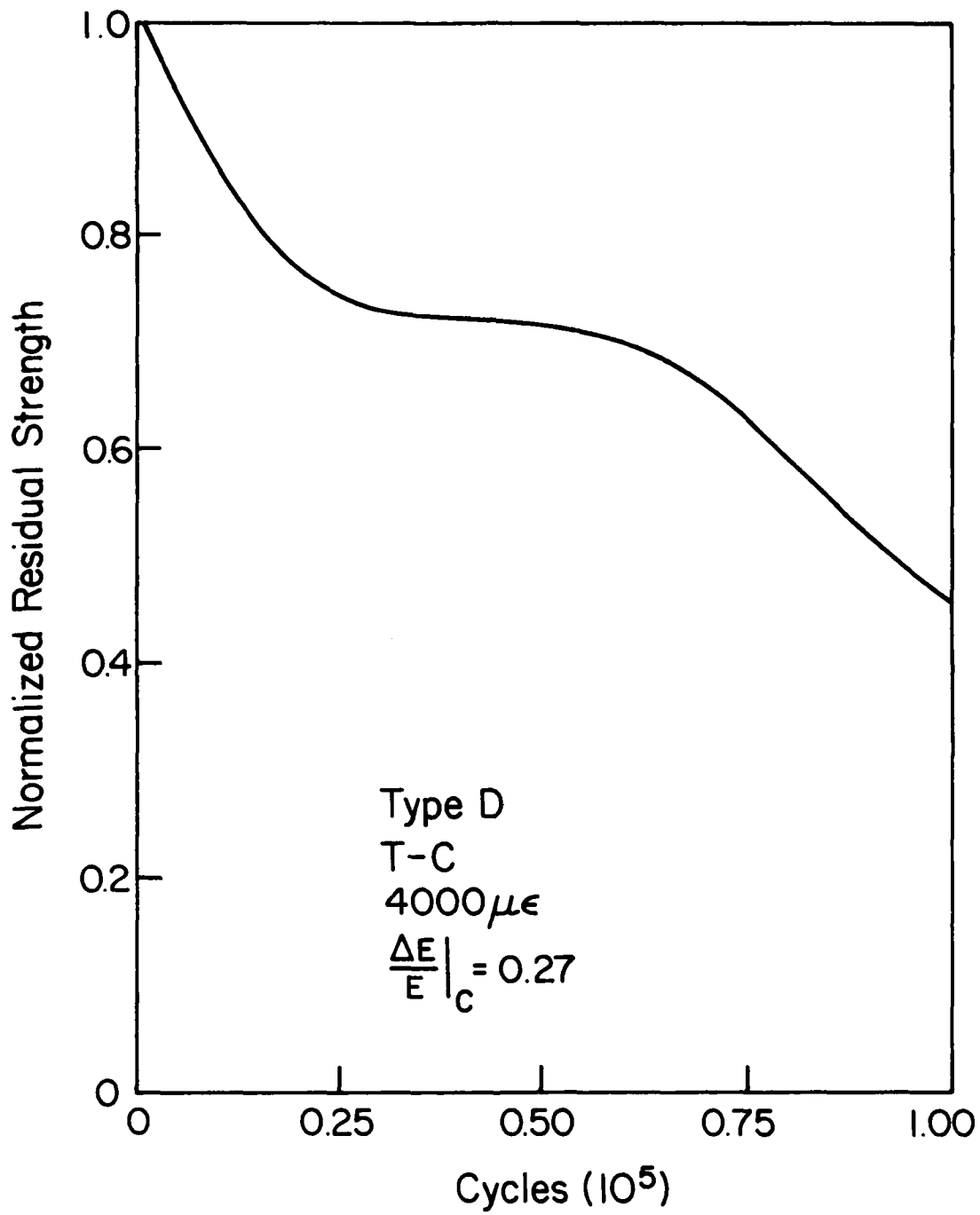


Figure 56: Predicted Residual Strength Data for Specimen D2-8

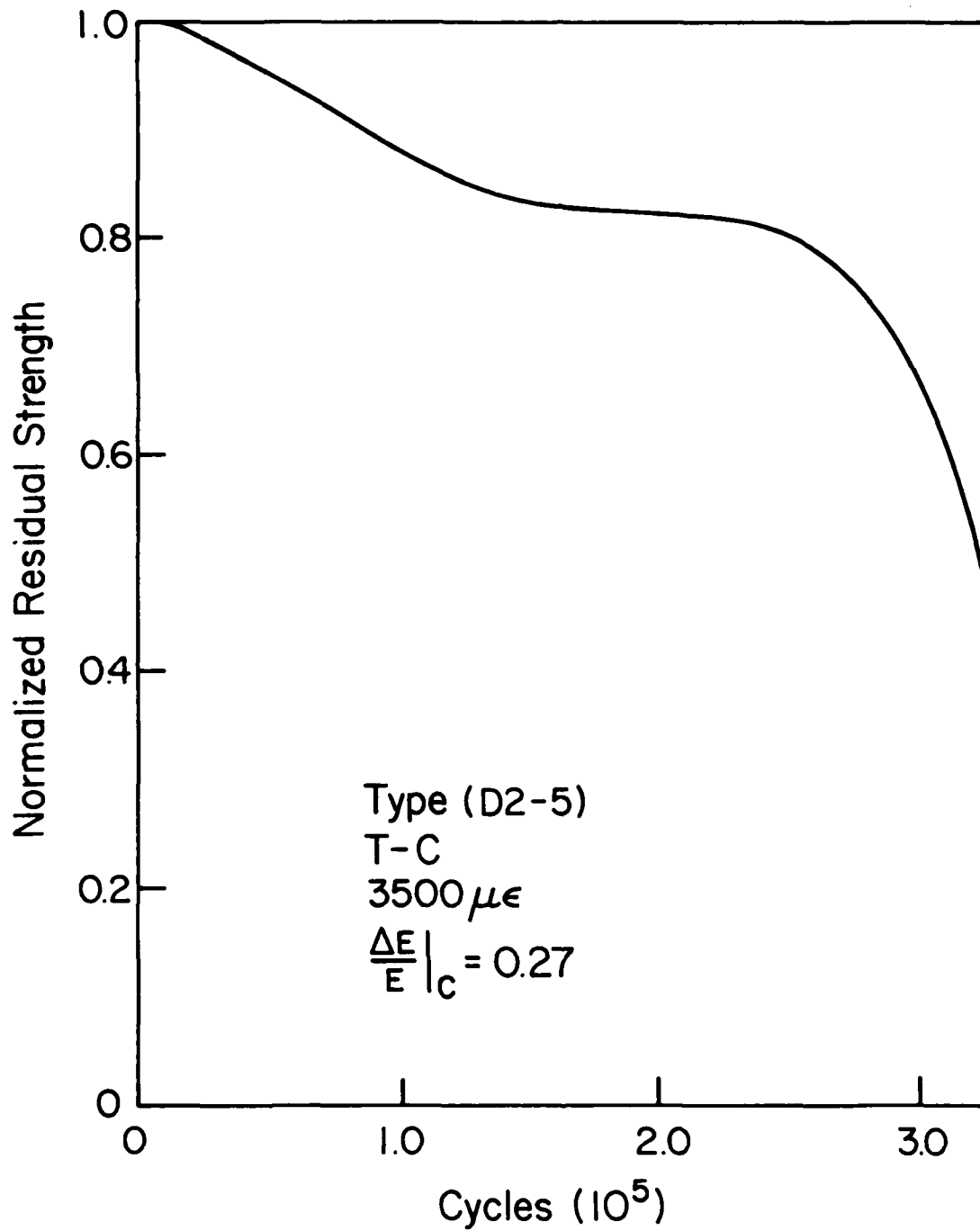


Figure 57: Predicted Residual Strength Data for Specimen D2-5

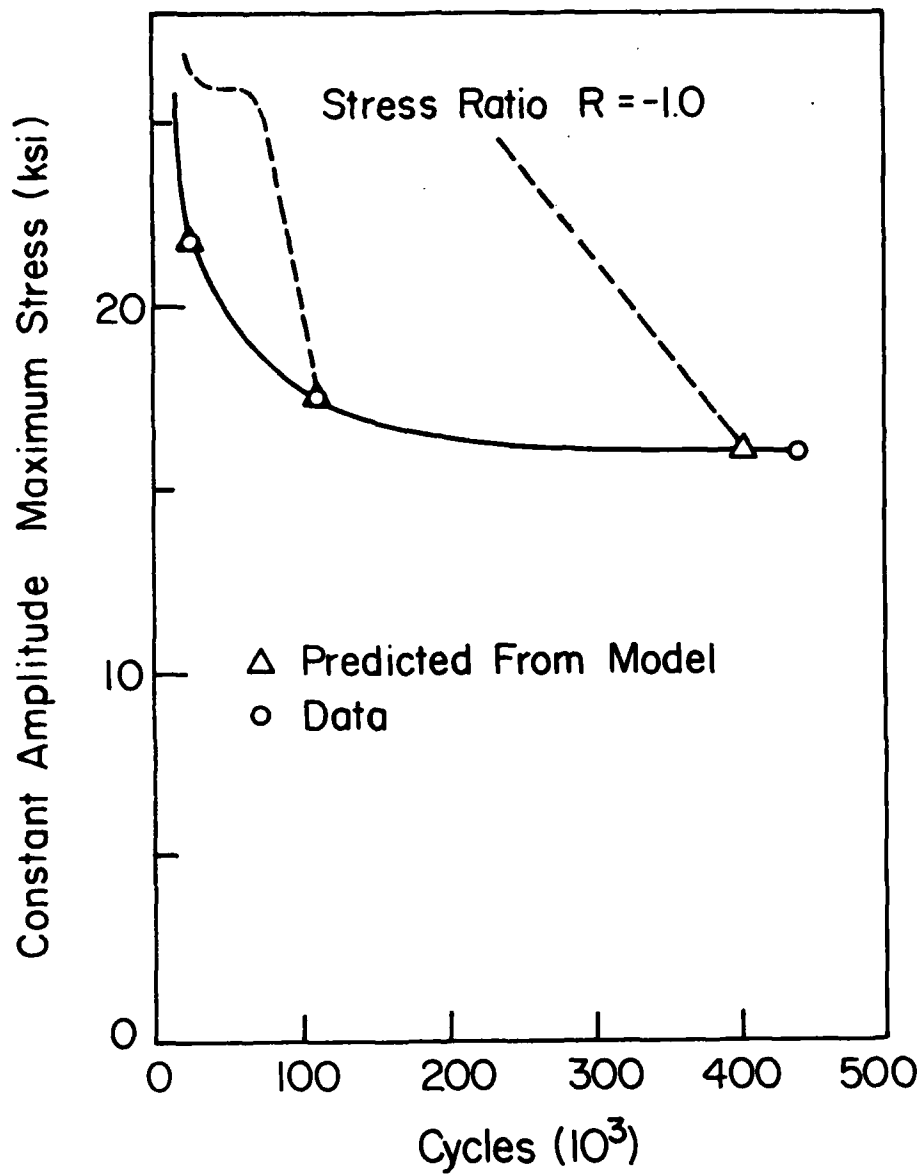


Figure 58: Summary of Observed and Predicted Data for T-C Loading of Type D Laminates Using Critical Stiffness Model

predicted and observed results is shown in Fig. 58. The predictions of life are virtually coincident with the observations for the two lower 5,000 $\mu\epsilon$ are also quite close together. Hence, this interpretation of the model appears to produce reasonable results.

We have mentioned earlier that the experimental behavior of the coupon specimens tested from the six laminates considered in this program was greatly affected by combined tension-compression loading in comparison to tensile or compressive loading alone. The experimental observations indicate that a very complex pattern of damage develops in that situation. One major aspect of that damage development is the influence and interaction of the transverse matrix cracks that form in tension with the edge delamination that forms and propagates predominantly during compressive load excursions. This interaction appears to be synergistic in the sense that the rate of delamination growth appears to be greatly enhanced by the presence of the matrix cracks. This is not surprising in view of the fact that large interlaminar stresses are known to occur at the tip of the transverse matrix cracks, stresses which certainly contribute to the tendency for the interface between the plies to separate. There is a great need for a vigorous research program to determine the details of this highly complex process. Some basic investigations are presently under way at Virginia Tech. It was not possible to resolve these issues during the course of the present investigation.

In an effort to include some aspects of the mechanisms involved, the cumulative damage model for T-C loading was altered to include the edge delamination mechanism. The form of the damage summation equation used for that purpose is given in Eqn. (18).

$$\Delta S(n) = (1 - F_r(n)) = \int (1 - E^*/E_L) d\left(\frac{a}{b}\right) \quad (18)$$

All of the quantities in that equation have been introduced earlier. The reader will recall that E^* is the longitudinal stiffness of a laminate which has completely delaminated along a given interface. The ratio a/b is the length of the delamination compared to the width of the specimen. Based on considerable evidence in the literature, we make the assumption that the crack length, a , is determined from the integral of a power law relationship between the rate of crack propagation and the strain energy release rate, G , as indicated in Eqn. (19).

$$a = a(n) = \alpha \int \mathcal{L}^\beta dn \quad (19)$$

The quantities α and β in that equation are constants (Refs. [12] and [13]). If we assume that the strain energy release rate includes all modes of crack propagation, then we can use an expression introduced by O'Brien [12] to write

$$\mathcal{L} = \mathcal{L}(n) = \frac{\epsilon^2 t}{2} (E_L - E^*) \quad (20)$$

where ϵ is the applied laminate strain, t is the laminate thickness and the other quantities have the values introduced earlier. We can also use an expression introduced by O'Brien for the laminate stiffness as a function of the length of the delamination to write the laminate strain as a function of the number of applied cycles for a fixed value of applied stress, σ^a .

$$\epsilon = \epsilon(n) = \frac{\sigma^a}{(E^* - E_L) \frac{a}{b} + E_L} \quad (21)$$

Hence, the model can be used if the constants α and β are known and if the value of the laminate stiffness for complete delamination, E^* , has been calculated.

The form of Eqn. (18) was chosen based on the following rationale. Equation (18) can be written in the following form:

$$(1 - F_r) = (1 - \sigma_r/\sigma_u) = (1 - E^*/E_L) \frac{a}{b} \quad (22)$$

If we assume that stress redistribution is to be ignored, so that all of the quantities in that equation and the equations (20) and (21) mentioned above become independent of the number of cycles of load application, n , then we can also write

$$\sigma_r/\sigma_u = (E^*/E_L - 1) \frac{a}{b} + 1 = \frac{[(E^* - E_L) \frac{a}{b} + E_L] \epsilon_c}{E_L \epsilon_c} \quad (23)$$

where the propagation length, a , can be determined by integration by quadratures of Eqn. (19). The critical strain, ϵ_c , in Eqn. (23) can be regarded as the critical strain to failure in a quasi-static test. Equation (23) can be rearranged as shown in Eqn. (24)

$$\sigma_r = [(E^* - E_L) \frac{a}{b} + E_L] \epsilon_c \quad (24)$$

That equation can be read as stating that the residual strength of a laminate which is delaminating is equal to the reduced stiffness times the critical strain of that laminate measured from a quasi-static

test. O'Brien has reached a conclusion of this type in an earlier investigation [14].

In order to apply this model, it is necessary to anticipate or to observe the delamination interfaces in a given laminate. From that information a laminate analysis can be used to estimate the completely delaminated modulus, E^* , from which the stiffness for a given crack length can be determined, and from which the strain and strain energy release rate can be determined using Eqns. (20) and (21). Then Eqn. (19) will yield a crack length (or an increment of crack length) and Eqn. (18) can be used to determine the amount of incremental change in residual strength. The process can then be iterated, the crack length increased by some increment, Eqn. (21) applied to find the strain, Eqn. (20) applied to find the strain energy release rate, and a new increment of crack length found from (an numerical integration of) Eqn. (19). We will look at a variety of calculations of this type. However, a second scenario is also possible. If the stiffness change of the specimen has been measured, or is otherwise available, one can use the measured stiffness change and the applied stress level to determine the laminate strain, ϵ , and then proceed to Eqns. (20), (19), and (18). This interpretation will also be used extensively in the following paragraphs, and the two approaches will be compared.

We begin by considering the application of this model to the Type C laminate. The reader will recall that the Type C laminate is a quasi-isotropic stacking sequence with the 90° plies interspersed between the 45° plies in the laminate. The experimental data indicates that delamination is likely to occur in that laminate at two different types of interfaces, the $0/+45$ and the $+45/90$ interfaces. The Poisson

mismatch for delamination along the 0/+45 interface is essentially zero since the transverse Poisson's ratio of the zero degree ply is about 0.31 which is essentially the same as the rest of the laminate. Hence, the calculation of the delaminated modulus, E^* , was done assuming that the +45/90 interface delaminates. The calculation was conducted by considering the stiffness of a 0,+45° sublaminates and a 90,-45,-45,90,+45,0° sublaminates. Following the suggestion of O'Brien, (Ref. [12]) the delaminated modulus was calculated using a rule of mixtures concept, i.e., the delaminated modulus was set equal to the summation of the products of the moduli of the sublaminates times the number of plies in each of those sublaminates divided by the total number of plies in the total laminate. Hence, the delaminated modulus for Type C material was calculated as shown in Eqn. (25).

$$E^* = \frac{2(11.569) + 6(6.4) + 2(8)7.844}{24} = 7.793 \quad (25)$$

In that equation, the stiffness of the first sublaminates mentioned above is 11.569 (msi), the stiffness of the second sublaminates mentioned is 6.4, and the stiffness of the remaining (undelaminated) laminate is 7.844. Hence, for a single delaminated interface, the delaminated modulus is 7.793 msi. These values are calculated from laminate analysis using the stiffnesses of the single plies tested in the quasi-static baseline series mentioned earlier. The actual value of the measured modulus of this laminate was 7.31 msi. Hence, it was assumed that the delaminated modulus was 7.26 msi when a single interface delaminates on each side of the centerline of the specimen. It should be mentioned that the experimental observations suggest that

delamination begins at the interface in the sublaminar that is closest to the outside surface of the laminate. As the damage develops, delaminations initiate at the same type of interface in sublaminates which are further from the surface in the thickness direction. Hence, the initiation process is progressive beginning at the exterior surfaces of the specimens and progressing toward the interior centerline of the laminates. Based on these observations, it was decided to postulate that laminate failure was controlled by the initiation and propagation of the outermost delamination, and that failure was defined by the incidence of that delamination progressing across the total width of the specimen. Hence, in the computer code used for the computation of the residual strength degradation, an undelaminated value of the laminate stiffness of 7.31 was used and a completely delaminated value of 7.262 msi was used.

The next matter of substance that needs to be considered to apply the model was the power law that characterizes the rate of delamination propagation in terms of the strain energy release rate, G . The most fundamental question involving that power law is the interpretation of the strain energy release rate. Depending upon the laminate type and stacking sequence, and upon the interface which delaminates, various modes of crack growth may be appropriate (crack opening mode, shear mode, etc.). If we assume that a shear mode is dominating the process for our situation, then one might be tempted to use values quoted in the literature which suggest that the coefficient of the power law should be something like 0.016 and the power should be something like 7.218 in English units (Ref [13]). However, it was found that in order to match the data for the Type C laminate, a value of the coefficient of about 0.16 was appropriate, but a power of about 10.7 was a better fit. Since

we did not have the opportunity to conduct the basic studies necessary to establish the appropriate analytical or experimental form of that equation by other means, a set of values for the power and coefficient were determined from an initial fit of one set of data, after which those quantities were held constant for all other predictions. However, it should be mentioned that this choice of power in the propagation rate equation greatly influences the delamination length at a given number of applied cycles. This is illustrated by the information shown in Fig. 59 which portrays the delamination length calculated for a given coefficient and three different powers of the strain energy release rate quantity. There is a substantial need for greater understanding of this sensitivity.

To indicate the applicability (or at least the internal consistency) of this delamination model, we will consider the block loading results discussed in the data section. Two sets of the block loading will be discussed, set 2 and set 3 as described earlier. The reader will recall that set 2 consisted of one block of loading of 150,000 cycles with a fully reversed strain amplitude of $3,500 \mu\epsilon$, followed by a second block of fully reversed loading at $4,500 \mu\epsilon$ until failure occurred. Table 6 shows some typical results of that type of loading. For the three tests indicated in that table, the average life observed for set 2 loading was 183,000 cycles. Set 3 loading consisted of a block of tension-tension loading with an R value of 0.1 having a maximum strain level of $4,000 \mu\epsilon$ for 150,000 cycles followed by fully reversed tension-compression loading at a strain amplitude of $4,000 \mu\epsilon$. Table 6 indicates that the average life for the three tests shown there was 474,000 cycles.

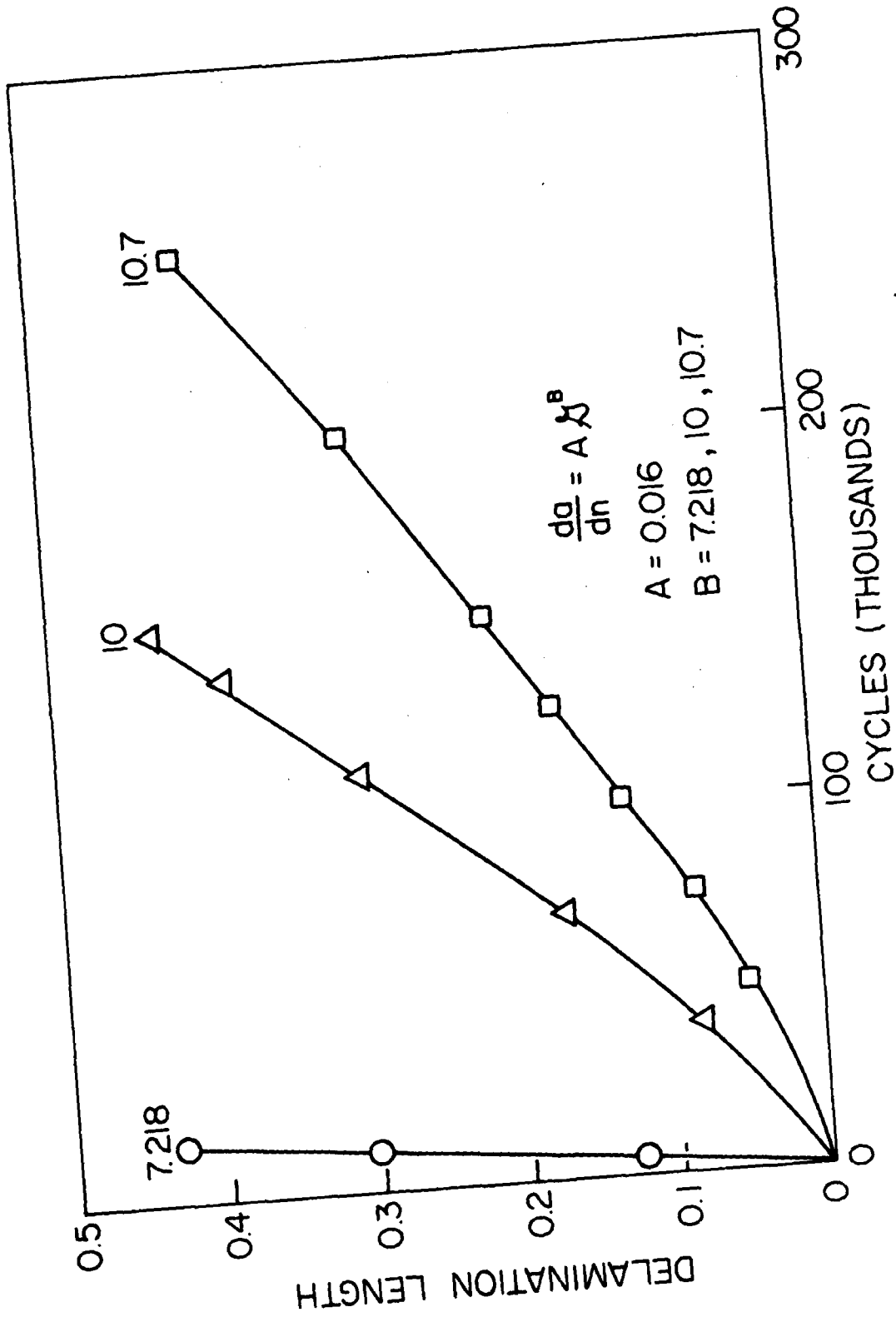


Figure 59: Parameter Study of the Power of Delamination Growth Law

TABLE 6.
RESULTS OF BLOCK LOADING TESTS AND PREDICTIONS

| <u>Set</u> | <u>Specimen</u> | <u>Block</u> | <u>Cycles (thousands)</u> | <u>Average Life (thousands)</u> | <u>Predicted Life (thousands)</u> | <u>Percent Error</u> |
|------------|-----------------|--------------|-------------------------------|---|---|--------------------------|
| 2 | 5-6 | 1 | 150 | 183 | 173 | 5.4 |
| | | 2 | 57 | | | |
| | 7-6 | 1 | 150 | | | |
| | | 2 | 32 | | | |
| | 8-7 | 1 | 150 | | | |
| | | 2 | 11 | | | |
| 3 | 8-5 | 1 | 150 | 474 | 451 | 4.8 |
| | | 2 | 327 | | | |
| | 7-4 | 1 | 150 | | | |
| | | 2 | 313 | | | |
| | 7-8 | 1 | 150 | | | |
| | | 2 | 232 | | | |

The delamination propagation model described above was applied to these block loading situations. The initial value of the strain energy release rate, G , was calculated from the initial strain (determined by dividing the applied stress by the initial modulus) the laminate thickness, and the difference between the fully delaminated modulus and the initial modulus of the laminate as indicated in Eqn. (20). Thereafter, as the number of cycles was incremented, the strain was increased according to Eqn. (21) based on the calculations of current crack length from Eqn. (19). The summation of the change in residual strength was determined from Eqn. (18) using an appropriate computer code. Equation (19) was integrated numerically. The results of those calculations are also shown in Table 6. For set 2 loading, the predicted life is about 173,000 cycles compared with the observed average life of 183,000. The difference of 5.4% is certainly tolerable. For Block 3 loading, the calculated life of 451,000 cycles compares well with the observed average life of 474,000 cycles, a difference of 4.8%. Hence, based on these limited results, the model appears to be self-consistent and to produce reasonable predictions, even for block loading situations.

Two very important points should be made here. First of all, the value of strain used in Eqn. (20) to calculate the strain energy release rate is the total strain range, not the strain amplitude. One can justify this choice on the basis of a variety of philosophies. The principal motivation for the authors was provided by the apparent importance of the shear stresses in the delamination process. If the interlaminar shear stresses are, indeed, a major part of the driving force for the delamination propagation, then a strain range (or stress range) is a more appropriate quantity to use in the propagation equation than a strain (or

stress) amplitude since the sign of the shear stress is immaterial to the process. Ultimately, the most convincing argument for the use of the strain range is the success and utility of the idea.

The second important matter to be mentioned is that the block loading was handled in the calculations mentioned above by using the delaminated crack length obtained in the first block of loading as a starting point for the second block of loading, an initial crack length concept. While this is consistent with the physical idea of the mechanism involved, a variety of other choices are certainly possible.

The above form of the T-C model was also applied to fully reversed loading of the Type F laminate. That laminate, which consists entirely of zero and 45° plies, was observed to separate into sublaminates consisting of 0,+45 and -45,-45 ply groups during delamination. A second type of delamination occurred with ply groups consisting of all of the 45° plies together separating from the zero degree plies. It was assumed that one of each of these types of delamination occurred on either side of the centerline of the laminates and that failure of the laminate specimen occurred when those interfaces had propagated across the entire width of the specimen. Since no basic data was available, it was assumed that both types of delamination propagated at the same rate, namely according to the power law described earlier with the coefficients and powers defined by our earlier experience. The laminate analysis calculation for the change in laminate stiffness due to the complete delamination of the two interfaces mentioned on either side of the centerline indicated that the initial stiffness value of 7 msi changed to a value of about 6.966 msi. The data for specimens F1-7, 3-9, 3-11, and 5-7 (which were essentially replicates) were analyzed using those numbers. The predicted life for that calculation was 386,000 cycles compared to values which ranged

between 375 and 712,000 cycles of observed life. As a point of reference, the values for the strain energy release rate, G , that were computed by the model were typically in the range between 0.3 and 0.5 inch pounds per square inch, a value that is "reasonable" in the context of published literature (Ref. [13]).

During the course of these computations it became apparent that another possible interpretation of the damage model described above would be useful. The reader will recall that the computed value of laminate strain as a function of the number of applied cycles was determined from Eqn. (21) using the constant applied stress amplitude, σ^d , divided by the current laminate modulus determined from an equation which estimates that value based on the amount of delaminated fractional width and the difference between the undelaminated and delaminated modulus. Hence, the model actually produces a predicted stiffness change as a function of cycles which, in turn, is used to estimate the current laminate strain. A comparison of these calculated changes in laminate stiffness with the observed values indicated that the stiffness changes were being underestimated by the model. One simple remedy for this situation is to use the measured values of stiffness change to compute the strain range as a function of the number of applied cycles and to enter that value into the calculation of the strain energy release rate according to the Eqn. (20). While it is true that this approach depends upon having measured values of stiffness change or upon having a method of estimating those changes, it was decided that such a model should be examined since it has the capability of incorporating more of the reality of the tests. Hence, a refined version of the model was programmed and a number of calculations made. A representative group of those calculations will be described below.

We will begin by considering the Type C laminate. We use an initial data set to "calibrate" the model as we have done earlier. For that purpose we analyze specimen C5-11 which has a stiffness change throughout the test of about 13%. We mention in passing that these large stiffness changes exceed the values calculated from delamination concepts at least in part because of the contribution of transverse cracking and the coupling between transverse cracking and delamination which is not accounted for in the earlier delamination model. As one would expect, this significant decrease in the modulus tends to increase the laminate strain by a comparable amount, and since the strain energy release rate depends on the square of that quantity, the crack propagation rate is accelerated greatly. Hence, it is not too surprising that the coefficient of the power law becomes 0.008 and the power of that propagation relationship becomes about 15 in order to obtain a match between the model and the data for that specimen. For that choice, there is essentially an identity between the predicted life of 77,000 and the observed life of about that value. However, while the strain energy release rate, G , was virtually constant during the delamination process in the previous model, it changes dramatically during the process modeled by this form of the equations. Hence, the integrations in Eqns. (18) and (19) perform a very necessary function since the arguments become strongly dependent upon the number of cycles, n . The cyclic stress amplitude for specimen C5-11 is 32.1 ksi which corresponds to a strain amplitude of about 3,900 $\mu\epsilon$. The total strain range was used in the model as before. The values of delaminated and undelaminated modulus for the Type C specimens calculated earlier were also used for this computation.

Having made our initial selection of the parameters in the model, we attempted to predict the results for other specimens. Specimen C7-1 was

oscillated at a stress amplitude of about 35.7 ksi. A stiffness change of about 6% was observed for that test. The calculated life for that specimen was about 12,500 cycles compared to an observed life of about 18,000 cycles. Specimen C8-8 was cycled at a stress amplitude of about 28.6 ksi which corresponds to a total strain range of about 7,820 $\mu\epsilon$. A stiffness change of about 8% was observed during that test. The calculated life for that situation was 325,000 cycles compared to an observed life of about 328,000 cycles. Data for specimen C6-2 at the intermediate strain level is also shown on Fig. 60. Agreement between predicted and observed results is excellent. Of course, we must remember that the model was set up to match one of these data points precisely, and we should also remember that the measured stiffness changes have a very strong influence on the accuracy of the model. To test the strength of this modeling concept, other situations should be examined.

We return now to the block loading results described earlier, and examine our predictions using this second form of our compression model. For the purpose of our computations, we require that stiffness changes be used. For that purpose we take data from Fig. 61 collected during the typical tests indicated there. We consider the Set 2 sequence and observe that during Block 1 loading a stiffness change of 1.5% is observed. A polynomial is fit to the resulting specimen axial strain over the course of 4×10^5 cycles of loading and used as input to the model. Block 1 of Set 2 loading consists of fully reversed cycling at a strain amplitude of about 3,500 $\mu\epsilon$ for 150,000 cycles. That computation produces a predicted delaminated crack length of about 6.2×10^{-5} inches. While it is true that this crack length is very small, it is, nevertheless, an initial crack when Block 2 loading begins. It should also be remembered that there has been a 1.5% stiffness change during Block 1 loading which influences the

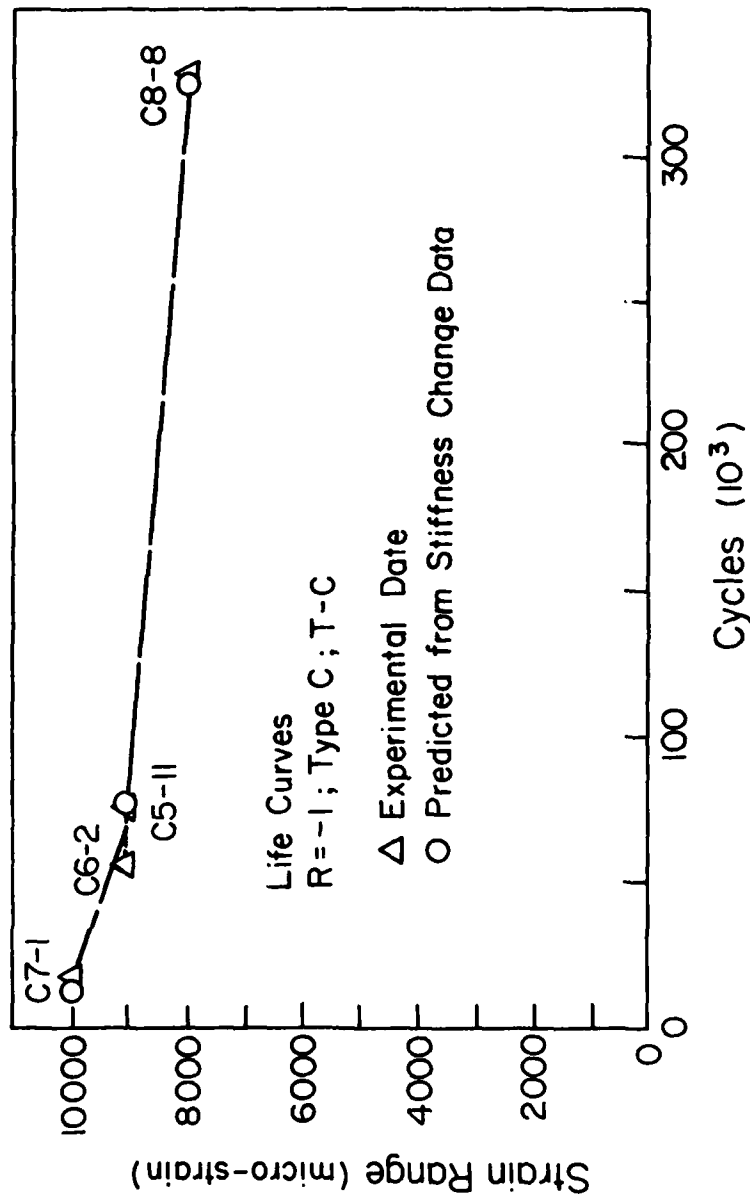


Figure 60: Predicted and Observed Life Data for T-C Model which Uses Observed Stiffness Changes

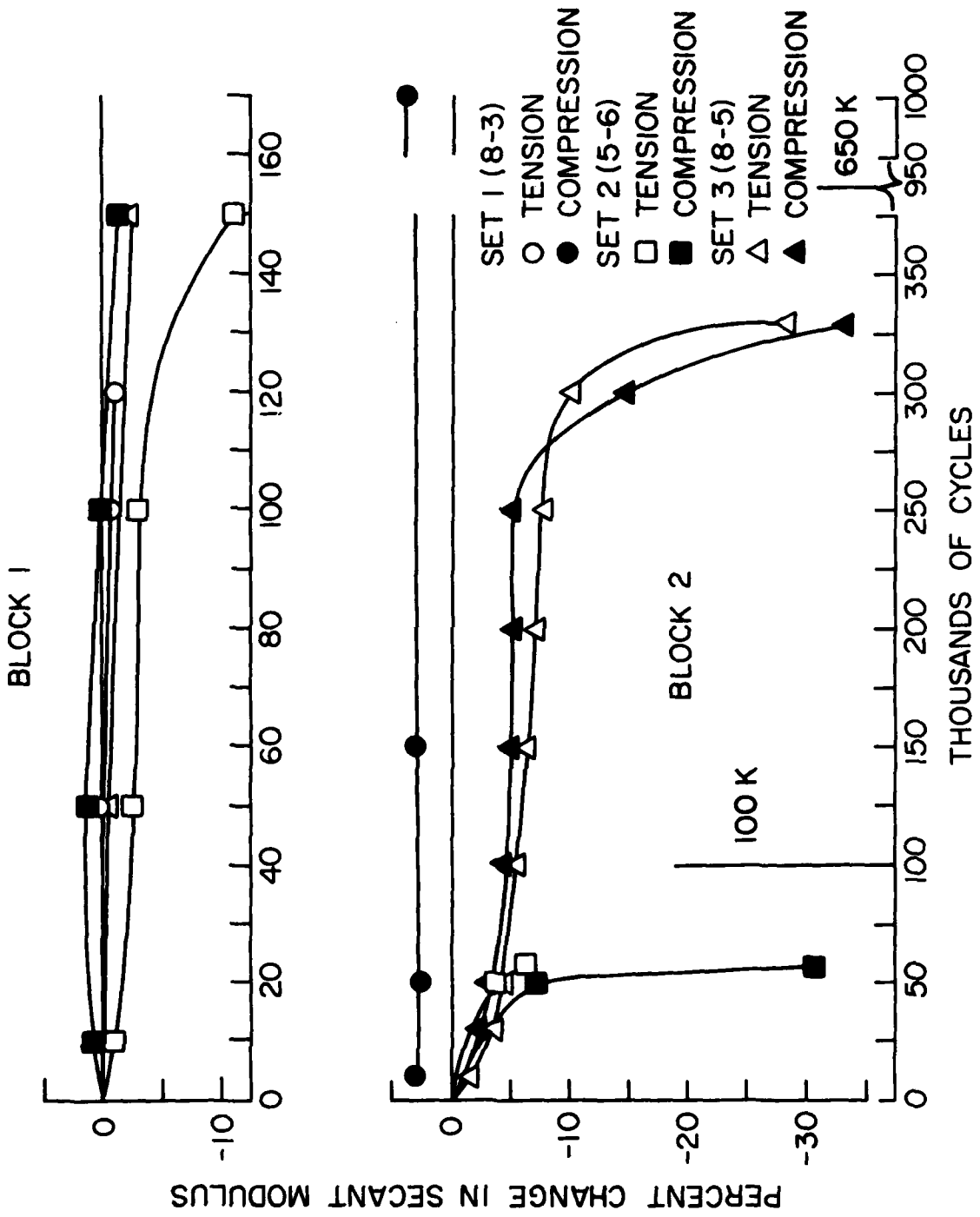


Figure 61: Stiffness Change During Block Loading of Three Specimens

laminate strain values that occur during Block 2 loading. Block 2 consists of fully reversed constant amplitude fatigue loading which corresponds to an initial value of about 4,500 $\mu\epsilon$ in amplitude. Block 2 loading is continued until specimen failure, an event that is defined by compressive instability at the value of applied load amplitude. A 7% change in the stiffness of the specimen is observed during Block 2 loading. The delamination model is used to calculate the life of the specimen (assumed to be coincident with the propagation of a delamination interface across the total width of the specimen) using the stiffness change and calculated crack length from Block 1 as initial values to the calculation for Block 2 loading. The Block 2 calculation then gives a life of 72,000 cycles compared to an observed life of about 57,000 cycles. If the change in stiffness in Block 1 is about 6%, then a predicted crack length of 8.5×10^{-5} is obtained, and a predicted life of 45,000 cycles for Block 2 loading is obtained from the model. If the Block 1 initial change in stiffness and crack length are ignored during the Block 2 calculation (to completely remove the influence of a prior loading history) the Block 2 calculation yields a predicted life of 71,500 cycles. The prediction of 45,000 cycles of life for the block loading results is to be compared with the average value of 33,000 cycles observed for three tests as recorded in Table 7, and a predicted life of 71,500 cycles when Block 1 loading is ignored is to be compared with an observed value of about 100,000 cycles for that loading applied alone. Hence, as indicated in Table 7, the block loading results are within about 7% of the observed data and the predictions for Block 2 alone differ by about 11% from the observations. This is thought to be reasonable agreement, quite similar to the accuracy of results obtained by using the delamination model that calculates the stiffness change rather than using observed values described earlier.

TABLE 7.
RESULTS OF BLOCK LOADING TESTS AND PREDICTIONS

| <u>Set</u> | <u>Specimen</u> | <u>Block</u> | <u>Cycles (thousands)</u> | <u>Average Life (thousands)</u> | <u>Predicted Life (thousands)</u> | <u>Percent Error</u> | | | |
|------------|-----------------|--------------|-------------------------------|---|---|--------------------------|--------------------|--------------------|----|
| 2 | 5-6 | 1 | 150 | 183 | 173 ¹ 195 ² | 5.4 7 | | | |
| | | 2 | 57 | | | | | | |
| | 7-6 | 1 | 150 | | | | | | |
| | | 2 | 32 | | | | | | |
| | 8-7 | 1 | 150 | | | | (250) ³ | (222) ³ | 11 |
| | | 2 | 11 | | | | | | |
| 3 | 8-5 | 1 | 150 | 474 | 451 ¹ 486 ² | 4.8 3 | | | |
| | | 2 | 327 | | | | | | |
| | 7-4 | 1 | 150 | | | | | | |
| | | 2 | 313 | | | | | | |
| | 7-8 | 1 | 150 | | | | (600) ³ | (490) ³ | 18 |
| | | 2 | 232 | | | | | | |

- ¹ delamination law driven calculation
² measured stiffness change driven calculation
³ block 2 without previous block 1; calculation using estimates of stiffness change data

For Set 3 block loading, the first block consists of T-T loading with a maximum initial maximum strain of about 4,000 $\mu\epsilon$ for 150,000 cycles, followed by T-C loading with an initial strain amplitude of about 4,000 $\mu\epsilon$. Again, stiffness changes from Fig. 61 were used to apply the cumulative damage model. The tension-tension calculation produced a drop in residual strength of about 1% with a 2% drop in the laminate stiffness. During Block 2 of Set 3 loading the stiffness change became quite large near the end of the test, about 30% for this particular test. This sharp drop in stiffness causes a rapid increase in strain which is interpreted by the model as a very rapid increase in the rate of crack growth. Hence, an accurate life prediction is virtually guaranteed by the data. The calculated life for this data set was 336,000 cycles compared to about 335,000 cycles for specimen C8-5 shown in Fig. 61. If we attempt to ignore Block 1 loading for this case, but still use the stiffness changes observed for specimen C8-5 to calculate a life prediction for the corresponding test condition not preceded by Block 1, the computation by the model is dominated by the rapid decrease of the modulus between about 250,000 and 350,000 cycles. Hence, the predicted life becomes only about 340,000 cycles compared to a measured value of roughly 600,000. As we mentioned before, when a model such as the present one is used which depends on measured values of stiffness change, it has the general major advantage of being highly accurate as a predictor of residual strength and life for the individual specimen for which the measurement was made. When that type of model is used for a prediction of residual properties for an arbitrary specimen for which no measurements are available, some reasonable means of estimating the stiffness changes must be used. For

the T-T model, a rationale has been established for that estimation process. For T-C loading, no well-established rationale is yet available, partly because of the large increases in stiffness that are caused by combined modes of damage development, specifically combinations of matrix cracking and edge delamination.

C. Variable R Value Testing and Modeling

So far we have considered the modeling of cumulative damage in situations where only tensile cyclic loading was applied, where only compressive cyclic loading was applied, and where an equal amplitude of tensile and compressive cyclic loading was applied in a fully reversed cyclic test. In terms of the common fatigue terminology, these loadings correspond to an R value of 0.1, 10, and -1. Of course, service loadings involve various combinations of tensile and compressive loading, i. e., various R values. Hence, two questions must be addressed. First, it must be determined if the fatigue loadings corresponding to other R values have a similar affect on material behavior as the classical cases already considered, or if the behavior can easily be extrapolated from the familiar results. And second, it must be determined if the models used to describe that behavior which are based on mechanisms peculiar to situations where either tensile or compressive damage modes dominate can be applied to intermediate situations. We have mentioned earlier that the R=-1 situation (T-C) is especially severe in the sense that tensile loading alone or compressive loading alone with the same stress range as the fully reversed stress amplitude produces dramatically less damage over the same number of cycles compared to the fully reversed case. It is reasonable to suspect that there is a transition range over which this synergism disappears.

Finally, the present model depends on two different analytical formulations, one for the situation where there is tensile loading alone, and one for the situation where there are compressive components. Is it appropriate to switch from the tensile model to the T-C model when only a small amount of compressive loading is present? All of these considerations have not been examined completely, but some of them will be considered below. Before examining these results, it is important to emphasize that a basic research investigation is needed to examine the actual processes of interaction between tensile and compressive damage modes so that a more rational approach to mechanistic modeling could be taken.

Based on the experimental observations, we have taken the following interim approach. Figure 62 presents a series of fatigue life data for five different R values. These data have been plotted as a function of the total strain range (actually total stress range), i.e., the absolute value of the maximum stress minus the minimum stress in the test. While it is true that plotting the results against the total strain range does not completely coalesce the data, it is also very clear that the results are closely grouped for such a plot, more closely grouped than any other portrayal that the authors were able to find. Another striking feature of the curves is the fact that they appear to be parallel to one another, that is, they appear to have a quite similar slope. Hence, it was decided to use the total strain range (or total stress range) in the model that we have been using for loading which includes compressive load excursions as we have done in earlier applications of that model, and to introduce a dependence on the stress ratio, R, by incorporating into the model a function of R which multiplies the strain range by a factor which is equal to the vertical separation of the curves in

Fig. 60. Since our model has been applied earlier to the fully reversed $R=-1$ case (for the Type C laminate), the data for that situation will be used as a baseline, and all other strain amplitudes will be adjusted accordingly. For the test data shown in Fig. 62, the correction factors become the values shown below.

| | |
|---------------|---------------------------|
| $R = -\infty$ | Correction factor = 1.188 |
| $R = -1$ | Correction factor = 1 |
| $R = -0.5$ | Correction factor = 1.093 |
| $R = -2$ | Correction factor = 1.227 |

A polynomial curve was fit to those points and used as the function of R which corrects the strain range input into the T-C model described in the previous section.

Two different types of calculations will be demonstrated below. We will discuss calculations for cyclic loading which includes some compressive load excursions, namely $R=-1$, $R=-2$, and $R=-0.5$. The two situations to be examined are the calculations for the T-C model in the two forms discussed earlier, namely, the form which uses the delamination propagation power law equation and calculated values of stiffness change to adjust the strain as a function of cycles, and the second form of the model which uses the measured stiffness change data as an input to adjust the strain level as a function of cycles. We will refer to the second form of the model as a "data driven model". Figure 63 shows the residual strength predictions as a function of cycles for three specimens, as well as the life predictions and observations for those three specimens. Since the $R=-1$ case was used as

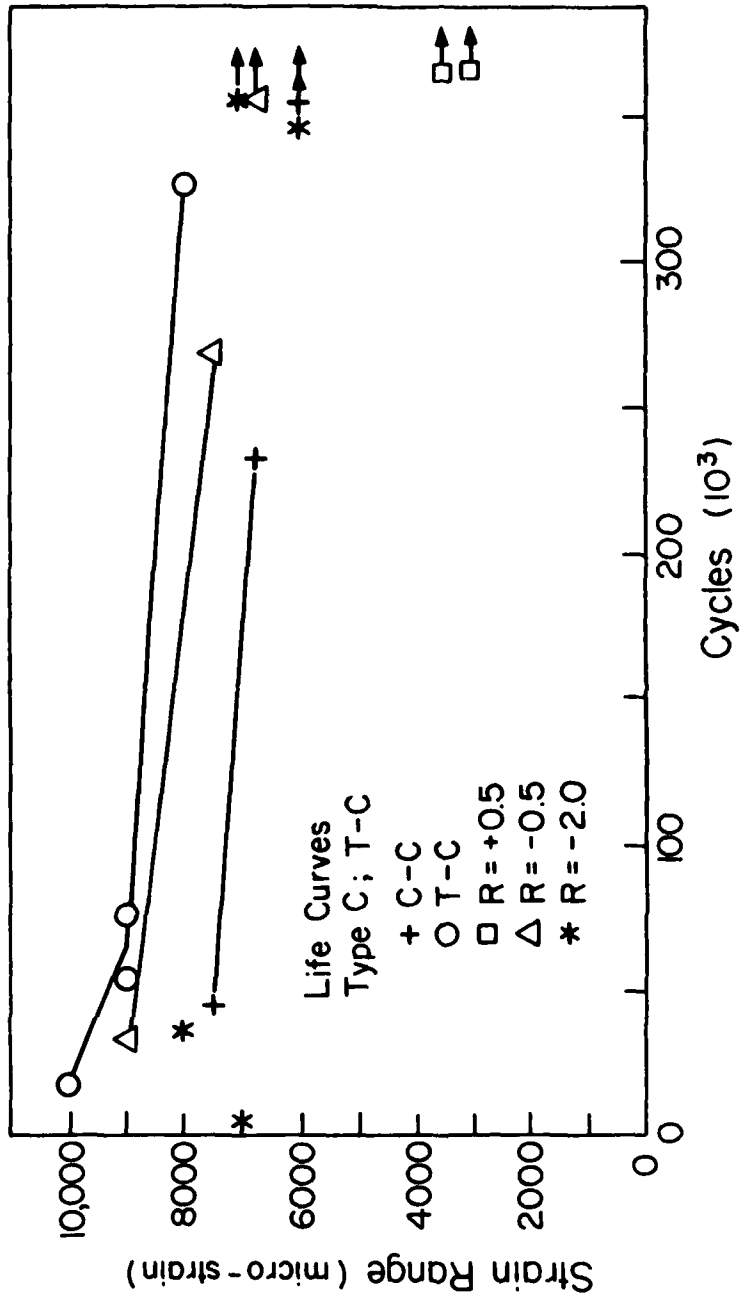


Figure 62: Fatigue Life Observations for Five Different R Values

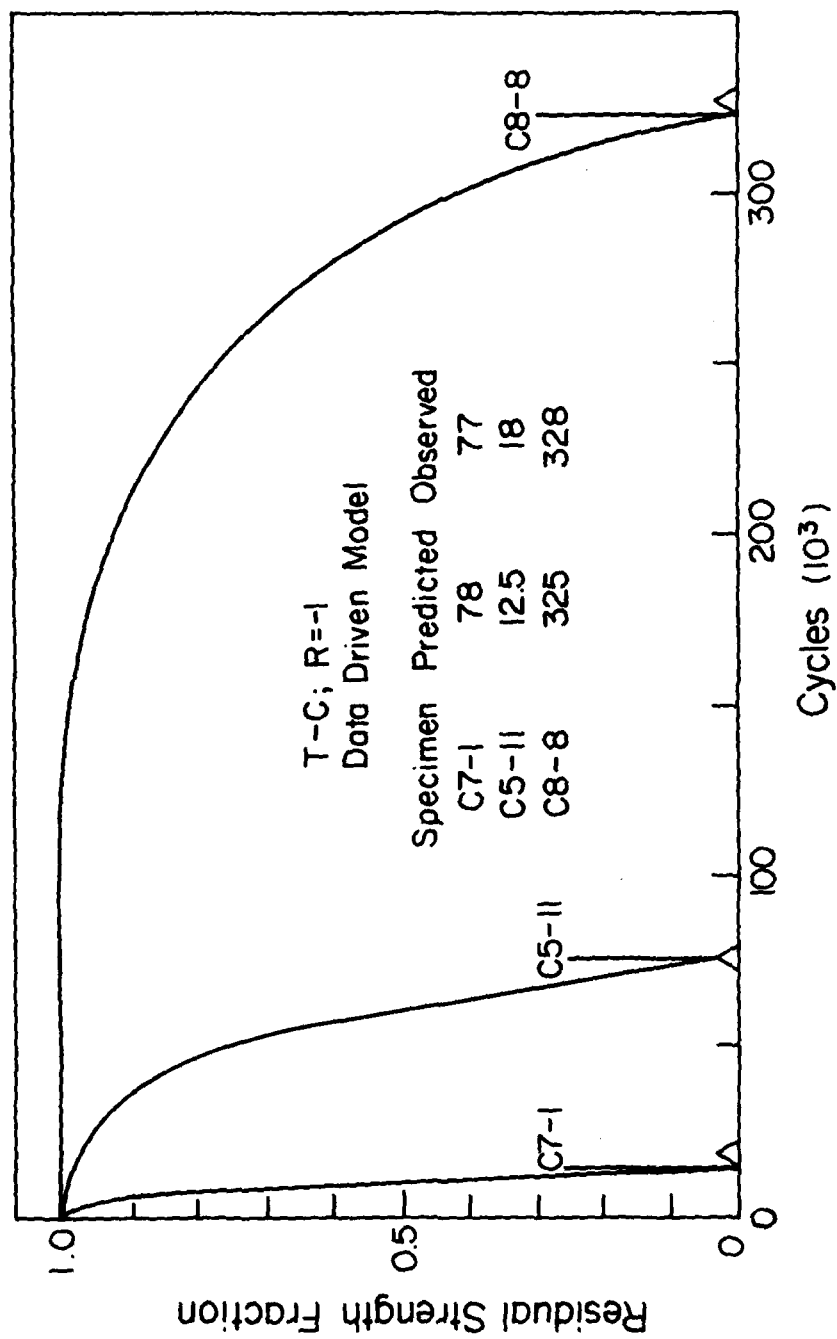


Figure 63: Residual Strength Prediction for R=-1, Type C

a baseline, and since the data driven model is strongly (and positively) influenced by the stiffness changes measured in a given test, the predicted results are very close to the observed values.

Figure 64 shows predicted and observed results for $R=-0.5$. Results predicted from the data driven model as well as the model which requires only the delamination equations are shown. It is interesting to note that the observed life values fall within the bracket formed by the two predicted values for each of the specimens analyzed. Moreover, the two predicted values and the observed value are quite close together. For specimen C8-12 the test was terminated at 350,000 cycles and a residual strength was measured. The strength of that specimen was observed to have been reduced by 4%. The predicted strength reduction using the data driven model was also 4%, an agreement that is certainly fortuitously close.

The results for the $R=-2$ tests are shown in Fig. 65. These tests are, of course, the counterpart to the $R=-0.5$ tests in the sense that for $R=-2$ the tensile component of loading is half as large as the magnitude of the compressive component, while for $R=-0.5$ the compressive component of loading is half as large in magnitude as the tensile component. However, the experimental results for the $R=-2$ situation were somewhat strange, as can be seen from the data plotted in Fig. 62. Figure 65 shows predicted and observed results for three specimens tested with $R=-2$. The observed stiffness changes were small for these tests, about 1% for specimen C8-10 and about 7% for specimen C7-9. Hence, the data driven model predicts values of life that are noticeably larger than the observed values. The model which uses the delamination equations alone is conservative as before. Hence, the observed results fall between the predicted ones. For the lowest strain

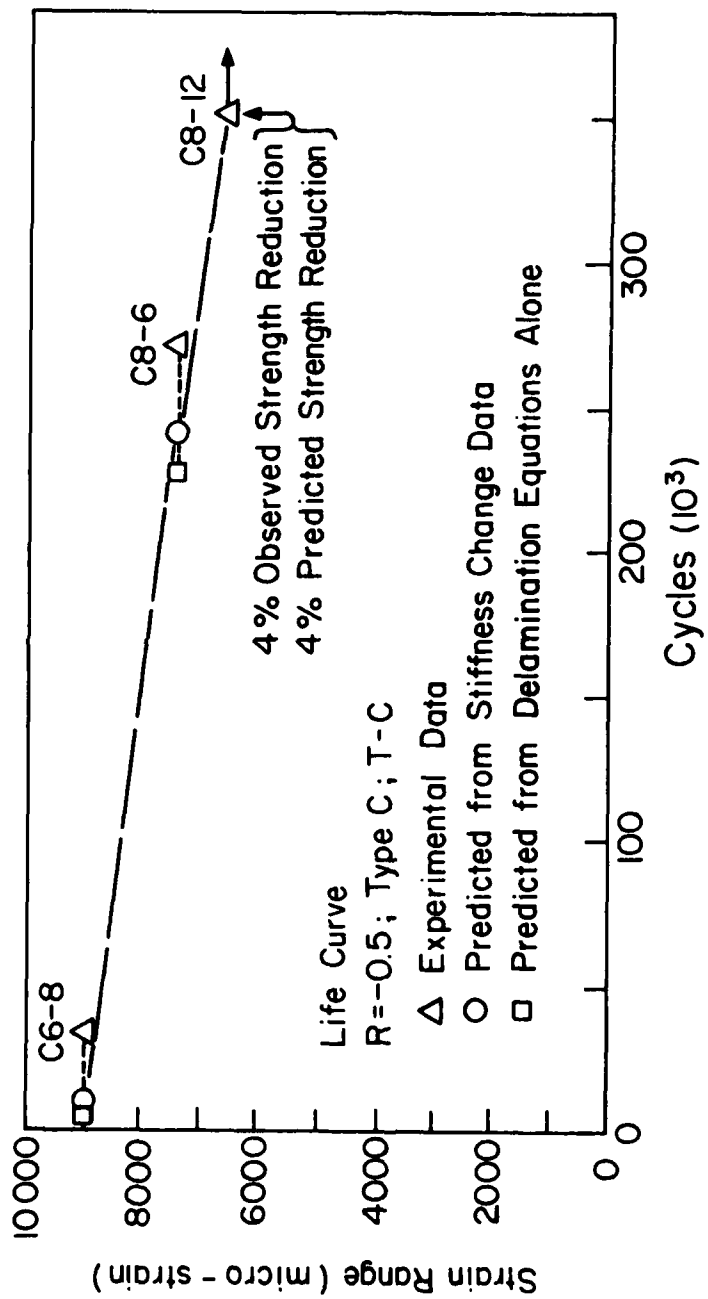


Figure 64: Life Predictions and Observations for $R = -0.5$ Tests

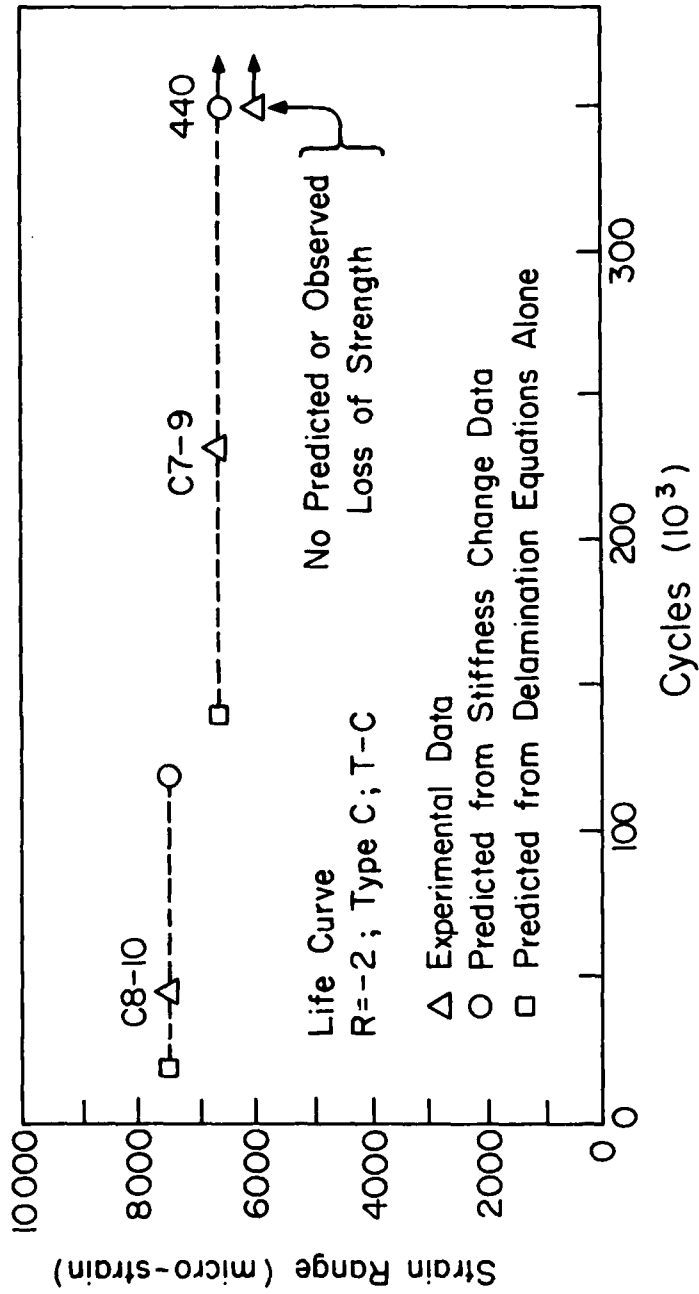


Figure 65: Predicted and Observed Life for R=-2 Tests

range in Fig. 65, the specimen did not fail in one million cycles, and was pulled to failure after the test to determine the residual strength at that point. The residual strength was essentially identical to the quasi-static baseline strengths measured earlier. Neither of the models predicted any strength loss for those amplitudes. While the life predictions in Fig. 65 are rather widely spaced, they are all within a factor of 2 or 3 of the observed data, a level of agreement that is generally tolerable in the context of fatigue behavior.

Table 8 is a summary of the results for the variable R series of tests and predictions. The life predictions and residual strength prediction are shown along with the observed data for the tests analyzed. It appears that engineering accuracy can be obtained with this rather simple approach to the modeling of fatigue loading spectra which involve compressive load excursions. However, it should be reemphasized that the basic mechanisms involved in these tests, the interaction of those mechanisms, the micro-damage states, and the micro-stress states have not been addressed in any detail here. Hence, it is not possible to define the boundaries of applicability of this model nor is it possible to imply that the cumulative damage behavior for all R values involving compressive load excursions can be predicted from this scheme.

Now we have come to the most important conclusions of our work.

Table 8. Summary results for variable R series

| R | Specimen | Max ϵ | Min ϵ | Observed | Life (10^3) | | Strength (%) | |
|------|----------|----------------|----------------|----------|------------------------|------------------------|--------------|-----------|
| | | | | | Predicted ¹ | Predicted ² | Observed | Predicted |
| -0.5 | C6-8 | 6000 | -3000 | 34 | 9.8 | 4.6 | | |
| -0.5 | C8-6 | 5000 | -2500 | 269 | 240 | 226 | | |
| -0.5 | C8-12 | 4500 | -2250 | 1000+ | | | 0.96 | 0.96 |
| -1 | C7-1 | 5000 | -5000 | 18 | 12.5 | | | |
| -1 | C6-2 | 4500 | -4500 | 56 | 77.4 | | | |
| -1 | C5-11 | 4500 | -4500 | 77 | 77.4 | | | |
| -1 | C8-8 | 4000 | -4000 | 328 | 325 | | | |
| -2 | C8-10 | 2500 | -5000 | 45.6 | 120 | 19 | | |
| -2 | C7-9 | 2250 | -4500 | 232 | 440 | 139 | | |
| -2 | C5-3 | 2000 | -4000 | 1000+ | | | 1.0 | 1.0 |

- 1 Predicted from stiffness change data
- 2 Predicted from delamination equations alone

5. Closure

The cumulative damage model that we have presented above has the following salient features:

- The model predicts the strength and life of engineering composite laminates under tension-tension, tension-compression, compression-compression, block-spectrum loading, and constant amplitude cyclic loading with R values between 0 and minus infinity.
- The model replaces Miner's Rule with an engineering model which is based on the physical mechanisms of damage and failure.
- Among other things, the model is able to account for the following features.
 - (a) Sequence effects in block loading.
 - (b) The effects of unknown load histories. (The model is able to predict the residual strength and life from the results of inspections, vis-a-vis, from measurements of stiffness changes for individual specimens, a critically unique feature.)
 - (c) Biaxial stress effects on the degradation of the 0 degree plies.
 - (d) Different changes in stiffness under the tensile load excursions compared to compressive load excursions for variable R value T-C loading.
 - (e) Different baseline quasi-static strength and stiffness (which enter as normalization factors).

- (f) Different laminate types, i. e., different combinations of ply orientations, physical dimensions, ply properties, stacking sequences, etc.

While the authors believe that this modeling effort has provided a firm foundation for continued work, it is only a first attempt to construct a mechanistic model of damage accumulation. During the course of the work it has become apparent that additional research and synthesis is needed in several areas. A few are listed below.

- Mechanistic models are only as good as our understanding of the damage events induced by fatigue loading in composite laminates. If progress is to continue in the area of mechanistic modeling of cumulative damage, progress must continue in the area of understanding these events. Perhaps the greatest need for investigation is associated with damage development that is induced by combined tension and compression load excursions, a process which is poorly documented and not well understood. A variety of other situations which involve combined damage modes also are in great need of further investigation.

- There is a need for a more thorough and complete analysis of the internal stress states that exist in the neighborhood of damage events. This is especially true of damage events which involve or induce three-dimensional stress states, such as transverse cracks which cross at the interface of two plies having different orientations.

- Mechanistic modeling to date has concentrated on the development of damage. The coalescence and localization of damage has not received sufficient attention. If accurate predictions of the fracture strength (or residual fracture strength) of laminates is to be obtained from mechanistic modeling, it is essential that additional attention be given to the development and precise nature of the fracture event, and to those events which precipitate the fracture process.
- The present investigation has been concerned with block loading or constant amplitude fatigue cycling. The modeling approach that has been used is, however, applicable in theory to spectrum loading. A logical next step in this investigative process would be to attempt to apply the present model or refinements thereof to a more general spectral loading.
- The present investigation has been concerned with coupon specimens for which the nominal stress state is uniform. The present approach could be, and should be, applied to nonuniform stress states such as those found in notched specimens.
- There is a continuing need to develop a nondestructive testing technique and associated damage parameter that can be used for mechanistic modeling purposes as well as for field interrogations for routine inspection purposes. For our present purposes, we have used stiffness change as a damage parameter

with considerable success. However, a development effort is needed if that damage parameter or other ones are to be applied to engineering components in field service.

- Another logical area of investigation as a follow on to this effort is the study of various environmental effects including temperature and moisture.
- There is a great need for an experimental investigation of the internal stress states associated with damage events and combination of damage events. In the past few years a number of experimental techniques such as moiré diffraction have been perfected which are capable of measuring the very small displacements and displacement gradients associated with small damage events such as matrix cracks, fiber fractures, and local debondings or delaminations. It is essential that these techniques be further developed and applied to fatigue damage development in composite laminates, not only for the purpose of validating various analysis methods, but also for the purpose of guiding the development of those methods and, most importantly, for the purpose of providing the physical information necessary for investigators to develop an understanding of the damage development processes.
- The philosophical, analytical, and conceptual generalities that investigators are able to make are always limited by experience. One of the greatest needs for further work is the

need for improved and more complete characterization of the fatigue behavior and damage development in various laminates and material systems.

- The transfer of techniques, understanding, and technology from the laboratory to the practitioner is always a challenge, but it is an extremely demanding challenge in the present case. A development program is needed which will address this transfer. A first step might be to generate interactive computer codes that can be used for design and analysis by practicing engineers without the continuous service of specialist scientists.

The ten areas of need above are only a few of the major topics that come to mind. The present investigation suggests that progress can be made when opportunities are provided.

SECTION III

CUMULATIVE DAMAGE EXPERIMENTAL INVESTIGATION

1. Background

The overall objective of the experimental portion of this program is to quantify material responses for the specific purpose of model development and refinement. Damages induced in selected laminates under the fundamental loading conditions of quasi-static tension and compression, constant amplitude fatigue at various R-ratios, and simple spectrum fatigue were thoroughly investigated. In addition to establishing the chronology and location of damage development, changes in specimen stiffness and strength were also established. These material responses were related to the damage state existing in the subject specimen at the time of measurement. Both nondestructive and destructive test techniques were employed to monitor the damage development and property changes. The nondestructive techniques applied included surface replication, enhanced X-ray radiography, and stiffness measurements. All data was input to the cumulative damage model development and refinement activities, as described in the previous section.

During Phase II, a total of 83 mechanical tests were conducted. The tests are illustrated in the Phase II test matrix shown in Table 9. Of these tests, 18 were conducted by Virginia Polytechnic Institute and State University Professors Reifsnider, Henneke, and Stinchcomb. The remaining 65 tests were conducted in the Materials

TABLE 9: PHASE II TEST MATRIX

| Test Type | Stress Ratio | Notes | Tests Scheduled | | |
|--|--------------|-------------------|-----------------|--------|-------|
| | | | C | F | Total |
| Monotonic Tension | - | Ramp to Failure | 0 | 3 | 3 |
| Monotonic Compression | - | Ramp to Failure | 0 | 5 | 5 |
| Quasi-Static Tension | - | Damage Monitoring | 0 | 2 | 2 |
| Quasi-Static Compression | - | Damage Monitoring | 0 | 1 | 1 |
| Constant Amplitude Fatigue | 0.1 | Baseline | 3 | 3 | 6 |
| | | Residual Strength | 3 | 3 | 6 |
| | 10 | Baseline | 1 | 2 | 3 |
| | | Residual Strength | 1 | 1 | 2 |
| | -1 | Baseline | 4 | 4 | 8 |
| | | Residual Strength | 5 | 4 | 9 |
| | 0.5 | Stress Ratio | 3 | 0 | 3 |
| | 2.0 | Stress Ratio | 0 | 3 | 3 |
| | -0.5 | Stress Ratio | 3 | 3 | 6 |
| | -2.0 | Stress Ratio | 3 | 3 | 6 |
| Simple Two-Stage Spectrum Load Histories | 0.1/10 | Set #1 Load Mode | 3 | 3 | 6 |
| | -1 | Set #2 Amplitude | 3 | 3 | 6 |
| | 0.1/-1 | Set #3 Load Mode | 3 | 0 | 3 |
| Unspecified | -- | Used As Required | 0 to 5 | 0 to 5 | 5 |

83

Research Laboratory of General Dynamics' Fort Worth Division.

The following sections describe the laminates, specimens, and test methods employed. The experimental results are then presented.

A. Specimen Description

Two laminate stacking sequences were chosen for Phase II evaluation. As in Phase I these stacking sequences were chosen to minimize the effects of the interlaminar stresses which develop at the free edge of the coupon specimens. The first stacking sequence, designated Type C, is a quasi-isotropic stack used in Phase I. This stacking sequence has been used to provide a more extensive data base on one laminate configuration. The other laminate configuration, designated Type F, has equal numbers of 0, +45, and -45 degree plies. The two stacking sequences are shown in Table 10.

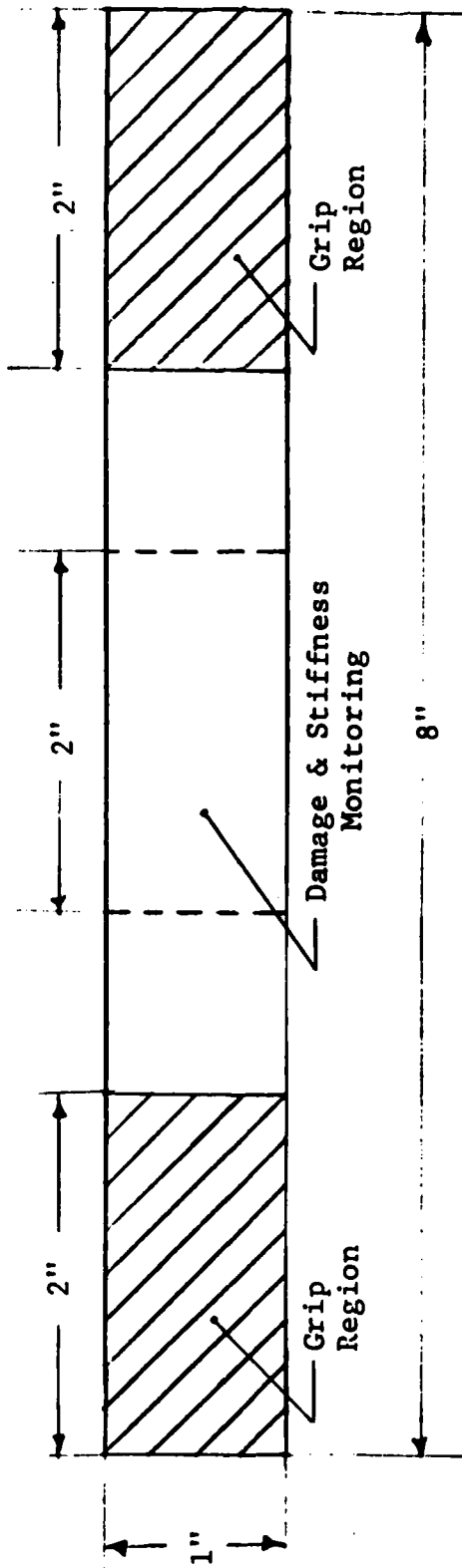
Figure 66 illustrates the basic specimen design. This basic specimen geometry consists of a 48 ply, one inch wide laminate with a four inch unsupported gage length between the grips. One minor change in this geometry when compared to that used in Phase I has been to increase the overall specimen length from seven to eight inches. This change was incorporated to provide a larger gripping area which reduces the effective gripping stress. The same material used in Phase I, AS1/3502, was used to fabricate all Phase II specimens.

Note that the two laminate stacking sequences used are both composed of repeated building blocks. Type C has six eight ply blocks of (0/+45/90/-45)s and Type F has eight six-ply (0/+45/-45)s blocks.

TABLE 10: LAMINATE STACKING SEQUENCES

| TYPE | FAMILY | STACKING SEQUENCE |
|------|------------|---|
| C | (25/50/25) | $[(0/+90/-)_{\text{S}} (0/+90/-)_{\text{S}} (0/+90/-)_{\text{S}}]_{\text{S}}_{\text{S}}$ |
| F | (33/67/0) | $[(0/\pm)_{\text{S}} (0/\pm)_{\text{S}} (0/\pm)_{\text{S}} (0/\pm)_{\text{S}}]_{\text{S}}_{\text{S}}$ |

(+) INDICATES A +45° PLY
 (-) INDICATES A -45° PLY



48 plies thick $\approx 0.265 - 0.290$

Figure 66: Specimen Geometry

These building blocks will be referred by number (1 through 6 for Type C and 1 through 8 for Type F) and identified as 'ply groups' to aid in the documentation of damage development through the specimen thickness. The use of this building block approach also results in the minimization of the interlaminar normal stress, σ_{zz} . The through the thickness interlaminar normal stress distributions are shown in Figures 67 and 68 for the Type C and Type F laminates, respectively. Note that the edge stress is zero between each ply group and that the magnitudes in the Type C are nearly the same as those in the Type F, though the signs are reversed. Type C has tensile interlaminar normal stresses under tensile loading while Type F interlaminar normal stresses are tensile under compressive loading.

The selection of these two laminate stacking sequences provides the modelling effort with different damage developments. The existence of 90 degree plies in the Type C, the +/-45 interface in the Type F, the difference in the number of 0 degree plies, and the differences in the interlaminar normal stress distribution all serve to generalize the cumulative damage model.

Phase II specimens have been numbered by the same method as the Phase I specimens. Each panel fabricated has been labeled according to stacking sequence and panel number. For example, Panel C5 refers to the fifth panel of Type C configuration. Each of the 12 specimens cut from each panel were labeled continuously one through twelve. Thus specimen labeled C5-10 is the tenth specimen cut from the fifth Type C panel. A total of four Type C panels and five Type F panels were fabricated for the Phase II effort. Panel designations for Phase II specimens are thus F1 through F5 and C5 through C8 (panels C1 to C4

TYPE C

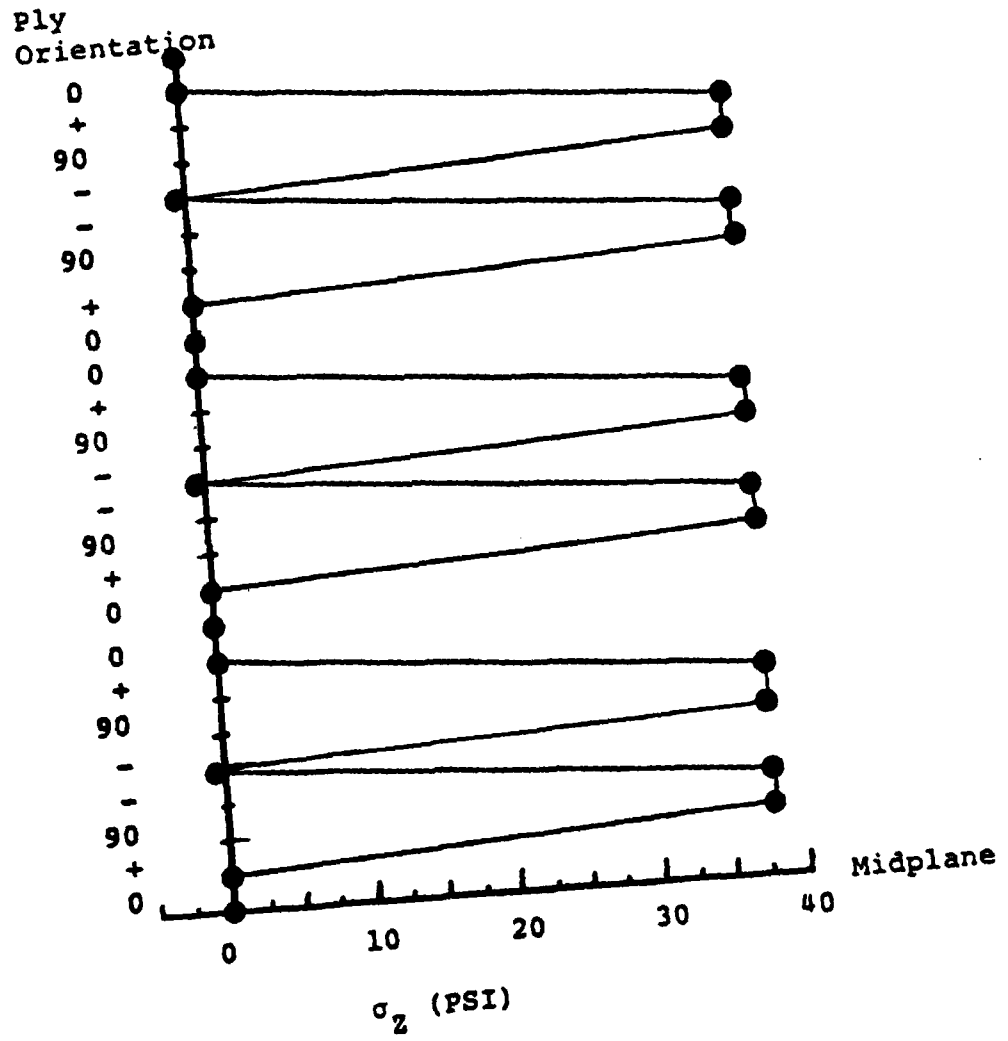


Figure 67 Interlaminar Normal Stress Distribution of Type C Laminates

TYPE F

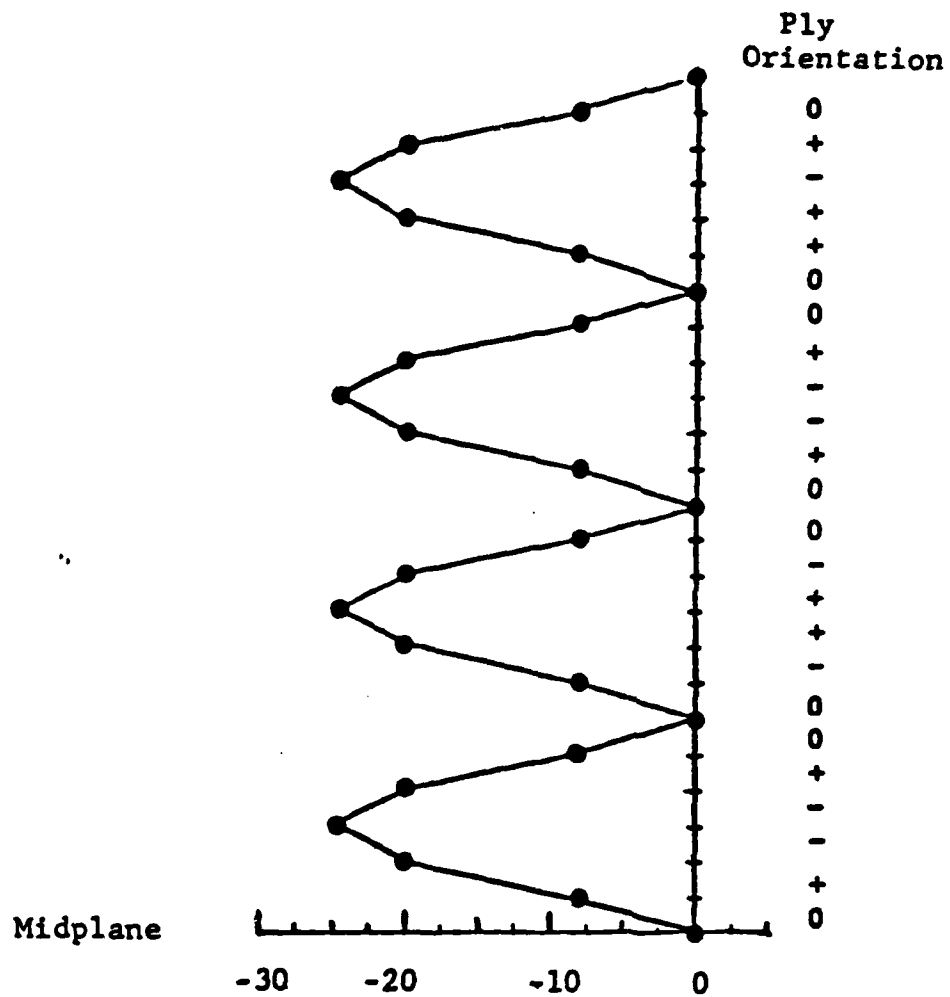


Figure 68 Interlaminar Normal Stress Distribution of Type F Laminates

were fabricated for the Phase I effort).

B. Nondestructive Test Techniques

Surface replication is a well-established metallographic procedure applied to optical and electron microscopy. This technique has only recently been applied to composite materials. The basic procedure is quite straightforward. A thin strip of .005"-thick cellulose acetate tape is anchored to the polished edge of the specimen by adhesive tape. A small amount of acetone is then injected between the specimen and the replicating tape. The acetone locally dissolves the replicating tape which flows into cracks in the composite laminate. The cellulose acetate hardens in a few minutes and is peeled from the specimen bearing an imprint of the specimen edge.

Edge replicas provide a permanent record of the damage state over the entire length of the specimen at the instant that a certain load level is reached. This technique can be applied while the specimen is in the test machine under load (+4 kip for Type C, +5 kip for Type F) so that the recordings capture the damage state in its most enlarged or open state. If the inspection is made after the load is removed from the specimen, many smaller cracks may close and not be detected. The replicas are easily stored for reexamination and future reference. Furthermore, replication is a simple technique that does not require complicated or extensive equipment.

Surface preparation is an important step in applying this

technique. The entire specimen edge is metallurgically polished on a polishing wheel using a 3 micron aluminum oxide/water suspension system on a felt polishing cloth.

A low voltage (25 kv and 2 ma) X-ray NDE technique modified for composite material application was used to monitor damage development through the specimen width. An opaque additive, zinc iodide, is introduced to the composite through the specimen edge. The ZnI_2 enters the cracks and delaminations which develop in the specimens by capillary action. The images of the voids and delaminations are greatly enhanced by the highly attenuating characteristics of the opaque additive.

X-ray records of the damage growth in the composite specimens were enlarged when prints were made from the exposed film. The darkened areas on the prints represent flawed areas where the opaque additive had penetrated. The actual length and area of the damage zones could be obtained from the prints using the appropriate scaling factor.

A 110 kv Picker portable X-ray unit was used in this study. It has a 2.25mm beryllium window and a focal spot of \emptyset .5mm. Kodak Type M industrial X-ray film was employed. A 69-second exposure time was required for each exposure.

Changes in specimen stiffness were also monitored during the mechanical testing. An extensometer was employed in the measurement of axial strain. It has a two inch gage length and was seated in aluminum blocks which were bonded to the specimens prior to testing. The two inch gage length provided a method for averaging of the damage so as to eliminate the effects of any local material variations. The

aluminum blocks provided reproducible seating of the extensometer which was removed during fatigue testing and mounted at discrete inspection times. The transverse strain was monitored through the use of a strain gage with a half inch gage length mounted in the center of the specimen span.

C. Test Procedures

1) Monotonic Tension and Compression

To determine the initial moduli of the laminates in this study, a series of ramp to failure tests was employed. In these tests, specimens having two longitudinal strain gages (front and back) and one transverse gage were mounted in the MTS machine. The specimens were then continuously loaded to failure at a rate calculated to correspond to that encountered in the constant amplitude fatigue tests. These tests were performed under computer control with load and strain channels being continuously recorded. Moduli were obtained by post-processing the data using a regression fit of the load (stress) and strain data.

2) Quasi-Static Tension and Compression

A series of tests was performed to determine the damage development and property changes of the laminates in this study under

static loading conditions. Since real-time methods of damage documentation of the type necessary in this program do not exist, these tests consisted of monotonic loadings in stages with load interruptions for the NDE evaluations.

The experimental procedure employed in both the quasi-static tension and compression tests was quite straightforward. The specimen was installed in the MTS hydraulic grips, a nominal initial tensile load was applied, and initial NDE evaluations were made. Once this initial examination was completed, the tensile load was removed, the extensometer was mounted on the specimen, and the initial specimen modulus determined by monotonically loading the specimen to a small predetermined load. The load was then returned to zero and the extensometer removed.

The specimen was then monotonically loaded (in either tension or compression, as appropriate) to a predetermined load value. The load was returned to zero and the NDE and stiffness procedures again employed. This process was repeated, with increasing load values in each step, until the specimen failed. The load reductions for each inspection were deemed necessary because the hold-at-load times required for the inspections were long and could adversely affect the results, especially at high loads.

3) Fatigue Testing

Three types of fatigue tests were conducted in this program: tension-tension, compression-compression, and tension-compression at

several R-ratios. All fatigue tests featured constant amplitude sinusoidal waveform loading, run under load control. A series of simplified spectrum tests, consisting of blocks of constant amplitude fatigue, were also performed.

The experimental procedure employed in these tests was identical to that used in the quasi-static testing, with the obvious exception that the loading between successive NDE evaluations was a predetermined number of fatigue cycles. This procedure thus results in a documentation of damage development and property changes as a function of fatigue cycles.

Each specimen was loaded in this manner until either a predetermined number of cycles, failure, or one million cycles. Those specimens which survived one million cycles and those for which testing was halted at a predetermined cycle count were monotonically loaded to failure to determine their residual strength. Thus data on life and strength reduction was obtained.

2. Summary of Test Results

A. Laminate Type C

The Phase II test matrix for the Type C laminate was designed to enhance the results obtained in Phase I both in a statistical sense by providing additional data for given load conditions, and in increasing the database by furnishing data for load conditions not included in the Phase I effort. The responses of this laminate to

tension-tension, compression-compression, and tension-compression constant amplitude fatigue loadings were studied using seven different R-ratios and several load levels within each R-ratio.

Static characterization of the Phase II Type C specimens was not performed as these specimens were prepared from the same material used in Phase I. These specimens were subject to the same quality control and assurance procedures described in previous reports. Confidence in the similarity of the Phase I and II specimens can be further established by comparison of responses under fatigue loading. Figure 69 presents the comparison of the S-N data generated for R=-1 load condition in the two phases of the program. Figure 70 is a comparison of the longitudinal stiffness retention obtained in a Phase I specimen and a Phase II specimen which were subjected to identical load conditions. As seen in both these figures, the responses of the Phase II specimens and those obtained in Phase I are comparable.

The results of the fatigue tests and damage inspections are summarized for each specimen in tables contained in the Appendix. These tables provide all the loading, property degradation, life, and damage information obtained for each specimen. The damage state at any inspection time is presented in a manner that allows the visualization of the actual damage within each ply group of the specimen. For example, the damage progression in specimen C5-5 is given in Table 11. Here it may be seen that the specimen contained no initial damage (no entries at 0 cycles) but that by 5000 cycles both the -45 degree and 90 degree plies within each ply group had cracked (as indicated by the damage code entries of '11' and '13', respectively) and that interfacial damage on the 90/-45 interface was

S-N CURVES OF LAMINATE TYPE C

R = -1.0

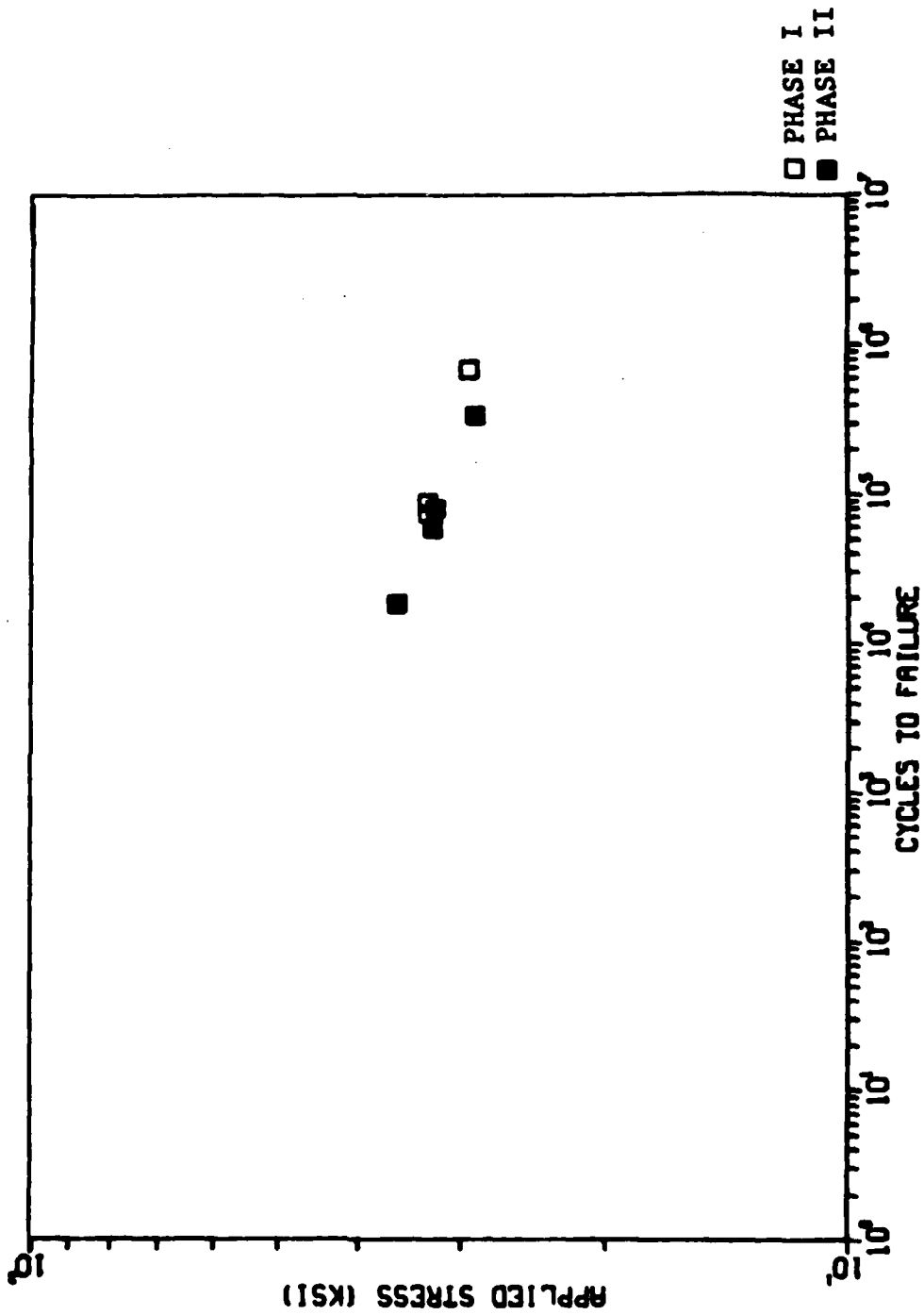


Figure 69 S-N Comparison: Phase I to Phase II Test Results

visible (damage code '36') within ply groups 2 through 6, while the same interface in ply group 1 was characterized as delaminated (code '46'). At 10000 cycles, the +45 ply had cracked in ply groups 1,3,4,5, and 6 (code '12'), delamination had begun on the +45/90 interface in groups 1 and 6 (code '45'), and delamination was also evident on the 90/-45 interface in group 6 (code '46'). Figure 71 shows the edge replicas for this specimen at these inspection intervals to allow a comparison of the tabulated damage state with the observed damage state. Note here that the two damage descriptors, delamination and transverse crack coupling, both refer to interfacial damage. Coupling refers to a damage state that is only detected on the edge replicas that has the appearance of a delamination but only extends along the interface for a distance of one to three cracks in adjacent plies. Delamination, on the other hand, may or may not appear in the X-radiographs but extends through at least four adjacent ply cracks along the interface.

A test matrix for the study of load history effects was designed to subject Type C (and Type F) laminates to sets of block loadings with two different constant amplitude loading blocks in each set. The loading modes and strain amplitudes for each block were determined to produce different responses based on the Phase I results. The load history test matrix for the Type C laminate is shown in Table 12.

Each specimen was quasi-statically loaded to the initial strain limits established for Block 1 of each set. The loads corresponding to the strain limits were recorded and used as the operating limits for the load controlled cyclic load histories at the specified R-ratios. For each of the three sets, the first loading block was

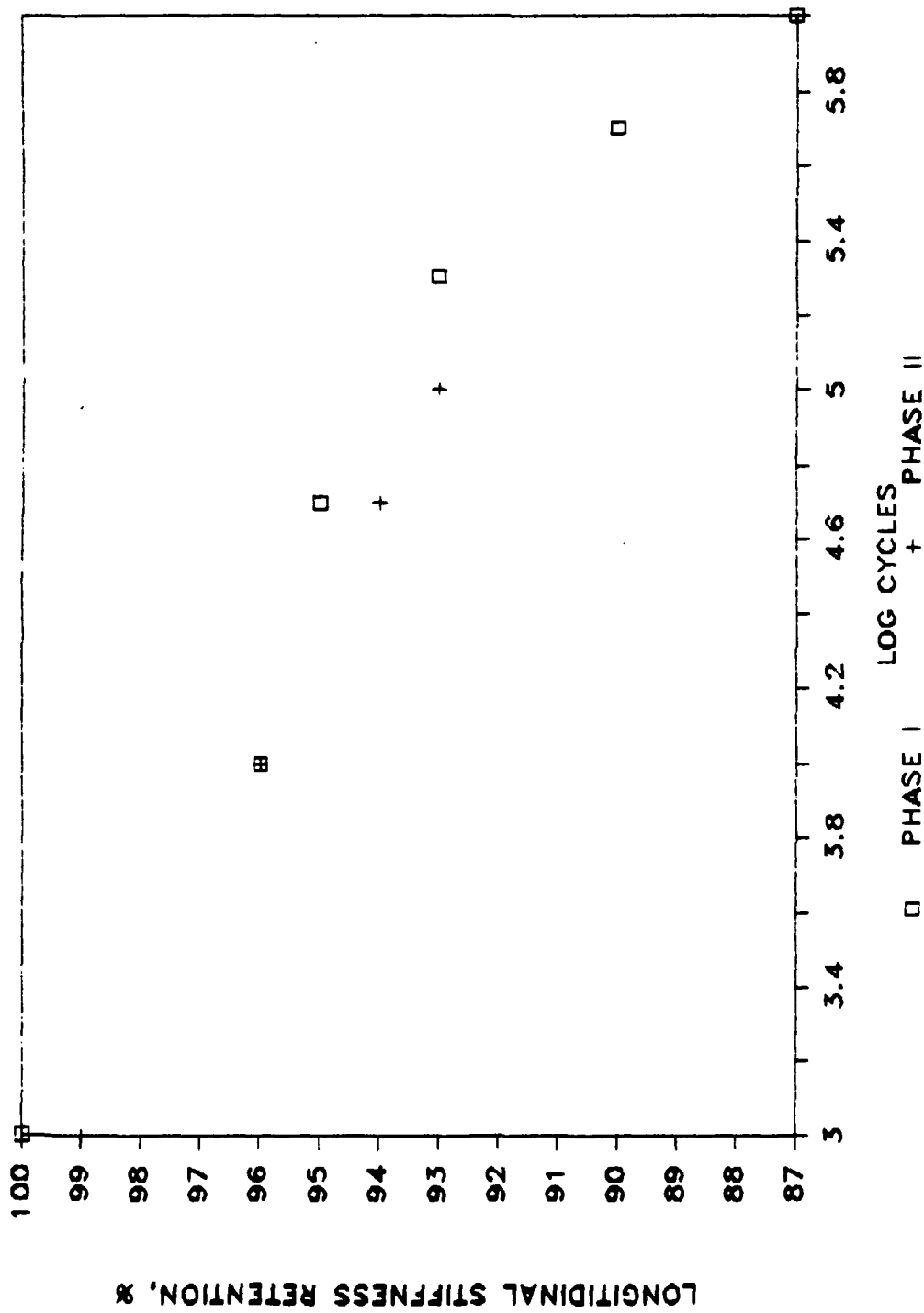


Figure 70: Longitudinal Stiffness Retention, Type C

Type C, T-T, R=0.1, $P_{max} = 12^k$

TABLE 11 : DAMAGE PROGRESSION IN SPECIMEN C5-5

Specimen: C5-5 Test Type: TT R=+0.1 f=10 Hz Area=0.277
 Pmax=+15 kip Life=32.2Kc Residual Strength=N/A

Damage Progression by Ply Group Observed via NDI

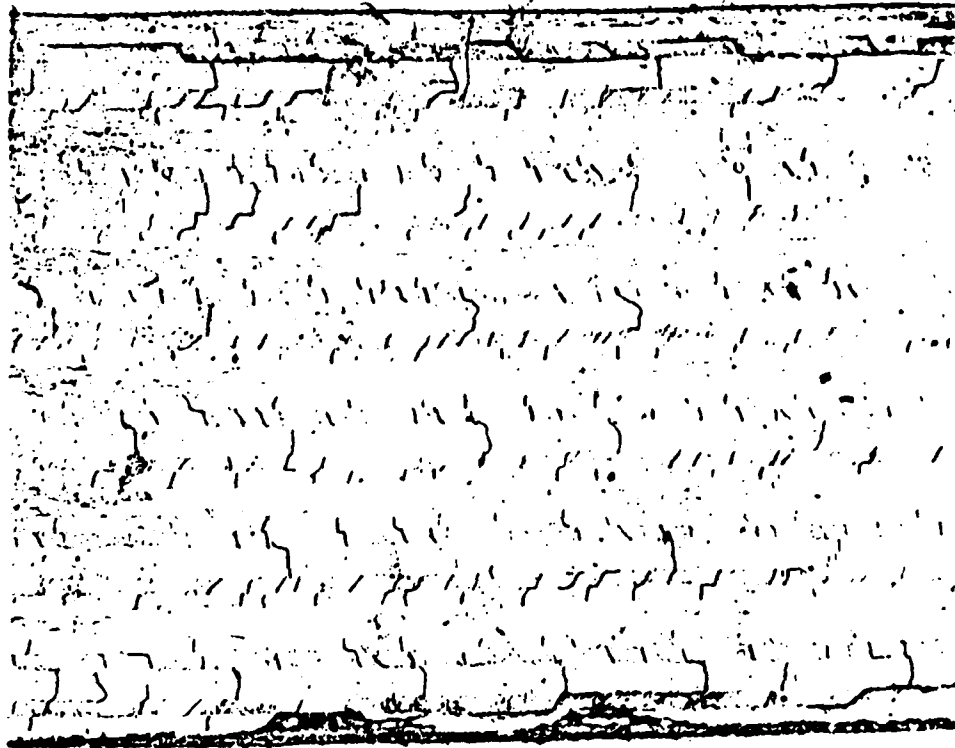
Damage Codes:

| | | | |
|------------|-----------------------------|------------|-----------------|
| 1st Digit: | | 2nd Digit: | |
| 1 | Transverse Crack Initiation | 1 | -45 ply |
| 2 | Transverse Crack Saturation | 2 | +45 ply |
| 3 | Transverse Crack Coupling | 3 | 90 ply |
| 4 | Delamination | 4 | 0/+ interface |
| | | 5 | +/-90 interface |
| | | 6 | 90/- interface |
| | | 7 | -/- interface |

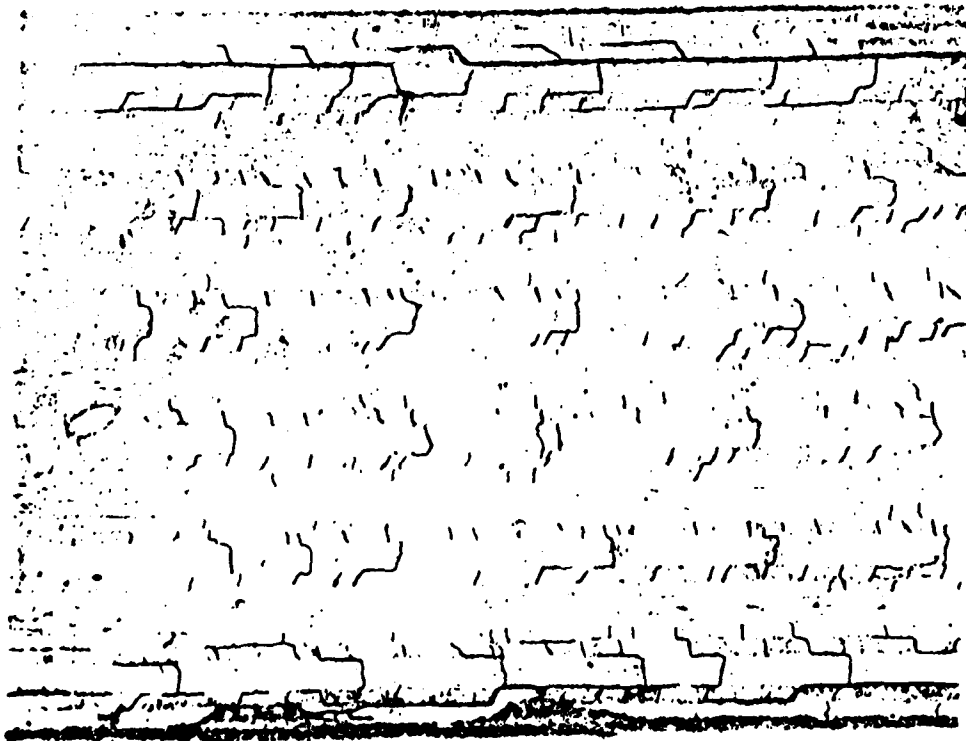
| Ply Group | K- Cycles at Inspection | | |
|-----------|-------------------------|------------|--------|
| | 0 | 5 | 10 |
| 1 | 11, 13, 46 | | 12, 45 |
| 2 | 11, 13, 36 | | |
| 3 | 11, 13, 36 | | 12 |
| 4 | 11, 13, 36 | | 12 |
| 5 | 11, 13, 36 | | 12 |
| 6 | 11, 13, 36 | 12, 45, 46 | |

% Stiffness Retention

| | | | |
|-----------|-----|----|----|
| E (long) | 100 | 96 | 94 |
| E (trans) | 100 | | |



a) 5 K-C



b) 10 K-C

Figure 71 Edge Replicas of Specimen C5-5

applied for 150 thousand cycles. During Block 1 loading, the maximum and minimum load and strain, secant modulus, and change in secant modulus were recorded every twelve seconds using an on-line computer which provided a hard copy of the data at every one percent change in secant modulus. The first two of the triplicate tests in each set were interrupted at several cyclic intervals for edge replication and enhanced radiography of the damage and for recording the quasi-static stress-strain curves. The third of the three replicates was not interrupted during Block 1 to provide a continuous record of stiffness change.

After 150 thousand cycles of Block 1 loading, the specimens were reloaded quasi-statically to determine the loads corresponding to the specified strain limits for Block 2. The cyclic loading was resumed under Block 2 conditions with on-line monitoring of cyclic data and interruptions at selected intervals for damage and stress-strain measurements. Block 2 loading was continued to failure or until a total (Block 1 plus Block 2) cycle count of one million, whichever occurred first. When a portion of the loading waveform was compressive, failure was defined as either reaching a minimum cyclic strain of $-6300\mu\epsilon$ (the onset of instability for Type C laminates as determined in Phase I) or reaching a damage state such that an increase in quasi-statically applied loads did not produce a corresponding increase in the compressive strain. The dual definition of failure was needed because the out-of-plane deformation due to compressive loading could either increase or decrease the strain on the side of the specimen to which the extensometer was attached.

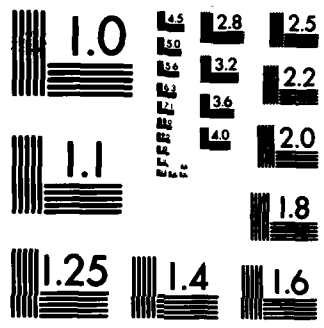
The fatigue lives for the specimens subjected to the three sets

Table 12- TEST MATRIX FOR LOADING HISTORY EFFECTS
TYPE C LAMINATES

| Set | Block | Loading Mode | $\epsilon_{\min}/\epsilon_{\max}$ (a) (microstrain) | R (b) | Number of Replicates |
|-----|-------|--------------|--|-------|----------------------|
| 1 | 1 | T-C | 400/4000 | 0.1 | 3 |
| | 2 | C-C | -4000/-400 | 10 | |
| 2 | 1 | T-C | -3500/3500 | -1 | 3 |
| | 2 | T-C | -4500/4500 | -1 | |
| 3 | 1 | T-T | 400/4000 | 0.1 | 3 |
| | 2 | T-C | -4000/4000 | -1 | |

(a) Strains shown are the initial cyclic strain limits in the load controlled tests.

(b) R is the value of $\epsilon_{\min}/\epsilon_{\max}$ for the initial cyclic strain limits in the load controlled tests.



MICROCOPY RESOLUTION TEST CHART
NATIONAL BUREAU OF STANDARDS-1963-A

of loading histories are shown in Table 13. Specimens loaded under Set 1 conditions survived 150 thousand cycles of tension-tension loading at $R=0.1$ with the initial maximum strain of $4000\mu\epsilon$ and an additional 850 thousand cycles of compression-compression loading at $R=10$ and $\epsilon_{\min}=-4000\mu\epsilon$. The attendant stiffness change was relatively small, Table 14. Edge replicas and radiographs after 150 thousand cycles of Block 1 loading showed an array of matrix cracks in the off-axis plies. However, the cyclic compression loading during Block 2 produced very little crack coupling along the ply interfaces and no delaminations even though 'initial damage' was present when Block 2 loading began, as shown in Fig. 72

The response under Set 2 and Set 3 conditions provides a sharp contrast to the response under Set 1 conditions. Block 1 of Sets 1 and 3 are identical and produced the same damage states in the specimens after 150 thousand cycles. Under Set 3, Block 2 conditions (tension-compression, $R=-1$, $4000\mu\epsilon$) the cracks in the off axis plies coupled along the interfaces producing delaminations which grew into the width of the specimens, Fig. 73. The attendant change in secant modulus was greater under Set 3 loading than under Set 1 loading, Table 14. Failure, at a mean life of 440,000 cycles, was due to the onset of instability caused by the compressive portion of the waveform during Block 2 as the minimum compressive strain changed from $-4000\mu\epsilon$ to $-6300\mu\epsilon$.

The shortest fatigue lives for the Type C laminate were caused by Set 2 loading where 150 thousand cycles of Block 1 (Tension-compression, $R=-1$, $3500\mu\epsilon$) were followed by Block 2 with $R=-1$, $4500\mu\epsilon$. Although the maximum strain in Block 1 was less than the

Table 13 FATIGUE LIFE DATA FROM LOADING HISTORY TESTS
TYPE C LAMINATES

| Set | Specimen | Block | Cycles (thousands) | Total Cycles (thousands) | Comments (a) |
|-----|----------|-------|-----------------------|--------------------------------|--------------|
| 1 | 8-3 | 1 | 150 | 1,000 | (1) |
| | | 2 | 850 | | |
| | 6-5 | 1 | 150 | 1,000 | (1) |
| | | 2 | 850 | | |
| | 5-10 | 1 | 150 | 1,000 | (1) |
| | | 2 | 850 | | |
| 2 | 5-6 | 1 | 150 | 207 | (2) |
| | | 2 | 57 | | |
| | 7-6 | 1 | 150 | 182 | (2) |
| | | 2 | 32 | | |
| | 8-7 | 1 | 150 | 161 | (3) |
| | | 2 | 11 | | |
| 3 | 8-5 | 1 | 150 | 477 | (2) |
| | | 2 | 327 | | |
| | 7-4 | 1 | 150 | 463 | (2) |
| | | 2 | 313 | | |
| | 7-8 | 1 | 150 | 382 | (2) |
| | | 2 | 232 | | |

(a)

Comments

- (1) Test terminated after one million cycles
- (2) Failure defined as $\epsilon_{min} = 6300 \mu\epsilon$
- (3) Failure defined as no increase in compressive strain corresponding to an increase in quasi-static compressive load.

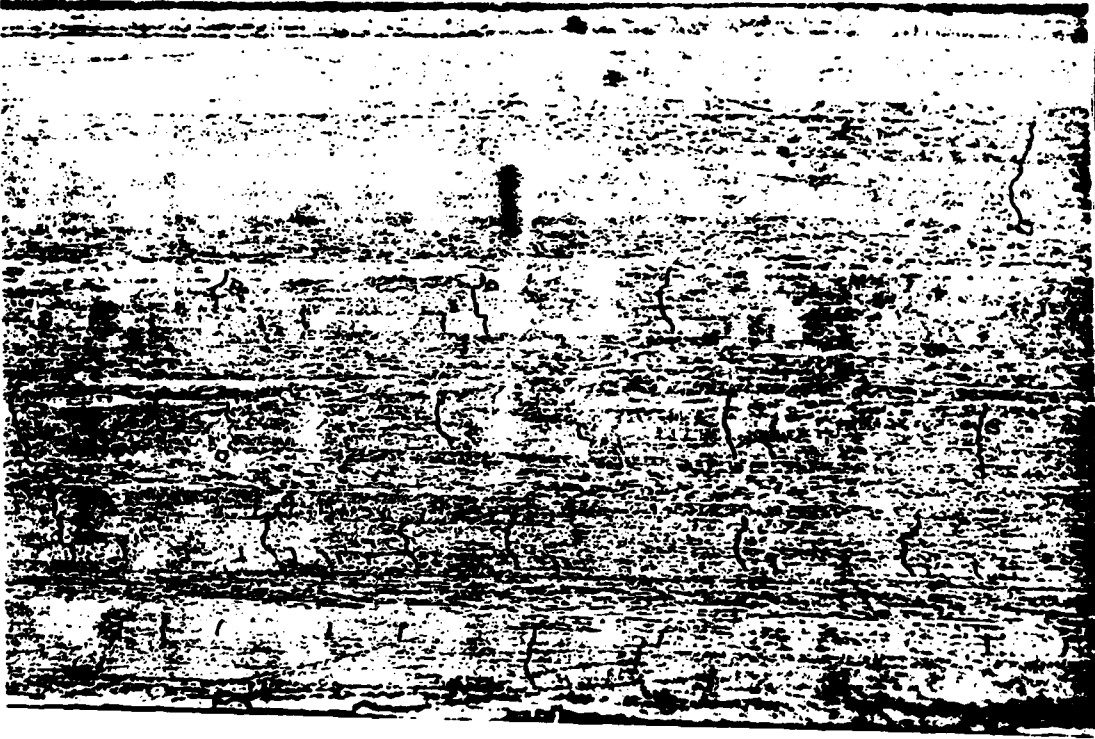
maximum strain in Block 1 of Sets 1 and 3, the strain range was greater by a factor of 1.9. The damage at the end of Block 1 consisted of matrix cracks in the off-axis plies and some interfacial damage in the form of local crack coupling as shown in Fig. 74. Changing the loading to Block 2 accelerated the development of damage along the length and through the width of the laminates. The increasing damage rate was reflected by a rapid and large reduction in the secant modulus as the delamination grew across the width of the specimen. In each of the three replicate tests, failure during Block 2 was determined by the onset of compressive instability. The mean fatigue life of 183,000 cycles for Set 2 conditions is the lowest of the three conditions investigated. Although the change in strain needed to reach the defined failure strain is less for Set 2 than for Set 3 (1800 μ e compared to 2300 μ e), the lower value of life is mainly due to the higher damage rate for Set 2, as indicated by the stiffness change data, Fig. 61. The change in secant modulus data in Table 14 and the data plotted in Figure 61 are determined from the values of static secant tensile and compressive modulus measured at selected intervals throughout the loading history. The secant modulus is calculated as σ/e , where e is the initial cyclic strain limit for the particular loading block and σ is the corresponding stress under static loading. The curves for Block 2 loading ($R=-1$) corresponding to Sets 2 and 3 show a very rapid and large stiffness reduction prior to reaching the defined failure condition. The rapid degradation of stiffness is due to delaminations which grow across the width of the specimen creating a 'deplied' ligament of material which deforms out of the plane of the laminate during the compressive portion of the

Table 14- CHANGE IN STATIC SECANT MODULUS
TYPE C LAMINATES

| Set | Specimen | Block | Cycles (thousands) | Percent Change ^(a) in Modulus | Comments ^(b) |
|-----|----------|-------|-----------------------|---|-------------------------|
| 1 | 8-3 | 1 | 120 | -1.1 (T) | 1 |
| | | 2 | 850 | +3.7 (C) | 2 |
| | 6-5 | 1 | 150 | -0.9 (T) | |
| | | 2 | 850 | +0.9 (C) | |
| | 5-10 | 1 | 150 | -1.2 (T) | |
| | | 2 | 850 | -0.5 (C) | |
| 2 | 5-6 | 1 | 150 | -11.3(T)/-1.5(C) | 3 |
| | | 2 | 57 | -6.5(T)/-30.8(C) | |
| | 7-6 | 1 | 150 | -6.1(T)/-6.4(C) | |
| | | 2 | 32 | -16.5(T)/-14.8(C) | |
| | 8-7 | 1 | 150 | -6.6(T)/-7.0(C) | |
| | | 2 | 11 | - / - | 4 |
| 3 | 8-5 | 1 | 150 | -2.5 (T) | |
| | | 2 | 327 | -28.4(T)/-33.4(C) | |
| | 7-4 | 1 | 150 | -0.3 (T) | |
| | | 2 | 313 | -34.1(T)/-36.9(C) | |
| | 7-8 | 1 | 150 | -0.6 (T) | |
| | | 2 | 232 | -24.4(T)/-35.1(C) | |

(a) Static secant modulus is calculated as σ/ϵ where ϵ is the strain limit for cyclic loading and σ is the corresponding stress recorded during monotonic loading.

(b) Comments
 (1) (T) refers to change in tensile secant modulus
 (2) (C) refers to change in compressive secant modulus
 (3) (change in tensile secant modulus)/(change in compressive secant modulus)
 (4) Compressive secant modulus at $-4500 \mu\epsilon$ could not be obtained. See Comment 3 in Table 13.

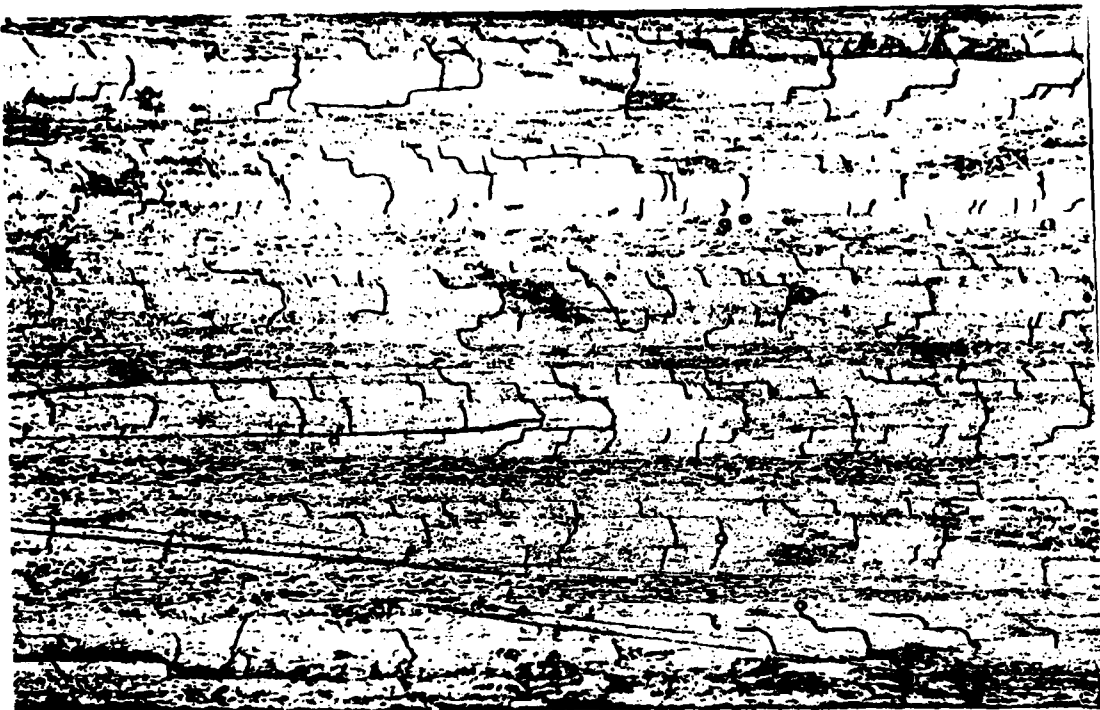


Set 1: Block 2, 850,000 cycles



Set 1: Block 1, 150,000 cycles

Figure 72: Edge Replicas of Specimen C8-3



Set 3: Block 2, 327,000 cycles



Set 3: Block 1, 150,000 cycles

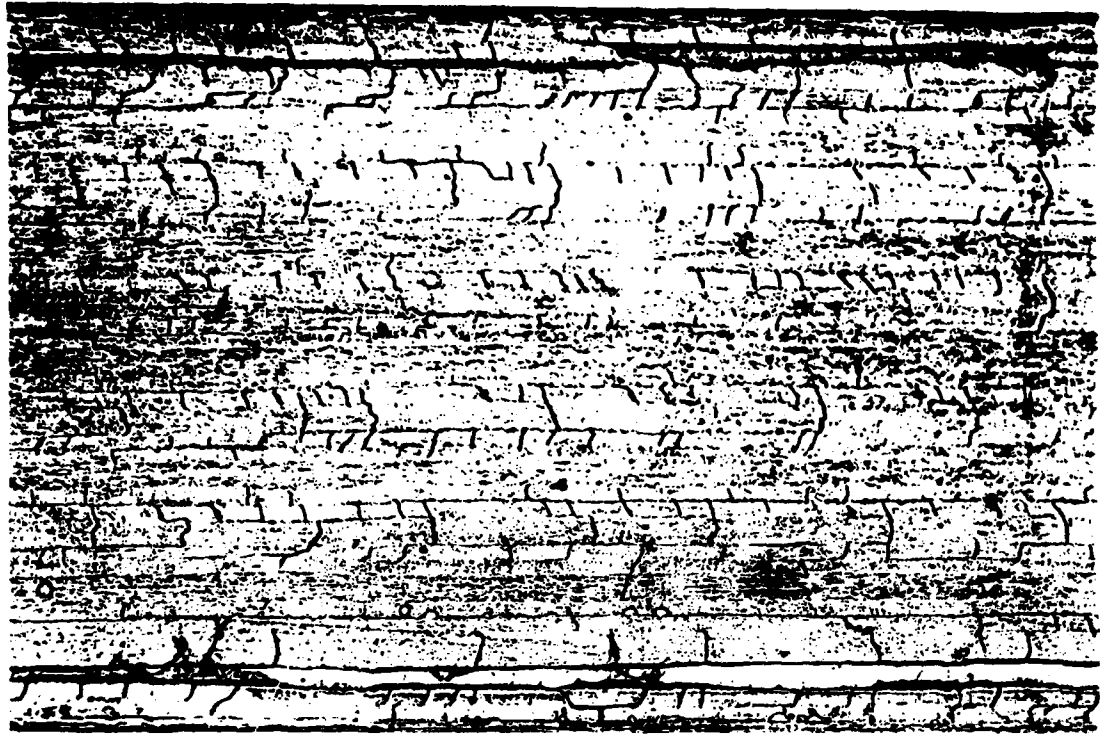
Figure 73 Edge Replicas of Specimen C8-5

loading waveform.

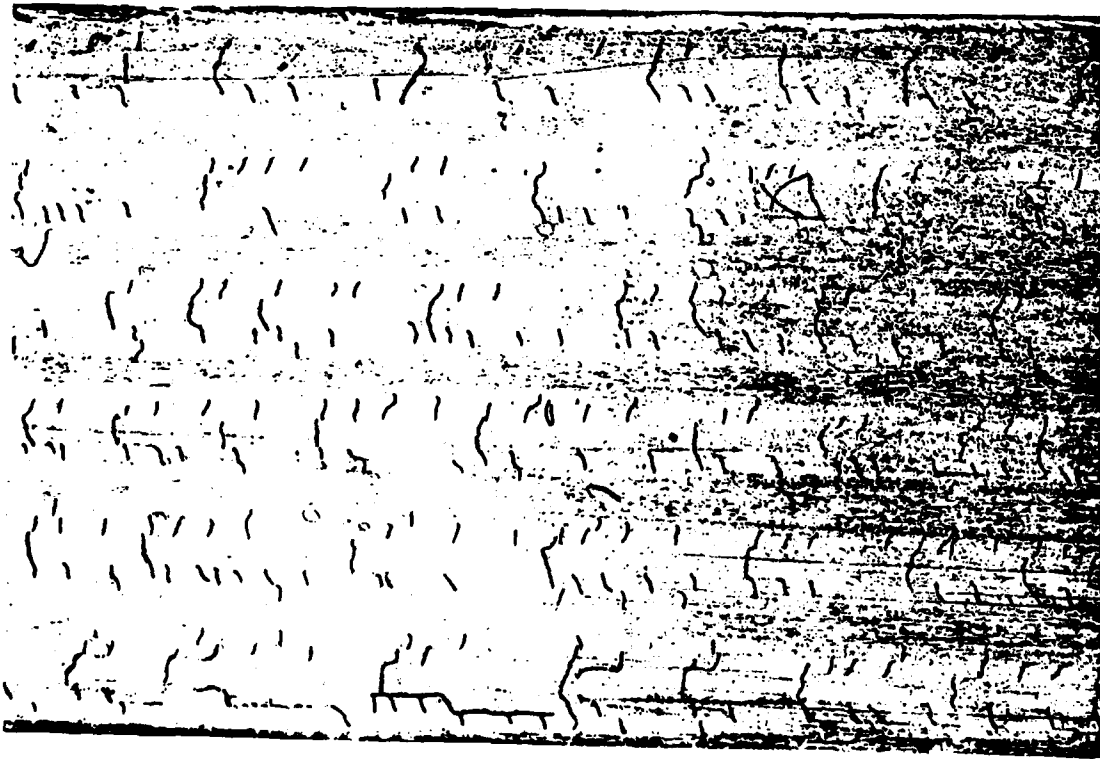
The stiffness and life data for each load history set are consistent and reproducible. Results from the Set 1 tests show that the cracks in the off-axis plies produced by tension-tension loading do not couple and do not form delaminations during compression-compression loading at $-4000\mu\epsilon$. However, matrix cracks do couple and do form life limiting delaminations when the tension-tension loading is followed by tension-compression loading at $\pm 4000\mu\epsilon$. The damage rate under tension-compression loading at $\pm 4500\mu\epsilon$ is much greater than that at $\pm 4000\mu\epsilon$.

B. Laminate Type F

The Type F laminate was introduced during Phase II to provide data on a relatively stiffer laminate without 90 plies. Therefore, a series of static laminate characterization tests were necessary. These tests have included both tensile and compressive, computer controlled, ramp to failure tests for the determination of the laminate moduli and strengths, and quasi-static tests for the determination of the static damage progression pattern. In these quasi-static tests, the load on the specimen was incrementally increased, with frequent loading interruptions to perform the NDI procedures previously described. Typical stress-strain diagrams obtained from the monotonic tests are shown in Figures 75 and 76 for tensile and compressive loadings, respectively. Laminate mechanical properties are shown, along with those of the Type C for comparison,



Set 2: Block 2, 57,000 cycles



Set 2: Block 1, 150,000 cycles

Figure 74: Edge Replicas of Specimen C5-6

in Table 15. The stiffness change data obtained from the quasi-static tension tests are shown in Figure 77.

The first series of fatigue tests performed were the $R=-1$ tests. In the first of these tests, run at a frequency of 10 Hertz, the specimen became too hot to touch. Consequently the cyclic frequency was reduced to 5 Hertz to alleviate any problems introduced by this phenomenon. A comparison of the longitudinal stiffness retention of a 10 Hertz specimen and a duplicate run at 5 Hertz is shown in Figure 77. As is seen, the 5 Hertz specimen exhibits a larger stiffness loss (also a slightly longer life) than that of the 10 Hertz specimen, though the general trends of both data sets are similar.

The damage and stiffness data collected for all tests on the Type F laminate are presented in the Appendix. As with the Type C laminate, much of this data has been included in the discussion on modeling (Section II) and will not be reviewed in detail here. Interpretation of the tables in the Appendix for the Type F laminate is identical to the description given for the Type C tables, with the exception of minor changes in the damage codes necessitated by the differing stacking sequences.

Block loading tests on the Type F laminate were performed in a different manner than those for the Type C. In particular, the blocks were alternated in 150 thousand cycle increments. Thus instead of Block 1 loading of 150 thousand cycles followed by Block 2 loading to failure, the specimens were subjected to 150 thousand cycles of Block 1 followed by 150 thousand cycles of Block 2, 150 thousand cycles of Block 1, and so forth until failure. The exact loading condition for each of the Type F block loading specimens is given in Table 16.

Results of these tests were similar to those of the Type C laminate. Under the tension-tension loading followed by compression-compression loading, all damage occurred during tensile loads and the damage was not driven to any extent under the compression loading. Also as noted in the Type C laminates, strain (or stress) range appears as a more sensitive parameter than absolute value maximum strain in determining the damage progression.

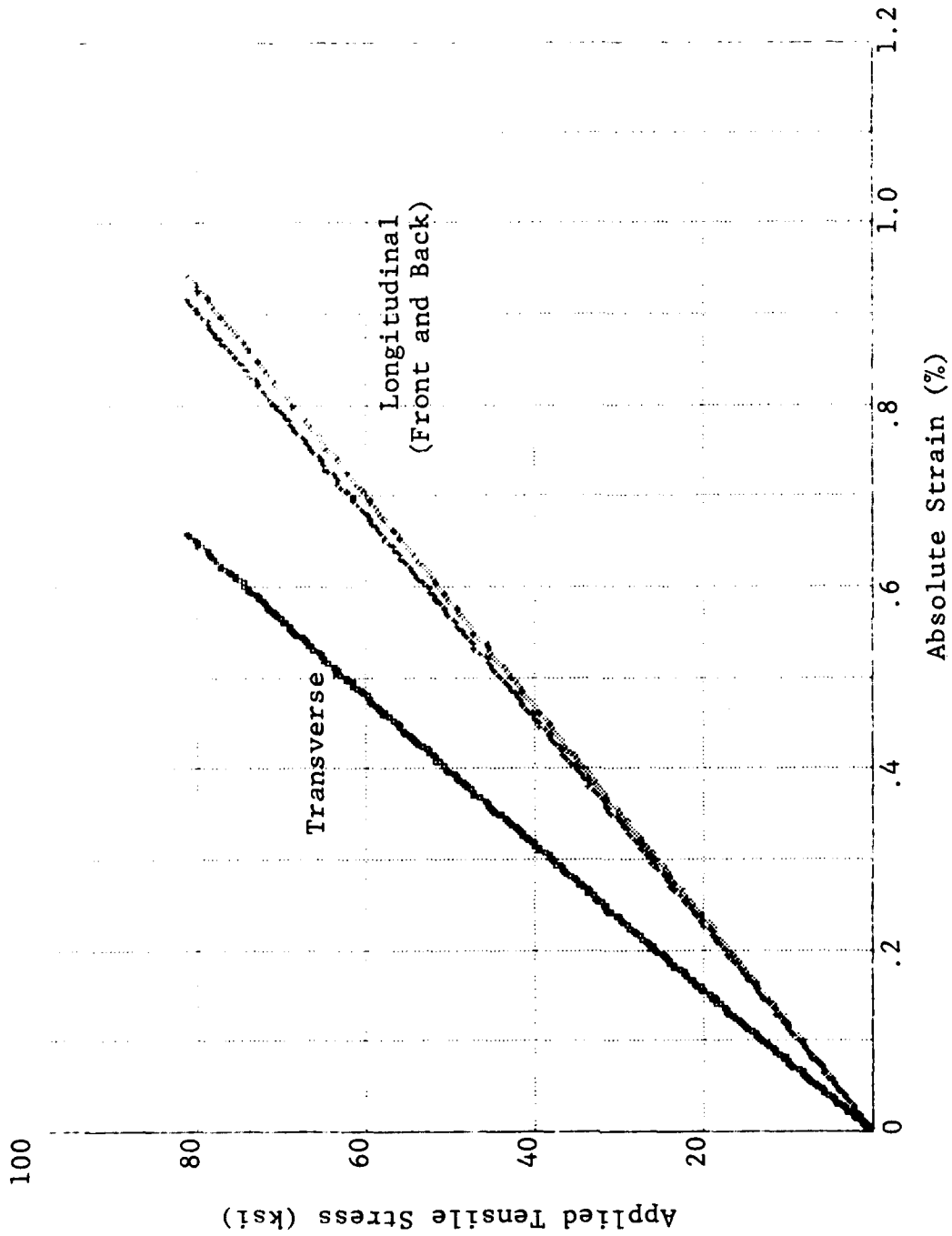


Figure 75: Stress-Strain Results for Type F Tensile Loading; Specimen F3-7

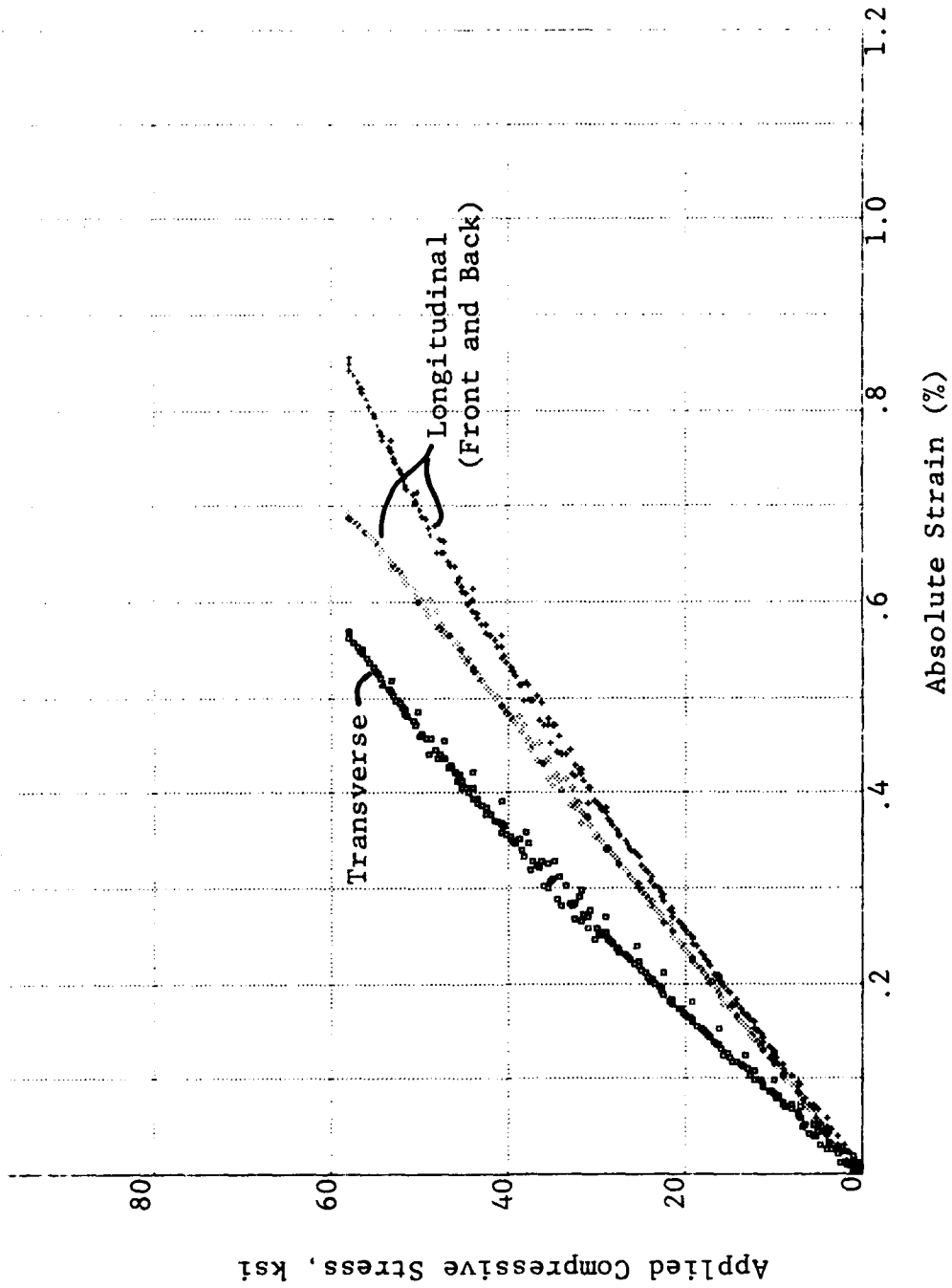


Figure 76: Stress-Strain Results for Type F Compression Loading, Specimen F1-12

Table 15 Laminate Tensile and Compressive Properties

| Property | Type C | | Type F | |
|---|---------|-------------|---------|-------------|
| | Tension | Compression | Tension | Compression |
| Modulus (MSI) | 7.31 | 7.16 | 8.56 | 8.11 |
| Poisson's Ratio | 0.29 | 0.28 | 0.73 | 0.68 |
| Stress at 3000 μ _e (KSI) | 22.4 | 21.3 | 25.7 | 24.3 |
| Stress at 4500 μ _e (KSI) | 33.6 | 31.6 | 38.5 | 36.5 |
| Ultimate Stress (KSI) | 72.3 | 43.0 | 94.6 | 56.1 |
| Ultimate Strain (%) | 1.01 | 0.63 | 1.10 | 0.77 |

STIFFNESS RETENTION

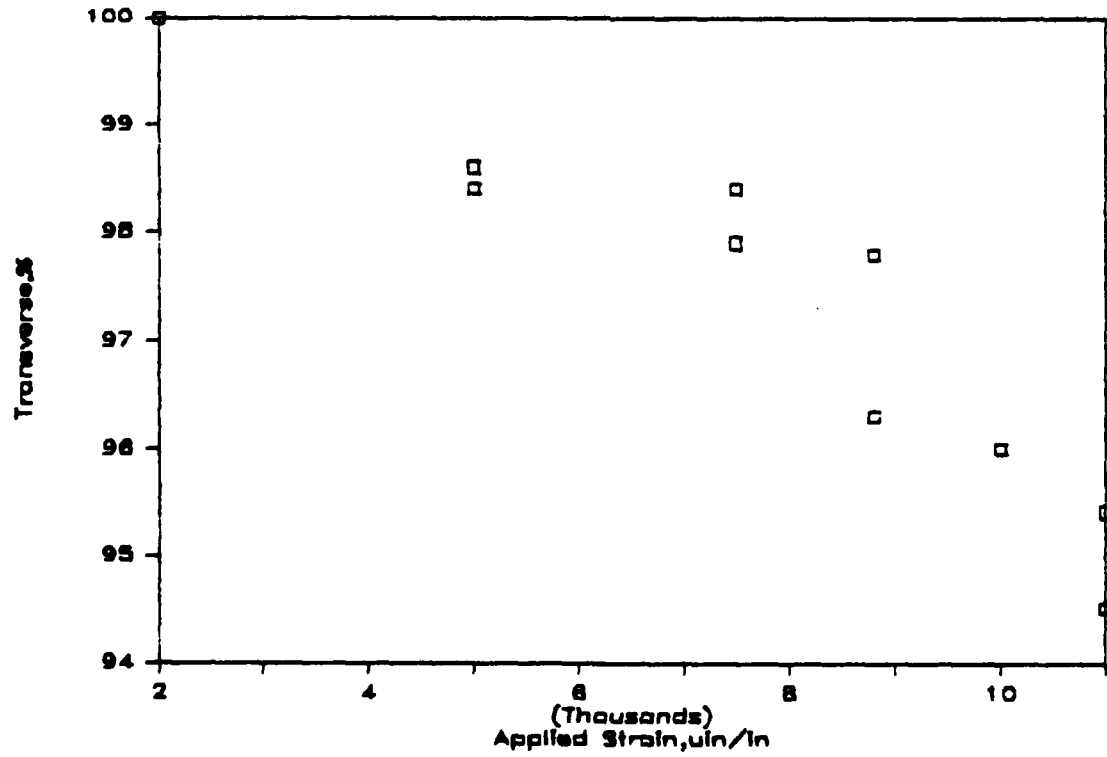
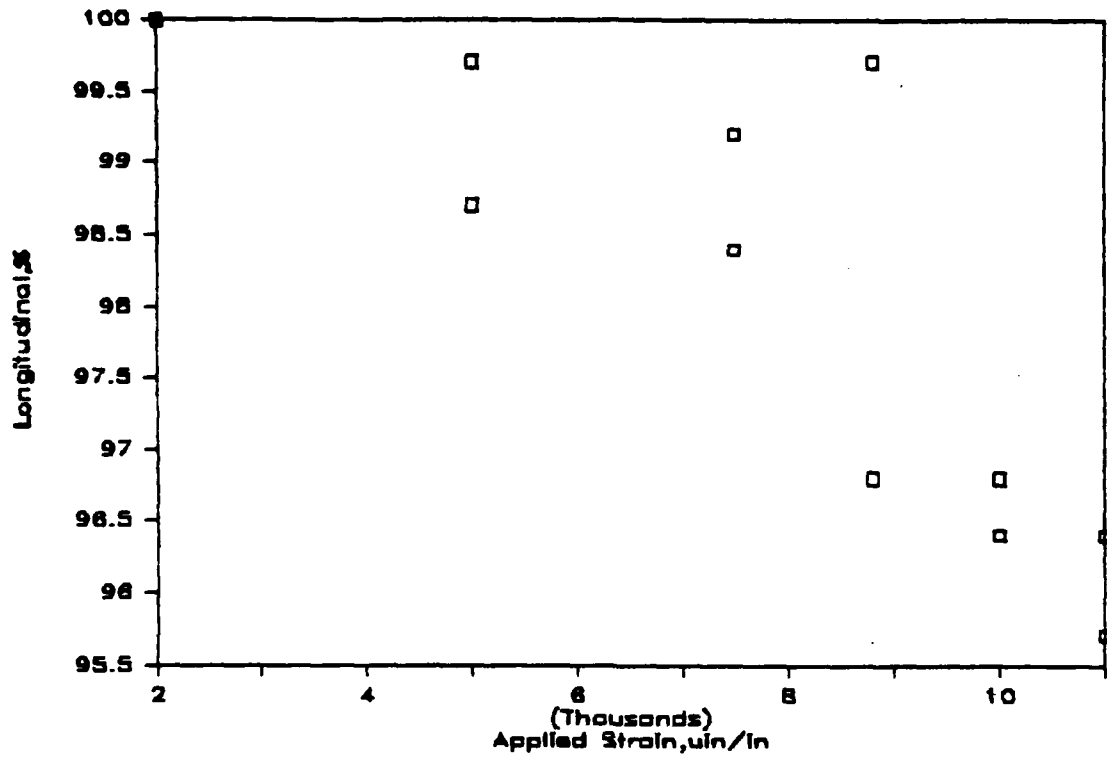


Figure 77 Type F Stiffness Change: Monotonic Tension

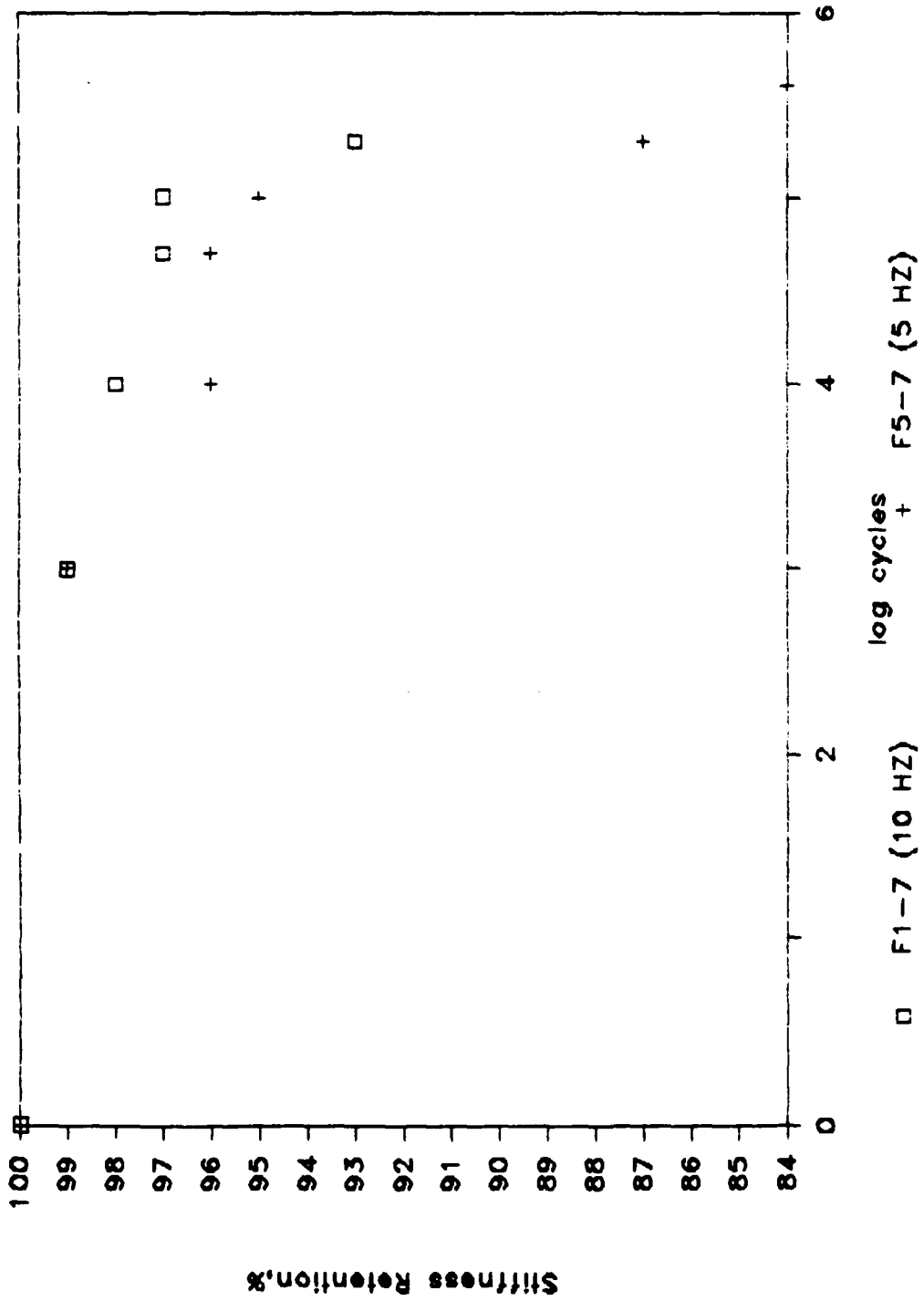


Figure 78: Type F Longitudinal Stiffness Retention

T-C, $k = -1$, $\sigma_{max} = 35$ ksi

TABLE 16: TYPE F BLOCK LOADING TESTS

| | Load Type | R | Maximum Load, kips | | | |
|-------|--------------|----|--------------------|----|----|------|
| | | | Specimen No. | | | |
| | | | 1 | 2 | 3 | |
| Set 1 | Block 1,3,.. | TT | 0.1 | 10 | 15 | 15 |
| | Block 2,4,.. | CC | 10 | -1 | -1 | -1.2 |
| Set 2 | Block 1,3,.. | TC | -1 | 10 | 9 | 10 |
| | Block 2,4,.. | TC | -1 | 8 | | |
| | Block 2,4,.. | TC | -2 | | | 6.66 |
| | Block 2,4,.. | TC | -0.5 | | 12 | |

SECTION IV

SUMMARY

This report has detailed the activities and results of the Phase II model refinement effort. In keeping with the contractual definition of Phase II, the activity has focused on refinement of the model developed in Phase I [15] by identifying critical model parameters and their values and through incorporating changes within the original model to obtain better alignment with experimental data. Thus the activities reported herein have included both the incorporation of data generated in this phase and a re-examination of data generated in Phase I.

The model as developed and refined has the following salient features:

Predicts the strength and life of engineering composite laminates under tension-tension, compression-compression, tension-compression, block-spectrum loading, and constant amplitude cyclic loading with R-values between 0 and -infinity.

Replaces Miner's rule with an engineering model which is based on the physical mechanisms of damage and failure.

Accounts for effects such as load sequence, biaxial stress state in critical elements, lamination differences, strength and/or stiffness differences, and

laminates response differences.

While the current model does not claim perfection, the results of this study to date provide confidence in the ability of the model to accurately predict, in most cases, the response of advanced composite materials under realistic load conditions. The accuracy and limitations of the model will be further explored during Phase III of this program.

APPENDIX

TABULAR DAMAGE DATA

TABLE 17 : DAMAGE PROGRESSION IN SPECIMEN C5-5

Specimen: C5-5 Test Type: TT R=+0.1 f=10 Hz Area=0.277
 Pmax=+15 kip Life=32.2Kc Residual Strength=N/A

Damage Progression by Ply Group Observed via NDI

Damage Codes:

| | | | |
|------------|-----------------------------|------------|-----------------|
| 1st Digit: | | 2nd Digit: | |
| 1 | Transverse Crack Initiation | 1 | -45 ply |
| 2 | Transverse Crack Saturation | 2 | +45 ply |
| 3 | Transverse Crack Coupling | 3 | 90 ply |
| 4 | Delamination | 4 | 0/+ interface |
| | | 5 | +/-90 interface |
| | | 6 | 90/- interface |
| | | 7 | -/- interface |

K- Cycles at Inspection

| Ply Group | 0 | 5 | 10 |
|-----------|------------|------------|--------|
| 1 | 11, 13, 46 | | 12, 45 |
| 2 | 11, 13, 36 | | |
| 3 | 11, 13, 36 | | 12 |
| 4 | 11, 13, 36 | | 12 |
| 5 | 11, 13, 36 | | 12 |
| 6 | 11, 13, 36 | 12, 45, 46 | |

% Stiffness Retention

| | 0 | 5 | 10 |
|-----------|-----|----|----|
| E (long) | 100 | 96 | 94 |
| E (trans) | 100 | | |

TABLE 18 : DAMAGE PROGRESSION IN SPECIMEN C7-3

Specimen: C7-3 Test Type: TT R=+0.1 f=10 Hz Area=0.279
 Pmax=+15 kip Life=58.85 Kc Residual Strength=N/A

Damage Progression by Ply Group Observed via NDI

Damage Codes:

| 1st Digit: | | 2nd Digit: | |
|------------|-----------------------------|------------|-----------------|
| 1 | Transverse Crack Initiation | 1 | -45 ply |
| 2 | Transverse Crack Saturation | 2 | +45 ply |
| 3 | Transverse Crack Coupling | 3 | 90 ply |
| 4 | Delamination | 4 | 0/+ interface |
| | | 5 | +/-90 interface |
| | | 6 | 90/- interface |
| | | 7 | -/- interface |

K- Cycles at Inspection

| Ply Group | 0 | 1 | 5 | 10 | 50 |
|-----------|---|------------|--------|----|--------|
| 1 | | 11, 13, 36 | 45, 46 | | |
| 2 | | 11, 13, 36 | | 12 | 45, 46 |
| 3 | | 11, 13, 36 | 12 | 12 | 45, 46 |
| 4 | | 11, 13, 36 | 12 | 12 | 45, 46 |
| 5 | | 11, 13, 36 | 12 | 12 | 45, 46 |
| 6 | | 11, 13, 36 | 45, 46 | | |

% Stiffness Retention

| | | | | | |
|-----------|-----|----|----|----|----|
| E (long) | 100 | 90 | 89 | 88 | 77 |
| E (trans) | 100 | 94 | 92 | 91 | 82 |

TABLE 19 : DAMAGE PROGRESSION IN SPECIMEN C5-7

Specimen: C5-7 Test Type: TT R=+0.1 f=10 Hz Area=0.280
 Pmax=+15 kip Life=81.5Kc Residual Strength=N/A

Damage Progression by Ply Group Observed via NDI

Damage Codes:

| | | | |
|------------|-----------------------------|------------|-----------------|
| 1st Digit: | | 2nd Digit: | |
| 1 | Transverse Crack Initiation | 1 | -45 ply |
| 2 | Transverse Crack Saturation | 2 | +45 ply |
| 3 | Transverse Crack Coupling | 3 | 90 ply |
| 4 | Delamination | 4 | 0/+ interface |
| | | 5 | +/-90 interface |
| | | 6 | 90/- interface |
| | | 7 | -/- interface |

K- Cycles at Inspection

| Ply Group | 0 | 1 | 5 | 10 | 50 |
|-----------|---|------------|------------|--------|--------|
| 1 | | 13 | 11, 12, 35 | 45, 46 | |
| 2 | | 11, 13 | 12 | 12 | 45, 46 |
| 3 | | 11, 13 | 12 | 12 | 45, 46 |
| 4 | | 11, 13 | 12 | 12 | 45, 46 |
| 5 | | 11, 13 | 12 | 12 | 45, 46 |
| 6 | | 11, 13, 35 | 12, 46 | | |

% Stiffness Retention

| | | | | | |
|-----------|-----|----|----|----|----|
| E (long) | 100 | 95 | 94 | 92 | 83 |
| E (trans) | 100 | 99 | 95 | 94 | 82 |

TABLE 20 : DAMAGE PROGRESSION IN SPECIMEN C5-1

Specimen: C5-1 Test Type: TT R=0.1 f=10 Hz Area=0.279
 Pmin=12 kip Life=1Mc+ Residual Strength=N/A

Damage Progression by Ply Group Observed via NDI

Damage Codes:

| | |
|--|---|
| <p>1st Digit:</p> <p>1 Transverse Crack Initiation</p> <p>2 Transverse Crack Saturation</p> <p>3 Transverse Crack Coupling</p> <p>4 Delamination</p> | <p>2nd Digit:</p> <p>1 -45 ply</p> <p>2 +45 ply</p> <p>3 90 ply</p> <p>4 0/+ interface</p> <p>5 +/90 interface</p> <p>6 90/- interface</p> <p>7 -/- interface</p> |
|--|---|

K- Cycles at Inspection

| Ply Group | 0 | 1 | 10 | 50 | 250 | 500 | 1000 |
|-----------|---|----|------------|--------|--------|-----|--------|
| 1 | | | 11, 13 | 35, 36 | 45, 46 | | |
| 2 | | 13 | 11, 12 | | 35, 36 | | 45, 46 |
| 3 | | | 11, 12, 13 | | 35, 36 | | 45, 46 |
| 4 | | | 11, 12, 13 | | 35, 36 | | 45, 46 |
| 5 | | 13 | 11 | 12 | 35, 36 | | 45, 46 |
| 6 | | | 11, 12, 13 | 35, 36 | 45, 46 | | |

% Stiffness Retention

| | | | | | | | |
|-----------|-----|-----|----|----|----|----|----|
| E (long) | 100 | 100 | 98 | 97 | 94 | 96 | 94 |
| E (trans) | | | | | | | |

TABLE 21 : DAMAGE PROGRESSION IN SPECIMEN C6-10

Specimen: C6-10 Test Type: TT R=+0.1 f=10 Hz Area=0.277
 Pmax=+12 kip Life=100+ Kc Residual Strength=68.2 ksi

Damage Progression by Ply Group Observed via NDI

Damage Codes:

| 1st Digit: | | 2nd Digit: | |
|------------|-----------------------------|------------|-----------------|
| 1 | Transverse Crack Initiation | 1 | -45 ply |
| 2 | Transverse Crack Saturation | 2 | +45 ply |
| 3 | Transverse Crack Coupling | 3 | 90 ply |
| 4 | Delamination | 4 | 0/+ interface |
| | | 5 | +/-90 interface |
| | | 6 | 90/- interface |
| | | 7 | -/- interface |

K- Cycles at Inspection

| Ply Group | 0 | 1 | 10 | 50 | 100 |
|-----------|---|------------|--------|----|--------|
| 1 | | 11, 13, 36 | 12 | | 45, 46 |
| 2 | | 13 | 11, 36 | 12 | |
| 3 | | 13 | 11, 36 | 12 | |
| 4 | | 13 | 11, 36 | 12 | |
| 5 | | 13 | 11, 36 | 12 | |
| 6 | | 11, 13, 36 | 12 | | 45, 46 |

% Stiffness Retention

| | | | | | |
|-----------|-----|----|----|----|----|
| E (long) | 100 | 99 | 96 | 94 | 94 |
| E (trans) | 100 | 99 | 97 | 95 | 95 |

TABLE 22 : DAMAGE PROGRESSION IN SPECIMEN C6-4

Specimen: C6-4 Test Type: TT R=+0.1 f=10 Hz Area=0.278
 Pmax=+15 kip Life=10+ Kc Residual Strength=70.7 ksi

Damage Progression by Ply Group Observed via NDI

Damage Codes:

| 1st Digit: | 2nd Digit: |
|-------------------------------|------------------|
| 1 Transverse Crack Initiation | 1 -45 ply |
| 2 Transverse Crack Saturation | 2 +45 ply |
| 3 Transverse Crack Coupling | 3 90 ply |
| 4 Delamination | 4 0/+ interface |
| | 5 +/90 interface |
| | 6 90/- interface |
| | 7 -/- interface |

| Ply Group | K- Cycles at Inspection | | |
|-----------|--------------------------|---|----|
| | 0 | 5 | 10 |
| 1 | 11, 12, 13 36, 44 | | |
| 2 | 11, 13, 36 | | |
| 3 | 11, 13, 36 | | |
| 4 | 11, 13, 36 | | |
| 5 | 11, 13, 36 | | |
| 6 | 11, 12, 13 36, 45, 44 | | |

% Stiffness Retention

| | | | |
|-----------|-----|----|----|
| E (long) | 100 | 95 | 95 |
| E (trans) | 100 | 96 | 95 |

TABLE 23 : DAMAGE PROGRESSION IN SPECIMEN C4-4

Specimen: C4-4 Test Type: CC R=10 f=10 Hz Area=0.278
 Pmin=-14 kip Life=5.5Kc Residual Strength=N/A

Damage Progression by Ply Group Observed via NDI

Damage Codes:

| 1st Digit: | | 2nd Digit: | |
|------------|-----------------------------|------------|----------------|
| 1 | Transverse Crack Initiation | 1 | -45 ply |
| 2 | Transverse Crack Saturation | 2 | +45 ply |
| 3 | Transverse Crack Coupling | 3 | 90 ply |
| 4 | Delamination | 4 | 0/+ interface |
| | | 5 | +90 interface |
| | | 6 | 90/- interface |
| | | 7 | -/- interface |

K- Cycles at Inspection

| Ply Group | 0 | .1 | 1 | 5 |
|-----------|---|----|----|--------|
| 1 | | | | |
| 2 | | | | |
| 3 | | | | |
| 4 | | | | |
| 5 | | | | |
| 6 | | | 44 | 45, 46 |

% Stiffness Retention

| | 0 | .1 | 1 | 5 |
|-----------|-----|-----|----|------|
| E (long) | 100 | 100 | 99 | 90.9 |
| E (trans) | | | | |

TABLE 24 : DAMAGE PROGRESSION IN SPECIMEN C6-2

Specimen: C6-2 Test Type: TC R=-1.0 f=10 Hz Area=0.280
 Pmax=+ 9 kip Life=56.5 Kc Residual Strength=N/A

Damage Progression by Ply Group Observed via NDI

Damage Codes:

| | | | |
|------------|-----------------------------|------------|-----------------|
| 1st Digit: | | 2nd Digit: | |
| 1 | Transverse Crack Initiation | 1 | -45 ply |
| 2 | Transverse Crack Saturation | 2 | +45 ply |
| 3 | Transverse Crack Coupling | 3 | 90 ply |
| 4 | Delamination | 4 | 0/+ interface |
| | | 5 | +/-90 interface |
| | | 6 | 90/- interface |
| | | 7 | -/- interface |

| Ply Group | K- Cycles at Inspection | | | | | |
|-----------|-------------------------|------------|--------|------------|--------|--------|
| | 0 | 5 | 10 | 20 | 50 | 56.5 |
| 1 | | 11, 12, 13 | | | 44 | |
| 2 | | 11, 13, 36 | 12 | | | |
| 3 | | 11, 13 | | | | |
| 4 | | 11, 13 | | | | |
| 5 | | | 11, 13 | | | 45, 46 |
| 6 | | | | 11, 13, 36 | 45, 46 | |

% Stiffness Retention

| | | | | | |
|-----------|-----|----|----|----|----|
| E (long) | 100 | 97 | 96 | 92 | 86 |
| E (trans) | 100 | | | | |

TABLE 25 : DAMAGE PROGRESSION IN SPECIMEN C7-1

Specimen:C7-1 Test Type: TC R=-1.0 f=10 Hz Area=0.280

Pmax=+10 kip Life=18 Kc Residual Strength=N/A

Damage Progression by Ply Group Observed via NDI

Damage Codes:

| 1st Digit: | | 2nd Digit: | |
|------------|-----------------------------|------------|-----------------|
| 1 | Transverse Crack Initiation | 1 | -45 ply |
| 2 | Transverse Crack Saturation | 2 | +45 ply |
| 3 | Transverse Crack Coupling | 3 | 90 ply |
| 4 | Delamination | 4 | 0/+ interface |
| | | 5 | +/-90 interface |
| | | 6 | 90/- interface |
| | | 7 | -/- interface |

K- Cycles at Inspection

| Ply Group | 0 | 1 | 5 | 10 |
|-----------|---|----|------------|--------|
| 1 | | 13 | 12, 13, 36 | 45, 46 |
| 2 | | 13 | 12, 13, 36 | |
| 3 | | 13 | 12, 13, 36 | |
| 4 | | 13 | 12, 13, 36 | |
| 5 | | 13 | 12, 13, 36 | |
| 6 | | 13 | 12, 13, 36 | 45, 46 |

% Stiffness Retention

| | | | | |
|-----------|-----|-----|----|----|
| E (long) | 100 | 100 | 95 | 94 |
| E (trans) | 100 | | | |

TABLE 26 : DAMAGE PROGRESSION IN SPECIMEN C8-8

Specimen: C8-8 Test Type: TC R=-1.0 f=10 Hz Area=0.280
 Pmax=+8 kip Life= 328 Kc Residual Strength=N/A

Damage Progression by Ply Group Observed via NDI

Damage Codes:

| 1st Digit: | 2nd Digit: |
|-------------------------------|-------------------|
| 1 Transverse Crack Initiation | 1 -45 ply |
| 2 Transverse Crack Saturation | 2 +45 ply |
| 3 Transverse Crack Coupling | 3 90 ply |
| 4 Delamination | 4 0/+ interface |
| | 5 +/-90 interface |
| | 6 90/- interface |
| | 7 -/- interface |

| Ply Group | K- Cycles at Inspection | | | | |
|-----------|-------------------------|---|------------|----|--------|
| | 0 | 1 | 10 | 50 | 100 |
| 1 | | | 11, 13, 36 | | 45, 46 |
| 2 | | | 11, 13, 36 | | |
| 3 | | | 11, 13, 36 | | |
| 4 | | | 11, 13, 36 | | |
| 5 | | | 11, 13, 36 | | 45, 46 |
| 6 | | | | | |

% Stiffness Retention

| | | | | | |
|-----------|-----|-----|----|----|----|
| E (long) | 100 | 99 | 98 | 97 | 92 |
| E (trans) | 100 | 100 | 98 | | |

TABLE 27 : DAMAGE PROGRESSION IN SPECIMEN C5-11

Specimen: C5-11 Test Type: TC R=-1.0 f=10 Hz Area=0.280
 Pmax=+ 9 kip Life=77.0Kc Residual Strength=N/A

Damage Progression by Ply Group Observed via NDI

Damage Codes:

| | | | |
|------------|-----------------------------|------------|----------------|
| 1st Digit: | | 2nd Digit: | |
| 1 | Transverse Crack Initiation | 1 | -45 ply |
| 2 | Transverse Crack Saturation | 2 | +45 ply |
| 3 | Transverse Crack Coupling | 3 | 90 ply |
| 4 | Delamination | 4 | 0/+ interface |
| | | 5 | +/90 interface |
| | | 6 | 90/- interface |
| | | 7 | -/- interface |

K- Cycles at Inspection

| Ply Group | 0 | 1 | 5 | 10 | 50 |
|-----------|---|--------------------|---|----|----|
| 1 | | | | | |
| 2 | | | | | |
| 3 | | | | | |
| 4 | | no damage observed | | | |
| 5 | | | | | |
| 6 | | | | | |

% Stiffness Retention

| | | | | | |
|-----------|-----|----|----|----|----|
| E (long) | 100 | 98 | 97 | 95 | 87 |
| E (trans) | 100 | 99 | 99 | 97 | 96 |

TABLE 28 : DAMAGE PROGRESSION IN SPECIMEN C6-6

Specimen: C6-6 Test Type: TT R=+0.5 f=10 Hz Area=0.279
 Pmax=+12 kip Life=1+ Mc Residual Strength=82.3 ksi

Damage Progression by Ply Group Observed via NDI

Damage Codes:

| | |
|-------------------------------|-------------------|
| 1st Digit: | 2nd Digit: |
| 1 Transverse Crack Initiation | 1 -45 ply |
| 2 Transverse Crack Saturation | 2 +45 ply |
| 3 Transverse Crack Coupling | 3 90 ply |
| 4 Delamination | 4 0/+ interface |
| | 5 +/-90 interface |
| | 6 90/- interface |
| | 7 -/- interface |

K- Cycles at Inspection

| Ply Group | 0 | 1 | 10 | 100 | 500 | 1000 |
|-----------|---|----|--------|-----|--------|------|
| 1 | | 13 | 11 | | 12, 35 | |
| 2 | | | 11, 13 | | 12 | |
| 3 | | | 11, 13 | | 12 | |
| 4 | | | 11, 13 | | | |
| 5 | | | 11, 13 | | | |
| 6 | | 13 | 11 | | 12, 36 | |

% Stiffness Retention

| | | | | | | |
|-----------|-----|----|----|----|----|----|
| E (long) | 100 | 99 | 97 | 97 | 98 | 98 |
| E (trans) | 100 | 99 | 98 | | | |

TABLE 29 : DAMAGE PROGRESSION IN SPECIMEN C7-11

Specimen: C7-11 Test Type: TT R=+0.5 f=10 Hz Area=0.277

Pmax=+15 kip Life= 1+ Mc Residual Strength=67.9 ksi

Damage Progression by Ply Group Observed via NDI

Damage Codes:

| 1st Digit: | | 2nd Digit: | |
|------------|-----------------------------|------------|-----------------|
| 1 | Transverse Crack Initiation | 1 | -45 ply |
| 2 | Transverse Crack Saturation | 2 | +45 ply |
| 3 | Transverse Crack Coupling | 3 | 90 ply |
| 4 | Delamination | 4 | 0/+ interface |
| | | 5 | +/-90 interface |
| | | 6 | 90/- interface |
| | | 7 | -/- interface |

| Ply Group | K- Cycles at Inspection | | | | | |
|-----------|-------------------------|------------|----|-----|-----|------|
| | 0 | 1 | 50 | 100 | 500 | 1000 |
| 1 | | 11, 13, 36 | 12 | 46 | | |
| 2 | | 11, 13, 36 | 12 | | | |
| 3 | | 11, 13, 36 | 12 | | | |
| 4 | | 11, 13, 36 | | 12 | | |
| 5 | | 11, 13, 36 | | 12 | | |
| 6 | | 11, 13, 36 | | 12 | 46 | |

% Stiffness Retention

| | | | | | | |
|-----------|-----|----|----|----|----|----|
| E (long) | 100 | 96 | 93 | 94 | 94 | 94 |
| E (trans) | 100 | 98 | 96 | 96 | 94 | 95 |

TABLE 30 : DAMAGE PROGRESSION IN SPECIMEN C8-4

Specimen: C8-4 Test Type: TT R=+0.5 f=10 Hz Area=0.281
 Pmax=+15 kip Life= 1+ Mc Residual Strength=78.8 ksi

Damage Progression by Ply Group Observed via NDI

Damage Codes:

| | | | |
|------------|-----------------------------|------------|-----------------|
| 1st Digit: | | 2nd Digit: | |
| 1 | Transverse Crack Initiation | 1 | -45 ply |
| 2 | Transverse Crack Saturation | 2 | +45 ply |
| 3 | Transverse Crack Coupling | 3 | 90 ply |
| 4 | Delamination | 4 | 0/+ interface |
| | | 5 | +/-90 interface |
| | | 6 | 90/- interface |
| | | 7 | -/- interface |

| Ply Group | K- Cycles at Inspection | | | | | |
|-----------|-------------------------|------------|----|-----|-----|------|
| | 0 | 10 | 50 | 100 | 300 | 1000 |
| 1 | | 11, 13, 36 | 12 | 46 | | 45 |
| 2 | | 11, 13, 36 | | | | |
| 3 | | 11, 13, 36 | | | | |
| 4 | | 11, 13, 36 | | | | |
| 5 | | 11, 13, 36 | | | | |
| 6 | | 11, 13, 36 | | 46 | | 45 |

| % Stiffness Retention | K- Cycles at Inspection | | | | | |
|-----------------------|-------------------------|----|----|-----|-----|------|
| | 0 | 10 | 50 | 100 | 300 | 1000 |
| E (long) | 100 | 95 | 95 | 95 | 95 | 95 |
| E (trans) | 100 | 96 | 97 | 98 | 95 | 93 |

TABLE 31 : DAMAGE PROGRESSION IN SPECIMEN C8-12

Specimen: C8-12 Test Type: TC R=-0.5 f=10 Hz Area=0.279
 Pmax=+9 kip Life= 1+ Mc Residual Strength=68.7 ksi

Damage Progression by Ply Group Observed via NDI

Damage Codes:

| 1st Digit: | | 2nd Digit: | |
|------------|-----------------------------|------------|-----------------|
| 1 | Transverse Crack Initiation | 1 | -45 ply |
| 2 | Transverse Crack Saturation | 2 | +45 ply |
| 3 | Transverse Crack Coupling | 3 | 90 ply |
| 4 | Delamination | 4 | 0/+ interface |
| | | 5 | +/-90 interface |
| | | 6 | 90/- interface |
| | | 7 | -/- interface |

K- Cycles at Inspection

| Ply Group | 0 | 10 | 100 | 500 | 1000 |
|-----------|---|------------|--------|--------|------|
| 1 | | 11, 13, 36 | 45, 46 | | |
| 2 | | 11, 13, 36 | | 45, 46 | |
| 3 | | 11, 13, 36 | | 45, 46 | |
| 4 | | 11, 13, 36 | | 45, 46 | |
| 5 | | 11, 13, 36 | | 45, 46 | |
| 6 | | 11, 13, 36 | 45, 46 | | |

% Stiffness Retention

| | | | | | |
|-----------|-----|----|----|----|----|
| E (long) | 100 | 99 | 93 | 85 | 85 |
| E (trans) | 100 | 96 | 92 | | |

TABLE 32 : DAMAGE PROGRESSION IN SPECIMEN C6-8

Specimen:C6-8 Test Type: TC R=-0.5 f=10 Hz Area=0.279
 Pmax=+12 kip Life=34 Kc Residual Strength=N/A

Damage Progression by Ply Group Observed via NDI

Damage Codes:

| 1st Digit: | | 2nd Digit: | |
|------------|-----------------------------|------------|-----------------|
| 1 | Transverse Crack Initiation | 1 | -45 ply |
| 2 | Transverse Crack Saturation | 2 | +45 ply |
| 3 | Transverse Crack Coupling | 3 | 90 ply |
| 4 | Delamination | 4 | 0/+ interface |
| | | 5 | +/-90 interface |
| | | 6 | 90/- interface |
| | | 7 | -/- interface |

K- Cycles at Inspection

| Ply Group | 0 | 1 | 5 | 10 | 25 |
|-----------|---|------------|----|------------|--------|
| 1 | | 11, 13, 36 | | 12, 45, 46 | |
| 2 | | 11, 13, 36 | | 12 | 45, 46 |
| 3 | | 11, 13, 36 | | | 45, 46 |
| 4 | | 11, 13, 36 | | | 45, 46 |
| 5 | | 11, 13, 36 | | | 45, 46 |
| 6 | | 11, 12, 36 | 46 | 45 | |

% Stiffness Retention

| | | | | | |
|-----------|-----|----|----|----|----|
| E (long) | 100 | 97 | 95 | 91 | 86 |
| E (trans) | 100 | 95 | 92 | 89 | |

TABLE 33 : DAMAGE PROGRESSION IN SPECIMEN C8-6

Specimen: C8-6 Test Type: TC R=-0.5 f=10 Hz Area=0.282
 Pmax=+10 kip Life= 269 Kc Residual Strength=N/A

Damage Progression by Ply Group Observed via NDI

Damage Codes:

| 1st Digit: | | 2nd Digit: | |
|------------|-----------------------------|------------|-----------------|
| 1 | Transverse Crack Initiation | 1 | -45 ply |
| 2 | Transverse Crack Saturation | 2 | +45 ply |
| 3 | Transverse Crack Coupling | 3 | 90 ply |
| 4 | Delamination | 4 | 0/+ interface |
| | | 5 | +/-90 interface |
| | | 6 | 90/- interface |
| | | 7 | -/- interface |

| Ply Group | K- Cycles at Inspection | | | | |
|-----------|-------------------------|--------|--------|--------|--------|
| | 0 | 1 | 10 | 50 | 100 |
| 1 | | 11, 13 | | 45, 46 | |
| 2 | | 11, 13 | 12 | 36 | 46 |
| 3 | | 11, 13 | | 36 | 45, 46 |
| 4 | | 11, 13 | | 36 | 45 |
| 5 | | 11, 13 | 36 | 35 | 45, 46 |
| 6 | | 11, 13 | 12, 36 | 45, 46 | |

% Stiffness Retention

| | | | | | |
|-----------|-----|-----|----|----|----|
| E (long) | 100 | 99 | 94 | 92 | 86 |
| E (trans) | 100 | 100 | 98 | 96 | 92 |

TABLE 34 : DAMAGE PROGRESSION IN SPECIMEN C7-9

Specimen: C7-9 Test Type: TC R=-2.0 f=10 Hz Area=0.275

Pmax=+4.5 kip Life=232 Kc Residual Strength=N/A

Damage Progression by Ply Group Observed via NDI

Damage Codes:

| 1st Digit: | | 2nd Digit: | |
|------------|-----------------------------|------------|-----------------|
| 1 | Transverse Crack Initiation | 1 | -45 ply |
| 2 | Transverse Crack Saturation | 2 | +45 ply |
| 3 | Transverse Crack Coupling | 3 | 90 ply |
| 4 | Delamination | 4 | 0/+ interface |
| | | 5 | +/-90 interface |
| | | 6 | 90/- interface |
| | | 7 | -/- interface |

K- Cycles at Inspection

| Ply Group | 0 | 1 | 50 | 100 | 200 |
|-----------|---|----|----|--------|------------------|
| 1 | | 13 | | | |
| 2 | | | | 11, 13 | |
| 3 | | | | | 11, 13 |
| 4 | | | 11 | 13 | |
| 5 | | | | 13 | |
| 6 | | | | | 11, 12, 13 45 |

% Stiffness Retention

| | | | | | |
|-----------|-----|-----|-----|-----|----|
| E (long) | 100 | 100 | 98 | 98 | 93 |
| E (trans) | 100 | 100 | 100 | 100 | |

TABLE 35 : DAMAGE PROGRESSION IN SPECIMEN C8-10

Specimen: C8-10 Test Type: TC R=-2.0 f=10 Hz Area=0.282
 Pmax=+5 kip Life= 45.6 Kc Residual Strength=N/A

Damage Progression by Ply Group Observed via NDI

Damage Codes:

| | |
|--|---|
| <p>1st Digit:</p> <p>1 Transverse Crack Initiation</p> <p>2 Transverse Crack Saturation</p> <p>3 Transverse Crack Coupling</p> <p>4 Delamination</p> | <p>2nd Digit:</p> <p>1 -45 ply</p> <p>2 +45 ply</p> <p>3 90 ply</p> <p>4 0/+ interface</p> <p>5 +/90 interface</p> <p>6 90/- interface</p> <p>7 -/- interface</p> |
|--|---|

K- Cycles at Inspection

| Ply Group | 0 | 1 | 5 | 10 | 20 |
|-----------|--------------------|---|---|----|----|
| 1 | | | | | |
| 2 | | | | | |
| 3 | | | | | |
| 4 | No damage observed | | | | |
| 5 | | | | | |
| 6 | | | | | |

% Stiffness Retention

| | | | | | |
|-----------|-----|-----|-----|-----|-----|
| E (long) | 100 | 100 | 100 | 99 | 98 |
| E (trans) | 100 | 100 | 100 | 100 | 100 |

TABLE 36 : DAMAGE PROGRESSION IN SPECIMEN C5-3

Specimen: C5-3 Test Type: TC R=-2.0 f=10 Hz Area=0.279
 Pmax=+4 kip Life=1Mc+ Residual Strength=79.9ksi

Damage Progression by Ply Group Observed via NDI

Damage Codes:

| | | |
|------------|-----------------------------|------------------|
| 1st Digit: | | 2nd Digit: |
| 1 | Transverse Crack Initiation | 1 -45 ply |
| 2 | Transverse Crack Saturation | 2 +45 ply |
| 3 | Transverse Crack Coupling | 3 90 ply |
| 4 | Delamination | 4 0/+ interface |
| | | 5 +/90 interface |
| | | 6 90/- interface |
| | | 7 -/- interface |

K- Cycles at Inspection

| Ply Group | 0 | 10 | 100 | 300 | 1000 |
|-----------|---|----|-----|--------|--------|
| 1 | | | | | 11, 13 |
| 2 | | | | 11, 13 | |
| 3 | | | | 11, 13 | |
| 4 | | | | 11, 13 | |
| 5 | | | | 11, 13 | |
| 6 | | | | | 11, 13 |

% Stiffness Retention

| | | | | | |
|-----------|-----|----|----|----|----|
| E (long) | 100 | 99 | 99 | 97 | 94 |
| E (trans) | 100 | 99 | 99 | 97 | 92 |

TABLE 37 : DAMAGE PROGRESSION IN SPECIMEN F2-7

Specimen: F2-7 Test Type: GST R=N/A f=N/A Area=0.282
 Pmax= 23.05 kip Life= N/A Residual Strength= 23.05 kip

Damage Progression by Ply Group Observed via NDI

Damage Codes:

| | | |
|------------|-----------------------------|-----------------|
| 1st Digit: | | 2nd Digit: |
| 1 | Transverse Crack Initiation | 1 -45 ply |
| 2 | Transverse Crack Saturation | 2 +45 ply |
| 3 | Transverse Crack Coupling | 3 +/- interface |
| 4 | Delamination | 4 0/+ interface |
| | | 5 -/- interface |

Load at Inspection, kips

| Ply Group | 5 | 10 | 15 | 17.5 | 20 | 22.5 |
|-----------|--------------------|----|----|------|----|------|
| 1 | | | | | | |
| 2 | | | | | | |
| 3 | | | | | | |
| 4 | No damage observed | | | | | |
| 5 | | | | | | |
| 6 | | | | | | |
| 7 | | | | | | |
| 8 | | | | | | |

% Stiffness Retention

| | | | | | | |
|-----------|-----|-----|----|----|----|----|
| E (long) | 100 | 100 | 99 | 98 | 99 | 97 |
| E (trans) | 100 | 100 | 99 | 97 | 98 | 96 |

TABLE 38 : DAMAGE PROGRESSION IN SPECIMEN F5-6

Specimen: F5-6 Test Type: QST R=N/A f=N/A Area=0.285
 Pmax= 22.50 kip Life= N/A Residual Strength= 22.50 kip

Damage Progression by Ply Group Observed via NDI

Damage Codes:

| | |
|-------------------------------|-----------------|
| 1st Digit: | 2nd Digit: |
| 1 Transverse Crack Initiation | 1 -45 ply |
| 2 Transverse Crack Saturation | 2 +45 ply |
| 3 Transverse Crack Coupling | 3 +/- interface |
| 4 Delamination | 4 0/+ interface |
| | 5 -/- interface |

| Ply Group | Load at Inspection, kips | | | | | |
|-----------|--------------------------|----|----|------|----|------------|
| | 5 | 10 | 15 | 17.5 | 20 | 22.5 |
| 1 | | | | | | 11, 12, 33 |
| 2 | | | | | | 43, 44 |
| 3 | | | | | | |
| 4 | | | | | | |
| 5 | | | | | | |
| 6 | | | | | | |
| 7 | | | | | | |
| 8 | | | | | | |

| % Stiffness Retention | Load at Inspection, kips | | | | | |
|-----------------------|--------------------------|-----|----|------|----|------|
| | 5 | 10 | 15 | 17.5 | 20 | 22.5 |
| E (long) | 100 | 100 | 98 | 98 | 99 | 96 |
| E (trans) | 100 | 100 | 99 | 97 | 95 | 95 |

TABLE 39 : DAMAGE PROGRESSION IN SPECIMEN F4-2

Specimen: F4-2 Test Type: OSC R=N/A f=N/A Area=0.277
 Pmax=-19.80 kip Life= N/A Residual Strength=-19.80 kip

Damage Progression by Ply Group Observed via NDI

Damage Codes:

| | |
|-------------------------------|-----------------|
| 1st Digit: | 2nd Digit: |
| 1 Transverse Crack Initiation | 1 -45 ply |
| 2 Transverse Crack Saturation | 2 +45 ply |
| 3 Transverse Crack Coupling | 3 +/- interface |
| 4 Delamination | 4 0/+ interface |
| | 5 -/- interface |

Load at Inspection, kips

| Ply Group | -5 | -10 | -15 | -17 | -18 | -19 |
|-----------|--------------------|-----|-----|-----|-----|-----|
| 1 | | | | | | |
| 2 | | | | | | |
| 3 | | | | | | |
| 4 | No damage observed | | | | | |
| 5 | | | | | | |
| 6 | | | | | | |
| 7 | | | | | | |
| 8 | | | | | | |

% Stiffness Retention

| | | | | | | |
|-----------|-----|-----|-----|-----|----|----|
| E(long),T | 100 | 100 | 98 | 98 | 97 | 96 |
| E(long),C | 100 | 99 | 100 | 100 | 99 | 99 |
| E(trns),T | 100 | 100 | 99 | 97 | 95 | 95 |
| E(trns),C | 100 | 100 | 99 | 98 | 99 | 97 |

TABLE 40 : DAMAGE PROGRESSION IN SPECIMEN F3-4

Specimen: F3-4 Test Type: TT R= 0.1 f=5 Hz Area=0.280
 Pmax= 15 kip Life= 1000+ Kc Residual Strength=N/A

Damage Progression by Ply Group Observed via NDI

Damage Codes:

| | |
|-------------------------------|-----------------|
| 1st Digit: | 2nd Digit: |
| 1 Transverse Crack Initiation | 1 -45 ply |
| 2 Transverse Crack Saturation | 2 +45 ply |
| 3 Transverse Crack Coupling | 3 +/- interface |
| 4 Delamination | 4 0/+ interface |
| | 5 -/- interface |

K- Cycles at Inspection

| Ply Group | 0 | 100 | 250 | 500 | 750 | 1000 |
|-----------|---|-----|------------|--------|-----|------|
| 1 | | | 11, 12, 33 | 43, 44 | | |
| 2 | | | 11 | 12, 33 | | |
| 3 | | | 11, 12, 33 | | | |
| 4 | | | 11, 12, 33 | | | |
| 5 | | | 11 | | | |
| 6 | | | 11 | | | |
| 7 | | | 11, 12, 33 | | | |
| 8 | | | 11, 12, 33 | | | |

% Stiffness Retention

| | | | | | | |
|-----------|-----|-----|----|----|----|----|
| E (long) | 100 | 100 | 95 | 93 | 93 | 91 |
| E (trans) | 100 | 98 | | | | |

TABLE 41 : DAMAGE PROGRESSION IN SPECIMEN F4-6

Specimen: F4-6 Test Type: TT R= 0.1 f=5 Hz Area=0.280
 Pmax= 16 kip Life= 330.0+ Kc Residual Strength= 22.90 kip

Damage Progression by Ply Group Observed via NDI

Damage Codes:

| 1st Digit: | | 2nd Digit: | |
|------------|-----------------------------|------------|---------------|
| 1 | Transverse Crack Initiation | 1 | -45 ply |
| 2 | Transverse Crack Saturation | 2 | +45 ply |
| 3 | Transverse Crack Coupling | 3 | +/- interface |
| 4 | Delamination | 4 | 0/+ interface |
| | | 5 | -/- interface |

K- Cycles at Inspection

| Ply Group | K- Cycles at Inspection | |
|-----------|-------------------------|----------------|
| | 0 | 330 |
| 1 | | 11, 12, 33 |
| 2 | | 11, 12, 33 |
| 3 | | 11, 12, 33 |
| 4 | | 11, 12, 33 |
| 5 | | 11, 12, 33 |
| 6 | | 11, 12, 33 |
| 7 | | 11, 12, 33 |
| 8 | | 11, 12, 33, 43 |

% Stiffness Retention

| | | |
|-----------|-----|----|
| E (long) | 100 | 92 |
| E (trans) | 100 | 88 |

TABLE 42 : DAMAGE PROGRESSION IN SPECIMEN F1-9

Specimen: F1-9 Test Type: TT R=0.1 f=5 Hz Area=0.283
 Pmax= 18 kip Life=290.80 Kc Residual Strength=N/A

Damage Progression by Ply Group Observed via NDI

Damage Codes:

| | |
|-------------------------------|-----------------|
| 1st Digit: | 2nd Digit: |
| 1 Transverse Crack Initiation | 1 -45 ply |
| 2 Transverse Crack Saturation | 2 +45 ply |
| 3 Transverse Crack Coupling | 3 +/- interface |
| 4 Delamination | 4 0/+ interface |
| | 5 -/- interface |

| Ply Group | K- Cycles at Inspection | | | |
|-----------|-------------------------|------------|--------|-----|
| | 0 | 50 | 100 | 250 |
| 1 | 11, 12, 44 | | | 43 |
| 2 | | 11 | | |
| 3 | | | 11, 12 | |
| 4 | | | 11 | |
| 5 | | | 11 | |
| 6 | | | 11 | |
| 7 | | | 11 | |
| 8 | | 11, 12, 43 | | 44 |

% Stiffness Retention

| | | | | |
|-----------|-----|----|----|----|
| E (long) | 100 | 99 | 95 | 91 |
| E (trans) | 100 | 96 | | |

TABLE 43 : DAMAGE PROGRESSION IN SPECIMEN F3-1

Specimen: F3-1 Test Type: TT R= 0.1 f=5 Hz Area=0.277
 Pmax= 18 kip Life= 200.0+ Kc Residual Strength= 24.10 kip

Damage Progression by Ply Group Observed via NDI

Damage Codes:

| 1st Digit: | 2nd Digit: |
|-------------------------------|-----------------|
| 1 Transverse Crack Initiation | 1 -45 ply |
| 2 Transverse Crack Saturation | 2 +45 ply |
| 3 Transverse Crack Coupling | 3 +/- interface |
| 4 Delamination | 4 0/+ interface |
| | 5 -/- interface |

K- Cycles at Inspection

| Ply Group | 0 | 200 |
|-----------|---|----------------|
| 1 | | 11, 12, 33, 43 |
| 2 | | 11, 12, 33 |
| 3 | | 11, 12, 33 |
| 4 | | 11, 12, 33 |
| 5 | | 11, 12, 33 |
| 6 | | 11, 12, 33 |
| 7 | | 11, 12, 33 |
| 8 | | 11, 12, 33, 43 |

% Stiffness Retention

E (long) 100
 E (trans) 100

TABLE 44 : DAMAGE PROGRESSION IN SPECIMEN F5-5

Specimen: F5-5 Test Type: TT R= 0.1 f=5 Hz Area=0.279
 Pmax= 20 kip Life= 10.0+ Kc Residual Strength= 21.80 kip

Damage Progression by Ply Group Observed via NDI

Damage Codes:

| | | |
|-------------------|-----------------------------|-------------------|
| 1st Digit: | | 2nd Digit: |
| 1 | Transverse Crack Initiation | 1 -45 ply |
| 2 | Transverse Crack Saturation | 2 +45 ply |
| 3 | Transverse Crack Coupling | 3 +/- interface |
| 4 | Delamination | 4 0/+ interface |
| | | 5 -/- interface |

K- Cycles at Inspection

| Ply Group | 0 | 10 |
|-----------|---|------------|
| 1 | | 11 |
| 2 | | 11, 12, 33 |
| 3 | | 11, 12, 33 |
| 4 | | 11 |
| 5 | | 11, 12, 33 |
| 6 | | 11, 12, 33 |
| 7 | | 11, 12, 33 |
| 8 | | 11 |

% Stiffness Retention

| | | |
|-----------|-----|-----|
| E (long) | 100 | 100 |
| E (trans) | 100 | 98 |

TABLE 45 : DAMAGE PROGRESSION IN SPECIMEN F2-2

Specimen: F2-2 Test Type: TT R=0.1 f=5 Hz Area=0.281
 Pmax= 20 kip Life=21.31 Kc Residual Strength=N/A

Damage Progression by Ply Group Observed via NDI

Damage Codes:

| | | |
|-------------------|-----------------------------|-------------------|
| 1st Digit: | | 2nd Digit: |
| 1 | Transverse Crack Initiation | 1 -45 ply |
| 2 | Transverse Crack Saturation | 2 +45 ply |
| 3 | Transverse Crack Coupling | 3 +/- interface |
| 4 | Delamination | 4 0/+ interface |
| | | 5 -/- interface |

K- Cycles at Inspection

| Ply Group | 0 | 10 |
|-----------|---|----------|
| 1 | | 11,12 |
| 2 | | 11 |
| 3 | | 11 |
| 4 | | 11 |
| 5 | | 11,12 |
| 6 | | 11 |
| 7 | | 11,12 |
| 8 | | 11,12,44 |

*** Stiffness Retention**

| | | |
|-----------|-----|----|
| E (long) | 100 | 91 |
| E (trans) | 100 | 98 |

TABLE 46 : DAMAGE PROGRESSION IN SPECIMEN F4-1

Specimen: F4-1 Test Type: TC R=-0.5 f=5 Hz Area=0.277
 Pmax= 10 kip Life= 1000 + Kc Residual Strength= 22.2 kip

Damage Progression by Ply Group Observed via NDI

Damage Codes:

| | | |
|-------------------------------|--|-------------------|
| 1st Digit: | | 2nd Digit: |
| 1 Transverse Crack Initiation | | 1 -45 ply |
| 2 Transverse Crack Saturation | | 2 +45 ply |
| 3 Transverse Crack Coupling | | 3 +/- interface |
| 4 Delamination | | 4 0/+ interface |
| | | 5 -/- interface |

K- Cycles at Inspection

| Ply Group | 0 | 100 | 300 | 400 | 700 | 1000 |
|-----------|---|------------|-----|------------|--------|------|
| 1 | | | | 11, 12, 33 | | |
| 2 | | | | 11, 12, 33 | | |
| 3 | | | | 11, 12, 33 | | |
| 4 | | 11 | | 12, 33 | | |
| 5 | | | | 11 | | |
| 6 | | | | 11, 12 | | |
| 7 | | | | 11 | 12, 33 | |
| 8 | | 11, 12, 33 | | 43 | | |

% Stiffness Retention

| | | | | | | |
|-----------|-----|----|----|----|----|----|
| E (long) | 100 | 97 | 95 | 95 | 95 | 94 |
| E (trans) | 100 | 98 | 98 | | | |

TABLE 47 : DAMAGE PROGRESSION IN SPECIMEN F5-8

Specimen: F5-8 Test Type: TC R=-0.5 f=5 Hz Area=0.277
 Pmax= 12 kip Life= 1000 + Kc Residual Strength= 19.55 kip

Damage Progression by Ply Group Observed via NDI

Damage Codes:

| | | | |
|------------|-----------------------------|------------|---------------|
| 1st Digit: | | 2nd Digit: | |
| 1 | Transverse Crack Initiation | 1 | -45 ply |
| 2 | Transverse Crack Saturation | 2 | +45 ply |
| 3 | Transverse Crack Coupling | 3 | +/- interface |
| 4 | Delamination | 4 | 0/+ interface |
| | | 5 | -/- interface |

| Ply Group | K- Cycles at Inspection | | | | |
|-----------|-------------------------|------------|------------|-----|------|
| | 0 | 239 | 471 | 720 | 1000 |
| 1 | | 11, 12, 33 | | | 43 |
| 2 | | 11, 12, 33 | | | 43 |
| 3 | | 11, 12, 33 | | | 43 |
| 4 | | 11, 12, 33 | | | 43 |
| 5 | | 11, 12, 33 | | | 43 |
| 6 | | 11, 12, 33 | | | 43 |
| 7 | | 11, 12, 33 | | | 43 |
| 8 | | 11, 12, 33 | 43, 44, 45 | | |

% Stiffness Retention

| | | | | | |
|-----------|-----|----|----|----|----|
| E (long) | 100 | 93 | 91 | 89 | 88 |
| E (trans) | 100 | | | | |

TABLE 48 : DAMAGE PROGRESSION IN SPECIMEN F4-7

Specimen: F4-7 Test Type: TC R=-0.5 f=5 Hz Area=0.280
 Pmax= 12 kip Life= 1000 + Kc Residual Strength= 22.5 kip

Damage Progression by Ply Group Observed via NDI

Damage Codes:

| | | | |
|------------|-----------------------------|------------|---------------|
| 1st Digit: | | 2nd Digit: | |
| 1 | Transverse Crack Initiation | 1 | -45 ply |
| 2 | Transverse Crack Saturation | 2 | +45 ply |
| 3 | Transverse Crack Coupling | 3 | +/- interface |
| 4 | Delamination | 4 | 0/+ interface |
| | | 5 | -/- interface |

K- Cycles at Inspection

| Ply Group | 0 | 50 | 100 | 500 | 600 | 1000 |
|-----------|---|------------|------------|-----|--------|------|
| 1 | | 11, 12, 33 | | | 43, 44 | |
| 2 | | 11, 12, 33 | | | | |
| 3 | | 11, 12, 33 | | | | |
| 4 | | 11, 12, 33 | | | | |
| 5 | | 11, 12, 33 | | | | |
| 6 | | | 11, 12, 33 | | | |
| 7 | | | 11, 12, 33 | | | |
| 8 | | | 11, 12, 33 | 43 | 44 | |

% Stiffness Retention

| | 0 | 50 | 100 | 500 | 600 | 1000 |
|-----------|-----|----|-----|-----|-----|------|
| E (long) | 100 | 99 | 98 | 90 | 90 | 88 |
| E (trans) | 100 | 98 | 96 | | | |

TABLE 49 : DAMAGE PROGRESSION IN SPECIMEN F1-7

Specimen: F1-7 Test Type: TC R=-1.0 f=10 Hz Area=0.283
 Pmax= 10 kip Life=375.72 Kc Residual Strength=N/A

Damage Progression by Ply Group Observed via NDI

Damage Codes:

| | |
|--|--|
| <p>1st Digit:</p> <p>1 Transverse Crack Initiation</p> <p>2 Transverse Crack Saturation</p> <p>3 Transverse Crack Coupling</p> <p>4 Delamination</p> | <p>2nd Digit:</p> <p>1 -45 ply</p> <p>2 +45 ply</p> <p>3 +/- interface</p> <p>4 0/+ interface</p> <p>5 -/- interface</p> |
|--|--|

K- Cycles at Inspection

| Ply Group | 0 | 1 | 10 | 50 | 100 | 200 |
|-----------|---|---|------------|----|--------|-----|
| 1 | | | 11, 12, 43 | | 44 | |
| 2 | | | | | 11, 12 | |
| 3 | | | | | 11, 12 | |
| 4 | | | | | 11, 12 | |
| 5 | | | | | 11, 12 | |
| 6 | | | | | 11, 12 | |
| 7 | | | | | 11, 12 | |
| 8 | | | | | 11, 12 | 44 |

% Stiffness Retention

| | | | | | | |
|-----------|-----|-----|-----|----|----|----|
| E (long) | 100 | 100 | 100 | 99 | 99 | 93 |
| E (trans) | 100 | 99 | 95 | | | |

TABLE 50 : DAMAGE PROGRESSION IN SPECIMEN F1-10

Specimen: F1-10 Test Type: TC R=-1.0 f=5 Hz Area=0.283
 Pmax= 10 kip Life=330.0 Kc+ Residual Strength= 23.15 kip

Damage Progression by Ply Group Observed via NDI

Damage Codes:

| 1st Digit: | | 2nd Digit: | |
|------------|-----------------------------|------------|---------------|
| 1 | Transverse Crack Initiation | 1 | -45 ply |
| 2 | Transverse Crack Saturation | 2 | +45 ply |
| 3 | Transverse Crack Coupling | 3 | +/- interface |
| 4 | Delamination | 4 | 0/+ interface |
| | | 5 | -/- interface |

K- Cycles at Inspection

| Ply Group | 0 | 330 |
|-----------|---|----------------|
| 1 | | 11, 12, 43, 44 |
| 2 | | 11, 12 |
| 3 | | 11, 12 |
| 4 | | 11, 12 |
| 5 | | 11, 12 |
| 6 | | 11, 12 |
| 7 | | 11, 12 |
| 8 | | 11, 12, 43, 44 |

% Stiffness Retention

| | | |
|-----------|-----|----|
| E (long) | 100 | 88 |
| E (trans) | 100 | |

TABLE 51 : DAMAGE PROGRESSION IN SPECIMEN F2-5

Specimen: F2-5 Test Type: TC R=-1.0 f=5 Hz Area=0.277
 Pmax= 10 kip Life= 285 + Kc Residual Strength= 18.95 kip

Damage Progression by Ply Group Observed via NDI

Damage Codes:

| | |
|-------------------------------|-----------------|
| 1st Digit: | 2nd Digit: |
| 1 Transverse Crack Initiation | 1 -45 ply |
| 2 Transverse Crack Saturation | 2 +45 ply |
| 3 Transverse Crack Coupling | 3 +/- interface |
| 4 Delamination | 4 0/+ interface |
| | 5 -/- interface |

K- Cycles at Inspection

| Ply Group | 0 | 35 | 285 |
|-----------|---|----|----------------|
| 1 | | | 11, 12 |
| 2 | | | 11 |
| 3 | | 11 | |
| 4 | | | 11 |
| 5 | | | 11 |
| 6 | | 11 | |
| 7 | | | 11 |
| 8 | | | 11, 12, 43, 44 |

% Stiffness Retention

| | | | |
|-----------|-----|-----|----|
| E (long) | 100 | 100 | 98 |
| E (trans) | 100 | 98 | |

TABLE 52 : DAMAGE PROGRESSION IN SPECIMEN F2-9

Specimen: F2-9 Test Type: TC R=-1.0 f=5 Hz Area=0.279
 Pmax= 10 kip Life= 280.0+ Kc Residual Strength= 22.75 kip

Damage Progression by Ply Group Observed via NDI

Damage Codes:

| | | |
|------------|-----------------------------|-----------------|
| 1st Digit: | | 2nd Digit: |
| 1 | Transverse Crack Initiation | 1 -45 ply |
| 2 | Transverse Crack Saturation | 2 +45 ply |
| 3 | Transverse Crack Coupling | 3 +/- interface |
| 4 | Delamination | 4 0/+ interface |
| | | 5 -/- interface |

K- Cycles at Inspection

| Ply Group | 0 | 45 | 280 |
|-----------|---|----|----------------|
| 1 | | | 11, 12, 33, 43 |
| 2 | | | 11, 12, 33 |
| 3 | | | 11, 12, 33 |
| 4 | | | 11, 12, 33 |
| 5 | | | 11, 12, 33 |
| 6 | | | 11, 12, 33 |
| 7 | | | 11, 12, 33 |
| 8 | | | 11, 12, 33, 43 |

% Stiffness Retention

| | | | |
|-----------|-----|----|----|
| E (long) | 100 | 96 | 87 |
| E (trans) | 100 | | |

TABLE 53 : DAMAGE PROGRESSION IN SPECIMEN F4-4

Specimen: F4-4 Test Type: TC R=-1.0 f=10 Hz Area=0.279
 Pmax= 10 kip Life= 138.59 Kc Residual Strength=N/A

Damage Progression by Ply Group Observed via NDI

Damage Codes:

| | |
|--|--|
| <p>1st Digit:</p> <p>1 Transverse Crack Initiation</p> <p>2 Transverse Crack Saturation</p> <p>3 Transverse Crack Coupling</p> <p>4 Delamination</p> | <p>2nd Digit:</p> <p>1 -45 ply</p> <p>2 +45 ply</p> <p>3 +/- interface</p> <p>4 0/+ interface</p> <p>5 -/- interface</p> |
|--|--|

K- Cycles at Inspection

| Ply Group | 0 | 100 |
|-----------|---|----------------|
| 1 | | 11, 12, 33 |
| 2 | | 11, 12, 33 |
| 3 | | 11, 12, 33 |
| 4 | | 11, 12, 33 |
| 5 | | 11, 12, 33 |
| 6 | | 11, 12, 33 |
| 7 | | 11, 12, 33 |
| 8 | | 11, 12, 33, 43 |

% Stiffness Retention

| | | |
|-----------|-----|----|
| E (long) | 100 | 99 |
| E (trans) | 100 | 99 |

TABLE 54 : DAMAGE PROGRESSION IN SPECIMEN F3-9

Specimen: F3-9 Test Type: TC R=-1.0 f=5 Hz Area=0.280
 Pmax= 10 kip Life= 712.50 Kc Residual Strength=N/A

Damage Progression by Ply Group Observed via NDI

Damage Codes:

| | | | |
|------------|-----------------------------|------------|---------------|
| 1st Digit: | | 2nd Digit: | |
| 1 | Transverse Crack Initiation | 1 | -45 ply |
| 2 | Transverse Crack Saturation | 2 | +45 ply |
| 3 | Transverse Crack Coupling | 3 | +/- interface |
| 4 | Delamination | 4 | 0/+ interface |
| | | 5 | -/- interface |

| Ply Group | K- Cycles at Inspection | | | | |
|-----------|-------------------------|-----|-----|-----|-----|
| | 0 | 200 | 300 | 347 | 550 |
| 1 | 11,12,33 | | 43 | 44 | |
| 2 | 11,12,33 | | 43 | | |
| 3 | 11,12,33 | | | | |
| 4 | 11,12,33 | | | | |
| 5 | 11,12,33 | | | | |
| 6 | 11,12,33 | | | | |
| 7 | 11,12,33 | | 43 | | |
| 8 | 11,12,33 | | 43 | 44 | |

% Stiffness Retention

| | | | | | |
|-----------|-----|----|----|----|----|
| E (long) | 100 | 93 | 90 | 86 | 85 |
| E (trans) | 100 | | | | |

TABLE 55 : DAMAGE PROGRESSION IN SPECIMEN F5-7

Specimen: F5-7 Test Type: TC R=-1.0 f=5 Hz Area=0.287
 Pmax= 10 kip Life= 494.65 Kc Residual Strength=N/A

Damage Progression by Ply Group Observed via NDI

Damage Codes:

| | |
|-------------------------------|-----------------|
| 1st Digit: | 2nd Digit: |
| 1 Transverse Crack Initiation | 1 -45 ply |
| 2 Transverse Crack Saturation | 2 +45 ply |
| 3 Transverse Crack Coupling | 3 +/- interface |
| 4 Delamination | 4 0/+ interface |
| | 5 -/- interface |

K- Cycles at Inspection

| Ply Group | 0 | 10 | 50 | 100 | 200 | 400 |
|-----------|---|----|------------|-----|------------|-----|
| 1 | | | 11, 12, 33 | | | |
| 2 | | | 11, 12, 33 | | | |
| 3 | | | 11, 12 | | | |
| 4 | | | 11, 12, 33 | | | |
| 5 | | | | 11 | | |
| 6 | | | 11, 12, 33 | | | |
| 7 | | | 11, 12, 33 | | | |
| 8 | | | | | 11, 12, 33 | |
| | | | | | 43 | |

% Stiffness Retention

| | | | | | | |
|-----------|-----|-----|----|----|----|----|
| E (long) | 100 | 96 | 96 | 95 | 87 | 84 |
| E (trans) | 100 | 100 | 99 | | | |

TABLE 56 : DAMAGE PROGRESSION IN SPECIMEN F2-6

Specimen: F2-6 Test Type: TC R=-1.0 f=5 Hz Area=0.280
 Pmax= 11 kip Life= 484.05 Kc Residual Strength=N/A

Damage Progression by Ply Group Observed via NDI

Damage Codes:

| | | | |
|------------|-----------------------------|------------|---------------|
| 1st Digit: | | 2nd Digit: | |
| 1 | Transverse Crack Initiation | 1 | -45 ply |
| 2 | Transverse Crack Saturation | 2 | +45 ply |
| 3 | Transverse Crack Coupling | 3 | +/- interface |
| 4 | Delamination | 4 | 0/+ interface |
| | | 5 | -/- interface |

| Ply Group | K- Cycles at Inspection | | | | | |
|-----------|-------------------------|-------|----------|-------|-----|-----|
| | 0 | 10 | 50 | 100 | 350 | 465 |
| 1 | | | 11,12,43 | 44 | | |
| 2 | | | 11,12,33 | | | |
| 3 | | | 11 | 12,33 | | |
| 4 | | | 11 | 12,33 | | |
| 5 | | | 11,12,33 | | | |
| 6 | | 11 | 12,33 | | | |
| 7 | | 11,12 | 33 | | | 44 |
| 8 | | 11,12 | | 44 | | |

| % Stiffness Retention | K- Cycles at Inspection | | | | | |
|-----------------------|-------------------------|-----|----|-----|-----|-----|
| | 0 | 10 | 50 | 100 | 350 | 465 |
| E (long) | 100 | 100 | 97 | 96 | 87 | 85 |
| E (trans) | 100 | 98 | | | | |

TABLE 57 : DAMAGE PROGRESSION IN SPECIMEN F3-11

Specimen: F3-11 Test Type: TC R=-1.0 f=10 Hz Area=0.279
 Pmax= 11 kip Life= 37.74 Kc Residual Strength=N/A

Damage Progression by Ply Group Observed via NDI

Damage Codes:

| | | | |
|------------|-----------------------------|------------|---------------|
| 1st Digit: | | 2nd Digit: | |
| 1 | Transverse Crack Initiation | 1 | -45 ply |
| 2 | Transverse Crack Saturation | 2 | +45 ply |
| 3 | Transverse Crack Coupling | 3 | +/- interface |
| 4 | Delamination | 4 | 0/+ interface |
| | | 5 | -/- interface |

K- Cycles at Inspection

| Ply Group | 0 | 1 | 5 | 10 | 20 |
|-----------|---|---|---|----|----|
| 1 | | | | | |
| 2 | | | | | |
| 3 | | | | | |
| 4 | | | | | |
| 5 | | | | | |
| 6 | | | | | |
| 7 | | | | | |
| 8 | | | | 43 | |

% Stiffness Retention

| | | | | | |
|-----------|-----|-----|----|----|----|
| E (long) | 100 | 100 | 99 | 98 | 96 |
| E (trans) | 100 | 99 | 98 | | |

TABLE 58 : DAMAGE PROGRESSION IN SPECIMEN F1-5

Specimen:F1-5 Test Type: TC R=-2.0 f= 5 Hz Area=0.280
 Pmin=-10 kip Life=1 Mc+ Residual Strength=>20.0 kip

Damage Progression by Ply Group Observed via NDI

Damage Codes:

| | |
|-------------------------------|-----------------|
| 1st Digit: | 2nd Digit: |
| 1 Transverse Crack Initiation | 1 -45 ply |
| 2 Transverse Crack Saturation | 2 +45 ply |
| 3 Transverse Crack Coupling | 3 +/- interface |
| 4 Delamination | 4 0/+ interface |
| | 5 -/- interface |

| Ply Group | K- Cycles at Inspection | | | | | |
|-----------|-------------------------|----|-----|-----|--------|------|
| | 0 | 50 | 200 | 427 | 700 | 1000 |
| 1 | | | | | | |
| 2 | | 11 | | | | |
| 3 | | | | 11 | | |
| 4 | | | | | 11, 12 | |
| 5 | | | | | 11, 12 | |
| 6 | | | | | 11, 12 | |
| 7 | | | | 11 | | 12 |
| 8 | | | | | | |

| % Stiffness Retention | K- Cycles at Inspection | | | | | |
|-----------------------|-------------------------|----|-----|-----|-----|------|
| | 0 | 50 | 200 | 427 | 700 | 1000 |
| E (long) | 100 | 97 | 97 | 97 | 94 | 92 |
| E (trans) | 100 | 99 | 97 | | | |

TABLE 59 : DAMAGE PROGRESSION IN SPECIMEN F1-11

Specimen: F1-11 Test Type: TC R=-2.0 f=5 Hz Area=0.283
 Pmax= 6 kip Life=271.74 Kc Residual Strength=N/A

Damage Progression by Ply Group Observed via NDI

Damage Codes:

| | | | |
|------------|-----------------------------|------------|---------------|
| 1st Digit: | | 2nd Digit: | |
| 1 | Transverse Crack Initiation | 1 | -45 ply |
| 2 | Transverse Crack Saturation | 2 | +45 ply |
| 3 | Transverse Crack Coupling | 3 | +/- interface |
| 4 | Delamination | 4 | 0/+ interface |
| | | 5 | -/- interface |

K- Cycles at Inspection

| Ply Group | 0 | 50 | 100 | 200 |
|-----------|---|----|----------------|-----|
| 1 | | | 11, 12, 43, 44 | |
| 2 | | | 11 | |
| 3 | | | 11 | |
| 4 | | | | |
| 5 | | | | |
| 6 | | | | |
| 7 | | | | |
| 8 | | | | |

% Stiffness Retention

| | 100 | 97 | 94 | 85 |
|-----------|-----|----|----|----|
| E (long) | | | | |
| E (trans) | 100 | | | |

TABLE 60 : DAMAGE PROGRESSION IN SPECIMEN F1-1

Specimen: F1-1 Test Type: TC R=-2.0 f= 5 Hz Area=0.276
 Pmin=-14 kip Life=61.84 Kc Residual Strength=N/A

Damage Progression by Ply Group Observed via NDI

Damage Codes:

| | | | |
|------------|-----------------------------|------------|---------------|
| 1st Digit: | | 2nd Digit: | |
| 1 | Transverse Crack Initiation | 1 | -45 ply |
| 2 | Transverse Crack Saturation | 2 | +45 ply |
| 3 | Transverse Crack Coupling | 3 | +/- interface |
| 4 | Delamination | 4 | 0/+ interface |
| | | 5 | -/- interface |

K- Cycles at Inspection

| Ply Group | 0 | 10 | 50 |
|-----------|---|----|--------|
| 1 | | | 43, 44 |
| 2 | | | |
| 3 | | | |
| 4 | | | |
| 5 | | | |
| 6 | | | |
| 7 | | | |
| 8 | | | 43, 44 |

% Stiffness Retention

| | | | |
|-----------|-----|----|------|
| E (long) | 100 | 94 | 88.8 |
| E (trans) | 100 | | |

TABLE 61 : DAMAGE PROGRESSION IN SPECIMEN F1-4

Specimen: F1-4 Test Type: CC R=2.0 f= 5 Hz Area=0.282
 Pmin=-14 kip Life=1 Mc+ Residual Strength= 25.9 kip

Damage Progression by Ply Group Observed via NDI

Damage Codes:

| | |
|-------------------------------|-----------------|
| 1st Digit: | 2nd Digit: |
| 1 Transverse Crack Initiation | 1 -45 ply |
| 2 Transverse Crack Saturation | 2 +45 ply |
| 3 Transverse Crack Coupling | 3 +/- interface |
| 4 Delamination | 4 0/+ interface |
| | 5 -/- interface |

K- Cycles at Inspection

| | | | | | | | | | | |
|-----------|---|----|----|----|-----|-----|-----|-----|-----|--------------------|
| | 0 | 10 | 25 | 50 | 100 | 200 | 350 | 500 | 650 | 1000 |
| Ply Group | | | | | | | | | | |
| 1 | | | | | | | | | | |
| 2 | | | | | | | | | | |
| 3 | | | | | | | | | | |
| 4 | | | | | | | | | | |
| 5 | | | | | | | | | | No damage observed |
| 6 | | | | | | | | | | |
| 7 | | | | | | | | | | |
| 8 | | | | | | | | | | |

% Stiffness Retention

| | | | | | | | | | | |
|-----------|-----|----|----|----|----|----|----|----|----|--|
| E (long) | 100 | 99 | 98 | 92 | 90 | | | | | |
| E (trans) | 100 | 98 | 98 | 99 | 97 | 97 | 96 | 95 | 95 | |

TABLE 62 : DAMAGE PROGRESSION IN SPECIMEN F3-12

Specimen: F3-12 Test Type: CC R= 2.0 f=5 Hz Area=0.278
 Pmin= -16 kip Life= 500+ Kc Residual Strength= 25.05 kip

Damage Progression by Ply Group Observed via NDI

Damage Codes:

| | | | |
|------------|-----------------------------|------------|---------------|
| 1st Digit: | | 2nd Digit: | |
| 1 | Transverse Crack Initiation | 1 | -45 ply |
| 2 | Transverse Crack Saturation | 2 | +45 ply |
| 3 | Transverse Crack Coupling | 3 | +/- interface |
| 4 | Delamination | 4 | 0/+ interface |
| | | 5 | -/- interface |

K- Cycles at Inspection

| Ply Group | 0 | 10 | 50 | 100 | 280 | 500 |
|-----------|--------------------|----|----|-----|-----|-----|
| 1 | | | | | | |
| 2 | | | | | | |
| 3 | | | | | | |
| 4 | | | | | | |
| 5 | No damage observed | | | | | |
| 6 | | | | | | |
| 7 | | | | | | |
| 8 | | | | | | |

% Stiffness Retention

| | 0 | 10 | 50 | 100 | 280 | 500 |
|-----------|-----|-----|-----|-----|-----|-----|
| E (long) | 100 | 101 | 102 | 102 | 100 | 102 |
| E (trans) | 100 | 97 | 96 | 96 | 92 | |

TABLE 63 : DAMAGE PROGRESSION IN SPECIMEN F5-1

Specimen: F5-1 Test Type: CC R= 10.0 f=5 Hz Area=0.282
 Pmin= -12 kip Life= 1000+ Kc Residual Strength= 27.15 kip

Damage Progression by Ply Group Observed via NDI

Damage Codes:

| | |
|-------------------------------|-----------------|
| 1st Digit: | 2nd Digit: |
| 1 Transverse Crack Initiation | 1 -45 ply |
| 2 Transverse Crack Saturation | 2 +45 ply |
| 3 Transverse Crack Coupling | 3 +/- interface |
| 4 Delamination | 4 0/+ interface |
| | 5 -/- interface |

K- Cycles at Inspection

| Fly Group | 0 | 100 | 200 | 500 | 700 | 1000 |
|-----------|--------------------|-----|-----|-----|-----|------|
| 1 | | | | | | |
| 2 | | | | | | |
| 3 | | | | | | |
| 4 | | | | | | |
| 5 | No damage observed | | | | | |
| 6 | | | | | | |
| 7 | | | | | | |
| 8 | | | | | | |

% Stiffness Retention

| | | | | | | |
|-----------|-----|-----|----|----|-----|----|
| E (long) | 100 | 100 | 99 | 99 | 100 | 99 |
| E (trans) | 100 | 99 | 99 | 98 | | |

TABLE 64 : DAMAGE PROGRESSION IN SPECIMEN F2-1

Specimen: F2-1 Test Type: S R=0.1/10 f=5 Hz Area=0.277
 Pmax= 10/-1 kip Life=1050 + Kc Residual Strength=23.6 kip

Damage Progression by Ply Group Observed via NDI

Damage Codes:

| | | | |
|------------|-----------------------------|------------|---------------|
| 1st Digit: | | 2nd Digit: | |
| 1 | Transverse Crack Initiation | 1 | -45 ply |
| 2 | Transverse Crack Saturation | 2 | +45 ply |
| 3 | Transverse Crack Coupling | 3 | +/- interface |
| 4 | Delamination | 4 | 0/+ interface |
| | | 5 | -/- interface |

K- Cycles at Inspection

| | | | | | | | | |
|-----------|---|-----|--------------------|-----|-----|-----|-----|------|
| | 0 | 150 | 300 | 450 | 600 | 750 | 900 | 1050 |
| Ply Group | | | | | | | | |
| 1 | | | | | | | | |
| 2 | | | | | | | | |
| 3 | | | | | | | | |
| 4 | | | No damage observed | | | | | |
| 5 | | | | | | | | |
| 6 | | | | | | | | |
| 7 | | | | | | | | |
| 8 | | | | | | | | |

% Stiffness Retention

| | | | | | | | | |
|-----------|-----|-----|-----|-----|----|----|----|-----|
| E (long) | 100 | 99 | 101 | 103 | 99 | 99 | 98 | 100 |
| E (trans) | 100 | 100 | 99 | | | | | |

TABLE 65 : DAMAGE PROGRESSION IN SPECIMEN F4-12

Specimen: F4-12 Test Type: S R=0.1/10 f=5 Hz Area=0.276
 Pmax= 15/-1 kip Life=1050 + Kc Residual Strength=23.45 kip

Damage Progression by Ply Group Observed via NDI

Damage Codes:

| | |
|-------------------------------|-----------------|
| 1st Digit: | 2nd Digit: |
| 1 Transverse Crack Initiation | 1 -45 ply |
| 2 Transverse Crack Saturation | 2 +45 ply |
| 3 Transverse Crack Coupling | 3 +/- interface |
| 4 Delamination | 4 0/+ interface |
| | 5 -/- interface |

| Ply Group | K- Cycles at Inspection | | | | | | | |
|-----------|-------------------------|-----|------------|-----|-----|-----|-----|------|
| | 0 | 150 | 300 | 450 | 600 | 750 | 900 | 1050 |
| 1 | | | 11, 12, 33 | | | | 43 | |
| 2 | | | 11, 12, 33 | | | | | |
| 3 | 11, 12, 33 | | | | | | | |
| 4 | 11, 12, 33 | | | | | | | |
| 5 | | | | | | | | |
| 6 | 11, 12, 33 | | | | | | | |
| 7 | 11, 12, 33 | | | | | | | |
| 8 | | 11 | | | | 43 | | |

% Stiffness Retention

| | | | | | | | | |
|-----------|-----|-----|-----|-----|-----|-----|-----|-----|
| E (long) | 100 | 105 | 104 | 107 | 106 | 106 | 105 | 106 |
| E (trans) | 100 | 94 | 94 | | | | | |

TABLE 66 : DAMAGE PROGRESSION IN SPECIMEN F3-5

Specimen:F3-5 Test Type: S R=.1/10 f=5 Hz Area=0.276
Pmax= 15/-1.2 kip Life=1.59710 Mc Residual Strength=N/A

Damage Progression by Ply Group Observed via NDI

Damage Codes:

| | |
|-------------------------------|-----------------|
| 1st Digit: | 2nd Digit: |
| 1 Transverse Crack Initiation | 1 -45 ply |
| 2 Transverse Crack Saturation | 2 +45 ply |
| 3 Transverse Crack Coupling | 3 +/- interface |
| 4 Delamination | 4 0/+ interface |
| | 5 -/- interface |

| Ply Group | K- Cycles at Inspection | | | | | | | |
|-----------|-------------------------|-------|-----|-------|-----|-----|-----|------|
| | 0 | 150 | 300 | 450 | 600 | 750 | 900 | 1574 |
| 1 | | 11,12 | | 44 | | 43 | | |
| | | 33 | | | | | | |
| 2 | | 11,12 | | | | | | 43 |
| | | 33 | | | | | | |
| 3 | | 11,12 | | | | | | 43 |
| | | 33 | | | | | | |
| 4 | | 11,12 | | | | | | 43 |
| | | 33 | | | | | | |
| 5 | | 11,12 | | | | | | 43 |
| | | 33 | | | | | | |
| 6 | | 11,12 | | | | | | 43 |
| | | 33 | | | | | | |
| 7 | | 11,12 | | | | | | 43 |
| | | 33 | | | | | | |
| 8 | | 11,12 | | 43,44 | | | | |
| | | 33 | | | | | | |

% Stiffness Retention

| | | | | | | | |
|-----------|-----|-----|-----|----|----|----|----|
| E (long) | 100 | 100 | 100 | 99 | 99 | 98 | 96 |
| E (trans) | 100 | 102 | 98 | | | | |

TABLE 67 : DAMAGE PROGRESSION IN SPECIMEN F2-8

Specimen:F2-8 Test Type: S R=-1 /- . f=5 Hz Area=0.277
 Pmax= 10/ 8 kip Life=1.00163 Mc Residual Strength=N/A

Damage Progression by Ply Group Observed via NDI

Damage Codes:

| | |
|-------------------------------|-----------------|
| 1st Digit: | 2nd Digit: |
| 1 Transverse Crack Initiation | 1 -45 ply |
| 2 Transverse Crack Saturation | 2 +45 ply |
| 3 Transverse Crack Coupling | 3 +/- interface |
| 4 Delamination | 4 0/+ interface |
| | 5 -/- interface |

| Ply Group | K- Cycles at Inspection | | | | | | |
|-----------|-------------------------|-------|-------|-------|-----|-----|-----|
| | 0 | 150 | 300 | 450 | 600 | 750 | 900 |
| 1 | | 11,12 | 43 | 44 | | | |
| | | 33 | | | | | |
| 2 | | 11,12 | | | | 43 | |
| | | 33 | | | | | |
| 3 | | 11,12 | | | | 43 | |
| | | 33 | | | | | |
| 4 | | 11 | 12,33 | | | 43 | |
| 5 | | 11 | 12,33 | | | 43 | |
| 6 | | 11,12 | | | | 43 | |
| | | 33 | | | | | |
| 7 | | 11,12 | | | | 43 | |
| | | 33 | | | | | |
| 8 | | 11,12 | | 43,44 | | | |
| | | 33 | | | | | |

% Stiffness Retention

| | | | | | | | |
|-----------|-----|----|----|----|----|----|----|
| E (long) | 100 | 91 | 94 | 92 | 90 | 87 | 85 |
| E (trans) | 100 | | | | | | |

TABLE 68 : DAMAGE PROGRESSION IN SPECIMEN F3-10

Specimen: F3-10 Test Type: S R=-1/-0.5 f=5 Hz Area=0.280
 Pmax= 9/12 kip Life= 250 + Kc Residual Strength= 19.25 kip

Damage Progression by Ply Group Observed via NDI

Damage Codes:

| | |
|-------------------------------|-----------------|
| 1st Digit: | 2nd Digit: |
| 1 Transverse Crack Initiation | 1 -45 ply |
| 2 Transverse Crack Saturation | 2 +45 ply |
| 3 Transverse Crack Coupling | 3 +/- interface |
| 4 Delamination | 4 0/+ interface |
| | 5 -/- interface |

| Ply Group | K- Cycles at Inspection | | |
|-----------|-------------------------|-----|-----|
| | 0 | 150 | 250 |
| 1 | | | 11 |
| 2 | | 11 | |
| 3 | | 11 | |
| 4 | | 11 | |
| 5 | | 11 | |
| 6 | | 11 | |
| 7 | | 11 | |
| 8 | | | 11 |

% Stiffness Retention

| | | |
|-----------|-----|-----|
| E (long) | 100 | 100 |
| E (trans) | 100 | 99 |

TABLE 69 : DAMAGE PROGRESSION IN SPECIMEN F5-2

Specimen: F5-2 Test Type: S R=-1/-2 f=5 Hz Area=0.282
 Pmax= 10/6.66 kip Life= 303.46 Kc Residual Strength=N/A

Damage Progression by Ply Group Observed via NDI

Damage Codes:

| 1st Digit: | | 2nd Digit: | |
|------------|-----------------------------|------------|---------------|
| 1 | Transverse Crack Initiation | 1 | -45 ply |
| 2 | Transverse Crack Saturation | 2 | +45 ply |
| 3 | Transverse Crack Coupling | 3 | +/- interface |
| 4 | Delamination | 4 | 0/+ interface |
| | | 5 | -/- interface |

| Ply Group | K- Cycles at Inspection | | | | |
|-----------|-------------------------|------------|-----|-----|-----|
| | 0 | 150 | 200 | 250 | 300 |
| 1 | | 43, 44 | | 45 | |
| 2 | | 11, 12, 33 | | | |
| 3 | | 11, 12, 33 | | | 43 |
| 4 | | 11, 12, 33 | | | |
| 5 | | 11, 12, 33 | | | |
| 6 | | 11, 12, 33 | | | 43 |
| 7 | | 11, 12, 33 | | | |
| 8 | | 11, 12, 33 | 43 | | |

% Stiffness Retention

| | | | | | |
|-----------|-----|-----|----|----|----|
| E (long) | 100 | 100 | 95 | 96 | 91 |
| E (trans) | 100 | 99 | | | |

REFERENCES

1. A. Highsmith and K. L. Reifsnider, "Stiffness Reduction Mechanisms in Composite Laminates", Proc. ASTM Conf. on Damage in Composite Laminates, STP 755, K. L. Reifsnider, Ed., Bal Harbour, FL, Nov. 12-14, 1980, pp. 103-117
2. K. L. Reifsnider, E. G. Henneke II, and W. W. Stinchcomb, "Defect-Property Relationships in Composite Materials," AFML-TR-76-81, Part IV, Air Force Materials Laboratory, June 1979
3. T. K. O'Brien, "Stiffness Change as a Nondestructive Damage Measurement," in Mechanics of Nondestructive Testing, W. W. Stinchcomb, Ed., Plenum Press, New York, 1980, pp. 101-121
4. K. L. Reifsnider, "Some Fundamental Aspects of the Fatigue and Fracture Response of Composite Materials," Proceedings, 14th Annual Meeting of the Society of Engineering Science, Lehigh Univ., Bethlehem, PA., Nov. 14-16, 1977, pp.373-384
5. R. N. Kriz, W. W. Stinchcomb, and D. R. Tenney, "Effects of Moisture, Residual Thermal Curing Stresses, and Mechanical Load on the Damage Development in Quasi-Isotropic Laminates," VPI-E-80-5, College of Engineering, Virginia Polytechnic Institute and State University, Feb. 1980
6. K. L. Reifsnider, W. W. Stinchcomb, and E. G. Henneke II, "Defect-Property Relationships in Composite Laminates," AFML-TR-76-81, Part III, April 1979
7. P. C. Yeung, W. W. Stinchcomb, and K. L. Reifsnider, "Characterization of Constraining Effects on Flaw Growth," Nondestructive Evaluation and Flaw Criticality for Composite Materials, STP 696, B. P. Pipes, Ed., American Society for Testing and Materials, 1979

8. J. E. Masters and K. L. Reifsnider, "An Investigation of Cumulative Damage Development in Quasi-Isotropic Graphite-Epoxy Laminates," in Damage of Composite Materials, K. L. Reifsnider, Ed., STP 775, American Society for Testing and Materials, 1982, pp. 40-62
9. K. L. Reifsnider and A. L. Highsmith, "Characteristic Damage States: A New Approach to Representing Fatigue Damage in Composite Materials," in Materials, Experimentation, and Design in Fatigue, Westbury House, Guildford, U.K., 1981, pp.246-260
10. R. D. Jamison, A. L. Highsmith, and K. L. Reifsnider, "Strain Field Response of θ Glass/Epoxy Composites under Tension," Composites Technology Review, Vol. 3, No. 4, 1981, pp.158-159
11. A. L. Highsmith and K. L. Reifsnider, "Non-uniform Microstrain in Composite Laminates," Composites Technology Review, Vol. 4, No. 1, 1982, pp. 20-22
12. T. K. O'Brien, "Characterization of Delamination Onset and Growth in a Composite Laminate," Damage in Composite Materials, ASTM STP-775, American Society for Testing and Materials, 1982
13. D. J. Wilkins, "A Comparison of the Delamination and Environmental Resistance of a Graphite/Epoxy and a Graphite/Bismaleimide," NAV-GD-0037, NASC, 1981
14. T. K. O'Brien, "Tension Fatigue Behaviour of Quasi-Isotropic Graphite Epoxy Laminates," Fatigue and Creep of Composite Materials, H. Lilholt and R. Talreja, Eds., Riso National Laboratory, Roskilde, Denmark, 1982
15. K. M. Liechti, K. L. Reifsnider, W. W. Stinchcomb, and D. A. Ulman, "A Cumulative Damage Model for Advanced Composite Materials: Phase I Final Report," AFWAL-TR-82-4094, July 1982

END

FILMED

10-84

DTIC